ALPHA-BUNGAROTOXIN-RESISTANT CHOLINERGIC RECEPTORS ON AN IDENTIFIED LOCUST FLIGHT MOTONEURONE

Linda J. Anderson

A Thesis Submitted for the Degree of PhD
at the
University of St Andrews

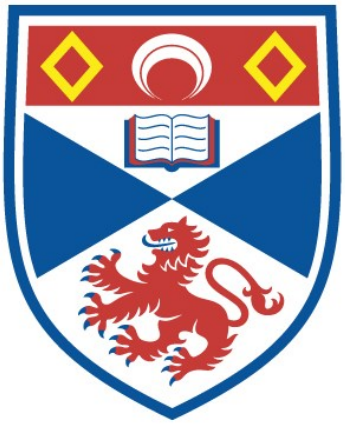

1995

ALPHA-BUNGAROTOXIN-RESISTANT CHOLINERGIC RECEPTORS ON AN IDENTIFIED LOCUST FLIGHT MOTONEURONE

A thesis submitted to the University of St. Andrews for the degree of Doctor of Philosophy

by

Linda J. Anderson

University of St. Andrews

School of Biological and Medical Sciences

March, 1995.

I, Linda J. Anderson, hereby certify that this thesis, which is approximately 40 000 words in length, has been written by me, that it is the record of work carried out by me and that it has not been submitted in any previous application for a higher degree.

date 30 March 1995 signature of candidate .....

I was admitted as a research student under Ordinance No. 12 in October, 1991 and as a candidate for the degree of Ph.D. in September, 1992; the higher study for which this is a record was carried out in the University of St. Andrews between 1991 and 1995.

date 30 March 1995 signature of candidate .....

I hereby certify that the candidate has fulfilled the conditions of the Resolutions and Regulations for the degree of Ph.D. in the University of St. Andrews and that the candidate is qualified to submit this thesis in application for that degree.

date 30 3 95 signature of supervisor .....

In submitting this thesis to the University of St. Andrews I understand that I am giving permission for it to be made available for use in accordance with the regulations of the University Library for the time being in force, subject to any copyright vested in the work not being affected thereby. I also understand that the title and abstract will be published, and that a copy of the work may be made and supplied to any *bona fide* library or research worker.

date 30 March 1995 signature of candidate .....

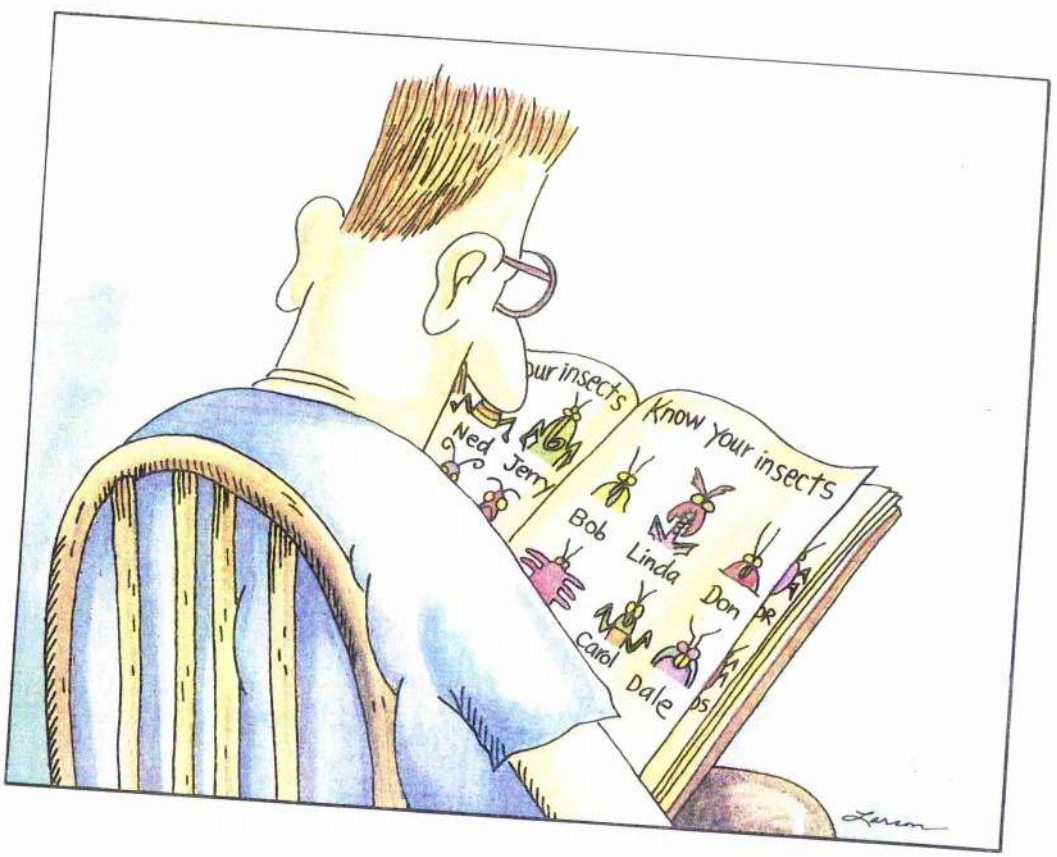

Cartoon by Gary Larson
From: The Prehistory of The Far Side: A 10th Anniversary Exhibit. Warner Books, London.

ACKNOWLEDGEMENTS

My sincerest thanks go to my supervisor, Bob Pitman, for his guidance and advice throughout the course of my PhD. I would also like to thank Jon David for many interesting discussions, especially over a pint of Arrolls on a Friday night. Special thanks are also due to my friends, especially Ali, Larissa, Carolyn, Kate, Sandra, Kevin, Karen, Gordon, Joe and Pat for their support and encouragement while I was writing up.

I would like to thank the members of the Photographic Department for their assistance with photography, and David Ogden for maintaining the locust colony.

Finally, I want to thank my family for their support throughout my studies.

This work was supported by a Maitland Ramsay Scholarship from the University of St. Andrews.

CONTENTS

ABSTRACT

1. There is a population of α-bungarotoxin-resistant cholinergic receptors on the soma of the first basalar motoneurone of the locust, *Schistocerca gregaria.*

2. The receptors have a broadly muscarinic pharmacology: the response to pressure-applied ACh can be reversibly reduced by the global muscarinic antagonists atropine and dexetimide, and the vertebrate muscarinic subtype-selective antagonists pirenzepine (M_1 subtype-selective), 4-DAMP (M_3), p-F-HHSiD ($M_3>M_1>M_2$) and methoctramine (M_2).

3. In the presence of α-bungarotoxin, however, nicotine evokes a current similar to those induced by the muscarinic agonists muscarine, McN-A-343 and carbachol under voltage clamp; the nicotine-induced current can be blocked by the muscarinic antagonist scopolamine, suggesting that these 'muscarinic' receptors have a 'mixed' cholinergic pharmacology.

4. Under voltage clamp, activation of the receptors by the muscarinic agonists muscarine and McN-A-343, and the cholinergic agonist carbachol (in the presence of α-bungarotoxin) evokes an inward current at command potentials between -100 and 0 mV. This current is time- and voltage-dependent: the current component evoked at potentials more negative than -40 mV is relatively small, and either increases continuously during 15 min exposure to agonist, or increases to a maximum after 5 or 10 min before decreasing. At potentials more positive than -40 mV, the current component is larger, and increases continuously in the presence of drug. In approximately 50 % of neurones voltage clamped at a holding potential of -50 mV, the inward current is preceded by an initial outward current at potentials positive to -40 mV. After 1 min exposure to agonist, the outward current reverses and becomes inwardly-directed, increasing in amplitude in the presence of agonist.

5. The apparent inward current evoked by McN-A-343 at potentials positive to -40 mV is due to the inhibition of a voltage-dependent K^+ current, and may involve the production of cAMP. Activation of the 'mixed' receptors also stimulates the release of Ca^{2+} from intracellular stores.

6. The input resistance of the neurone, measured under current clamp, is increased by McN-A-343 in some preparations and decreased in others. The agonist decreases the spike threshold of the neurone, and therefore the physiological role of these 'mixed' receptors may be to modulate the excitability of the neurone.

CHAPTER 1

General Introduction

1. GENERAL INTRODUCTION

1.1. ACETYLCHOLINE

Cholinergic receptors were first classified in vertebrate preparations by Dale in 1914 according to their sensitivity to nicotine and muscarine, although it was not until 1921 that the first convincing evidence for the presence of acetylcholine (ACh) as a neurotransmitter in the vertebrate peripheral nervous system was produced (Loewi, 1921). The criteria which must be met for a substance to be classified as a neurotransmitter have been reviewed by Werman (1966):

1. the presence of an inactivating enzyme;
2. the presence of the putative neurotransmitter;
3. the substance must be detectable in the extracellular fluid of the synapse upon stimulation of the presynaptic nerve;
4. the presence of the synthesising enzyme and precursor molecules;
5. the existence of a specific release mechanism;
6. application of the putative neurotransmitter must mimic the actions of the endogenous neurotransmitter;
7. pharmacological agents must have the same effect on the postsynaptic actions of the putative neurotransmitter as on those of the endogenous neurotransmitter.

There is no single synapse in the CNS of any insect for which all of these criteria have been met, although the evidence that exists is strongly indicative that ACh is a neurotransmitter in the insect CNS (for reviews see Pitman, 1985; Sattelle, 1985; Breer & Sattelle, 1987). ACh has been found in nervous tissue of the fly *Musca domestica* (Tobias et al, 1946), blowflies (Lewis, 1953), the honey bee *Apis mellifera* (Augustinsson & Grahn, 1954), the cockroach *Periplaneta americana* (Tobias et al, 1946; Colhoun, 1958a), the tobacco hornworm *Manduca sexta* (Sanes & Hildebrand, 1976) and the locust *Locusta migratoria* (Breer,

1981a). Colhoun (1958a) demonstrated that stimulation of the nerve cord or of a sensory pathway of the cockroach resulted in an increase in the ACh content of the nerve cord. The presence of the synthesising enzyme choline acetyltransferase (ChAT) has been demonstrated in *Musca* (Tobias et al, 1946), cockroach (Tobias et al, 1946; Colhoun, 1958b), woodroach (Schafer, 1973), locust (Emson et al, 1974; Breer, 1981a) and *Manduca* (Sanes & Hildebrand, 1976). Emson et al (1974) showed that large amounts of ChAT were located in sensory neurones, rather than motoneurones. Work on locust synaptosomes (pinched-off presynaptic nerve terminals) has demonstrated that ^{3}H-choline is accumulated via a high affinity uptake system (Breer, 1981a, 1982, 1983). Acetylcholine is synthesised in locust synaptosomes and can be subsequently released upon depolarisation of the synaptosome by increasing the external K^{+} concentration (Breer, 1982; Breer & Knipper, 1984). Cholinesterase, the enzyme responsible for the degradation of ACh, is present in *Musca* (Tobias et al, 1946), cockroach (Tobias et al, 1946), locust (Emson et al, 1974; Breer, 1981a) and *Manduca* (Sanes & Hildebrand, 1976). Electrophysiological experiments on cockroach central neurones (Callec & Boistel, 1967; Kerkut et al, 1969; Kerkut et al, 1970; Shankland et al, 1971; Sattelle et al, 1976) demonstrated that cholinergic agonists mimicked the actions of the natural transmitter, thus providing more evidence for the role of ACh as a neurotransmitter in the insect CNS.

The majority of research on cholinergic receptors has been performed on vertebrate preparations, and it has become apparent that there are major differences between nicotinic and muscarinic receptors in terms of ligand binding properties, physiology, biochemistry and molecular biology. The following overview of cholinergic receptors describes some of the pharmacology and structure of vertebrate receptors, and compares these properties with those of the receptors found in the insect CNS.

1.1.1. Pharmacology

1.1.1.1. Vertebrate nicotinic receptors

Vertebrate nicotinic receptors were divided into two subtypes when it was realised that the nicotinic receptors at the neuromuscular junction had different pharmacological properties to those of the autonomic ganglia. Table 1.1. lists the major nicotinic agonists and antagonists (see Bowman & Rand, 1980 for review). In general, nicotinic agonists such as nicotine and DMPP (1,1-dimethyl-4-phenylpiperazinium) show little selectivity between neuromuscular junction receptors and ganglionic receptors, but nicotinic antagonists show more specificity. Antagonists of receptors at the neuromuscular junction can be either non-depolarising blockers or depolarising blockers. Non-depolarising antagonists (for example d-tubocurarine) simply bind to the nicotinic receptor without activating it. Depolarising antagonists (for example decamethonium), are nicotinic agonists and persistently activate the receptor, producing a sustained depolarisation of the endplate region thus inactivating the voltage-sensitive Na^+ channels and rendering the membrane inexcitable. Nicotinic antagonists that block ganglionic receptors include hexamethonium and pentamethonium. The mechanism of block is similar to that of non-depolarising neuromuscular receptor antagonists.

α-Bungarotoxin (α-BTX) is a snake toxin which was thought to bind specifically to neuromuscular nicotinic receptors, and therefore could be used to differentiate between neuromuscular and ganglionic nicotinic receptors. However, it is now known that the toxin also blocks ganglionic nicotinic receptors in some preparations (see below). α-BTX was first isolated from the venom of the snake *Bungarus multicinctus* by Chang & Lee in 1963 and binds irreversibly to neuromuscular nicotinic receptors (Chang & Lee, 1963; Lee et al, 1967; Barnard et al, 1971; Miledi & Potter, 1971; Berg et al, 1972; Bursztajn & Gershon, 1977). The electroplax tissue of electric fishes is modified muscle, and, perhaps not surprisingly, also expresses α-BTX-sensitive nicotinic receptors (Changeux et al,

Table 1.1. Cholinergic receptor ligands.

NICOTINIC RECEPTOR LIGANDS

AGONISTS	ANTAGONISTS		
	neuromuscular		ganglionic
	non-depolarising	depolarising	
ACh	*d*-tubocurarine	decamethonium	hexamethonium
carbachol	benzoquinonium	suxamethonium	pentamethonium
nicotine	gallamine	suxethonium	pentolinium
DMPP	pancuronium	carbolonium	

MUSCARINIC RECEPTOR LIGANDS

AGONISTS	ANTAGONISTS
ACh	QNB
carbachol	atropine
muscarine	dexetimide
muscarone	scopolamine
oxotremorine	benzilylcholine mustard
bethanecol	
acetyl β-methyl choline	

1970; Miledi et al, 1971; Raftery, 1973). Toxin binding sites have been found on neurones throughout the central and autonomic nervous systems, including guinea-pig cerebral cortex (Bosmann, 1972), cultured chick sympathetic neurones (Greene et al, 1973), rat sympathetic ganglia (Fumagalli et al, 1976) and rat carotid body (Chen & Yates, 1981). However, not all of these binding sites have been found to be functional nicotinic receptors. Whereas α-BTX blocks nicotinic receptor-mediated events in guinea-pig cerebral cortex (Bosmann, 1972), pigeon sympathetic neurones (Chiappinelli & Zigmond, 1978), frog (Marshall, 1981) and chick (Chiappinelli & Zigmond, 1978) sympathetic ganglia and rat olfactory bulb (Alkondon & Albuquerque, 1994), it has no effect on the nicotinic receptors in the rat superior cervical ganglion (Brown & Fumagalli, 1977), guinea-pig and rabbit autonomic ganglia (Bursztajn & Gershon, 1977) and rat parasympathetic ganglion (Ascher et al, 1979). The differential sensitivity to α-BTX of neuronal nicotinic receptors suggests that they are not a homogeneous group.

1.1.1.2. Vertebrate muscarinic receptors

The major global muscarinic ligands are summarised in Table 1.1. (see Bowman & Rand, 1980 for review). Muscarinic agonists include muscarine and oxotremorine, and muscarinic antagonists include atropine and scopolamine. Quinuclidinyl benzilate (QNB) is a potent muscarinic antagonist in the vertebrate CNS (Yamamura & Snyder, 1974a, b; Yamamura et al, 1974; Waelbroeck et al, 1991) which is often used to identify muscarinic receptors. α-BTX has no effect on muscarinic receptors.

Evidence to suggest that more than one subclass of vertebrate muscarinic receptors existed was first provided by binding studies which showed that muscarinic receptors in rat brain had a greater affinity for the antagonist pirenzepine than receptors located in heart, smooth muscle and glands, including the submaximal and parotid (Hammer et al, 1980). Pirenzepine-sensitive muscarinic receptors were later classed as M_1 receptors, and pirenzepine-

insensitive as M_2 receptors. Pirenzepine-insensitive receptors differ in their pharmacology: AF-DX 116 (Giachetti et al, 1986) and methoctramine (Melchiorre et al, 1987) are more potent on cardiac M_2 receptors than those located in smooth muscle. 4-Diphenylacetoxy-N-methylpiperidine methiodide (4-DAMP), hexahydrosiladifenidol (HHSiD) and its p-Fluoro derivative were proven to be more potent on the receptors on smooth muscle than heart (Barlow et al, 1976; Lambrecht et al, 1989). These three receptor subtypes with distinct pharmacologies were termed M_1 (brain), M_2 (cardiac) and M_3 (smooth muscle).

1.1.1.3. Insect cholinergic receptors

There are both α-BTX and QNB binding sites in the insect CNS, implying that both nicotinic and muscarinic cholinergic receptors are present. In contrast to the vertebrate CNS, in which there are more muscarinic than nicotinic receptors (Ben-Barak & Dudai, 1979; Salvaterra & Foders, 1979), binding studies using α-BTX and QNB have shown that nicotinic receptors outnumber muscarinic receptors by a factor of ten in the insect CNS (Dudai & Ben-Barak, 1977; Breer, 1981b; Lummis & Sattelle, 1985). α-BTX binding sites are widespread in the insect CNS, including cerebral ganglia of the locust (Breer, 1981b) and *Manduca* (Sanes et al, 1977), terminal abdominal ganglia of the cricket *Acheta domesticus* (Meyer & Edwards, 1985), cockroach nerve cords (Lummis & Sattelle, 1985) and the heads of the fruitfly *Drosophila melanogaster* (Dudai & Amsterdam, 1977), housefly (Dudai, 1977) and honey bee (Huang & Knowles, 1990). α-BTX-sensitive ACh receptors have been detected using electrophysiological techniques on giant interneurone 2 (Sattelle et al, 1983; Harrow & Sattelle, 1983), motoneurone D_s (Carr & Fourtner, 1980) and motoneurone D_f of the cockroach (Sattelle et al, 1980), and isolated unidentified neurones of *Locusta* (Benson, 1992). There may be some heterogeneity of nicotinic receptors in the insect CNS as they are not all sensitive to α-BTX: receptors on dorsal unpaired midline (DUM) neurones of *Periplaneta* (Sattelle et al, 1980) and *Schistocerca nitens*

(Goodman & Spitzer, 1980) have been shown to be insensitive to α-BTX at concentrations up to 10^{-6} M. However, Lapied & Hue (1991) found that the response of DUM neurones to nicotine was partly blocked by α-BTX. Nicotine evokes a biphasic depolarisation in these cells, consisting of a fast initial depolarisation followed by a slower depolarisation. The slow depolarisation was blocked by the toxin, but the fast depolarisation was unaffected.

A QNB-binding site has been identified in the heads of *Drosophila* (Dudai & Ben-barak, 1977) and *Locusta* (Breer, 1981b), the terminal abdominal ganglion of the cricket (Meyer & Edwards, 1980; Meyer & Reddy, 1985), the supraoesophageal ganglion of *Schistocerca gregaria* (Aguilar & Lunt, 1984), *Periplaneta* nerve cords (Lummis & Sattelle, 1985) and the brain of *Apis* (Huang & Knowles, 1990). Electrophysiological experiments have identified functional postsynaptic cholinergic receptors with muscarinic properties on principal planta retractor (PPR) motoneurones of *Manduca* (Trimmer & Weeks, 1989), cockroach giant interneurones (Le Corronc & Hue, 1993), motoneurone D_f and DUM neurone somata of the cockroach (David & Pitman, 1990; Bai et al, 1992) and isolated *Locusta* thoracic cell bodies (Benson, 1992). Muscarinic receptors in the insect CNS are also located presynaptically (see Section 1.1.3.), and have been identified in locust synaptosomes (Knipper & Breer, 1988) and at the cercal nerve-giant interneurone synapse of the cockroach (Hue et al, 1989; Le Corronc et al, 1991). The pharmacology of insect muscarinic receptors differs between preparations and between pre- and postsynaptic locations. For example, the muscarinic receptors on PPR motoneurone of *Manduca* (Trimmer & Weeks, 1993), motoneurone D_f (David & Pitman, 1993a) and the giant interneurone (Le Corronc & Hue, 1993) of *Periplaneta*, have been shown to be most sensitive to the M_1 antagonist pirenzepine. Similarly, muscarinic receptors present on the somata of locust neurones have a high affinity for pirenzepine (Knipper & Breer, 1988). A study on *Musca*, *Apis* and *Periplaneta* brains (Abdallah et al, 1991) showed that muscarinic receptors in these tissues have a high affinity for 4-DAMP

and therefore appear to be similar to vertebrate M_3 receptors. In contrast, presynaptic receptors present in locust synaptosomes (Knipper & Breer, 1988) and at the cercal nerve-giant interneurone synapse of the cockroach (Le Corronc et al, 1991) have an M_2-like pharmacology.

1.1.2. Receptor structure

1.1.2.1. Nicotinic receptors

Nicotinic acetylcholine receptors have been purified from electroplax tissue (Olsen et al, 1972; Schmidt & Raftery, 1972) and mammalian skeletal muscle (Brockes & Hall, 1975; Dolly & Barnard, 1975). Because of the very high concentration of nicotinic receptors in electroplax tissue - receptor protein can be purified in mg amounts - receptors from this tissue rather than muscle have been used extensively for biochemical and molecular biology studies. The nicotinic acetylcholine receptor isolated from electroplax tissue contains four different polypeptide chains (Weill et al, 1974; Raftery et al, 1975). Subsequent research proved that the nicotinic receptor is made up of five polypeptide subunits with the stoichiometry $\alpha_2\beta\gamma\delta$ (Reynolds & Karlin, 1978; Lindstrom et al, 1979), arranged around a water-filled ion channel (Brisson & Unwin, 1985). A diagrammatic representation of the nicotinic receptor is shown in Figure 1.1. The α subunits are not adjacent to each other in the receptor complex, and are probably separated by either the β or γ subunit (Karlin et al, 1983; Hamilton et al, 1985). Nicotinic receptors are members of a superfamily of ligand-gated ion channels. Included in this group are $GABA_A$, glycine and some glutamate and serotonin receptors (reviewed by Karlin, 1993); all are macromolecules, and are comprised of an integral receptor composed of subunits arranged around an ion channel.

Affinity labelling experiments in the early 1970s showed that the acetylcholine binding site was located on the α subunit (Reiter et al, 1972; Karlin & Cowburn, 1973; Weill et al, 1974). This implies that there are two ACh binding

Figure 1.1. The pentameric structure of the nicotinic cholinergic receptor of *Torpedo* electroplax tissue. The receptor is a macromolecule comprising an integral receptor and non-specific cation channel, and is made up of five polypeptide chains arranged around the pore. The agonist-binding sites are located on the α subunits (but see Karlin, 1993), implying that two molecules of ACh must bind to the receptor in order for the channel to open. Conserved tyramine, tryptophan and cysteine residues located at the agonist-binding sites are thought to be involved in ligand binding (Karlin, 1993).
(Figure adapted from Rang & Dale, 1987.)

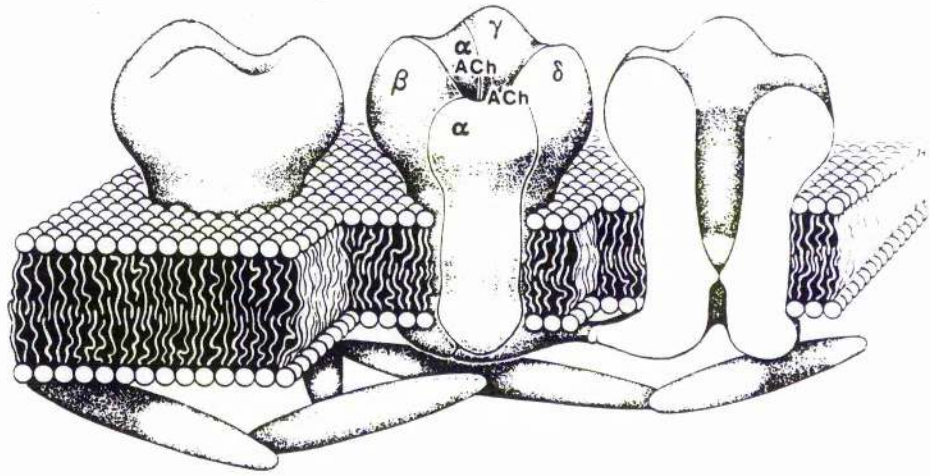

sites per receptor protein, a result which had been indicated by pharmacological analysis.

The first nicotinic receptor to be sequenced was that of *Torpedo californica* (Noda et al, 1982, 1983a; Claudio et al, 1983). All subunits have the same secondary structure, and share a high degree of homology (approximately 40 %). They contain four stretches of hydrophobic amino acids, M1 to M4, which are assumed to be membrane spanning domains. M2 is the most highly conserved domain, and is thought to be involved in ion channel formation: mutagenesis studies have demonstrated that replacement of residues in the M2 domains of each subunit affects the conductance of the channel when the receptor is expressed in *Xenopus* oocytes (Imoto et al, 1991). The amino termini of the subunits are extracellular, but there has been some debate as to whether the carboxy termini of the peptide chains are extracellular (McCrea et al, 1987; Dwyer, 1991) or intracellular (Lindstrom et al, 1984; Young et al, 1985). However, evidence now suggests that the carboxy termini are extracellular (Karlin, 1993).

Cloning of the nicotinic receptor of bovine calf skeletal muscle showed that the nicotinic receptor found in this tissue also consisted of α, β, γ and δ subunits and shared a high degree of amino acid sequence homology with the receptor present in fish electroplax (Noda et al, 1983b; Takai et al, 1984; Tanabe et al, 1984; Kubo et al, 1985). The γ subunit of calf muscle was sequenced from RNA extracted from foetal or newborn tissue (Takai et al, 1984), but when older muscle was used, a novel subunit was uncovered (Takai et al, 1985) which was termed ε. This subunit showed a high degree of homology with the calf γ subunit. When injected into *Xenopus* oocytes with α, β and δ subunits a functional ACh receptor was expressed. Mishina et al (1986) demonstrated that the kinetics of a receptor containing the γ subunit differed from an ε-containing receptor, and that these differences corresponded to those found in foetal and mature calf muscle, suggesting that the two subunits are differentially expressed during development.

Neuronal nicotinic receptors are also composed of five subunits, which are classified as α or β (or non-α) (Conti-Tronconi et al, 1994). To date, seven α (α2 to α8) and four β (β2 to β5) subunits have been sequenced from both mammalian and non-mammalian autonomic ganglia and CNS tissue (muscle subunits are conventionally known as α1 and β1). No sequences corresponding to γ, δ or ε have yet been identified. Sensitivity to α-BTX is conferred by the α subunit: toxin-sensitive receptors contain α7 or α8 subunits, and toxin-insensitive receptors contain α2, α3 or α4 subunits. The effect of α-BTX on nicotinic receptors composed of α5 or α6 subunits is unknown.

Insect nicotinic acetylcholine receptors are assumed to have a similar pentameric structure to vertebrate nicotinic receptors. The first insect nicotinic receptor subunits to be cloned were a non-α subunit, or ARD (Hermans-Borgmeyer et al, 1986) and an α subunit (ALS; Bossy et al, 1988) from *Drosophila*. Since then, a second α, termed Dα2 (Jonas et al, 1990) and non-α subunit (SBD; Sawruk et al, 1990) have also been cloned from *Drosophila*. An α subunit (αL1) has also been cloned from *Schistocerca* (Marshall et al, 1990). Perhaps not surprisingly, these subunits have a higher homology for vertebrate neuronal receptor subunits than muscle or electroplax receptors: ALS, ARD, αL1 and Dα2 show approximately 40, 46, 46 and 60 % homology respectively with vertebrate neuronal α subunits (Bossy et al, 1988; Hermans-Borgmeyer et al, 1986; Marshall et al, 1990; Jonas et al, 1990). Little pharmacological work has been done on the nicotinic receptors which can be reconstituted from these subunits, but it has been found that α-BTX binds to αL1 (Marshall et al, 1990) and to ALS (Bertrand et al, 1994), but not to Dα2 (Bertrand et al, 1994).

The subunits of the insect nicotinic receptor could combine to form either homo-oligomeric receptors or hetero-oligomeric receptors, and there is evidence for the occurrence of both. Initial attempts to purify nicotinic receptors from locust nervous tissue resulted in the detection of a single polypeptide, implying

that the natural receptor was a homo-oligomer (Breer et al, 1985). When expressed in lipid bilayers a functional nicotinic receptor was obtained (Hanke & Breer, 1986). However, the existence of a *Drosophila* non-α subunit (Hermans-Borgmeyer et al, 1986), which is presumably a non-ligand binding subunit, would suggest that insect nicotinic receptors are hetero-oligomers because an α subunit would be required for ligand binding. In support of this hypothesis, expression studies have shown that both ALS and ARD *Drosophila* subunits must be injected into *Xenopus* oocytes in order to form a functional receptor (Schloss et al 1991). These conflicting observations suggest that insect nicotinic receptors can exist as both homo-oligomeric and hetero-oligomeric structures.

1.1.2.2. Muscarinic receptors

Whereas the nicotinic ACh receptor is a macromolecule comprising an integral receptor and non-specific cation channel, muscarinic receptors are members of a superfamily of plasma membrane receptors that couple to guanine nucleotide-binding proteins (G proteins; see Section 1.2.1.) to mediate signal transduction (Hulme et al, 1990). Other members of this superfamily include receptors for catecholamines, metabotropic glutamate receptors, serotonin, $GABA_B$, most neuropeptides and rhodopsin. These G protein-linked receptors consist of a single polypeptide chain, with seven hydrophobic transmembrane helices (TM1-TM7), joined by alternating intracellular (i1-i4) and extracellular (o1-o3) loops. The amino terminal of the protein is extracellular, and the carboxy terminal is cytoplasmic. A diagrammatic representation of a muscarinic receptor is shown in Figure 1.2.

Pharmacological experiments had shown that muscarinic receptors existed in more than one subtype (Section 1.1.1.2.); the development of molecular biology techniques enabled researchers to classify muscarinic receptors further. Physiologically-defined receptors are represented by 'M', whereas genetically-defined muscarinic receptors are represented by 'm'. Muscarinic receptors were

Figure 1.2. The muscarinic cholinergic receptor consists of one polypeptide chain with seven hydrophobic transmembrane helices, joined by alternating intracellular and extracellular loops. The amino terminal is extracellular, and the carboxy terminal is intracellular.
(Adapted from Brann et al, 1993a.)

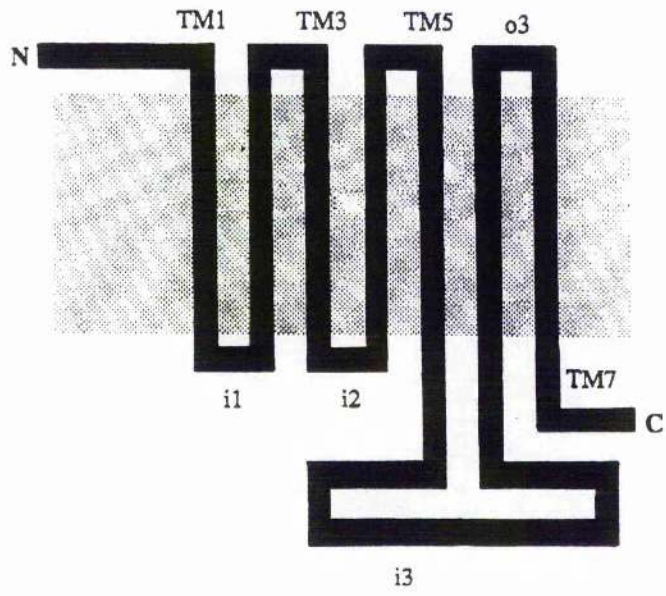

first purified from porcine brain (Haga & Haga, 1983) and heart (Peterson et al, 1984). Kubo et al (1986a) successfully cloned muscarinic receptors from porcine brain, expressed them in *Xenopus* oocytes and proposed that they were similar to M_1 receptors due to their high affinity for pirenzepine. In another paper (Kubo et al, 1986b), the same group reported the sequence of the cDNA encoding the M_2 receptor in porcine cardiac muscle. The receptors were subsequently expressed in Chinese hamster ovary cells and confirmed as being of the M_2 subtype due to their low affinity for pirenzepine (Peralta et al, 1987a). Bonner et al (1987) isolated three cDNAs from rat cerebral cortex: one is the homologue of the porcine brain muscarinic receptor (m_1), and the other two were similar, but distinct from both the brain and cardiac (m_2) receptors already identified and were termed m_3 and m_4. When transfected into COS-7 cells, the m_1, m_3 and m_4 receptors had a high affinity for pirenzepine. A fifth muscarinic receptor was later cloned from rat brain (Liao et al, 1989), which had similar antagonist binding properties to the M_1 receptor.

The distribution of mRNAs in vertebrate tissues is displayed in Table 1.2. The m_1 to m_5 receptor proteins have been detected throughout the brain (Brann et al, 1988, 1993b; Buckley et al, 1988; Weiner & Brann, 1989). Several brain areas express more than one receptor subtype, such as the hippocampus, cortex, thalamus and striatum. Similar observations have been made in rabbit peripheral tissues (Dörje et al, 1991). Significant amounts of m_5 mRNA have not been found in the periphery (Dörje et al, 1991).

The five mammalian receptor proteins show a high level of sequence homology, and share approximately 145 invariant amino acids (Wess, 1993). The majority of these common amino acids are located in the seven transmembrane regions. The third cytoplasmic loop, referred to as i3, is very large in all muscarinic receptors, but there is very little sequence homology between the different subtypes (Bonner, 1989).

Table 1.2. Distribution of mRNAs encoding muscarinic receptors.

m_1	m_2	m_3	m_4	m_5
		brain		
hippocampus	hippocampus	hippocampus	hippocampus	hippocampus
cortex	cortex	cortex	cortex	substantia nigra
striatum	thalamus	thalamus	thalamus	
	striatum		striatum	
		peripheral tissues		
sympathetic ganglia	sympathetic ganglia	submaxillary gland	lung	
vas deferens	vas deferens			
submaxillary gland	submaxillary gland			
	atrium			
	ileum			
	lung			

It has been suggested that ligand binding to the muscarinic receptor occurs in the pocket formed by the circular arrangement of the seven transmembrane domains in a helical wheel arrangement, as shown in Figure 1.3. (Hulme et al, 1990). Practically all muscarinic ligands have a positively charged amino head group, and affinity labelling studies suggested that ligand binding occurs due to ion-ion interaction between the amino group and an aspartate residue located in TM3 (Curtis et al, 1989; Kurtenbach et al, 1990). This was further demonstrated by site-directed mutagenesis (Fraser et al, 1989) in which substitution of this aspartate with the uncharged amino acid asparagine resulted in a receptor that was unable to bind [^{3}H]QNB. In addition to this binding site, the hydrophobic core of the receptor contains a series of conserved threonine and tyramine residues: it is postulated that the hydroxyl groups in the side chains of these amino acids interact with the ACh molecule by forming hydrogen bonds. This theory is supported by experiments in which Thr residues were replaced by alanine, or tyramine by phenylalanine, which resulted in receptors with a much lower affinity for ACh and carbachol (Wess et al, 1991). However, the binding of antagonists to the mutant receptors was unaffected, suggesting that these residues are only involved in agonist binding.

Binding of a muscarinic agonist to the receptor results in a conformational change in the protein which enables it to bind to a G protein. Expression studies have shown that the m_1, m_3 and m_5 receptors generally couple to G proteins that stimulate phosphoinositide hydrolysis (see Section 1.2.3.), and the m_2 and m_4 receptors selectively couple to G proteins that cause the inhibition of adenylate cyclase (see Section 1.2.2.) (Fukuda et al, 1988; Peralta et al, 1988; Pinkas-Kramarski et al, 1988; Liao et al, 1989; HM4 and HM3 of Peralta et al correspond to m_3 and m_4 respectively). One exception is the muscarinic receptors of the heart, in which the receptor-activated G protein interacts directly with the ion channel (see Sections 1.2.1. and 1.3.1.3.). The intracellular loops of the receptor protein are involved in G protein recognition: mutagenesis studies involving M_1 receptors

Figure 1.3. The muscarinic cholinergic receptor is arranged in the membrane in a circular 'helical wheel' arrangement, and agonist binding occurs in the pocket formed in the centre of the receptor. The positively charged amino head group interacts with a negatively charged aspartate (D) residue in TM3. In addition, hydroxyl groups of threonine (T) and tyramine (Y) residues form hydrogen bonds with the ACh molecule. The numbering of amino acid residues refers to the rat M_3 receptor.
(Adapted from Wess, 1993.)

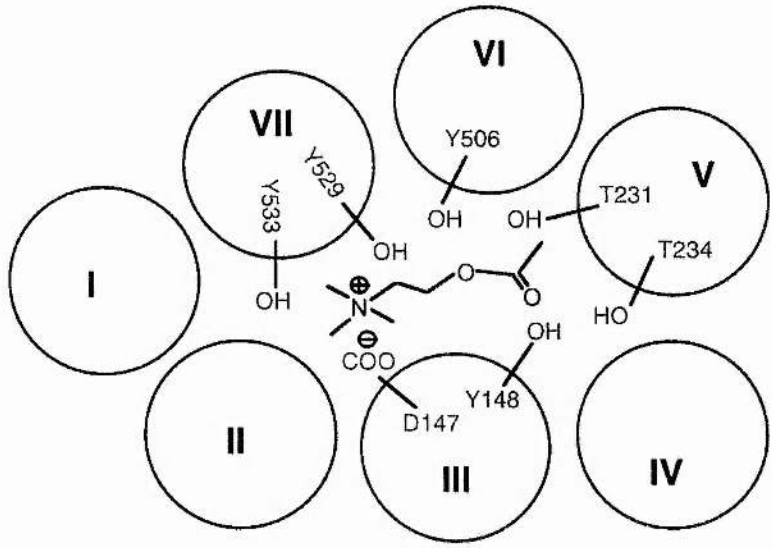

(Fraser et al, 1989) and β-adrenergic receptors (Fraser et al, 1988) have shown that a highly conserved aspartate residue at the beginning of i2 is necessary for efficient G protein coupling. However, experiments have suggested that the i3 domain is sufficient to determine which G protein the receptor subtype will bind to (Kubo et al, 1988). The specificity of the receptor is conveyed by the N-terminal 16-21 amino acids of i3 (Wess et al, 1989; Lechleiter et al, 1990). It is in this region that the sequences of m_1, m_3 and m_5 differ most from those of m_2 and m_4 (Peralta et al, 1987b; Wess et al, 1989).

Only one invertebrate muscarinic receptor has been cloned: both Onai et al (1989) and Shapiro et al (1989) cloned a *Drosophila* receptor which contains the conserved residues common to most G protein-linked receptors, as well as those common to all muscarinic receptors. The receptor isolated by Onai et al has 66 more amino acids than that reported by Shapiro and colleagues (788 amino acids compared with 722); both were considerably longer than mammalian muscarinic receptors (460-590 amino acids; Shapiro et al, 1989). The discrepancy between the receptor molecules isolated by the two groups can be explained by the presence of an alternative splicing site in i3 (Shapiro et al, 1989), which will result in slight variations in the protein produced. Onai et al (1989) found that both the i3 domain and the amino terminus were longer than those reported for most of the mammalian receptor proteins; i3 was approximately double the length. These authors showed that the *Drosophila* muscarinic receptor displayed approximately 60 % homology with mammalian muscarinic receptors, and was most similar to m_1. When only the transmembrane domains were considered, the homology was increased to a maximum of 88 % in TM3 and 4. Shapiro et al (1989) obtained a lower homology of 45 to 50 % when the amino acids of i3 proposed to be involved in G protein recognition in mammalian receptors were excluded. These 20 amino acids were more similar to mammalian m_1, m_3 and m_5 (45, 50 and 60 % homology respectively) than to m_2 and m_4 (25 and 15 % homology respectively).

Both groups showed that there was very little similarity between the i3 domain of the *Drosophila* muscarinic receptor and the mammalian muscarinic receptors.

Shapiro et al (1989) expressed the *Drosophila* muscarinic receptor protein Y1 adrenal carcinoma cells, and found that it bound pirenzepine and thus appeared to be similar to the vertebrate M_1 receptor. In addition, the receptor mediated a carbachol-induced increase in phosphoinositide hydrolysis, suggesting that it is similar to the mammalian m_1, m_3 and m_5 receptors. The *Drosophila* receptor was also expressed in COS 7 cells and *Xenopus* oocytes (Blake et al, 1993); the order of potency of muscarinic receptor antagonists was 4-DAMP > pirenzepine > AF-DX 116, implying that the pharmacology of the receptor broadly resembled that of the vertebrate M_1 and M_3 receptors.

1.1.3. Functional muscarinic receptors in the insect CNS

The first evidence for a physiological role for presynaptic muscarinic receptors in the insect CNS came from experiments on locust synaptosomes (Breer & Knipper, 1984). Synaptosomes are pinched-off nerve terminals and can be used to study the characteristics of neurotransmitter release: when the external K^+ concentration is increased, the synaptosomes are depolarised, thus stimulating the release of ACh. Breer & Knipper (1984) demonstrated that in the presence of muscarinic agonists the amount of ACh released was reduced, and in the presence of muscarinic antagonists it was increased. The results of their experiments were strongly indicative of the presence of presynaptic muscarinic receptors that were involved in regulating ACh release. Further experiments confirmed the muscarinic properties of these receptors, and demonstrated than they were insensitive to pirenzepine and therefore resembled vertebrate M_2 receptors (Knipper & Breer, 1988, 1989). The involvement of muscarinic autoreceptors in synaptic transmission has been demonstrated in electrophysiological studies by investigating the effects of muscarinic ligands on the epsps evoked in central neurones of cockroach (Hue et al, 1989; Le Corronc et al, 1991), locust (Leitch et

al, 1993) and *Manduca* (Trimmer & Weeks, 1989). In these experiments, muscarinic agonists decreased the amplitude of the epsps, and muscarinic antagonists increased the amplitude of the epsps. The work of Le Corronc et al (1991) pointed to the same conclusions as Knipper & Breer (1988, 1989), that the presynaptic muscarinic receptors had a pharmacological profile similar to vertebrate M_2 receptors (for detailed review see Trimmer, 1995).

For many years, the functional role of postsynaptic muscarinic receptors remained unclear. Recently, however, it has been demonstrated that the addition of muscarinic agonists to neurones of *Manduca* (Trimmer & Weeks, 1989, 1993), locust (Baines & Bacon, 1994) and cockroach (Le Corronc & Hue, 1993) increased the excitability of the cells and lowered the spike threshold. In the intact animal, this would facilitate synaptic transmission and increase the probability of a nicotinic receptor-mediated depolarisation evoking an action potential.

1.1.4. 'Mixed' cholinergic receptors

Evidence for a putative third type of cholinergic receptor emerged in 1971 from work on the electroplax of *Electrophorus* (Eldefrawi et al, 1971). Biochemical studies revealed the existence of receptors which bound muscarone, nicotine and decamethonium, a nicotinic antagonist at the vertebrate neuromuscular junction. It was also found that the binding of muscarone was reduced by nicotine, curare (vertebrate neuromuscular junction and electroplax nicotinic receptor antagonist) and decamethonium and thus appeared to have a mixed muscarinic-nicotinic pharmacology. Binding studies have also provided evidence for mixed muscarinic-nicotinic receptors in the head of *Musca* (Aziz & Eldefrawi, 1973; Mansour et al, 1977; Harris et al, 1981), cultured neurones from the brain of *Periplaneta* (Lees et al, 1983) and bovine chromaffin cells (Shirvan et al, 1991). However, the density of these putative receptors is much higher than that found for other receptors, which could suggest that the binding sites do not correspond to receptor proteins. Electrophysiological experiments have

demonstrated the existence of functional mixed muscarinic-nicotinic receptors in several different preparations: the response evoked by nicotine can be blocked by muscarinic antagonists in isolated, unidentified neurones of *Locusta* (Benson & Neumann, 1987; Benson, 1992), motoneurone D_f of *Periplaneta* (David & Pitman, 1993a) and the skin of *Rana catesbiana* (Cox, 1993). In addition, the effects of muscarinic agents are mimicked by nicotine in D_f neurone somata (David & Pitman, 1993a). The effect of α-BTX on the mixed muscarinic-nicotinic receptors of these preparations differs: the toxin did not bind to the receptor identified by Mansour et al (1977), but did bind to the receptor located on cultured *Periplaneta* neurones (Lees et al, 1983). Similarly, the functional mixed muscarinic-nicotinic receptors of motoneurone D_f were insensitive to α-BTX (David & Pitman, 1993a) but those of isolated, unidentified neurones of *Locusta* (Benson & Neumann, 1987; Benson, 1992) can be blocked by α-BTX. As yet, the molecular biology of such receptors has not yet been studied. In fact, they may correspond to one of the muscarinic receptor subtypes.

1.1.5. Evolution of cholinergic receptors

The question thus arises, how have two very different receptor molecules which utilise the same neurotransmitter evolved? There is no evidence that the receptors are closely related: the two receptor proteins differ greatly in structure and physiology. Additionally, when the amino acid sequences of the nicotinic receptor subunits are compared with those of the muscarinic receptor, there is only random homology. These data strongly suggest that the receptors evolved convergently to bind ACh.

1.2. SIGNAL TRANSDUCTION PATHWAYS

Muscarinic receptors are not directly coupled to ion channels, but exert their effects via guanine nucleotide-binding proteins (G proteins) which regulate second messenger pathways, and these in turn can regulate a large number of physiological and biochemical processes in the cell. Two pathways which have been well described are (1) the production of cyclic adenosine monophosphate (cAMP) from adenosine triphosphate (ATP) catalysed by the activation of membrane bound adenylate cyclase, and (2) a combination of second messengers resulting from the hydrolysis of a membrane phospholipid (phosphatidyl inositol 4,5-bisphosphate, or PIP_2) by activation of a membrane associated phospholipase C (PLC). Hydrolysis of PIP_2 results in the production of inositol 1,4,5-trisphosphate (IP_3) and diacylglycerol (DAG). IP_3 binds to specific receptors on the endoplasmic reticulum causing the release of Ca^{2+}. In both these pathways, there are a number of ways that the second messengers can exert their effects: they can bind directly to a target protein, thus affecting a conformational change, or they can activate a protein kinase which phosphorylates specific proteins, causing a conformational change. cAMP activates a cAMP-dependent protein kinase (PKA) and DAG activates protein kinase C (PKC).

This thesis presents evidence consistent with the involvement of both cAMP and Ca^{2+} in muscarinic receptor-mediated events. The following outline of second messengers therefore concentrates on Ca^{2+} and cAMP; PIP_2 hydrolysis is also described because IP_3 may be involved in Ca^{2+} release from intracellular stores. A description of G proteins is also included.

1.2.1. G proteins

G proteins allow amplification of a signal and provide an additional level of control. Amplification can occur at three stages: one receptor-agonist complex can activate several G proteins, and each G protein can then activate several enzyme molecules, which in turn can generate many second messenger molecules.

G proteins are membrane bound heterotrimeric proteins comprising α, β and γ subunits. The involvement of a G protein in transmembrane signalling was initially suggested from investigations into the actions of glucagon in the rat liver, where it was discovered that the hormone required the presence of guanyl nucleotides in order to break down glycogen (Rodbell et al, 1971). There is a superfamily of G protein-coupled receptors, which includes those for the neurotransmitters ACh, catecholamines, glutamate, GABA, neuropeptides and serotonin (Hulme et al, 1990).

The enzyme which is modulated by a particular G protein depends upon the α subunit. There are four main classes of G protein: G_s, G_i, G_q and G_{12}, and within each class there are several types of α subunit (reviewed by Hepler & Gilman, 1992). G_s and G_i are generally coupled to adenylate cyclase (see Section 1.2.2.), whereas G_q and G_{12} are coupled to phospholipase C. There is a relatively high degree of similarity between β and γ subunits (Hepler & Gilman, 1992).

Figure 1.4 shows the five stages of G protein-mediated transmembrane signalling. In the inactivated state (a), GDP (guanosine diphosphate) is bound to the G protein. However, binding of a receptor-agonist complex to the α subunit (G_α) alters the guanyl nucleotide binding site on G_α, resulting in dissociation of the GDP molecule and binding of GTP (guanosine triphosphate) (b). The binding of GTP activates the G protein and allows G_α (with an associated GTP molecule) to dissociate from $G_{\beta\gamma}$ and the receptor-agonist complex (c). The free G_α subunit can then bind to and modify the activity of one of several enzymes, the particular one depending on the particular G_α subunit (d). G_α is activated for as long as GTP is bound; the subunit has GTPase activity (Brandt et al, 1983) and will slowly hydrolyse the GTP molecule to GDP. When this occurs, the G protein is inactivated and dissociates from the enzyme (e) and returns to the basal state.

The receptor-agonist complex is only necessary to initially activate the G protein: G_α will activate the enzyme independently of the receptor-agonist complex. This was first demonstrated by Schramm & Rodbell (1975), who

Figure 1.4. The five stages of G protein-mediated transmembrane signalling. In the inactivated state (a), G proteins exist as heterotrimers, with GDP bound to the G protein. Upon agonist binding and receptor activation, the receptor-agonist complex binds to the α subunit, altering the guanyl nucleotide binding site on G_α; the GDP molecule dissociates and GTP binds to G_α (b). The binding of GTP activates the G protein and allows G_α-GTP to dissociate from $G_{\beta\gamma}$ and the receptor-agonist complex (c). The free G_α subunit can now bind to and modify the activity of an effector molecule (d). In some cases, $G_{\beta\gamma}$ interacts with a second effector, E_2. G_α possesses an intrinsic GTPase activity and will slowly hydrolyse the GTP molecule to GDP. When this occurs, the G protein is inactivated and dissociates from the enzyme (e) and returns to the basal state (a).
(From Hepler & Gilman, 1992.)

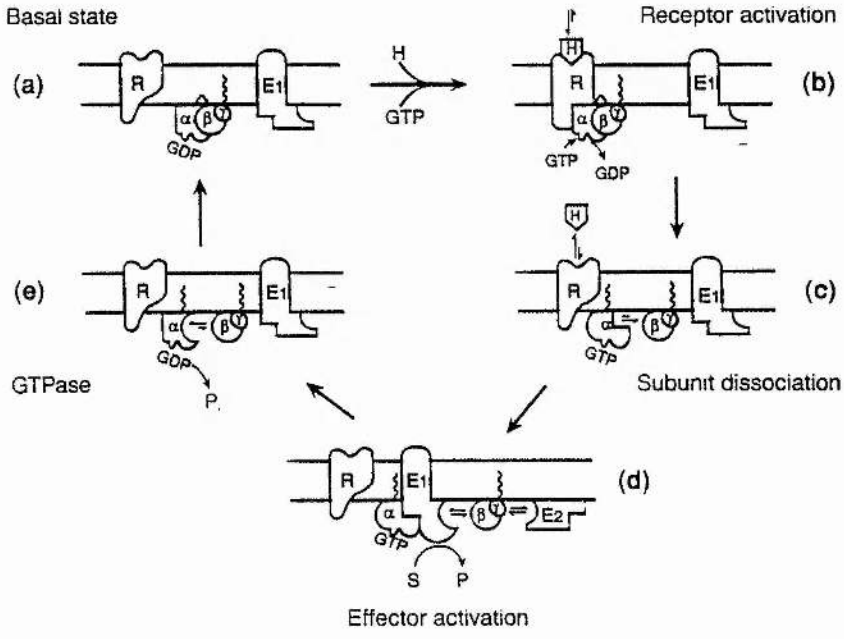

showed that the addition of the β-adrenergic antagonist propranolol only inhibited the effect of the β-adrenergic agonist isoproterenol if added prior to the agonist.

G proteins can modulate ion channels directly without involving a second messenger pathway. This has been observed in vertebrate heart, where muscarinic receptors activate G proteins which bind directly to K^+ channels and thus increase the K^+ conductance of the cell (Noma, 1986).

1.2.2. Cyclic AMP

The existence of cAMP was first discovered in liver homogenates by Rall et al (1957), and there is now abundant evidence that the modulation of cAMP production is a major intracellular signalling system (Schramm & Selinger, 1984; Berridge, 1985). Receptor activation modulates adenylate cyclase activity via G proteins. There are two types of G protein involved: those which mediate an increase in cAMP are termed stimulatory G proteins, or G_s, and those mediating a decrease in cAMP production, inhibitory G proteins (G_i) (Berridge, 1985). Pertussis toxin and cholera toxin (isolated from the bacteria *Bordetella pertussis* and *Vibrio cholerae* respectively) have been important tools in the determination of the role of G proteins in adenylate cyclase activity. Cassel & Pfeuffer (1978) showed that cholera toxin ADP ribosylates the α subunit of G_s, thus blocking its GTPase ability and locking the G protein in the active form. Pertussis toxin ADP ribosylates (Katada & Ui, 1982) the α subunit of G_i, which prevents the binding of GTP. Both toxins result in the persistent stimulation of adenylate cyclase.

Initial work on cAMP was concerned with the stimulation, rather than inhibition, of cAMP production: when the membrane receptor is activated by the binding of an agonist molecule, it undergoes a conformational change and binds to G_s. The α subunit of the G protein then couples to the membrane-bound enzyme adenylate cyclase, which converts ATP (adenosine triphosphate) to cAMP. Alternatively, activation of a receptor which is coupled to G_i inhibits adenylate

cyclase and leads to a decrease in the concentration of cAMP. These events are shown in Figure 1.5.

cAMP is released into the cytoplasm and may regulate some ion channels by binding to them directly (Nakamura & Gold, 1987). However, in the majority of known examples it activates cAMP-dependent protein kinase (PKA or A-kinase), first described in rabbit skeletal muscle by Walsh et al (1968). This enzyme consists of two regulatory subunits and two catalytic subunits: cAMP molecules bind to the regulatory subunits, liberating the catalytic subunits. The catalytic subunits are now activated and phosphorylate specific amino acid residues of target proteins such as ion channels, resulting in their opening or closing (Levitan, 1988).

There are two major mechanisms by which the adenylate cyclase system is deactivated. Firstly, the modulation of adenylate cyclase only continues for as long as GTP is bound to G_α, thus when GTP is hydrolysed to GDP the G protein is inactivated and will cease to stimulate (G_s) or inhibit (G_i) adenylate cyclase. Secondly, cAMP is hydrolysed to the inactive AMP by cAMP phosphodiesterase (Sutherland & Rall, 1958) and cAMP-dependent protein kinase will no longer be activated because of the decrease in cytosolic cAMP.

1.2.3. Inositol phospholipids

Phosphatidyl inositol 4,5-bisphosphate (PIP_2) is a plasma membrane phospholipid. Binding of a neurotransmitter to its receptor activates a G protein (G_p) which in turn activates the membrane-bound enzyme phospholipase C (or phosphoinositidase), leading to the hyrolysis of PIP_2. Two compounds are produced, inositol 1,4,5-trisphosphate (IP_3) and diacylglycerol (DAG), both of which act as second messengers (Nahorski, 1988). IP_3 is cytosolic whereas DAG is membrane-bound (Berridge & Irvine, 1984). The processes involved in PIP_2 hydrolysis are shown in Figure 1.6.

Figure 1.5. The modulation of adenylate cyclase activity by receptor activation. The left side of the diagram shows agonist-receptor complex binding to a stimulatory G protein, G_s, which results in the activation of adenylate cyclase and the production of cAMP. The nucleotide binds to the regulatory subunits (R) of A-kinase (R·cAMP) which causes the catalytic subunits (C) to dissociate and become activated. Target proteins are subsequently phosphorylated by A-kinase.

When an agonist molecule binds to a receptor which is associated with an inhibitory G protein (G_i), adenylate cyclase activity is inhibited. This is depicted on the right side of the diagram.

The actions of the bacterial toxins cholera toxin and pertussis toxin are also shown.

(Adapted from Berridge, 1985.)

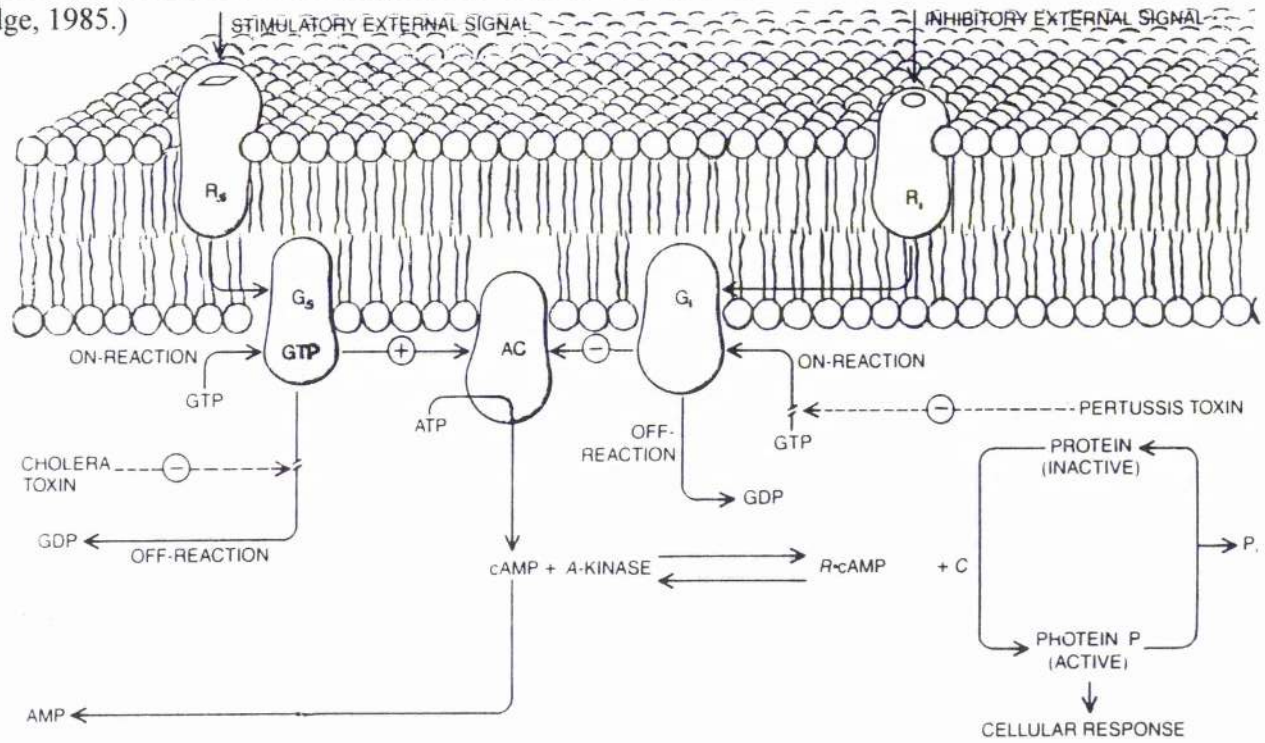

Figure 1.6. The hydrolysis of the membrane phospholipid PIP_2 by receptor activation. Binding of an agonist molecule to the receptor allows interaction with a G protein, which stimulates phospholipase C to hydrolyse PIP_2, resulting in the production of IP_3 and DAG. IP_3 stimulates the release of Ca^{2+} from intracellular stores, which can bind to calmodulin and activate Ca^{2+}/calmodulin dependent protein kinase leading to protein phosphorylation. DAG activates kinase-C and thus phosphorylates target proteins.
(Adapted from Berridge, 1985.)

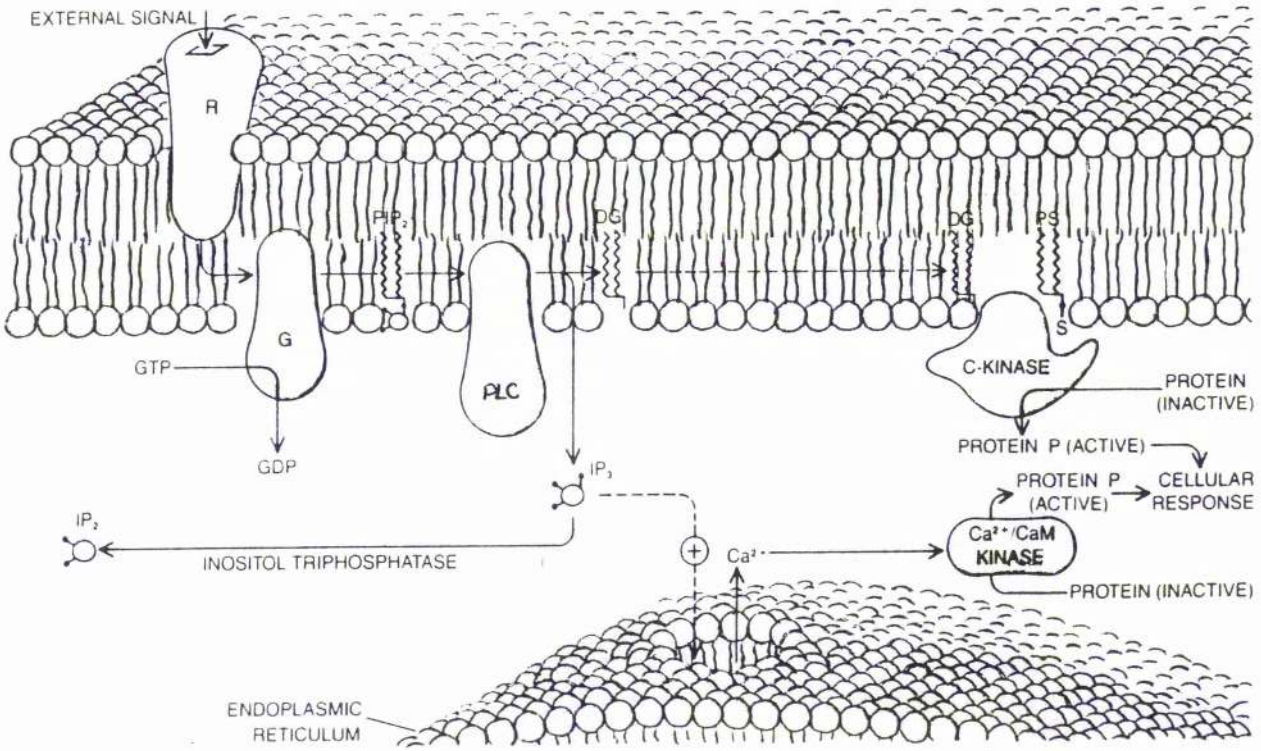

The first demonstration that IP_3 stimulated the release of Ca^{2+} from intracellular stores came from work on permeabilised rat pancreatic acinar cells (Streb et al, 1983), and it has since been verified for numerous cell types (Berridge & Irvine, 1984). The increase in Ca^{2+} is only transient because it is efficiently buffered and sequestered as described in Section 1.2.4., and the IP_3 is inactivated. There are two pathways by which IP_3 may be metabolised, and they are shown in Figure 1.7a: it can be converted to inositol by the sequential action of three phosphatases which hydrolyse it to 1,4-IP_2, then inositol 4-phosphate and finally to inositol. This is assumed to be an inactivation pathway because there is no evidence for a signalling role for IP_2 (Nahorski, 1988). Alternatively, it can be phosphorylated to inositol 1,3,4,5-tetrakisphosphate, which is progressively hydrolysed to inositol 1,3,4-trisphosphate, 3,4-IP_2, inositol 3-phosphate and inositol. The intermediaries produced by both of these pathways may also function as intracellular messengers (Nahorski, 1988).

The other product of PIP_2 hydrolysis, DAG, activates protein kinase C (PKC or C-kinase), a phospholipid- and Ca^{2+}-dependent enzyme (Takai et al, 1979), by increasing the affinity of the kinase for Ca^{2+} so that it can be activated at resting levels of Ca^{2+} (Kishimoto et al, 1980). Protein kinase C phosphorylates target proteins including ion channels, thus opening or closing them. DAG is only present for a few seconds, and can be phosphorylated to phosphatidate, which reacts with CTP (cytidine triphosphate) to form CDP-DAG. Phosphatidyl inositol is subsequently produced by the reaction of CDP-DAG and inositol (Figure 1.7b). DAG can also be hydrolysed to glycerol and its constituent fatty acids, releasing arachidonic acid which is used in the synthesis of lipid signalling molecules such as prostaglandins.

1.2.4. Calcium

Calcium is a major second messenger substance in cells (Berridge, 1985), and can enter across the external membrane, or can be released from intracellular

Figure 1.7a. Metabolic pathways of 1,4,5-IP_3. Inactivation of the second messenger occurs by hydrolysis to 1,4-IP_2, inositol 4-phosphate and inositol. Alternatively, 1,4,5-IP_3 can be phosphorylated to 1,3,4,5-IP_4, which is then hydrolysed via 1,3,4-IP_3, 3,4-IP_2 and inositol 3-phosphate to inositol.

Figure 1.7b. DAG is metabolised by phosphorylation to phosphatidate, which reacts with CTP to form CDP-DAG. This compound reacts with inositol to form phosphatidyl inositol, a precursor of PIP_2.
(From Stryer, 1988)

a

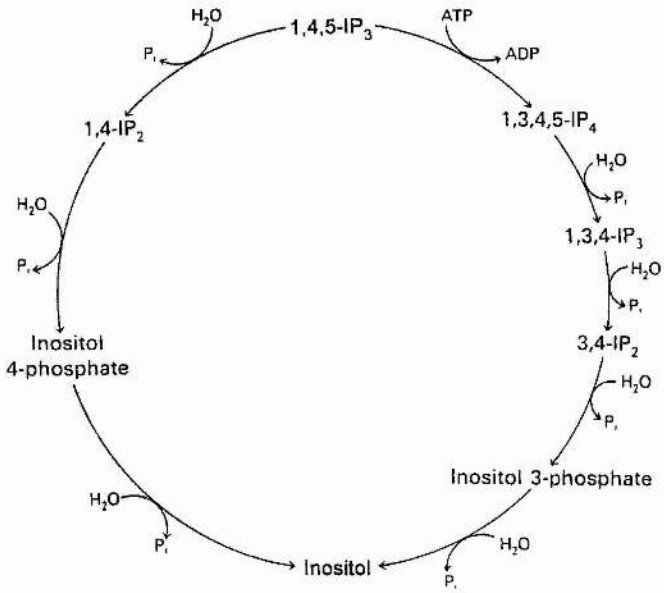

b

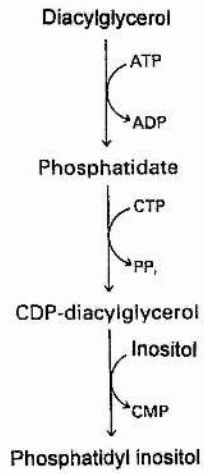

stores - primarily the smooth endoplasmic reticulum (SER) (or sarcoplasmic reticulum (SR) in muscle) - triggered by second messengers such as Ca^{2+} itself or IP_3 (see Section 1.2.3.). It has been suggested (Taylor & Marshall, 1992) that the two sources of Ca^{2+} are involved in distinct functions: Ca^{2+} entry into the cell through voltage sensitive ion channels in the surface membrane is probably the major supply of the ion for Ca^{2+}-dependent release of neurotransmitter from nerve terminals, although intracellular Ca^{2+} stores is also an important source of Ca^{2+} (Tsien & Tsien, 1990). In smooth muscle, Ca^{2+} release from intracellular stores plays a large part in contraction (Taylor & Marshall, 1992), whereas in cardiac and skeletal muscle contraction results from a combination of these two mechanisms: Ca^{2+} entry into the cell stimulates Ca^{2+} release from the SR (Taylor & Marshall, 1992).

Two groups of intracellular Ca^{2+}-release channels have been identified, those sensitive to ryanodine ('ryanodine receptors'; activated by low concentrations of ryanodine, and inhibited at higher concentrations) and those sensitive to IP_3 ('IP_3 receptors'). They are distinct entities which respond to different signals and are specialised for different roles (Ehrlich et al, 1994). Both channel types are present in intracellular membranes of numerous cell types, although they are not usually localised together in the same membrane (Hille, 1992). This would imply that the ryanodine-sensitive and IP_3-sensitive Ca^{2+} stores are distinct. Ryanodine receptors are the main Ca^{2+} release channels in skeletal muscle, whereas IP_3 receptors are more common in smooth muscle. Neurones have significant amounts of both receptor types (Hille, 1992).

There are several mechanisms by which ryanodine receptors are activated, but the main one is Ca^{2+}-induced Ca^{2+} release, in which an increase in free cytosolic Ca^{2+} triggers the release of more Ca^{2+} from the intracellular stores. The only known physiological substance which can activate IP_3 receptors is IP_3 itself (Ehrlich et al, 1994). Both channels are strongly modulated by cytosolic Ca^{2+}: at

low concentrations the channels can be opened by their appropriate activator, but at higher concentrations they are inhibited (Bezprozvanny et al, 1991). Supattapone et al (1988) found that Ca^{2+} inhibits binding of IP_3 to rat cerebellar membranes, but not to the purified receptors, which suggests the involvement of a Ca^{2+} binding protein which regulates the IP_3 receptor.

After release of Ca^{2+} from the intracellular stores, the stores must be refilled. Two mechanisms for this are (1) sequestration into intracellular stores by Ca^{2+} ATPase, a Ca^{2+} pump located in the membranes of Ca^{2+} storage organelles and (2) refilling from the external environment; the decrease in the Ca^{2+} content of the stores activates a class of surface membrane Ca^{2+} channels called Ca^{2+}-release-activated channels (CRAC), a mechanism which appears to involve at least one type of cytosolic factor (reviewed by Fasolato et al, 1994). It has also been suggested that the IP_3 receptor undergoes a conformational change so that it can interact with, and activate, a Ca^{2+} channel in the cell membrane (Irvine, 1990).

It is very important that the concentration of Ca^{2+} does not remain elevated for longer than necessary, and to this end there are highly efficient mechanisms by which the increased Ca^{2+} concentration is returned to that of rest (Blaustein, 1988). One mechanism is the buffering of Ca^{2+} by Ca^{2+}-binding proteins in the cytoplasm such as parvalbumin and vitamin D-dependent Ca^{2+}-binding protein; binding to these proteins renders Ca^{2+} inactive. This is a rapid process, but is likely to become saturated quickly. Ca^{2+} that is not bound can be sequestered into intracellular stores by Ca^{2+} ATPase, as described above. Ca^{2+} can alternatively be expelled from the cell by either a second type of Ca^{2+} ATPase, or the Na^{+}-Ca^{2+} exchanger. The latter extrudes one Ca^{2+} from the cell for the entry of three Na^{+}, and is driven by the Na^{+} electrochemical gradient rather than ATP.

The effects of Ca^{2+} can be mediated directly or through a Ca^{2+}-binding protein such as calmodulin, found in the cytoplasm of both vertebrate and invertebrate cells. The protein behaves as a multipurpose intracellular Ca^{2+}

receptor and mediates many Ca^{2+}-regulated processes. Four Ca^{2+} ions bind to one molecule of calmodulin to affect a change in its conformation, resulting in activation of the complex. One of the major targets of the Ca^{2+}/calmodulin complex is a group of kinases known as Ca^{2+}/calmodulin-dependent protein kinases, which phosphorylate specific amino acid residues of target proteins. A major consequence of an increase in the concentration of intracellular Ca^{2+} in neurones is the modulation of Ca^{2+}-dependent K^+ channels, which will be discussed in Section 1.3.1.4.

1.2.5. Crosstalk between signal transduction pathways

The adenylate cyclase and phospholipid pathways are not completely isolated, so they may interact. The products of PIP_2 hydrolysis can affect the activity of adenylate cyclase: the first demonstration of a synergistic relationship between protein kinase C and transmitter-activated adenylate cyclase stimulation was in rat pineal gland cells (Sugden et al, 1985), in which the addition of phorbol esters, or the DAG compound, OAG (1-oleoyl-2-acetylglycerol), resulted in the potentiation of cAMP production by isoprenaline. Yoshimasa et al (1987) showed that protein kinase C, stimulated by phorbol esters, could phosphorylate the catalytic subunit of adenylate cyclase of frog erythrocytes. Carbachol stimulated PIP_2 hydrolysis in Chinese hamster ovary (CHO) cells (Buck & Fraser, 1990) or A9 L fibroblasts (Felder et al, 1989) transfected with m_1 receptors which subsequently caused an increase in cAMP levels; the effect was proposed to be due to activation of adenylate cyclase by Ca^{2+} release from intracellular stores by IP_3 (Felder et al, 1989). A class of adenylate cyclase in mammalian brain (Brostrom et al, 1975; Cheung et al, 1975) and invertebrates (Abrams et al, 1991; Yovell et al, 1992) is Ca^{2+}/calmodulin-sensitive. cAMP production in SH-SY5Y human neuroblastoma cell lines was increased by both Ca^{2+} and protein kinase C (Jansson et al 1991), whereas in canine iris smooth muscle (Tachado et al, 1994) only Ca^{2+} appears to be involved.

cAMP has been found to modulate PIP_2 hydrolysis in several preparations. Akil & Fisher (1989) demonstrated that increasing intracellular levels of cAMP in SK-N-SH human neuroblastoma cell lines by stimulating adenylate cyclase activity or inhibiting phosphodiesterase activity resulted in a decrease in muscarinic agonist-stimulated phosphoinositide turnover. Similarly, glutamate-stimulated PIP_2 hydrolysis in rat brain astrocytes was inhibited by either the activation of adenylate cyclase or the addition of the membrane permeable cAMP analogue dibutyryl cAMP (Robertson et al, 1990). Conversely, muscarinic receptor-mediated stimulation of PIP_2 hydrolysis is enhanced by β adrenergic receptor-mediated stimulation of cAMP production in neuroepithelioma cells (Fisher et al, 1992).

1.3. MEMBRANE CURRENTS

The apparent inward current induced by activation of the α-BTX-resistant receptors on the first basalar motoneurone may be due to inhibition of an outward current or stimulation of an inward current. The experiments presented in this thesis were designed to investigate whether muscarinic receptor activation modulated either an outward K^+ current or an inward Ca^{2+} current. The following introductory section is an overview of K^+ and Ca^{2+} currents.

1.3.1. K^+ currents

K^+ channels have been found in almost every eukaryotic cell (Rudy, 1988). K^+ currents are hyperpolarising and thus play an important role in regulating the excitability of neurones. There are several types of K^+ channels and they have different kinetics, voltage dependency, pharmacology and single channel properties. However, the ionic selectivity of the channels is similar: $Tl^+ > K^+ > Rb^+ > NH_4^+$. Neurones must be capable of generating numerous patterns of activity, which may underlie the need for a diversity of K^+ channels. This diversity is not due to differences in cell types, because more than one K^+ current can be present in the same cell. In addition, different cells express similar K^+ currents, and may not express every type of K^+ channel.

Two general classes of K^+ channel are described here, and their characteristics are summarised in Table 1.3: voltage-dependent (delayed rectifier, A-current and inward rectifier) and Ca^{2+} dependent. The properties of individual types of K^+ channel can also be modulated by neurotransmitters. In the context of this thesis, the M-current, modulated by activation of muscarinic receptors is particularly relevant and is described below.

Table 1.3. Properties of K^+ channels

	Delayed rectifier	**A-current**	**Inward rectifier**	**Ca^{2+}-dependent: BK(Ca)**	**Ca^{2+}-dependent: SK(Ca)**	**M-current**
Activation threshold	positive to -50 to -20 mV	positive to -60 to -50 mV; inactivated at resting potential	Dependent on E_m and E_k	Dependent on $[Ca^{2+}]_i$	Dependent on $[Ca^{2+}]_i$	Positive to -60 mV
Inactivation	Slow	Rapid	Slow	Slow	Slow	Slow
Single channel conductance	15-20 pS	15-20 pS	Approximately 20 pS	150-250 pS	4-14 pS	7 to 19 pS
Voltage dependent	Yes	Yes	Yes	Yes	No	Yes
Ca^{2+} dependent	No	No	No	Yes (1 to 10 μM)	Yes (10 to 100 nM)	No
Channel blockers	TEA^+, Cs^+, Ba^{2+}, 4-AP, β & γ dendrotoxin, noxiustoxin	TEA^+, 4-AP, α & δ dendrotoxin	TEA^+ (variable), Cs^+, Ba^{2+}	TEA^+, Cs^+, Ba^{2+}, charybdotoxin, iberiotoxin, kaliotoxin	Cs^+, Ba^{2+}, apamin, charybdotoxin, scyllatoxin	Ba^{2+}
Physiological role	Action potential repolarisation	Regulation of firing rate; latency to first spike	Resting conductance; maintenance of long plateaux in action potentials; cardiac pacemaking	Fast AHP; action potential repolarisation; regulation of firing rate	Slow AHP; spike frequency adaptation	Regulation of neuronal excitability

1.3.1.1. Delayed rectifier

The voltage-dependent K^+ current of the squid giant axon first described by Hodgkin & Huxley (1952a,b,c) is known as a delayed rectifier ($I_{K(V)}$), because it is activated with a delay after a depolarising voltage step, and because current flows more readily in one direction, namely out of the cell. This name is still used to describe axon-like K^+ channels, although the majority of known K^+ channels also change the conductance of the membrane with a delay. The original work by Hodgkin & Huxley did not report inactivation of $I_{K(V)}$, although using longer depolarising pulses it has been shown that the delayed rectifier of the squid giant axon does inactivate over a period of several seconds (Ehrenstein & Gilbert, 1966). Similar observations have also been made in both molluscan neurones (Connor & Stevens, 1971a) and frog skeletal muscle (Adrian et al, 1968).

The activation threshold for the delayed rectifier varies between preparations, but tends to be between -50 and -20 mV (Rudy, 1988). The single channel conductance is between 15 and 20 pS (Rudy, 1988). When a depolarising voltage step is applied to a neurone under voltage clamp such that the delayed rectifier is activated, the conductance of the membrane increases sigmoidally and inactivates slowly. Upon repolarisation, the conductance decreases exponentially. The physiological role of $I_{K(V)}$ is to repolarise the membrane during the falling phase of the action potential, thus keeping the duration of the action potential brief.

The delayed rectifier is the main K^+ current in many cells, and is present in both invertebrate cells such as the squid giant axon, crab axons, *Aplysia* bag cell neurones and *Drosophila* muscle, and vertebrate cells including frog sciatic nerve, hippocampal neurones, cardiac muscle and skeletal muscle (reviewed by Rudy, 1988). There are two criteria used to distinguish it from other K^+ currents: first, the macroscopic current displays similar kinetics and voltage-dependency to the current described by Hodgkin & Huxley (1952a,b,c). The second criterion is one of exclusion: if a K^+ current is not an A-current and is not Ca^{2+}-sensitive, it is

classified as a delayed rectifier. This has therefore resulted in a class of delayed rectifiers with diverse kinetics, voltage-dependency and pharmacology.

Delayed rectifier K^+ channels can be blocked by a variety of drugs and toxins. Tetraethylammonium ions (TEA^+) are membrane impermeant and block delayed rectifier K^+ channels when applied either intra- or extracellularly (Hille, 1992), although the concentrations required vary. For example, 50 % block of $I_{K(V)}$ of frog node of Ranvier is achieved by 0·4 mM external TEA^+ (Hille, 1967), whereas 8 mM is required for the same effect in frog skeletal muscle (Stanfield, 1970a). Armstrong & Binstock (1965) found that 100 mM TEA^+ had no effect on the squid giant axon when applied externally, although Tasaki & Hagiwara (1957) had previously reported that intracellular perfusion of the ion blocked the K^+ channels of this preparation.

Delayed rectifier K^+ channels are also blocked by Cs^+ (Chandler & Meves, 1965; Bezanilla & Armstrong, 1972) and Ba^{2+} (Eaton & Brodwick, 1980; Armstrong et al, 1982). Armstrong and colleagues (1982) showed that the block by externally applied Ba^{2+} ions was voltage dependent, and could be decreased by holding the cell at a more positive holding potential, or by applying depolarising pulses. 4-Aminopyridine (4-AP) is a membrane permeable drug which is often used as a diagnostic agent for the A-current, although it also blocks delayed rectifier K^+ channels of squid giant axon at similar concentrations (Yeh et al, 1976; Meves & Pichon, 1977). In the basalar/coxal depressor motoneurone of the cockroach *Periplaneta* (Nightingale & Pitman, 1989), 4-AP and the related compound 3,4-DAP shifted the peak in the N-shaped I/V relationship to less positive potentials.

Toxins isolated from the venoms of snakes and scorpions have been found to block delayed rectifier channels. Dendrotoxin is isolated from the venom of the green mamba snake *Dendroapsis*, and blocks both the delayed rectifier (Bräu et al, 1990) and the A-current (Halliwell et al, 1986). Benishin et al (1988) obtained four polypeptide fractions from the venom (designated α, β, γ and δ), and showed

that the β and γ peptides blocked the delayed rectifier, whereas α and δ inhibited the A-current. The venom of the scorpion *Centruroides noxius* contains the toxin noxiustoxin, which blocks the delayed rectifier of the squid giant axon (Carbone et al, 1987). The mode of action of the toxin was dependent on the concentration applied: at concentrations less than 1·5 μM the block was voltage-independent, but was voltage-dependent at higher concentrations.

1.3.1.2. A-current

A transient outward K^+ current was first reported by Hagiwara et al (1961) in neurones of the mollusc *Onchidium*. It was further studied in *Anisodoris* neurones by Connor & Stevens (1971b), and *Helix* by Neher (1971), and was termed the A-current ($I_{K(A)}$) by Connor & Stevens. Their experiments showed that a transient current with fast activation and inactivation kinetics was evoked when the membrane was voltage clamped at a holding potential of approximately -100 mV and stepped to potentials close to the normal resting potential of -50 to -35 mV. The magnitude of the current increased when either the command potential was made more positive, or the holding potential was made more negative. The single channel conductance is between 15 and 20 pS (Rudy, 1988).

The greatest difference between the delayed rectifier and the A-current is in their kinetics: $I_{K(A)}$ shows extremely fast activation (5-20 ms) upon depolarisation of the cell membrane, and rapidly inactivates exponentially (50-150 ms) during steady-state depolarisation. The A-current also differs in the activation threshold: it is activated at more negative membrane potentials, typically between -50 and -60 mV. Thus it is activated over a range of membrane potentials more negative than the threshold for action potential generation. However, there are some preparations in which the threshold for activation is more positive, and lies between -25 and -40 mV (Salkoff & Wyman, 1983; Tachibana, 1983; Giles & van Ginneken, 1985). A possible explanation for this phenomenon is that the inward current in these cells is carried exclusively by

Ca^{2+}, and therefore activation of the Ca^{2+} current occurs at more positive potentials. Thus the action potential threshold will be more positive. In all cases, A channels open transiently when the cell is depolarised from hyperpolarised potentials, opposing the depolarisation of the membrane. However, the A-current rapidly inactivates and the neurone can fire an action potential. The hyperpolarisation following the action potential removes the inactivation of the channels, which can open transiently; the resulting outward current slows down the return of the membrane potential to the spike threshold and therefore increases the interspike interval. The A-current regulates the frequency of repetitive firing, and increases the latency to the first spike (Rudy, 1988).

The A-current usually occurs in cells with the delayed rectifier and other K^+ currents, and is present in many excitable cells including neurones of molluscs, crustaceans, insects, amphibians and mammals, and insect and mammalian muscles (see Rogawski, 1985; Rudy, 1988 for reviews).

The study of the A-current has been facilitated by the observation that in *Drosophila* the A-current appears earlier in development than either the delayed rectifier or the inward current (Salkoff & Wyman, 1981a). In a 72 h pupa, the A-current of the dorsal longitudinal flight muscle (dlm) is present and has a similar amplitude to that found in adult muscle fibres. The inward current appears at approximately 84 h and the delayed rectifier at 96 h, just prior to adult eclosion. Thus, the A-current can be investigated in a 72 h pupa without contamination by other currents. The results of this experiment initiated a detailed comparison (Salkoff & Wyman, 1981b) between wild-type flies and those expressing an X-linked mutation referred to as *Shaker*, so-called because under ether anaesthesia the legs of the fly shake. *Shaker* mutants of *Drosophila* have been central to the understanding of the A-current. Early experiments on the neuromuscular junction of larval *Shaker* mutants (Jan et al, 1977) showed that there was an increase in transmitter release due to a prolonged presynaptic Ca^{2+} conductance after stimulation of the nerve. The addition of 4-AP to a wild-type fly mimicked every

aspect of the *Shaker* phenotype: prolonged Ca^{2+} conductance, increased transmitter release and leg shaking. It was therefore suggested that the mutation affected a K^+ conductance. Salkoff & Wyman (1981b) studied various *Shaker* mutations in 72 h pupae and found that the mutations affected the kinetics of the A-current, and even whether it was present in the dlm muscle, thereby confirming the observations of Jan et al (1977) that *Shaker* mutations affect a K^+ conductance.

The pharmacology of the A-current is distinct from that of the delayed rectifier. It is less sensitive to TEA^+: Neher & Lux (1972) found that 50 % block of $I_{K(V)}$ of *Helix* neurones required between 5 and 12 mM TEA^+, whereas to reduce $I_{K(A)}$ by the same amount required between 20 and 80 mM. In neurones of *Tritonia*, Thompson (1977) demonstrated that 50 mM TEA^+ reduced the delayed rectifier by 50 %, but 100 mM was required to decrease the A-current by 50 %. Conversely, 2 mM 4-AP blocked $I_{K(A)}$, whereas the delayed rectifier was unaffected by 10 mM. Unlike the effect of TEA^+ on the delayed rectifier, the concentration of 4-AP required to block the A-current is similar throughout several phyla, which suggests that the molecular structure of the channel has been conserved (Rogawski, 1985).

1.3.1.3. Inward rectifier

Inward rectifier K^+ channels (K_{IR}) were first discovered in frog skeletal muscle by Katz (1949) and have since been found in skeletal and cardiac muscle, vertebrate and invertebrate neurones and the eggs of several animals (reviewed by Rudy, 1988). They have been most thoroughly described in frog skeletal muscle and the eggs of tunicates and starfish. There are two features of inward rectifier channels which are not shared by other K^+ channels. First, they open with a steep voltage-dependency upon hyperpolarisation: the currents evoked exhibit a large instantaneous inward current, which increases over a few hundred milliseconds to a steady state. Second, the voltage dependence of the channels depends on both

the membrane potential and the external K^+ concentration. Early experiments on starfish eggs (Hagiwara et al, 1976) suggested that the kinetics of the inward rectifier channels were dependent on the electrochemical gradient of K^+, that is, the difference between the membrane potential and the K^+ equilibrium potential (E_M-E_K). However, further work on starfish eggs (Hagiwara & Yoshii, 1979) and frog skeletal muscle (Leech & Stanfield, 1981) showed that the kinetics were unaffected by the intracellular K^+ concentration, and were thus only dependent on the membrane potential and external K^+ concentration.

Inward rectifiers can be divided into two groups based on the steepness of voltage gating (Hille, 1992); the mechanism of rectification appears to differ between the two groups. The first group of channels are steep inward rectifiers and includes those found in skeletal muscle, endothelial cells and eggs. The second group are mildly rectifying and are located in cardiac muscle. Patch clamp studies of guinea-pig ventricular myocytes suggested that mild rectification was due to a block of the open ion pore by intracellular Mg^{2+} (Matsuda et al, 1987; Vandenberg, 1987): in the absence of intracellular Mg^{2+}, the I/V relationships of the cells were linear. The involvement of Mg^{2+} in steep rectifiers differs between preparations: inwardly rectifying channels of frog and human skeletal muscle are Mg^{2+}-sensitive (Burton & Hutter, 1990), whereas those of endothelial cells are Mg^{2+}-insensitive (Silver & DeCoursey, 1990).

The blocking capabilities of extracellular TEA^+ on inward rectifiers is variable. The channels of frog skeletal muscle are sensitive to TEA^+ (Stanfield, 1970b; Standen & Stanfield, 1980), whereas those of starfish eggs (Hagiwara et al, 1976) and guinea-pig olfactory neurones (Constanti & Galvan, 1983) are not blocked by up to 100 mM TEA^+. Cs^+ and Ba^{2+} are more global channel blockers: external Cs^+ inhibits the inward rectifier current in starfish eggs (Hagiwara et al, 1976), frog skeletal muscle (Gay & Stanfield, 1977) and guinea-pig ventricular myocytes (Trube et al, 1981). Ba^{2+} added to the bathing solution blocks inward rectifier channels of starfish eggs (Hagiwara et al, 1978), frog skeletal muscle

(Standen & Stanfield, 1978) and guinea-pig ventricular myocytes (Trube et al, 1981).

The inward rectifier contributes to the resting conductance at the membrane potential in several cells (Stanfield, 1970b; Johns et al, 1987). In cardiac cells, the inward rectifier is a major determinant of the resting potential, and because it is inactivated with depolarisation, it also contributes to the long plateau phase of the action potential (Reuter, 1984). The long duration fertilisation action potential in eggs, which may last for several minutes (Hagiwara & Jaffe, 1979), is thought to be due to the presence of an inward rectifier.

There are two types of inward rectifier channels in the heart (Sakmann et al, 1983). Those in the sino-atrial and atrio-ventricular nodes are sensitive to ACh: release of the neurotransmitter upon parasympathetic stimulation activates the channels, resulting in an increase in K^+ conductance and thus a slowing of the heart rate. The muscarinic receptors are directly linked to the K^+ channels via a G protein, and no second messenger pathway is involved (Noma, 1986). Consequently, the channels are activated more slowly than a ligand-gated channel such as the nicotinic receptor, but more quickly than a second messenger-linked channel. The inward rectifier channels of the atrial and ventricular muscle cells are insensitive to ACh, and also exhibit different kinetics to the ACh-sensitive channels (Sakmann et al, 1983).

1.3.1.4. Ca^{2+}-dependent K^+ currents

The sustained outward current evoked in many neurones during a depolarising pulse comprises the voltage-dependent delayed rectifier and a Ca^{2+}-dependent K^+ current ($I_{K(Ca)}$). This latter class of currents is activated by an increase in the concentration of free Ca^{2+} in the cytoplasm of the cell. The first report of a Ca^{2+}-dependent K^+ current was in *Aplysia* neurones, when injection of intracellular Ca^{2+} increased the K^+ conductance of the cell (Meech, 1972). The voltage- and time-dependence of $I_{K(Ca)}$ will include the voltage- and time-

dependence of Ca^{2+} entry or release into the cytoplasm, although the $I_{BK(Ca)}$ current (described below) is voltage dependent at a constant intracellular free Ca^{2+} concentration. In the experiments of Meech (1972), when the cell was stepped from -50 mV to increasingly more positive potentials, the current-voltage (I/V) relationship was N-shaped, which is now accepted as a characteristic feature of Ca^{2+}-dependent K^+ currents. The amplitude of the total outward current increased to + 50 mV then began to decrease up to + 80 mV when it started to further increase. The N-shape was blocked in the presence of Ca^{2+}-free saline suggesting that it was due to an influx of Ca^{2+}. When these experiments were performed, the 'late calcium channel' of squid axons had recently been described (Baker et al, 1971), which mediated an inward current which was maximal at + 70 mV; Meech (1972) proposed that the similarity between the voltage dependence of the Ca^{2+} current in squid axons and the K^+ current of *Aplysia* was further evidence for the Ca^{2+}-dependence of the K^+ current. It is now clear that Ca^{2+}-dependent K^+ currents are a ubiquitous feature of cells (Rudy, 1988).

Patch clamp studies have shown that Ca^{2+}-dependent K^+ channels can be divided into two main subtypes depending on their conductance: high conductance (BK channel; BK_{Ca}; maxi-K channel) or small conductance (SK channel; SK_{Ca}; slow AHP K_{Ca}). The currents passing through these channels are referred to as $I_{BK(Ca)}$ (or I_C) and $I_{SK(Ca)}$ (or I_{AHP}) respectively. BK channels were originally found in cultured bovine chromaffin cells by Marty (1981), and have since been identified in rat skeletal muscle, rabbit sympathetic neurones and smooth muscle and toad smooth muscle (reviewed by Latorre et al, 1989). Patch clamp studies of *Helix* neurones uncovered a smaller Ca^{2+}-dependent K^+ conductance mediated by SK channels (Lux et al, 1981). SK channels are also located in rat skeletal muscle, mouse olfactory cells, human red blood cells and *Aplysia* neurones (reviewed by Latorre et al, 1989). In addition to conductance, these channels differ in their voltage dependence, Ca^{2+} sensitivity, kinetics and pharmacology.

BK channels are voltage dependent (Adams et al, 1982a) and behave in a similar manner to the delayed rectifier channels, activating with depolarisation. Unlike the delayed rectifier channels however, the probability of the channel opening is increased by a rise in intracellular Ca^{2+}. 1 to 10 μM intracellular free Ca^{2+} is required for channel activation. The single channel conductance of BK channels is between 150 and 250 pS (Hille, 1992). SK channels are voltage independent (Pennefather et al, 1985), and have a much lower conductance of 4 to 14 pS (Hille, 1992) and are activated by a lower Ca^{2+} concentration of 10 to 100 nM.

The two Ca^{2+}-dependent K^+ currents can be differentiated according to their sensitivities to drugs and toxins. The Ca^{2+}-dependent K^+ current of *Aplysia* neurones was shown to be comprised of two components: a large component which was blocked by 200 mM TEA^+, and a smaller one which was unaffected by 200 mM TEA^+ (Deitmer & Eckert, 1985). Patch clamp experiments on rabbit smooth muscle (Inoue et al, 1985) showed that the large conductance channel (BK) was blocked by 0·1-1 mM TEA^+, whereas the smaller conductance channel (SK) was insensitive to this concentration of TEA^+. Similarly, there are several toxins present in the venoms of certain scorpions which can be used to differentiate between the two channel types. Kaliotoxin has been isolated from the venom of *Androctonus mauretanicus mauretanicus* and blocks BK channels of *Helix* neurones and rabbit sympathetic ganglion cells (Crest et al, 1992). BK channels of bovine smooth muscle are also sensitive to iberiotoxin, a toxin present in the venom of *Buthus tamulus* (Galvez et al, 1990; Giangiacomo et al, 1992). Charybdotoxin and scyllatoxin (leiurotoxin I) are both present in the venom of *Leiurus quinquestriatus hebraeus*; the former blocks BK channels of rat skeletal muscle incorporated into planar lipid bilayers (Miller et al, 1985) and bullfrog sympathetic ganglion cells (Goh et al, 1992). However, this toxin is not as specific as was originally proposed because it also blocks SK channels of *Aplysia* neurones (Hermann & Erxleben, 1987) and bullfrog sympathetic ganglion cells (Goh et al,

1992), and also Ca^{2+}-independent, voltage dependent K^+ channels of rat brain synaptosomes (Schneider et al, 1989) and cultured rat dorsal root ganglion neurones (Schweitz et al, 1989). Scyllatoxin blocks SK channels (Goh et al, 1992). SK channels in bullfrog sympathetic neurones (Pennefather et al, 1985) and rat skeletal muscle (Blatz & Magleby, 1986) can be blocked by apamin, a fraction of the venom of the honey bee *Apis mellifera*. BK channels are insensitive to apamin.

Ca^{2+}-dependent K^+ channels can be blocked by Cs^+ applied to either side of the membrane (Yellen, 1984; Smart, 1987). Intracellular Ba^{2+} fails to activate Ca^{2+}-dependent K^+ channels (Connor, 1979), as well as directly blocking the ion pore from either side of the membrane (Vergara & Latorre, 1983; Smart, 1987).

Due to the requirement of Ca^{2+} for activation of $I_{K(Ca)}$, any drug which alters the availability of Ca^{2+} will indirectly affect $I_{K(Ca)}$. There are two ways that this can occur: sequestration of intracellular Ca^{2+}, and prevention of Ca^{2+} entry into the cell. Injection of Ca^{2+} chelators such as EGTA and BAPTA into a neurone will block or reduce the activation of $I_{K(Ca)}$ (Connor, 1979; Lancaster & Nicoll, 1987). Ca^{2+} channel blockers will be described in Section 1.3.2.

Following an action potential, the membrane is briefly hyperpolarised (afterhyperpolarisation, or AHP). In some neurones, the amplitude of the AHP increases as the number of evoked action potentials increases (Madison & Nicoll, 1984; Bourque et al, 1985). The AHP is due to the activation of both types of Ca^{2+}-dependent K^+ channels, which are in turn activated by the influx of Ca^{2+} during the action potential. The AHP can be divided into two components: the fast AHP and the slow AHP. The fast AHP lasts for 1 to 2 ms and is due to current flow through BK channels; it is only brief because the voltage-dependency of the current results in its inactivation at potentials close to the resting potential. $I_{BK(Ca)}$ contributes to the repolarisation of the neurone after an action potential (Adams et al, 1982a; Lancaster & Nicoll, 1987); the current hyperpolarises the membrane sufficiently to delay return to the action potential threshold and therefore regulates

the frequency of the first few spikes during a depolarisation (Lancaster & Nicoll, 1987). The slow AHP, on the other hand, is the result of current flow through SK channels. This current is also known as I_{AHP} and may be 50 to 1000 ms in duration. I_{AHP} is involved in spike frequency adaptation (Madison & Nicoll, 1984; Bourque et al, 1985): during a depolarising stimulus, action potentials are evoked at first, but the frequency decreases until the spikes cease, even though the depolarising stimulus continues. This is caused by the accumulating slow AHP, which increases steadily during the action potentials until it is large enough to prevent the neurone from reaching the spike threshold.

Certain molluscan neurones called 'burster' neurones generate endogenous bursts of action potentials separated by quiescent periods during which the membrane is hyperpolarised (reviewed by Meech, 1979; Benson & Adams, 1987). The interburst hyperpolarisation gives way to a slow depolarisation and another burst of action potentials. This rhythm is due to cyclical variations in the concentration of intracellular free Ca^{2+}, which has been demonstrated by measuring fluctuations in Ca^{2+} concentration with the fluorescent Ca^{2+}-sensitive dye Arsenazo III (Thomas & Gorman, 1977). During a train of action potentials, Ca^{2+} ions enter the cell and accumulate because the rate of entry is greater than the rate of buffering. The concentration of Ca^{2+} gradually rises until the threshold concentration for activation of $I_{K(Ca)}$ is reached and the membrane is hyperpolarised, thus inhibiting Ca^{2+} entry into the cell. The concentration of intracellular Ca^{2+} falls, decreasing $I_{K(Ca)}$ and allowing depolarisation leading to the next burst of action potentials.

Several types of cells possess a transient current activated by a rise in intracellular Ca^{2+} concentration. Bullfrog sympathetic ganglion neurones, for example, exhibit a transient current which is inhibited by either Ca^{2+} channel blockers or Ca^{2+}-free saline (MacDermott & Weight, 1982). The current could be blocked by external TEA^+ but was unaffected by 4-AP. Hippocampal neurones exhibit two transient outward currents (Zbicz & Weight, 1985). A fast transient

current (duration 15 to 20 ms) is 4-AP-insensitive and TEA^+-sensitive and is activated by Ca^{2+}. This current resembled the one described by MacDermott & Weight (1982). The slower, Ca^{2+}-independent transient current, similar to the A-current, can be blocked by 4-AP but is unaffected by TEA^+. Two transient currents have also been recorded in sheep cardiac Purkinje fibres (Boyett, 1981), one of which can be blocked by 4-AP, and the other which is Ca^{2+}-dependent and unaffected by 4-AP. Further support for the existence of two independent transient K^+ currents has come from the work of Salkoff (1983). The transient current in D*rosophila* flight muscle is composed of two currents, one of which is Ca^{2+}-sensitive. *Shaker* mutants, in which the Ca^{2+}-independent A-current is defective, have Ca^{2+}-dependent transient currents similar to those found in wild-type flies.

1.3.1.5. M current

The M-current (I_M) was first described by Brown & Adams (1980) in bullfrog sympathetic neurones, and is so-called because it is sensitive to muscarine. It is a non-inactivating, voltage-dependent K^+ current, and is activated at potentials positive to -60 mV in bullfrog sympathetic ganglion cells (Brown & Adams, 1980). It differs from the delayed rectifier conductance in having slower kinetics and a more negative activation threshold. Three single channel conductances - 7 pS, 12 pS and 19 pS - were found for M-channels of cultured rat dorsal root ganglion (DRG) cells (Selyanko et al, 1992), although it was not clear whether this reflected three substrates of the same channel or three different M-channels. In the presence of muscarinic agonists, the M-current is reduced (Brown & Adams, 1980). The physiological role of the M-current is to increase the excitability of the neurone upon synaptic excitation and thus increase the likelihood of action potential propagation. The M-current is classically studied by voltage clamping a cell more positive than the membrane potential and applying hyperpolarising pulses. The slow current relaxation following the hyperpolarisation represents the activation of the M-current.

Experiments on a variety of preparations have shown that the M-current is widespread throughout vertebrate excitable cells, including rat sympathetic neurones, hippocampal cells, human neocortical cells, spinal motoneurones, NG108-15 cells and toad smooth muscle (reviewed by Brown, 1988). There is no evidence for its occurrence in invertebrate cells. The M-current in bullfrog sympathetic neurones is insensitive to TEA^+ (10 mM) (Brown & Adams, 1980), although it can be blocked by Ba^{2+} in bullfrog sympathetic ganglion cells (Constanti et al, 1981) and NG108-15 mouse neuroblastoma x rat glioma hybrid cells (Brown & Higashida, 1988a).

The M-current is inhibited by other putative neurotransmitter substances. Luteinising hormone releasing hormone (LHRH) suppresses the current in bullfrog sympathetic ganglion neurones (Jan et al, 1979; Jones, 1987); substance P inhibits the current in toad smooth muscle (Sims et al, 1986) and guinea-pig sympathetic ganglion cells (Vanner et al, 1993); and bradykinin decreases the M-current in NG108-15 cells (Higashida & Brown, 1986; Brown & Higashida, 1988b) and rat neurosecretory PC12 cell lines (Villaroel et al, 1989).

It is likely that the inhibition of the M-current by agonists is mediated by a second messenger pathway, because the receptors involved, for example the muscarinic receptor, are G protein-linked. The involvement of a G protein has been demonstrated in rat sympathetic neurones (Marrion, 1987; Brown et al, 1989) by whole cell patch clamp experiments in which the inclusion of non-hydrolysable GTP analogues in the patch pipette suppressed I_M and prevented recovery from subsequent muscarine-induced inhibition. However, there is some debate as to the second messenger pathway that is subsequently activated. It is unlikely that cyclic nucleotides are involved because the addition of membrane permeable analogues of cAMP and cGMP have no effect in bullfrog sympathetic neurones (Adams et al, 1982b), rat sympathetic neurones (Brown et al, 1989) or NG108-15 cells (Robbins et al, 1993). Biochemical experiments have shown that muscarine and LHRH increased PI turnover in whole bullfrog sympathetic ganglia

(Pfaffinger et al, 1988). Ca^{2+} does not play a major role in M-current inhibition because intracellular injection of Ca^{2+} (Adams et al, 1982b), or exposure to a Ca^{2+} ionophore (Brown & Adams, 1987) did not inhibit the M-current. In rat hippocampal cells, injection of IP_3 inhibited the M-current, although loading the cells with BAPTA or EGTA did not prevent M-current suppression by carbachol. However, it blocked the AHP (Dutar & Nicoll, 1988a, b). This could suggest an action of IP_3 independent of Ca^{2+} mobilisation. Muscarinic agonists and LHRH induce Ca^{2+} transients in cells expressing M channels (Pfaffinger et al, 1988; Marrion et al, 1991), but this does not appear to be linked to M-current suppression: repeated application of agonist to bullfrog sympathetic neurones decreases the amplitude of the Ca^{2+} transient but has no effect on the magnitude of the M-current. Nevertheless, Ca^{2+} may have some modulatory role of the M-current as it has been demonstrated that a small increase in intracellular Ca^{2+} enhances the M-current, whereas a larger amount of Ca^{2+} inhibits it (Marrion et al, 1991). The experiments described above imply that the production of IP_3 and the subsequent mobilisation of Ca^{2+} has little effect on M-current inhibition. There is evidence to suggest that the other product of PIP_2 hydrolysis, DAG, may be involved. This comes from experiments in which stimulation of protein kinase C by phorbol esters inhibited the M-current (Brown & Adams, 1987; Brown et al, 1989; Schäfer et al, 1991; Marrion, 1994). Brown & Adams (1987) reported that the degree of M-current suppression by phorbol esters in bullfrog sympathetic neurones, however, was smaller than that produced by agonists, and that it developed more slowly. Moreover, although the M-current appears to be decreased by activation of protein kinase C, inhibitors of the enzyme do not prevent the inhibition of the M-current by agonists (Schäfer et al, 1991; Marrion, 1994). The M-current of rat hippocampal cells is unaffected by phorbol esters (Dutar & Nicoll, 1988a, b) and only slightly decreased in NG108-15 cells (Robbins et al, 1993). This suggests that there could be some tissue heterogeneity in the mechanism of M-current inhibition and a role for protein kinase C is far

from proven. The possibility exists that the M channels are directly modulated by a G protein without the activation of a second messenger pathway, in the same way as the ACh-sensitive inward rectifier channels of the heart, or that an as yet unidentified pathway is involved.

1.3.2. Ca^{2+} currents

Since the first demonstration of Ca^{2+} permeability in crustacean muscle fibres (Fatt & Katz, 1953), experiments have shown that voltage-dependent Ca^{2+} channels are a ubiquitous feature of all excitable cells, both vertebrate and invertebrate (reviewed by Hagiwara & Byerly, 1981). Because Ca^{2+} channels inactivate more slowly than Na^{+} channels, they can generate a more maintained inward current during prolonged depolarisations. An influx of Ca^{2+} across the cell membrane triggers the release of neurotransmitter from presynaptic terminals, controls bursting in rhythmically active cells and shapes the action potentials produced in muscle and neurones. Ca^{2+} ions are also a key requirement in the excitation-contraction coupling of muscle. In many invertebrate muscles - crustacean, insect and molluscan (reviewed by Hagiwara & Byerly, 1981) - Ca^{2+} carries the inward current of the action potential, unlike squid axon and frog skeletal muscle.

In biophysical studies of Ca^{2+} channels, Ca^{2+} ions are often replaced by Ba^{2+} because they carry current through Ca^{2+} channels and also block K^{+} channels, enabling currents through Ca^{2+} channels to be observed more readily. A feature of Ca^{2+} channels is Ca^{2+}-dependent inactivation, in which a rise in the concentration of intracellular free Ca^{2+} results in a decrease in the amplitude of the Ca^{2+} current (Brehm & Eckert, 1978; Tillotson, 1979). Substituting Ba^{2+} for Ca^{2+} decreases the inactivation of the Ca^{2+} current (Brehm & Eckert, 1978; Tillotson, 1979; Eckert & Tillotson, 1981). Evidently, although Ba^{2+} ions behave in a similar manner to Ca^{2+} in being able to pass through Ca^{2+} channels, they are relatively ineffective in stimulating the inactivation process.

All Ca^{2+} channels open upon depolarisation after a delay. However, Ca^{2+} channels differ in their kinetics, voltage dependency, ionic selectivity, single channel conductance and pharmacology. One method of classification is according to the voltage dependence of activation. Channels which are activated at membrane potentials positive to -50 mV are referred to as low voltage activated

(LVA) channels (Carbone & Swandulla, 1989). LVA channels inactivate rapidly; inactivation is complete within 100 ms, and is voltage-dependent and Ca^{2+}-independent (Carbone & Lux, 1988). High voltage activated (HVA) channels are activated at membrane potentials positive to -10 mV (Carbone & Swandulla, 1989). Inactivation is less pronounced, and is both voltage- and Ca^{2+}-dependent (Brown et al, 1981; Gutnick et al, 1989).

An alternative classification scheme divides Ca^{2+} channels into L-, T-, N- and P-type channels; the properties of these Ca^{2+} channels are summarised in Table 1.4. A fifth type of channel, named Q-type, has been identified using molecular biology techniques (reviewed by Zhang et al, 1993; Tsien et al, 1995). Q-type Ca^{2+} channels are expressed predominantly in the nerve terminals of the mammalian CNS.

1.3.2.1. L-type Ca^{2+} channels

L-type channels (*l*arge conductance (25 pS), *l*ong lasting) are slowly inactivating HVA channels which are activated by depolarising pulses to potentials positive to -10 mV (Nowycky et al, 1985). They are not inactivated at holding potentials as positive as 0 mV. The current carried by Ba^{2+} through L-type channels is larger than that carried by Ca^{2+} (Fox et al, 1987). They are the most extensively studied Ca^{2+} channel, and are widely distributed, particularly in cardiac, smooth and skeletal muscle. In cardiac cells, L-type Ca^{2+} channels are involved in both the propagation of electrical impulses and in the initiation of contraction; in smooth muscle, they are involved in tension development, and in skeletal muscle they are necessary for excitation-contraction coupling (Hofmann et al, 1994). L-type channels are not involved in neurotransmitter release (Hofmann et al, 1994).

A group of organic drugs which have been used as diagnostic agents for L-type channels are dihydropyridines (DHPs). These include the channel blockers nifedipine and nitrendipine, and the channel activator Bay K 8644. L-type

Table 1.4. Properties of Ca^{2+} channels

	LVA		HVA	
	T-type	**L-type**	**N-type**	**P-type**
Activation threshold	Positive to -50 mV	Positive to -10 mV	Positive to -20 mV	Positive to -15 mV
Inactivation:	Rapid: voltage-dependent, Ca^{2+} independent; inactivated at holding potentials positive to -80 mV	Slow: voltage- and Ca^{2+} dependent	Rapid: voltage- and Ca^{2+} dependent; inactivated at holding potentials positive to -80 mV	Slow; voltage- and Ca^{2+} dependent
Single channel conductance	8 pS	25 pS	13 pS	10-12 pS
Ba^{2+} permeability	Equal to Ca^{2+}	Greater than Ca^{2+}	Greater than Ca^{2+}	Greater than Ca^{2+}
Channel blockers	μM Ni^{2+} Flunarizine U-92032	DHPs phenylalkylamines benzothiazepines μM Cd^{2+}	ω conotoxin μM Cd^{2+}	Funnel web spider toxin
Physiological role	Burst formation	Muscle contraction	Neurotransmitter release	Neurotransmitter release

channels are also sensitive to phenylalkylamines (e.g. verapamil and D600) and benzothiazepines (e.g. diltiazem) (reviewed by Spedding & Paoletti, 1992). All Ca^{2+} channels are blocked by millimolar concentrations of polyvalent metal ions, such as the transition metals (Ni^{2+}, Cd^{2+}, Co^{2+} and Mn^{2+}) and La^{3+}. However, when the metal ions are applied at micromolar concentrations, there is some selectivity between channel types: L- and N-type channels are blocked by 20-50 μM Cd^{2+}, whereas T-type channels are unaffected (Fox et al, 1987).

1.3.2.2. T-type Ca^{2+} channels

T-type channels (*t*ransient, *t*iny conductance: 8 pS) are LVA channels, and open transiently upon depolarising pulses from a holding potential more negative than -100 mV to command potentials positive to -50 mV (Nowycky et al, 1985). They are inactivated at holding potentials more positive than -80 mV. The Ba^{2+} current through T-type channels is the same amplitude as the Ca^{2+} current (Nilius et al, 1985; Fox et al, 1987). T-type channels are located in a number of tissues and are concentrated in the sino-atrial node (Hagiwara et al, 1988) and ventricles (Nilius et al, 1985) of the heart, as well as in smooth muscle (Loirand et al, 1989) and neurones (Nowycky et al, 1985), and have been proposed to be involved in burst formation (Hagiwara et al, 1988; Tsien et al, 1988; Huguenard & Prince, 1992).

There are no highly selective T-type channel blockers. Micromolar Ni^{2+} blocks T-type channels but is less effective at L- and N-type channels (Fox et al 1987). Flunarizine has also been found to block T-type channels in rat hippocampal neurones (Takahashi & Akaike, 1991), although it also blocks N-type channels in the same tissue (Tytgat et al, 1991). U-92032 has been suggested as a possible specific T-type channel blocker as it blocked T-type channels in guinea-pig atrial cells without affecting L-type channels (Xu & Lee, 1994).

1.3.2.3. N-type Ca^{2+} channels

HVA channels which are inactivated at holding potentials positive to -100 mV and require larger depolarising pulses for activation than T-type channels (activation threshold -20 mV) are termed N-type Ca^{2+} channels (*n*either T- nor L-type; *n*euronal) (Nowycky et al, 1985). N-type channels are similar to L-type channels in that they are activated by large depolarisations, but also resemble T-type channels because they are inactivated at holding potentials more negative than -80 mV and rapidly inactivate during a depolarising pulse (Nowycky et al, 1985). However, the single channel conductance of N-type channels (13 pS) is larger than the conductance of T-type channels. Ba^{2+} ions carry more charge through N-type channels than Ca^{2+} (Fox et al, 1987). N-type channels appear to be almost completely restricted to neurones and play a major role in neurotransmitter release (Tsien et al, 1988).

N-type Ca^{2+} channels can be identified due to their sensitivity to a toxin from the venom of the marine snail *Conus geographus* called ω-conotoxin GVIA (CTX); there are reports of this toxin also blocking L-type Ca^{2+} channels of sympathetic neurones (Fox et al, 1987; Hirning et al, 1988), but N-type channels can be distinguished by their insensitivity to DHPs.

1.3.2.4. P-type Ca^{2+} channels

The existence of a fourth, P-type (*P*urkinje cell), HVA channel in guinea-pig cerebellar Purkinje cells and squid giant synapses was proposed by Llinás et al (1989) on the basis that the channels were insensitive to agents that block L-and N-type channels, but could be blocked by venom from the funnel web spider, *Agelenopsis aperta*, called FTX (Llinás et al, 1989). P-type channels are activated at potentials positive to -15 mV (Uchitel & Protti, 1994), and have a single channel conductance of 10 to 12 pS (Spedding & Paoletti, 1992). The current carried by Ba^{2+} through P-type channels is larger than that carried by Ca^{2+} (Uchitel & Protti, 1994).

Polyclonal antibody studies have shown that P-type channels are distributed widely throughout the mammalian CNS, for example in the dendrites and axon terminals of Purkinje cells, and in the hippocampus, neocortex, olfactory bulb, thalamus and medulla (Llinás et al, 1992). The original work of Llinás and colleagues (Llinás et al, 1989) demonstrated that neurotransmitter release from squid axons was mediated by these channels, and it is now thought that they play a large part in neurotransmitter release throughout the CNS and peripheral nervous system (Uchitel & Protti, 1994).

1.4. LOCUST FLIGHT

The experiments described in this thesis were performed on the first basalar motoneurone of the locust mesothoracic ganglion. This motoneurone receives excitatory input from the forewing stretch receptor, and innervates one of the principal wing depressor muscles. To enable the reader to put the current work into a neuroethological context, the remainder of this introductory section is a brief overview of locust flight and the effect of sensory input from the wing hinge stretch receptors on the motor rhythm.

The locust possesses two pairs of wings: the forewings are attached to the mesothoracic segment, and the hindwings to the metathoracic segment. Each thoracic segment contains all the muscles and motoneurones involved in generating the movement of the wings in that segment. During free flight, the wingbeat frequency is approximately 23 Hz (Baker et al, 1981). A detailed study of the mechanics of the flying locust was carried out in the early 1960s by Wilson & Weis-Fogh (1962). Throughout the flight cycle, the wings are rotated so that the leading edge cuts through the air: during the downstroke the wing is pronated (leading edge held downwards), and during the upstroke it is supinated (leading edge upwards). Lift and thrust are produced mainly during the downstroke, and are maximal halfway through the downstroke.

Supination of the wing is caused simply by passive elastic forces and is not under muscular control (Wilson & Weis-Fogh, 1962); the muscles responsible for the upstroke of the wing are purely elevators. However, three of the wing depressor muscles - the first basalar and second basalar muscles, and the subalar muscle - control pronation of the wing during the downstroke. The subalar muscle produces supination of the wing during the downstroke, and counteracts the pronation caused by the two basalar muscles; it is not involved in supination of the wing during the upstroke. It also controls the wing twist imposed by changes in the orientation of the body during flight (Wilson & Weis-Fogh, 1962).

Flight muscles can be divided into three main groups: dorso-ventral elevators, dorsal longitudinal depressors and dorso-ventral depressors. The latter group includes the basalar and the subalar muscles, and are responsible for producing the powerful downstroke (Wilson & Weis-Fogh, 1962).

There are forty excitatory motoneurones located in the mesothoracic ganglion of the locust that are involved in flight (Bentley, 1970). The axons of the motoneurones exit the ganglion through ipsilateral nerve roots; the somata of motoneurones whose axons exit through the same nerve root are grouped together. In addition, the somata of motoneurones which innervate the same muscle are grouped together. The position of a soma in the ganglion reflects the approximate position in the thorax of the muscle which it innervates: somata located in the anterior of the ganglion generally innervate muscles in the anterior region of the thorax, those in the posterior of the ganglion drive muscles in the posterior of the thorax, those on the midline drive the midline muscles and the more lateral somata innervate more lateral muscles (Bentley, 1970).

The locust flight system was one of the first in which it was demonstrated that sensory feedback was unnecessary for generating the basic rhythm underlying a behaviour (Wilson, 1961). However, although the rhythmic activity was present, the wingbeat frequency was reduced by approximately 50 %, implying that sensory input is necessary to produce normal flight. An important source of such information is the wing hinge stretch receptor (Gettrup, 1962), located at the base of each wing. The stretch receptor sensory neurones exhibit extensive arborisation in the ipsilateral halves of the thoracic ganglia (Burrows, 1975; Altman & Tyrer, 1977). The forewing stretch receptor branches in the mesothoracic ganglion and extends into both the prothoracic and metathoracic ganglia; the hindwing stretch receptor branches in the metathoracic ganglion and sends a process into the mesothoracic ganglion. Both send fine axons into the abdominal ganglia (Altman & Tyrer, 1977).

The original work by Gettrup (1962) demonstrated that the stretch receptor responds to elevation of the wing with a train of action potentials, the intensity of which was dependent on the extent of wing elevation. When the upward movement ceased, the stretch receptor slowly adapted to a tonic frequency corresponding to the position of the wing. The activity of the neurone halted when the wing was lowered. If the stretch receptor was destroyed, the flight rhythm was drastically reduced, which suggested that the stretch receptors were part of a peripheral feedback system which played an important part in the control of the flight rhythm.

Experiments to try to elucidate the function of the stretch receptors suggested that they provided a tonic influence to increase the average flight frequency (Wilson & Gettrup, 1963). This conclusion was reached on the observation that stimulation of the stretch receptors did not influence the flight rhythm on a cycle by cycle basis; rather stimulation of the stretch receptors led to a slow increase in the flight frequency. Several years later, it was demonstrated that manually moving a wing up and down could reset the flight rhythm within a few wingbeats if the stimulating frequency was close to that of the previous rhythm (Wendler, 1974). A detailed study of the connections made between the stretch receptor and flight motoneurones of the locust was carried out by Burrows (1975). He found that an action potential in the forewing stretch receptor evoked an epsp in the ipsilateral mesothoracic depressor motoneurones (including the first basalar motoneurone) and an ipsp in the elevator motoneurones, and proposed that the excitatory connections were monosynaptic due to the short latency (the latency of the epsp was 1 ms, whereas that of the ipsp was 4-6 ms). The hindwing stretch receptor projected onto the metathoracic ganglion motoneurones in a similar manner. There were no connections of either stretch receptor with contralateral motoneurones, although interganglionic connections did exist. Thus the stretch receptors and flight motoneurones form a resistance reflex, in which elevation of

the wing excites the stretch receptor, which inhibits the elevator motoneurones and excites the depressor motoneurones, thereby reinforcing the wing downstroke.

The work of Wendler (1974) and Burrows (1975) described above cast some doubt on the theory of Wilson & Gettrup (1963) that the stretch receptors provided only a tonic influence on the flight rhythm. The experiments performed by Pearson and colleagues (Pearson et al, 1983; Reye & Pearson, 1987) proved conclusively that this was not the case and the stretch receptors are indeed involved in flight rhythm generation on a cycle by cycle basis. If the stretch receptor neurone was stimulated close to the onset of depressor motoneurone activity, the flight rhythm could be reset; however, there was no effect if the stimulus was presented in the period between the bursts. The flight rhythm could be entrained if the stretch receptor was stimulated at a constant rate close to the wingbeat frequency. In addition, if the stretch receptor was stimulated at the same time as the depressor motoneurones were spiking, the flight rhythm frequency increased and the period of flight activity was prolonged; thus the influence exerted upon the flight central pattern generator is phase-dependent.

The interneurones involved in flight rhythm generation are located in the three thoracic ganglia and the first three abdominal ganglia, which are fused with the metathoracic ganglion (Robertson & Pearson, 1983). Rather than the forewings and hindwings being under the control of separate rhythm generators, the interneurones all form one pattern generator. It has been proposed that the flight pattern is produced by the oscillatory properties of the circuit rather than due to endogenously oscillating neurones: there is evidence that the circuitry between two interneurones, 301 and 501, comprises delayed excitation and feedback inhibition (Robertson & Pearson, 1985) and is capable of producing oscillatory activity. Recent experiments have shown, however, that at least some flight interneurones have the ability to generate plateau potentials in the presence of octopamine (Ramirez & Pearson, 1991a, b). The connectivity between the interneurones in the pattern generator and other neurones is complex; for example,

interneurone 511 is involved in elevation of the wing, and in addition to inhibiting depressor motoneurones, it also inhibits excitatory premotor interneurones to depressor motoneurones and disinhibits elevator motoneurones (Robertson, 1986).

1.5. THESIS IN CONTEXT

A major reason for the study of insects as a group is that they are the most successful group of animals in the world: there are more species in the class Insecta than the rest of the Animal Kingdom put together. Insects are essentially terrestrial animals and occupy every environmental niche on land, but they are also found in aquatic environments. Insects were the first animals to develop flight, and this feature has contributed greatly to their present day success, enabling them to escape predators, and find food and better environmental conditions.

Many studies of insects are directed to their control: although many insects are useful to man in that they pollinate important food crops, they are also highly destructive, and attack crops, forests and timber buildings, causing social and economic hardship. However, because of their simplicity compared to higher animals, insects can also be used to study fundamental physiological principles. In addition, insects are a phylogenetically ancient class of animal, and by examining their physiology, a comparison can be made with higher animals to investigate how the latter have evolved.

There are several advantages to the use of insects in neurobiology research. The main advantage is that the nervous system is relatively simple, containing large neurones which are easily identifiable and accessible for microelectrode studies. Insects are also ideal for the study of neural bases of behaviour such as flight and walking, because the neurones involved can be uniquely identified and their roles in the behaviour examined.

Information on cholinergic receptors with muscarinic properties in the insect CNS is sparse. Although the existence of muscarinic ligand binding sites in the insect CNS has been known about for almost two decades, electrophysiological evidence for functional postsynaptic 'muscarinic' receptors was not provided until several years later. Furthermore, a physiological role for such receptors has only been suggested in the last few years. The effects of

muscarinic receptor activation are more complex and subtle than those of nicotinic receptor activation, which has made the effects more elusive, but renders them potentially extremely interesting. The work described here was therefore carried out to investigate the pharmacology and function of a population of 'muscarinic' receptors on an identified motoneurone of the locust, *Schistocerca gregaria*. The soma of this motoneurone provides a readily accessible and identifiable preparation to investigate these receptors. The motoneurone innervates a major flight muscle, and therefore the receptors could be involved in long-term cholinergic modulation of the flight rhythm.

The aims of this thesis were:

1. to examine the pharmacology of a population of α-bungarotoxin-resistant cholinergic receptors on the first basalar motoneurone of the locust, *Schistocerca gregaria*, both in current- and voltage-clamp,
2. to investigate the mechanism by which receptor activation results in the production of a current,
3. to determine the ionic basis of the evoked current, and
4. to identify the possible physiological role of these receptors in the locust CNS.

CHAPTER 2

Materials and Methods

2. MATERIALS AND METHODS

2.1. ANIMALS: MAINTENANCE AND DISSECTION

Male *Schistocerca gregaria* were obtained from a laboratory colony provided with a diet of fresh barley shoots and bran. When necessary the colony was supplemented with animals from Blades Biological (Kent). Only males were used for experiments to ensure that the colony was maintained and to avoid any effects of sexual dimorphism.

The animals were killed by decapitation and pinned ventral surface upwards on a Sylgard dish. The cuticle covering the thorax was removed, revealing the three thoracic ganglia below. They were dissected out into normal locust saline (see Appendix I). Dissections were carried out under a Nikon binocular microscope (magnification 8X - 45X).

The nerve cord was attached to a small Perspex preparation slide (10 x 19 mm; see Figure 2.1) using two small silicone elastic bands, with the mesothoracic ganglion, ventral surface uppermost, positioned over the Araldite ridge of the slide. A drop of 4 % Methylene Blue was applied with a fine hypodermic needle to the surface of the mesothoracic ganglion in order to visualise the neural sheath before it was mechanically removed with a pair of sharpened watchmakers' forceps. The slide was immediately placed in the saline-filled Perspex experimental chamber.

One set of experiments was conducted on isolated cell bodies; for this, the axon was severed close to the cell body with a pair of fine scissors (Fine Science Tools; U.K. agents Interfocus Ltd., Withersfield, Suffolk).

2.2. ELECTROPHYSIOLOGY

2.2.1. Experimental Chamber

The experimental chamber was constructed from a block of Perspex (81 x 25 x 36 mm) and had a volume of 2.5 ml (see Figure 2.2). Pure oxygen (BOC)

Figure 2.1. The preparation slide showing the front (A) and side (B) views. The nerve cord was positioned on the slide in such a way that the mesothoracic ganglion lay on the Araldite ridge. Silicone elastic bands were used to secure the nerve cord in position. (Figure adapted from Nightingale, 1988).

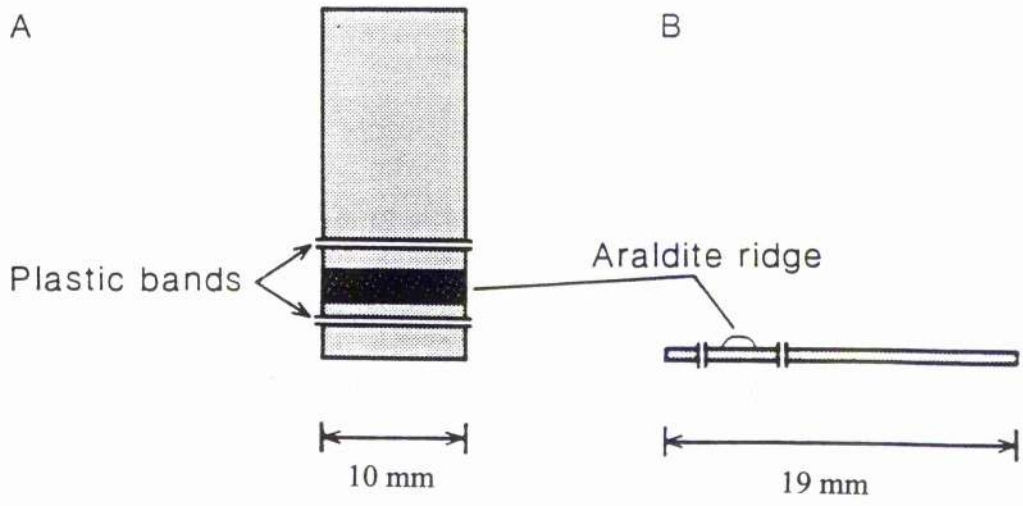

Figure 2.2. The experimental chamber showing the left (A), front (B) and right (C) side views. The areas containing saline are shown with 'stippling'. Saline enters the right hand compartment under gravity and is circulated throughout the chamber by means of bubbling oxygen into the right hand compartment. The arrow shows the direction of circulation. The site of addition of pharmacological agents is shown by the asterisks in (B) and (C). (Figure adapted from Nightingale, 1988).

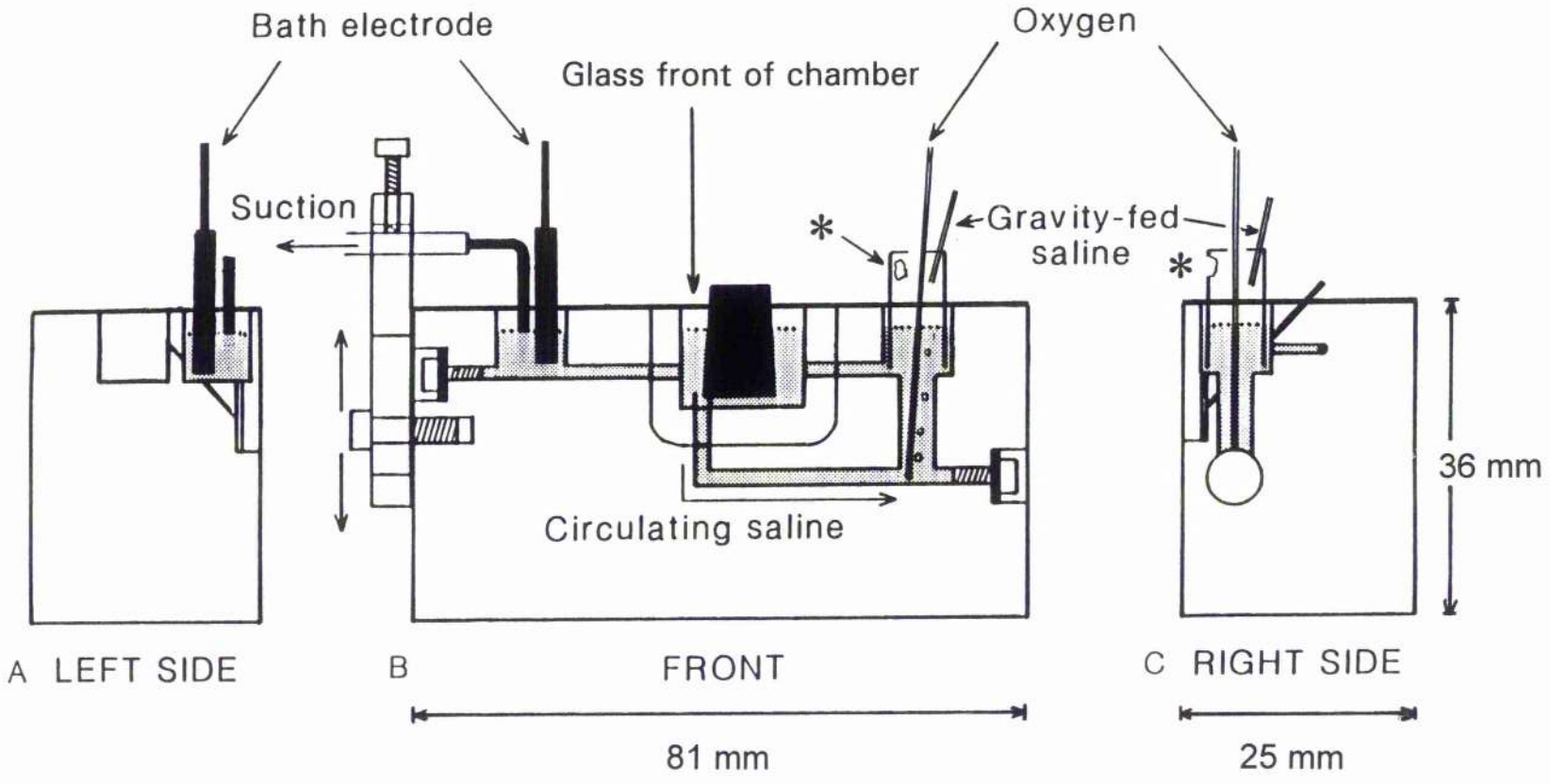
Bath electrode
Oxygen
Glass front of chamber
Suction
Gravity-fed saline
Circulating saline
36 mm
A LEFT SIDE
B FRONT
C RIGHT SIDE
81 mm
25 mm

was bubbled through a narrow tube into the right hand compartment; this maintained the viability of the preparation and circulated the saline in an anticlockwise direction. Saline was added to this compartment, and the bath volume was kept constant by continuous surface suction from the left hand compartment.

The bath electrodes were positioned in the left hand compartment of the chamber. In the majority of experiments, a flat tip probe containing a silver-silver chloride amalgam (Clark Electromedical Instruments) was used. In the remaining experiments, the electrodes were made from 1 mm silver wire, hammered flat (2 to 3 mm wide) to increase the conducting surface area. They were electrolytically coated with chloride using 1 M potassium chloride and a 9 V battery. This prevented electrical polarisation of the electrodes and hence allowed the recording of stable potentials.

All drugs were applied in a single aliquot (25μl) to the right hand compartment of the experimental chamber, and concentrations referred to in the text are final bath concentrations. Drugs were dissolved in normal saline. Drugs used are listed in Appendix II.

2.2.2. Illumination

A laboratory-built lamp (12 V, 55 W halogen bulb) was positioned outside the Faraday cage so that the light reflected off a mirror inside the cage. The beam was focused onto the preparation by a convex lens which could be moved in two planes. A Nikon binocular microscope could be swung in front of the experimental chamber and the illuminated preparation viewed horizontally through the glass front of the chamber at magnifications between 16X and 80X.

2.2.3. Intracellular Recording

2.2.3.1. Microelectrodes

Microelectrodes were drawn from thick-walled filament glass (Clark Electromedical Instruments) (internal diameter 0.86 mm) using either a Narishige type puller or a Kopf Vertical Pipette type puller. For the majority of experiments, the microelectrodes were filled routinely with 2 M potassium acetate (KAc), and had a resistance of 15 to 20 MΩ. When the neurone was to be injected with Lucifer Yellow after the experiment (see Section 2.5 for protocol), the tip was filled with 2.5 % Lucifer Yellow (made up in 1.5 M lithium acetate) and the shaft filled with 1 M lithium chloride. The resistance was 20 to 25 MΩ. Some experiments required that BAPTA be injected into the cell: the tip was filled with 100 mM BAPTA and the shaft with 2 M KAc. For other experiments in which K^+ channels were blocked, microelectrodes were filled with either 1 or 2 M CsCl. The microelectrodes were positioned in the bath using a pair of Prior micromanipulators fitted with reduction drives in two orthogonal planes. The recording microelectrode was connected to an amplifier headstage via a screened cable connected to an earth point on the base-plate. The headstage was attached outside the Faraday cage to a laboratory-made intracellular recording amplifier/bridge system.

2.2.3.2. Impalement

The recording microelectrode was lowered onto the surface of the cell until a slight depression was observed in the cell surface, and a small deflection was seen in the oscilloscope signal. A succession of approximately 100 nA, 30 ms hyperpolarising current pulses were applied to the microelectrode to facilitate impalement. To impale the cell with a second microelectrode, hyperpolarising current pulses (approximately 150 nA, 10 ms) were applied to this microelectrode while monitoring the membrane potential with the first microelectrode.

Penetration was marked by a large hyperpolarisation of the cell caused by the current pulse.

2.2.3.3. Pressure application

Thin-walled filament glass (internal diameter 1 mm) was used to make the agonist-containing microelectrodes for the pressure-application experiments. The pressure-microelectrode was filled with a solution of 10^{-2} M acetylcholine containing 0.02 % fast green to visualise the agonist when it was applied to the cell. To facilitate the expulsion of the agonist, the tip of the microelectrode was broken off by carefully touching the specimen slide. A 'puff' of agonist, 200 to 300 ms in duration was applied to the cell body of the motoneurone once every two minutes, using a garden spray unit (Killaspray Courier 8) to generate a pressure of 20 psi. Pressure pulses were applied using a Picospritzer II (General Valve Corporation) driven by a Grass S44 stimulator (100 ms, 15 V) through a laboratory-made relay switch. A block diagram for this experiment is shown in Appendix III.

2.2.3.4. Input resistance

This experiment was carried out in two-microelectrode current clamp, and the block diagram is shown in Appendix IV. An earthed brass shield was positioned between the recording and current microelectrodes prior to impalement to reduce capacitative coupling. The input resistance of the neurone was measured by injecting current pulses into the cell with one microelectrode of sufficient magnitude to hyperpolarise it by 10 mV (500 ms pulses) The amplitude of the applied current was measured by a current monitor and displayed on the second oscilloscope channel. Current pulses were applied by a Grass S44 stimulator, through a Grass stimulus isolation unit (SIU) and an amplifier/bridge.

The input resistance is calculated from Ohm's Law as follows:

$$\text{input resistance (M}\Omega\text{)} = \frac{\text{voltage deflection (V)}}{\text{applied current (A)}} = \frac{\text{membrane potential change (V)}}{\text{applied current (A)}}$$

2.2.3.5. Spike threshold

A block diagram representing the equipment used in this experiment is illustrated in Appendix V. A Grass S44 stimulator and a Servomex Waveform Generator (Type L.F. 141) were used to apply a ramp depolarisation to the neurone in two-microelectrode current clamp, and the membrane potential at which one or more axonal action potentials were evoked was measured. The current was measured by a current monitor and displayed on the second oscilloscope channel. This was repeated four times before and during the application of agonist, and after washing the drug off to obtain a mean value.

2.2.3.6. Voltage clamp

The current microelectrode was connected to a second amplifier headstage by a driven shield cable to reduce capacitance in the cable. The output from the voltage amplifier was fed directly to the (laboratory-made) voltage-clamp amplifier, and the output from the voltage-clamp amplifier was fed to the current microelectrode. A switch on the second amplifier (record/stimulate) converted the circuit from 'current clamp' to 'voltage clamp'. Command potentials were generated by a Grass S44 stimulator, through a Grass stimulus isolation unit (SIU) into the voltage-clamp amplifier. After switching the circuit to 'voltage clamp', the gain of the voltage clamp amplifier was increased so that the command potential was rapidly attained and maintained throughout the voltage step. Current was measured using a current monitor and displayed on the second oscilloscope channel. The block diagram is shown in Appendix VI.

2.2.4. DATA CAPTURE AND GRAPHS

Both current and voltage responses were displayed on a Tektronix 5103N Dual Beam Storage Oscilloscope. For the pressure application and input resistance experiments, the membrane potential was continually recorded directly onto a JJ Instruments pen recorder. In the spike threshold current clamp experiments and the voltage clamp experiments, responses were recorded on FM tape (AMPEX) using a RACAL Store 4DS recorder. After an experiment, data were replayed and displayed on the oscilloscope screen, enabling the spike threshold or the amplitude of the currents to be measured. Hard copies were produced by playback onto a Gould 1604 Oscilloscope and printed with a Gould Colorwriter 6120.

2.4. STATISTICS

Statistical analysis was carried out on the data investigating the effect of McN-A-343 on the input resistance and spike threshold of the motoneurone. Minitab (PC) was used to perform a t-test for two independent samples.

The membrane potential, input resistance and current amplitudes are expressed as the mean ± S.E.M. where appropriate.

2.5. NEURONE IDENTIFICATION

The cell body of the first basalar motoneurone is relatively large, paired and situated near the midline of the ventral surface of the mesothoracic ganglion. It was identified visually prior to impalement, and could be confirmed as the correct cell by injecting with the fluorescent dye Lucifer Yellow at the end of an experiment. Hyperpolarising current pulses (100 nA, 500 ms, 1 Hz) were applied for approximately 20 min to inject the dye into the cell. The preparation was then transferred to 5 % formalin for 15 min to prevent leaching of the Lucifer Yellow, before dehydration through an ascending alcohol series (70, 90, 95, 100, 100 % ethanol; 10 min each) and clearing in methyl salicylate. The preparation was mounted temporarily in methyl salicylate on a cavity slide and viewed with a

fluorescence microscope (Zeiss) using a 495 nm filter. The mesothoracic ganglion was photographed with Fujichrome 400 slide film using an Olympus OM-2 camera back; the film was developed commercially. Figure 2.3a is a photograph of the mesothoracic ganglion after injecting the right first basalar motoneurone with Lucifer Yellow. The axon extends through the neuropil and leaves the ganglion through ipsilateral nerve 3 (N3). The neurone arborises extensively in the neuropil ipsilateral to its axon.

After injection of the first basalar motoneurone with Lucifer Yellow, the preparation can be counterstained with Toluidine Blue (see Appendix VII for composition) to stain other cell bodies of the ganglia. This allows unique identification of BA1 according to its position relative to the other somata in the mesothoracic ganglion. The preparation was rehydrated through a descending alcohol series (100, 100, 95, 90, 70 % ethanol; 10 min each) and transferred from 70 % ethanol to Toluidine Blue stain. After 15 minutes the preparation was transferred to Bodian's fixative (see Appendix VII for composition) until the cells could be seen clearly under a binocular microscope. This usually took 10-15 minutes depending on the age of the stain. The tissue was dehydrated through an ascending alcohol series (70, 90, 95, 100, 100% ethanol; 10 min each) and cleared in methyl benzoate. The preparation was mounted temporarily in methyl benzoate on a cavity slide and photographed as above. A photograph of a Toluidine Blue-stained mesothoracic ganglion is shown in Figure 2.3b (different preparation to Figure 2.3a). The cell bodies of the ventral surface of the ganglion are arranged in three groups: two bilaterally symmetrical clusters at the anterior end (top in photograph) of the ganglion, and in a third group extending distally from the posterior region of the midline. The first basalar motoneurones (only one has been injected with Lucifer Yellow here) lie on the caudal margin of the anterior groups of cells, close to the midline of the ganglion. Each motoneurone soma is approximately 50 μm in diameter. The large, unstained area of the ganglion contains neuropil and nerve tracts rather than cell bodies.

Figure 2.3a. The ventral surface of the mesothoracic ganglion, showing the first basalar motoneurone after injection with Lucifer Yellow. The cell body lies close to the midline of the ganglion; it is out of focus in this photograph because it is not in the same plane as the axon. The axon extends through the neuropil and leaves the ganglion through ipsilateral nerve 3.

Figure 2.3b. The ventral surface of the mesothoracic ganglion after staining with Toluidine Blue. The first basalar motoneurone has been injected with Lucifer Yellow and its position in the ganglion relative to the other cell bodies can be determined. It lies on the periphery of the anterior group of somata, close to the midline of the ganglion. The diameter of the cell is approximately 50μm. The large, unstained area of the ganglion contains neuropil rather than cell bodies.

The anterior region of each ganglion is at the top of the figures.

Scale bar: 200 μm

a

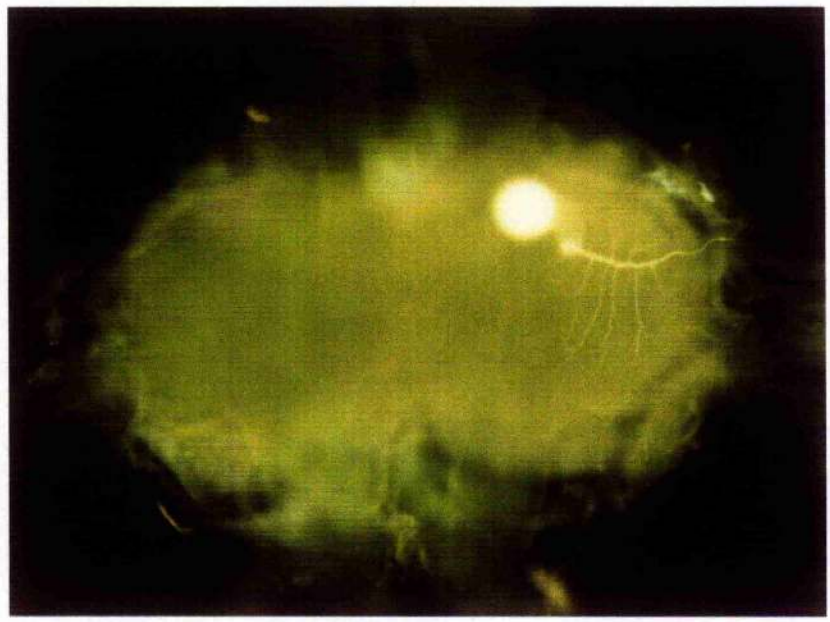

b

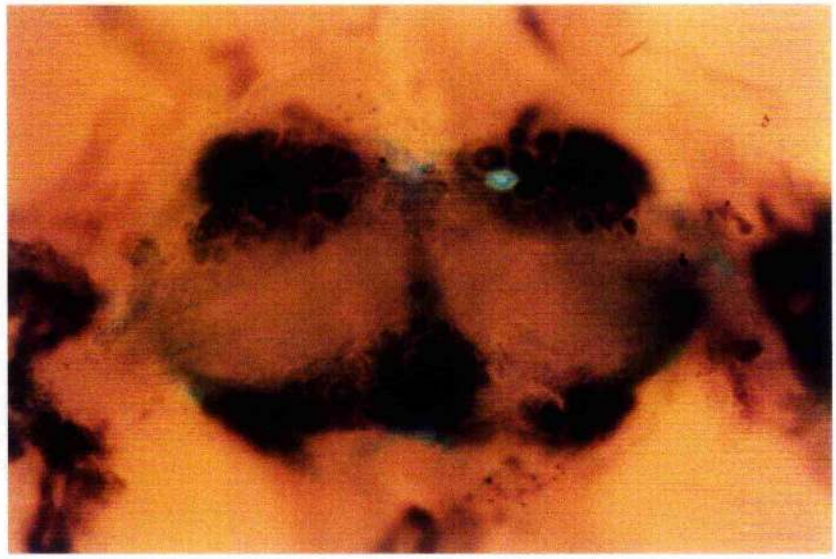

CHAPTER 3

Current clamp study of the pharmacology of α-BTX-resistant cholinergic receptors on the first basalar motoneurone and their possible physiological role

3.1. INTRODUCTION

ACh is a major excitatory neurotransmitter in the insect CNS (Pitman, 1985; Sattelle, 1985). The majority of insect cholinergic receptors are nicotinic, in contrast to the vertebrate CNS, where most cholinergic receptors have a muscarinic pharmacology (Ben-Barak & Dudai, 1979; Salvaterra & Foders, 1979). It is becoming apparent from work on *Manduca* (Trimmer & Weeks, 1989), locust (Baines & Bacon, 1994) and cockroach (David & Pitman, 1990; Lapied & Hue, 1991; Harrow & Sattelle, 1983), however, that nicotinic and muscarinic receptors can be colocalised on the same neurone. There is evidence to suggest that these muscarinic receptors modulate the excitability of the neurone (Trimmer & Weeks, 1989, 1993; Le Corronc & Hue, 1993; Baines & Bacon, 1994), thereby increasing the probability that a nicotinic receptor-mediated depolarisation will result in the propagation of an action potential.

In vertebrates, muscarinic cholinergic receptors can be grouped into subtypes according to their pharmacology. This was first proposed by Hammer et al (1980) on the basis that muscarinic receptors in rat brain could be blocked by pirenzepine (classed as M_1 receptors), whereas those located in the peripheral tissues were insensitive to the drug (M_2 receptors). It soon became apparent that the pirenzepine-insensitive receptors were not a homogeneous group and could be further classified according to their sensitivities to particular antagonists. Those in the heart could be blocked by AF-DX 116 (Giachetti et al, 1986) and methoctramine (Melchiorre et al, 1987), whereas those in smooth muscle were blocked by 4-DAMP (Barlow et al, 1976), HHSiD and p-F-HHSiD (Lambrecht et al, 1989). These three receptor subtypes were termed M_1 (brain), M_2 (cardiac) and M_3 (smooth muscle).

These antagonists were designed for vertebrate muscarinic receptors, but studies have demonstrated that they also show some selectivity for insect muscarinic receptors, although they are less specific. Pirenzepine-sensitive

muscarinic receptors have been found on isolated locust neurones (Benson, 1992), motoneurone D_f of the cockroach (David & Pitman, 1993a), PPR motoneurone of *Manduca* (Trimmer & Weeks, 1993) and cockroach giant interneurones (Le Corronc & Hue, 1993). However, HHSiD and methoctramine also decrease the response to exogenously applied ACh in motoneurone D_f, but are less effective (David & Pitman, 1993a). HHSiD and 4-DAMP have similar potencies to pirenzepine in isolated locust neurones (Benson, 1992), whereas methoctramine has virtually no effect. There is a binding site in the brains of honey bee, housefly and cockroach with a relatively low affinity for pirenzepine and AF-DX 116 compared with 4-DAMP (Abdallah et al, 1991). 4-DAMP and methoctramine have no effect on the muscarinic receptor-mediated depolarisation of cockroach giant interneurones (Le Corronc & Hue, 1993); these antagonists, as well as HHSiD and AF-DX 116, were weak antagonists at the muscarinic receptors of PPR motoneurone (Trimmer & Weeks, 1993).

α-BTX blocks most, but not all, of the response of the first basalar motoneurone to exogenous ACh (Leitch et al, 1993). The experiments presented here were performed to investigate this α-BTX-resistant component: the effects of muscarinic antagonists on the ACh-mediated depolarisation of the neurone were studied to determine whether the receptors have a muscarinic pharmacology; and the effect of the vertebrate M_1 subtype-selective agonist McN-A-343 on the input resistance and spike threshold of the neurone was investigated to examine whether these receptors can modulate the excitability of the motoneurone.

3.2. RESULTS

The resting membrane potential of the first basalar motoneurone was generally between -50 and -60 mV, measured 15 min after impalement. The mean value of the resting potential was -54·0 mV (S.E.M. ± 0·93 mV, n=25). The input resistance of the neurone was measured in two-electrode current clamp: current was injected with one electrode to hyperpolarise the membrane by 10 mV, and the deflection of the membrane potential monitored with the second electrode. The input resistance varied between 3 and 10 MΩ; the mean value was 4·3 MΩ (S.E.M. ± 0·31 MΩ, n=25).

3.2.1. MUSCARINIC PHARMACOLOGY

When ACh is pressure-applied onto the surface of the first basalar motoneurone, the cell is transiently depolarised. This response can be reduced by the addition of 10^{-6} M α-BTX (Figure 3.1; n=3). After 60 min, the amplitudes of the depolarisations were between 15 and 35 % of the control (mean 26·7 %; S.E.M. ± 4·9 %, n=3). α-BTX was added to the preparations in the following experiments to block the nicotinic receptors on the cell in order to study the α-BTX-resistant response to ACh. The toxin was used as supplied by the manufacurer and was not further purified. The agonist was pressure-applied to the cell (10^{-2} M, 200-300 ms) once every 2 min. Figure 3.2 shows that applying ACh in this way does not cause the receptors to desensitise. The effect of more frequent application of ACh was not investigated.

There is the possibility that the α-BTX-resistant component of the ACh-induced depolarisation is the result of incomplete block of the nicotinic receptors. The effect of an increased concentration of α-BTX was not examined; however, the results of the experiments in this chapter suggest that the toxin-resistant component has a muscarinic pharmacology and is not due to partial antagonism of the nicotinic receptors.

Figure 3.1. The effect of 10^{-6} M α-BTX on the response of the first basalar motoneurone to pressure applied ACh (10^{-2} M, 200 ms). The neurone was exposed to the toxin for 60 min, and the amplitude of the depolarisation has been reduced to approximately 30 % of the control.

Scale: vertical 2 mV
horizontal 1 min

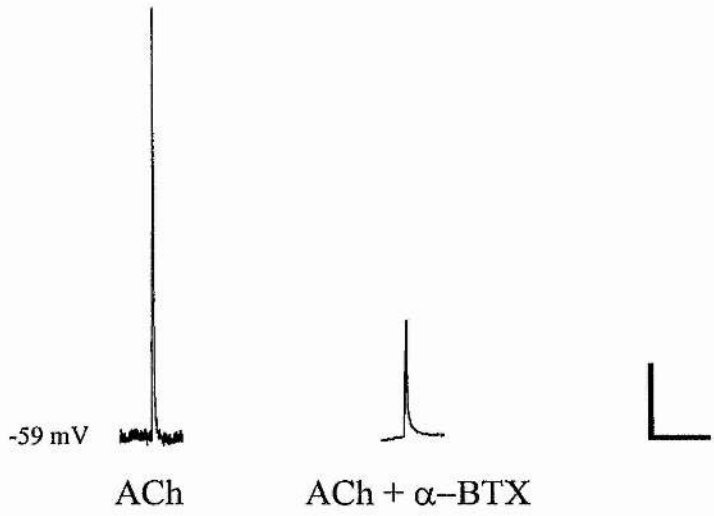

Figure 3.2. The effect of repeated application of ACh. The response does not desensitise when the agonist is applied once every 2 min.

Scale: vertical 2 mV
horizontal 2 min

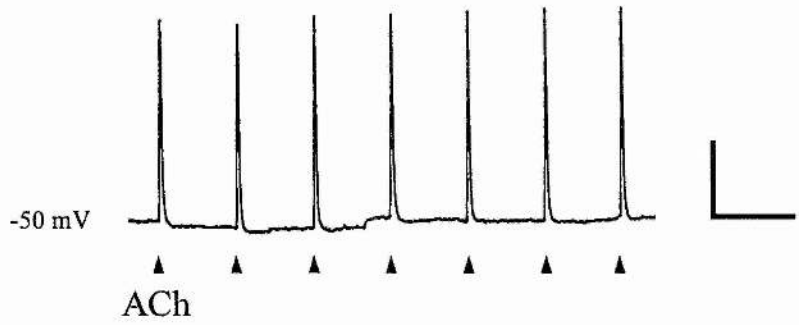

The general muscarinic antagonists applied were atropine and dexetimide to determine whether the receptors have a muscarinic pharmacology: α-BTX-resistant cholinergic receptors of other insect preparations have been shown to have a muscarinic pharmacology (David & Pitman, 1990; Benson, 1992). The antagonists selective for muscarinic receptor subtypes were pirenzepine (vertebrate M_1 subtype-selective), p-F-HHSiD (M_3>M_1>M_2), 4-DAMP (M_3 subtype selective) and methoctramine (M_2 subtype selective). These drugs were used to study the pharmacology of the α-BTX-resistant receptors in more detail.

The amplitude of the ACh-induced depolarisation is dependent on the duration of agonist application and the distance between the ACh-containing electrode and the soma membrane. ACh was applied when the neurone was at its normal resting potential; the effect of membrane potential on the amplitude of the depolarisation was not investigated. In the majority of preparations, the amplitude of the response was between 1 and 3 mV (n=20), but could be as large as 10 mV (n=3).

The antagonists were applied at concentrations of 10^{-4} M or $5x10^{-5}$ M. This relatively high concentration of antagonist was used to produce a fast block of the ACh depolarisation so that the neurone could be exposed to antagonist for the minimum length of time, so facilitating recovery of the response upon washing the preparation

3.2.1.1. Non-subtype-selective muscarinic antagonists

The effect of 10^{-4} M atropine (n=5) on the amplitude of the ACh-induced depolarisation in the presence α-BTX is shown in Figure 3.3. After 6 min, the amplitude was reduced to between 20 and 30 % of the control value (mean 26·0 %; S.E.M. ± 2·3 %), and could be reversed after washing the preparation with fresh saline.

Dexetimide (10^{-4} M) had a similar action on the ACh response obtained in the presence α-BTX (n=2), as shown in Figure 3.4. After 6 min the ACh

Figure 3.3. The addition of 10^{-4} M atropine reversibly reduces the amplitude of the ACh depolarisation, measured after 6 min. The membrane potential is -45 mV. In this preparation the cell started to depolarise slightly 4 min after the application of atropine; the membrane potential in the 'atropine' and 'wash' records was -44 mV. The small ACh-induced depolarisation remaining in the presence of atropine could be fully blocked if the concentration of antagonist was increased.

Scale: vertical 1 mV
horizontal 1 min

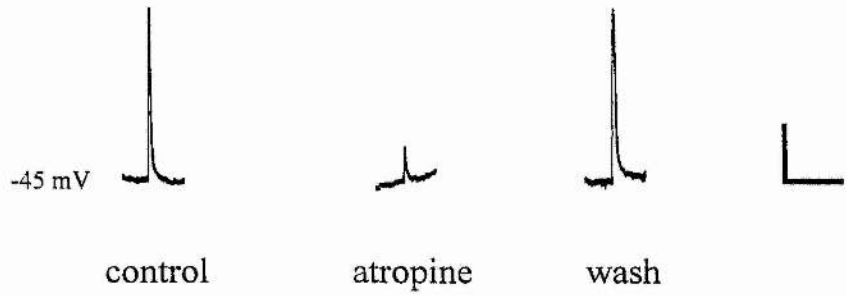

Figure 3.4. The response evoked in the first basalar motoneurone to pressure application of 10^{-2} M ACh can be reversibly reduced by 10^{-4} M dexetimide (recorded after 6 min). The membrane potential of the cell is shown beside the trace.

Scale: vertical 1 mV
horizontal 1 min

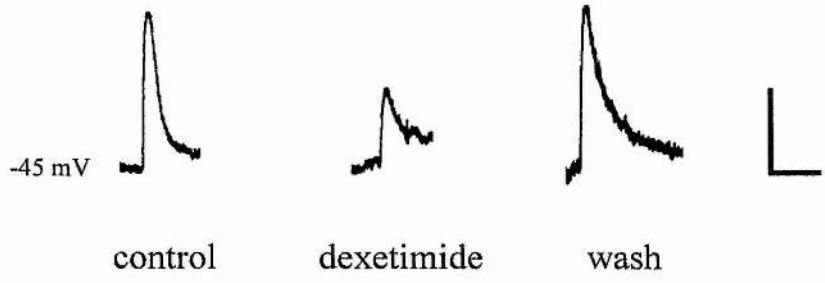

depolarisation had decreased to 30 (n=1) or 45 % (n=1) of the response obtained prior to the addition of antagonist. This effect of dexetimide was reversible.

3.2.1.2. Muscarinic receptor subtype-selective antagonists

Muscarinic antagonists selective for vertebrate M_1, M_2 and M_3 subtypes were applied to the motoneurone to determine whether these receptors showed any differential sensitivities to these compounds, as do vertebrate muscarinic receptors.

Pirenzepine is selective for vertebrate M_1 receptors, and Figure 3.5 shows that 10^{-4} M pirenzepine (n=3) reversibly decreased the transient depolarisations caused by ACh. The ACh responses were reduced to 43, 56 and 87 % of the control after 6 min exposure to pirenzepine (mean 62·0 ± 13·1 %, n=3). After washing, the amplitude of the depolarisations evoked in two neurones were larger than before the addition of pirenzepine. This antagonist would appear to be less potent than either atropine or dexetimide, but it was applied in the absence of α-BTX, therefore a comparison cannot be made. A proportion of the ACh response in the absence of α-BTX would be mediated by nicotinic receptors which would be unaffected by pirenzepine. However, pirenzepine did reduce the amplitude of the ACh-induced depolarisation, showing that pirenzepine-sensitive receptors are located on the first basalar motoneurone.

p-F-HHSiD is an M_3 antagonist, but also blocks vertebrate M_1 receptors, as well as having some antagonistic action on M_2 receptors. As Figure 3.6 illustrates, 10^{-4} M p-F-HHSiD (n=3) reduced the amplitude of the ACh-induced depolarisations of the neurone in the presence of α-BTX. Six minutes after the addition of the antagonist, the amplitude of the depolarisation was between 37 and 42 % (mean 38·7 %; S.E.M. ±1·4 %). Some recovery of the ACh response was observed upon washing, although it never reached control levels.

The effect of applying the vertebrate M_3 subtype-selective antagonist 4-DAMP (5×10^{-5} M; n=5) is shown in Figure 3.7. The response to ACh in the

Figure 3.5. Pirenzepine (10^{-4} M) decreases the amplitude of the depolarisation of BA1 produced by picospritzing 10^{-2} M ACh onto the motoneurone, measured after 6 min. The effect is reversible. The membrane potential of the cell is shown beside the trace. There is a small degree of depolarisation throughout the experiment; the membrane potential of the 'pirenzepine' record is -45 mV.

Scale: vertical 1 mV
horizontal 1 min

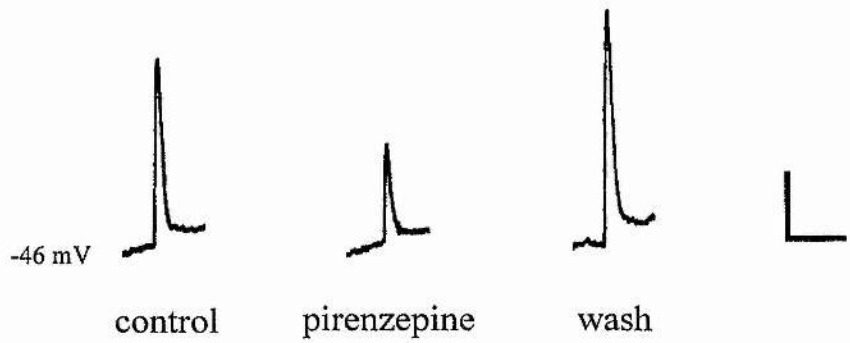

Figure 3.6. 10^{-4} M HHSiD reduces the amplitude (measured after 6 min) of the ACh-induced depolarisation (10^{-2} M) caused by pressure application of the agonist onto BA1. There is some recovery after washing. The membrane potential of the cell is shown beside the trace.

Scale: vertical 1 mV
horizontal 1 min

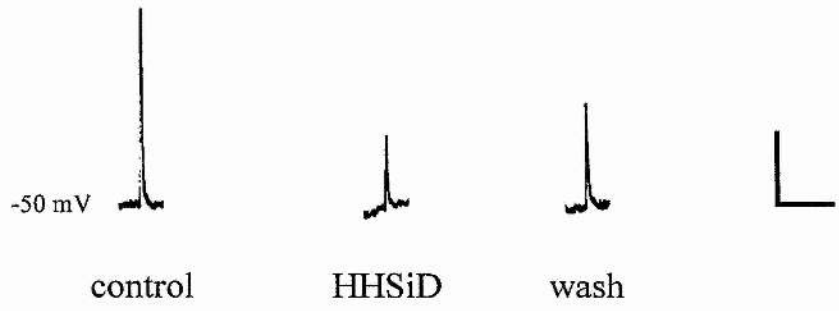

Figure 3.7. 4-DAMP ($5x10^{-5}$ M) reversibly decreases the amplitude of the depolarisation of the motoneurone produced by pressure application of ACh (10^{-2} M) onto the first basalar motoneurone (recorded after 6 min). The membrane potential of the cell is shown beside the trace.

Scale: vertical 1 mV
horizontal 1 min

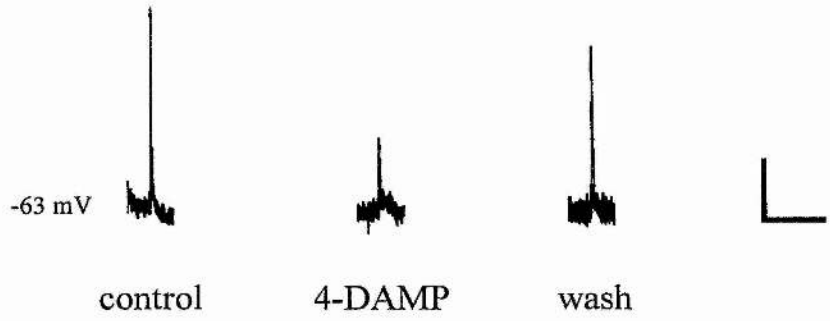

presence of α-BTX was reversibly reduced to between 5 and 30 % (mean 17·8 %; S.E.M. ± 4·6 %). In two preparations, the ACh-induced depolarisation was larger after washing than before the addition of 4-DAMP. In Figure 3.7, the amplitude of the response to ACh after washing is 82 % of the control.

Methoctramine ($5x10^{-5}$ M) selectively blocks vertebrate M_2 receptors (Figure 3.8; n=5); the amplitude of the ACh depolarisation in the presence of α-BTX was reduced to between 20 and 40 % (mean 33·0 %; S.E.M. ± 5·1 %). At this concentration some recovery was observed, but at higher concentrations of methoctramine the blocking effect was essentially irreversible.

3.2.2. EFFECT OF McN-A-343 ON INPUT RESISTANCE

The vertebrate M_1 receptor selective agonist McN-A-343 (10^{-4} M) was applied to the neurones (n=5) for 15 min at the normal resting potential of the cell, and the input resistance determined 1, 5, 10 and 15 min after application. This drug has been used as a benchmark agonist to stimulate α-BTX-resistant receptors in an identified cockroach motoneurone (David & Pitman, 1993a, 1995). The mean of four input resistance measurements was calculated, and t-tests for two independent samples were carried out for each neurone. One minute's exposure to McN-A-343 had no significant effect on the input resistance. However, after 5 (n=4) or 10 min (n=1) the input resistance was significantly affected ($P < 0·05$). The effect of McN-A-343 on the input resistance was variable and developed slowly during exposure, so that after 15 min the input resistance was decreased by 0·5, 1·5 or 2·8 MΩ, or increased by 0·7 MΩ (n=2). Typical traces are shown in Figure 3.9a & b.

McN-A-343 also had two effects on the membrane potential: in two preparations in which the input resistance decreased, there was an accompanying depolarisation of 2 mV after 15 min. The remaining neurones, in which the input resistance decreased (n=1) or increased (n=2), there was no change in the

Figure 3.8. The response of the first basalar motoneurone to pressure application of ACh (10^{-2} M) is reduced by $5x10^{-5}$ M methoctramine, measured after 6 min. The effect of the antagonist is partly relieved by washing. Before and during the addition of antagonist, the cell in this figure was spiking, resulting in the noisy baseline. The membrane potential of the cell is shown beside the trace.

Scale: vertical 1 mV
horizontal 1 min

Figure 3.9. The effect of 15 min exposure to 10^{-4} M McN-A-343 on the input resistance of the first basalar motoneurone. Hyperpolarising current pulses were applied to the cell once every 20 (a) or 30 s (b). In three preparations (a), the agonist reversibly decreased the input resistance by 0·5, 1·5 or 2·8 MΩ after 15 min, and reversibly increased it in two preparations (b) by 0·7 MΩ after 15 min. The input resistance was significantly affected after 5 (n=4) or 10 min (n=1) exposure to McN-A-343.
The effect of McN-A-343 on the membrane potential was also variable. In two preparations the cell was depolarised by 2 mV (a); this was accompanied by a decrease in input resistance. The agonist had no effect on the membrane potential in the remaining three cells (b); the input resistance of these neurones either increased (n=2) or decreased (n=1). The membrane potential returned to the control value after washing.

Scale: vertical 2 mV
horizontal 5 min

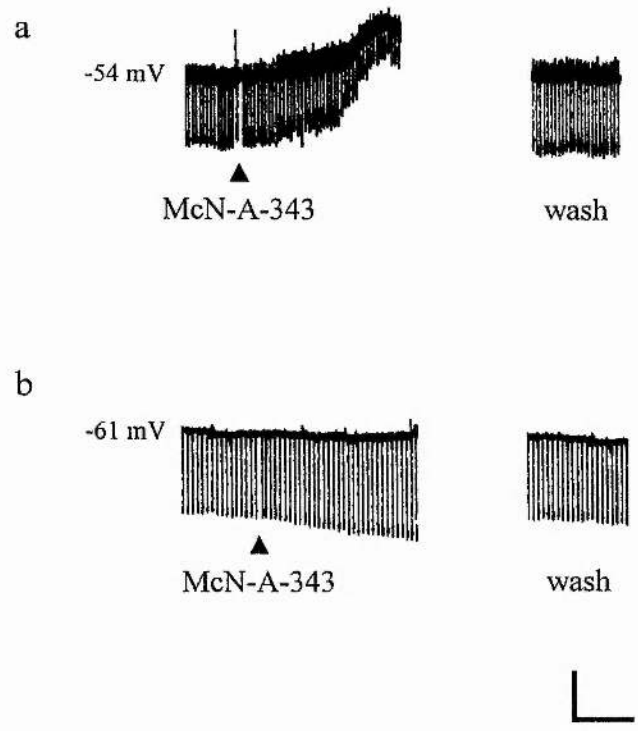

membrane potential. Both the input resistance and membrane potential returned to control values after washing with fresh saline.

3.2.3. EFFECT OF McN-A-343 ON SPIKE THRESHOLD

To establish whether McN-A-343 influenced the spike threshold of the neurone, depolarising current ramps (duration approximately 150 ms, followed by a sustained current pulse of the same duration) were injected through one electrode, and the membrane potential was monitored with the second electrode. The current was applied as a ramp which increased at a rate of 20 (n=2) or 40 nA s^{-1} (n=4), to reach an amplitude of 6 to 16 nA. The maximum current reached was between 6 and 16 nA.

Prior to the addition of McN-A-343 (n=3), the spike threshold of the motoneurone was -35, -36 and -46 mV in each neurone. The effect of 10^{-4} M McN-A-343 on the spike threshold was measured after 1, 5, 10 and 15 min (repeated four times), and a t-test for two independent samples was carried out for each neurone. Figure 3.10 shows the effect of 15 min exposure to McN-A-343 in a typical neurone. McN-A-343 had no significant effect on spike threshold after 1 min exposure (n=2); but in one preparation it decreased and became more negative ($P < 0{\cdot}05$). In the presence of the agonist the spike threshold decreased steadily, and was significantly decreased after 5 min exposure to McN-A-343; after 15 min the spike threshold was significantly decreased by between 1·5 and 3 mV. The decrease in threshold was not always accompanied by a change in membrane potential (n=2); when the cell did depolarise (n=1; 2 mV), returning it to the control membrane potential did not alter the effect of McN-A-343 on the spike threshold. Washing the preparation returned the spike threshold to control values.

Figure 3.10. The effect of 15 min exposure to 10^{-4} M McN-A-343 on the spike threshold of the first basalar motoneurone. Depolarising current ramps (20 or 40 nA s^{-1}; bottom traces) were applied to the neurone and the membrane potential monitored (top traces). Action potentials are highlighted by asterisks. Prior to the addition of McN-A-343, the spike threshold was -35, -36 or -46 mV and is represented by the dashed line. After drug treatment the threshold was significantly decreased ($P < 0{\cdot}05$) by between 1·5 and 3 mV. In this example, a second action potential was evoked in the presence of McN-A-343. The effect was reversed with washing.

Scale: vertical 5 mV
20 nA
horizontal 200 ms

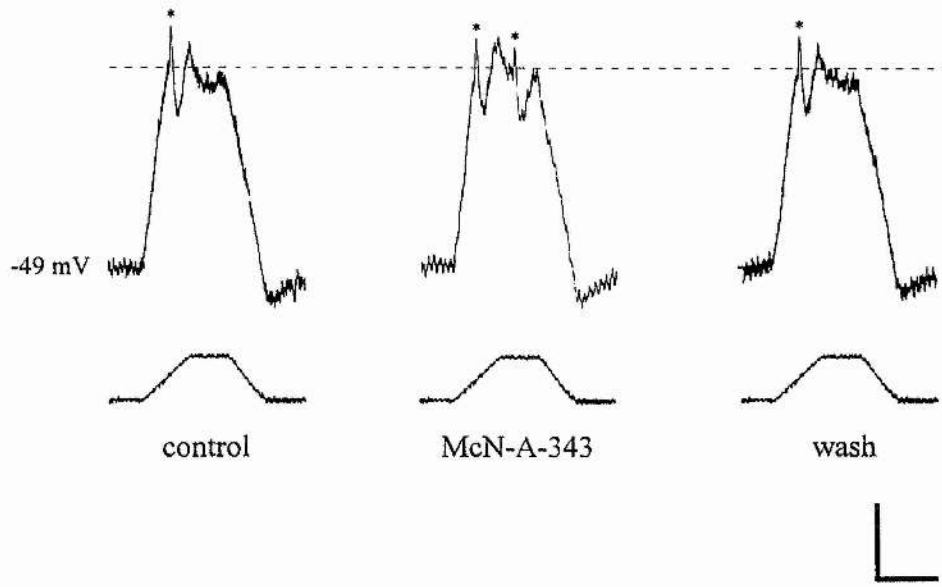

3.3. DISCUSSION

Pressure application of 10^{-2} M ACh onto the soma membrane of the first basalar motoneurone resulted in a transient depolarisation which could be reduced by 10^{-6} M α-BTX. The amplitude of the ACh depolarisation in the presence of α-BTX was usually between 1 and 3 mV, but in some preparations could be as large as 10 mV. These results provide the first suggestion for the co-existence of both nicotinic and muscarinic receptors on the first basalar motoneurone. It is unlikely that the α-BTX-resistant component of the ACh-induced depolarisation is due to incomplete block of the nicotinic receptors because the remaining depolarisation could be reversibly reduced by muscarinic antagonists. Muscarinic and nicotinic receptors are also colocalised on motoneurone PPR of *Manduca* (Trimmer & Weeks, 1989), cockroach motoneurone D_f (David & Pitman, 1990), DUM neurones of the cockroach (Lapied & Hue, 1991), cockroach giant interneurones (Le Corronc & Hue, 1993) spinal neurones of *Xenopus* embryos (Perrins & Roberts, 1994), cultured rat CNS astrocytes (Hösli et al, 1994) and sympathetic ganglion neurones (Yarosh et al, 1988; Furukawa et al, 1994).

The addition of muscarinic antagonists reduced the amplitude of the ACh-evoked depolarisations in the presence of α-BTX, suggesting that these receptors have a muscarinic pharmacology. Further evidence for the muscarinic nature of these receptors is that they are sensitive to the muscarinic agonist McN-A-343. Both general muscarinic antagonists and antagonists selective for vertebrate muscarinic receptor subtypes were effective. The vertebrate muscarinic M_1 antagonist pirenzepine decreased the amplitude of the ACh-induced depolarisation, indicating that the neurones possess a population of pirenzepine-sensitive receptors. However, pirenzepine cannot be directly compared with the other antagonists because it was added to the preparation in the absence of α-BTX, whereas all other antagonists were added in the presence of the toxin. The order of potency of the remaining antagonists is 4-DAMP > atropine =

methoctramine > p-F-HHSiD = dexetimide. Because all four of the subtype-selective antagonists decreased the ACh-induced depolarisation, the receptors cannot be classified as M_1, M_2 or M_3 receptors. This classification applies to vertebrate receptors, and the muscarinic antagonists available have been developed for vertebrate preparations. It is possible that the ligand binding site of invertebrate muscarinic receptors does not resemble that of vertebrate receptors because the two groups of animals are evolutionally distant. Insects are a phylogenetically ancient class of animal compared to vertebrates, therefore the receptors present in vertebrate species can be expected to have evolved significantly from those of insects. This would result in the different ligand binding properties of the muscarinic receptors of the two groups of animals.

Muscarinic receptors of other insect preparations are similar to BA1 in that they are sensitive to more than one subtype-selective antagonist. Of the antagonists tested, pirenzepine has been shown to be the most potent in blocking α-BTX-insensitive cholinergic receptors in motoneurone D_f of the cockroach. These receptors could, however, also be blocked by p-F-HHSiD and methoctramine (David & Pitman, 1993a). HHSiD, pirenzepine and 4-DAMP have similar potencies in isolated locust neurones, whereas methoctramine has virtually no effect (Benson, 1992). However, there appears to be some differential selectivity to different antagonists in cockroach GI neurones (Le Corronc & Hue, 1993) and the PPR motoneurone of *Manduca* (Trimmer & Weeks, 1993). In these preparations, pirenzepine reduces the response to muscarinic agonists, but methoctramine and 4-DAMP were ineffective. HHSiD was also found to be without effect in *Manduca* (Trimmer & Weeks, 1993). In contrast, a binding site with a relatively high affinity for 4-DAMP has been uncovered in the brains of honey bee, housefly and cockroach (Abdallah et al, 1991), whereas pirenzepine and AF-DX 116 (M_2 antagonist) were less potent.

Other research carried out on a variety of neurotransmitter receptors in insects has also provided evidence for variation between vertebrate and

invertebrate receptors. For example, GABA receptors appear to differ between vertebrates and invertebrate neurones: GABA receptors of cockroach motoneurone D_f (Sattelle et al, 1988), locust thoracic neurones (Lees et al, 1987) and lobster thoracic neurones (Jackel et al, 1994) are activated by $GABA_A$ agonists but are not blocked by the classical vertebrate $GABA_A$ antagonist bicuculline. GABA receptors of *Limulus* heart appear to be similar to vertebrate $GABA_A$ receptors but they can be blocked by the $GABA_B$ antagonist 3-aminopropyl-phosphonous acid and are insensitive to bicuculline (Benson, 1989). Picrotoxin, which blocks the ion channel of vertebrate $GABA_A$ receptors, has no effect on *Limulus* heart (Benson, 1989) or the stomatogastric ganglion of the crab (Marder & Paupardin-Tritsch, 1978) but does block the GABA receptors of cockroach central neurones (Pitman & Kerkut, 1970; Sattelle et al, 1988), lobster thoracic neurones (Jackel et al, 1994) and locust thoracic neurones (Lees et al, 1987).

The response to ACh did not always return to control amplitude after the application of HHSiD and methoctramine. These antagonists may bind with a higher affinity to the receptors than the other antagonists tested and therefore would be more difficult to wash off. However, there was always some degree of recovery, suggesting that the decrease observed in the presence of antagonist was due to the drug and not deterioration of the cell. Further evidence against the partial recovery of the response to ACh being due to deterioration of the cell comes from the observation that there was no associated change in the resting membrane potential, a measure which can be used to assess the viability of a neurone. After washing off the other antagonists, the amplitude of the ACh-response was sometimes greater than control values. The reason for this is unclear, although it is possible that washing the preparation could lead to a decrease in the concentration of cholinesterase in the extracellular fluid surrounding the motoneurone resulting in an enhancement of the response to ACh. Alternatively, it

could alter the ionic gradients across the membrane causing an increased driving force on the ions responsible for the ACh-induced depolarisation.

The input resistance of a neurone is a measure of the conductance of the membrane: an agonist-induced increase in input resistance is equivalent to a decrease in conductance caused by closure of ion channels. A decrease in input resistance, or increase in membrane conductance, results from the opening of channels. The addition of the vertebrate M_1 receptor selective agonist McN-A-343 to the first basalar motoneurone in some preparations decreased while in others increased the input resistance of the cell. This suggests that McN-A-343 may have two effects on the motoneurone, causing either an opening or a closure of ion channels. Muscarinic and global cholinergic agonists increased the input resistance of bullfrog sympathetic neurones (Weight & Votava, 1970; Kuba & Koketsu, 1976; Brown & Adams, 1980), cat thalamocortical neurones (Curró Dossi et al, 1991), basolateral amygdaloid neurones of the rat (Washburn & Moises, 1992) and rat hippocampal cells (Cole & Nicoll, 1984). These neurones possess a population of voltage-dependent K^+ channels which are sensitive to muscarinic receptor activation (M-channels; see Section 1.3.1.5.); in the presence of muscarinic agonists, the channels are inhibited, leading to a decrease in the K^+ conductance of the membrane. A decrease in input resistance in the presence of muscarinic agonists has been found in isolated *Locusta* neurones (Benson, 1992). These results are in contrast to the observation made by Trimmer & Weeks (1989, 1993) in *Manduca* that muscarinic agonists had no noticeable effect on input resistance.

The change in the input resistance of the first basalar motoneurone in the presence of McN-A-343 was not necessarily accompanied by a change in the membrane potential. In two neurones the cell depolarised by 2 mV, but in three McN-A-343 had no effect. The neurones which were depolarised by McN-A-343 exhibited a decrease in the input resistance, whereas those which were not

depolarised generally exhibited an increase in input resistance. The increase in input resistance suggests that K^+ channels may be closed by the agonist, a hypothesis confirmed by the experiments presented in Chapter 5. If the K^+ reversal potential was close to the resting membrane potential of a neurone, closure of K^+ channels need not have a large effect on the membrane potential. However, the decrease in input resistance and the depolarisation recorded from two neurones cannot be explained in terms of modulation of K^+ channels. One explanation is that the decrease in input resistance is secondary to the depolarisation: closure of K^+ channels causes depolarisation of the membrane and opens voltage-dependent Ca^{2+} and Na^+ channels. When ACh, carbachol or muscarinic agonists were applied to rat hippocampal neurones (Cole & Nicoll, 1984), rat basolateral amygdaloid neurones (Washburn & Moises, 1992), cat sensorimotor cortical neurones (Schwindt et al, 1988), the membrane was depolarised in only a proportion of preparations. In the preparations which did depolarise, the increased input resistance was unrelated to the depolarisation, because when the membrane potential was returned to the control potential the change in input resistance persisted.

The preliminary results presented here suggest that the addition of McN-A-343 to the first basalar motoneurone significantly decreases the spike threshold of the cell by 1·5 to 3 mV without necessarily affecting the membrane potential. This would suggest that the physiological role of these muscarinic receptors is to increase the excitability of the neurone.

Studies of postsynaptic muscarinic receptors of other insect preparations - *Manduca* larval PPR motoneurones (Trimmer & Weeks, 1989, 1993), cockroach giant interneurones (Le Corronc & Hue, 1993) and locust VPLI interneurones (Baines & Bacon, 1994) - have shown that these receptors do appear to be involved in modulating spike threshold. Muscarinic receptor activation caused a decrease of the spike threshold which was accompanied by membrane depolarisation. The change in threshold was independent of the depolarisation as

artificial repolarisation of the neurone to the control membrane potential did not abolish the increase in excitability. Trimmer & Weeks (1993) reported that 10 min treatment with oxotremorine lowered the spike threshold by approximately 5 mV, and Baines & Bacon (1994) reported that a 200 ms application of muscarine decreased the spike threshold by the same amount. The spike threshold of cockroach giant interneurones (Le Corronc & Hue, 1993) was lowered by approximately 2 mV after 1 min exposure to arecoline. However, in the experiments described here, 15 min exposure to McN-A-343 only decreased the spike threshold by a maximum of 3 mV. Although they appeared to reverse upon washing, there remains the possibility that these variations are due to drug-unrelated fluctuations in the spike threshold. Clearly, further investigations must be carried out. The addition of muscarinic antagonists would be expected to have the opposite effect and increase the spike threshold, as well as blocking the increase in excitability induced by muscarinic agonists. Activation of the receptors should also potentiate the effects of nicotine, a result obtained by Baines & Bacon (1994).

There are many examples of a muscarinic receptor-mediated increase in excitability in vertebrate preparations. Muscarinic receptor activation increased the excitability of bullfrog sympathetic neurones (Weight & Votava, 1970; Adams et al, 1982b), cat sensorimotor cortical neurones (Schwindt et al, 1988), rat hippocampal neurones (Cole & Nicoll, 1984; Lancaster & Nicoll, 1987) and rat basolateral amygdaloid neurones (Washburn & Moises, 1992). The effect was accompanied by an increase in the input resistance of the neurone (Weight & Votava, 1970; Adams et al, 1982b; Cole & Nicoll, 1984; Washburn & Moises, 1992). These authors reported that in many cases, muscarinic agonists had no effect on the membrane potential (Cole & Nicoll, 1984; Schwindt et al, 1988; Washburn & Moises, 1992); when the membrane did depolarise, the increased excitability was independent of the depolarisation because it was still observed when the membrane was returned to the control potential.

McN-A-343 did not affect the input resistance or the spike threshold until 5 min after the addition of the drug. This would suggest therefore, that the modulation of the excitable properties would only occur when there is prolonged activity of the synapse, for example while the locust is flying. If a similar time lag occurs *in vivo*, activation of the muscarinic receptors by ACh would have no effect on the motoneurone at the start of flight. However, after a few minutes, these receptors would mediate an increase in the excitability of the cell and may influence the flight pattern: if the spike threshold is lowered such that an action potential will be evoked at a more negative potential, this would obviously occur earlier as the motoneurone is depolarised from the resting potential and could therefore accelerate the rhythmic discharge of the first basalar motoneurones. To further investigate the functional role of these receptors, recordings could be made from neurones involved in the flight pattern generator and a muscarinic agonist applied to examine whether it has an effect on the flight rhythm.

SUMMARY

When ACh (in the presence of α-BTX) is pressure-applied onto the soma of the first basalar motoneurone, the cell is transiently depolarised. The amplitude of the depolarisation was usually between 1 and 3 mV.

This α-BTX-resistant component of the ACh-evoked depolarisation appears to be muscarinic in nature, because it can be reversibly decreased by muscarinic antagonists. It is sensitive to the non-subtype-selective muscarinic antagonists atropine and dexetimide, and the vertebrate subtype-selective receptor antagonists pirenzepine, HHSiD, 4-DAMP and methoctramine. The relative potencies of the antagonists is 4-DAMP > atropine = methoctramine > HHSiD = dexetimide; pirenzepine cannot be compared because it was added in the absence of α-BTX. The results suggest that these receptors have different characteristics to vertebrate muscarinic receptors because they are sensitive to more than one subtype-selective antagonist.

Activation of the α-BTX-resistant receptors studied here decreases the spike threshold of the motoneurone, and has a variable effect on the input resistance. Both features were affected significantly after 5 min exposure to McN-A-343. The physiological role of these receptors may be to modulate the excitability of the first basalar motoneurone and hence influence the flight pattern.

CHAPTER 4

Voltage clamp study of the currents evoked by activation of α-BTX-resistant cholinergic receptors in the first basalar motoneurone

4.1. INTRODUCTION

The experiments described in the following two chapters were performed using voltage clamp, a technique developed independently by Cole (1949) and Marmot (1949) which has become a powerful tool for studying the ionic currents across the cell membrane. Two microelectrodes were used in the experiments presented here: briefly, the membrane potential is monitored by one microelectrode, and is kept at a constant holding potential by current delivered through a second microelectrode from a high gain, high voltage feedback amplifier. The membrane was stepped to a pre-determined command potential by applying command pulses to the feedback amplifier.

The currents underlying the muscarinic receptor-mediated depolarisation of the first basalar motoneurone described in Chapter 3 were studied here using voltage clamp. In addition to this, experiments were performed to determine whether the current evoked by muscarinic agonists is mimicked by nicotine (in the presence of α-BTX), which would suggest that these muscarinic receptors may have a 'mixed' cholinergic pharmacology. The first report of putative receptors that bound both nicotinic and muscarinic ligands came from experiments on electroplax tissue of *Electrophorus* (Eldefrawi et al, 1971). A similar binding component was found in the CNS of the housefly *Musca* (Aziz & Eldefrawi, 1973), an observation which was later confirmed by Mansour et al (1977) and Harris et al (1981). Binding studies have identified putative 'mixed' cholinergic receptors in cultured cockroach neurones (Lees et al, 1983) and bovine chromaffin cells (Shirvan et al, 1991). However, the results of these binding studies must be interpreted with caution because the density of these putative receptors is much higher than that found for other receptors, which could suggest that the binding sites do not correspond to receptor proteins. Evidence for functional 'mixed' cholinergic receptors has been provided by electrophysiological experiments on motoneurone D_f of the cockroach (David & Pitman, 1993a), isolated unidentified

thoracic neurones of *Locusta* (Benson & Neumann, 1987; Benson, 1992) and the skin of *Rana catesbiana* (Cox, 1993).

Unlike vertebrate neurones, there are no known examples of chemical synapses onto the cell bodies of insect neurones. However, experiments on freshly isolated cell bodies of locust neurones, from which the axons have been severed, have provided conclusive evidence for the presence of somatic receptors for several different neurotransmitters, including ACh (Usherwood et al, 1980; Suter & Usherwood, 1985; Benson, 1992), L-glutamate (Usherwood et al, 1980; Giles & Usherwood, 1985), GABA (Giles & Usherwood, 1985; Lees et al, 1987; Whitton et al, 1994), serotonin (Usherwood et al, 1980; Bermudez et al, 1992) and octopamine (Usherwood et al, 1980; Suter, 1986).

The experiments performed in Chapter 3 demonstrated that there is a population of α-BTX-resistant cholinergic receptors on the first basalar motoneurone. The aims of the present experiments were (1) to use two-electrode voltage clamp to study the currents evoked in the first basalar motoneurone, (2) to further characterise the pharmacology of these receptors by investigating the effects of carbachol, muscarine and McN-A-343, (3) to determine whether the receptors also respond to nicotine and therefore have a 'mixed' cholinergic pharmacology, and (4) to investigate whether the receptors are present on the soma membrane of the motoneurone.

4.2. RESULTS

4.2.1. CURRENTS EVOKED IN THE FIRST BASALAR MOTONEURONE UNDER VOLTAGE CLAMP

For this first set of voltage clamp experiments a holding potential of -50 mV was selected because this is close to the mean resting membrane potential of this neurone. The membrane was stepped to potentials between -100 mV and 0 mV; the membrane was not jumped to potentials more positive than 0 mV because this has a deleterious effect on the long term stability of the cell. Examples of the evoked currents are displayed in Figure 4.1. Using command steps 250-300 ms long the current reached a steady state. At potentials more negative than the holding potential a square shaped inward current was evoked (n=22). This current was generally only a few nA in magnitude. At potentials more positive than the holding potential an outward current was evoked. The currents evoked in the majority of preparations consisted of an outward relaxation that gave way to a sustained outward current. At 0 mV the sustained outward current was reached after 50 to 100 ms. An outward current relaxation was recorded at -40 (n=4), -20 (n=16) and 0 mV (n=12). In the example shown in Figure 4.1a, the currents evoked at -20 and 0 mV exhibit outward current relaxations; however, at -40 mV the current lacks the outward current relaxation and appears square. This was recorded at -40 mV from a total of 18 neurones.

A transient outward current preceded the sustained current in the remaining preparations at -20 (n=6) and 0 mV (n=10), as shown in Figure 4.1b. An outward current relaxation was recorded at -40 mV in this neurone. The duration of this transient current was typically between 10 and 20 ms with an amplitude of 10 to 15 nA, and was larger at 0 mV than at -20 mV.

The currents evoked in eighteen neurones were similar at command potentials of -20 and 0 mV: an outward relaxation into a sustained outward current was recorded from twelve preparations (Figure 4.1a), and an initial transient

Figure 4.1. Currents evoked in the first basalar motoneurone by stepping the membrane from a holding potential of -50 mV to -100, -40, -20 and 0 mV. The voltage steps are shown below the currents. Inward currents evoked at -100 mV were small and appeared square-shaped; however, outward currents produced at potentials positive to the holding potential varied between preparations. The arrow in (a) shows the point at which the current amplitude was measured to construct the I/V relationship of each neurone.

Scale: vertical 100 nA
horizontal 100 ms

Figure 4.1a. The outward currents evoked at -20 and 0 mV in this cell exhibited an outward relaxation into a non-inactivating outward current. This was recorded at -40 mV (n=18), -20 mV (n=16) and 0 mV (n=12). The steady state current was reached within 50 to 100 ms at 0 mV. In this preparation at -40 mV, the current did not include an outward relaxation, and appeared square. This was observed in a total of four preparations.

Figure 4.1b. The non-inactivating outward current could be preceded by a transient outward current at -20 mV (n=6) and 0 mV (n=10). The duration of this transient was between 10 and 20 ms and the amplitude was 10 to 15 nA. In this neurone an outward relaxation was recorded at -40 mV.

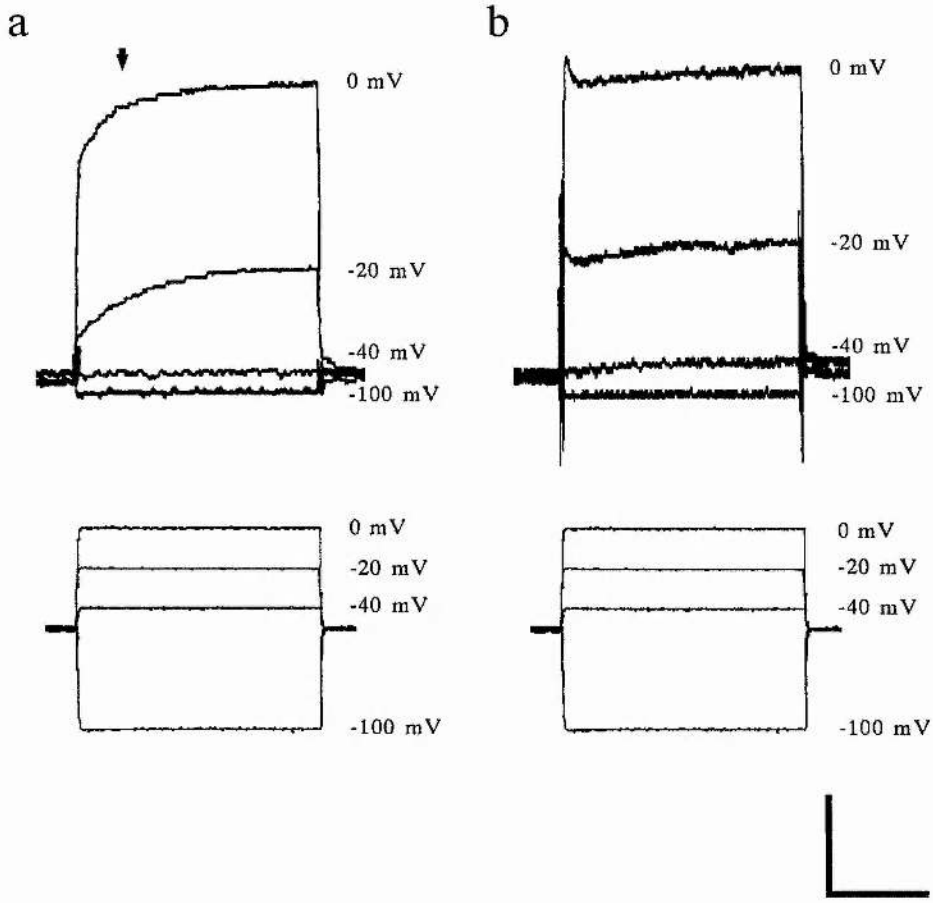
a
b
0 mV
-20 mV
-40 mV
-100 mV
0 mV
-20 mV
-40 mV
-100 mV
0 mV
-20 mV
-40 mV
-100 mV
0 mV
-20 mV
-40 mV
-100 mV

outward current preceding the sustained current was recorded from six preparations (Figure 4.1b). In the remaining cells (n=4), the outward relaxation gave way to a transient outward current as the command potential became more positive.

The current/voltage (I/V) relationship of the first basalar motoneurone is displayed in Figure 4.2. This was constructed by measuring the amplitudes of the evoked currents, such as those in Figure 4.1, after 50 ms (arrow, Figure 4.1a). The current is inwardly directed at command potentials more negative than the holding potential, -50 mV, and outwardly directed at more positive potentials. At command potentials between -100 and -40 mV the I/V relationship is approximately linear. However, at potentials more positive than about -40 mV the I/V relationship shows strong outward rectification and a large outward current develops.

4.2.2. EFFECT OF MUSCARINIC AGONISTS AND NICOTINE IN THE PRESENCE OF α-BTX

To confirm that the α-BTX-resistant receptors identified in the preceding chapter have a cholinergic pharmacology, the non-selective cholinergic agonist carbachol (carbamylcholine chloride; CCh) was applied to the motoneurone (n=5) in the presence of α-BTX (10^{-6} M). Carbachol is an analogue of ACh, and was applied rather than ACh because it is non-hydrolysable and cannot be broken down by cholinesterase. If the α-BTX-resistant receptors do not desensitise in the presence of agonist (which the following experiments demonstrate), the current evoked by CCh will continue as long as the neurone is exposed to agonist, allowing a study of the time dependency of the response. In addition to CCh, the currents evoked in the motoneurone by the specific muscarinic agonists L-(+)-muscarine (n=3) and McN-A-343 (n=3) were examined.

Cholinergic receptors of certain insect preparations which were previously assumed to be muscarinic receptors are now known to be activated by nicotine as

Figure 4.2. The I/V relationship of the first basalar motoneurone. The membrane potential was stepped from a holding potential of -50 mV to -100, -80, -60, -40, -20 and 0 mV, and the evoked currents were measured after 50 ms (to allow a comparison with later experiments in which the duration of the command pulse was decreased to 50 ms). At potentials between -100 and -40 mV the I/V relationship is approximately linear, and the evoked current is small. However, at potentials positive to -40 mV the I/V relationship shows strong outward rectification and the amplitude of the evoked currents greatly increases.

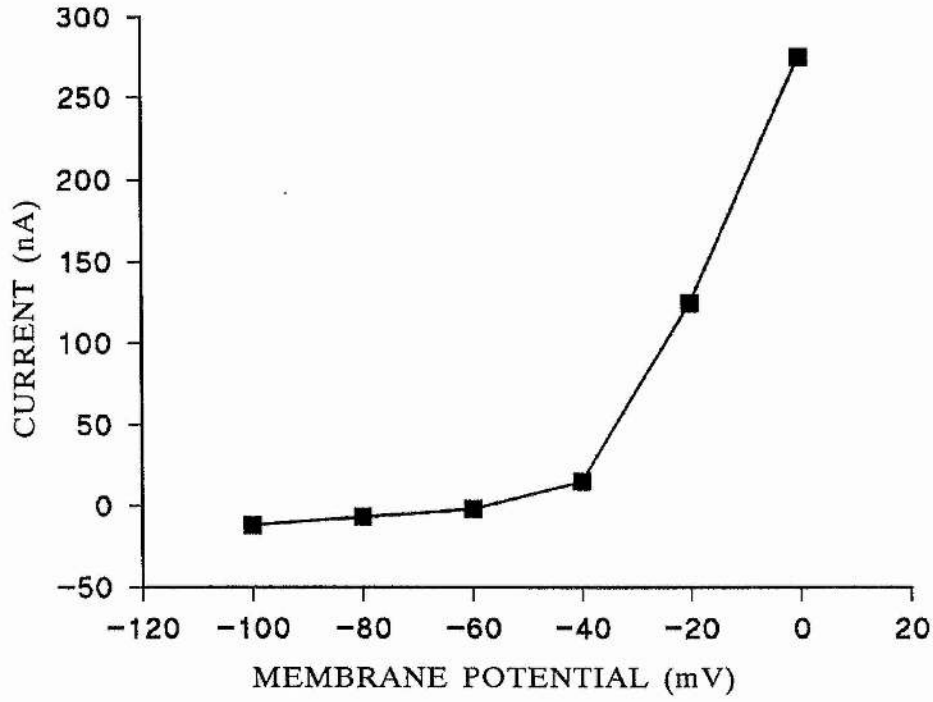

well as muscarinic agonists (Benson & Neumann, 1987; Benson, 1992; David & Pitman, 1993a). The effect on the first basalar motoneurone of (-)-nicotine (n=4) in the presence of α-BTX (10^{-6} M) was examined to determine whether these receptors have a mixed pharmacology.

Each drug was administered to give a bath concentration of 10^{-4} M. This is a relatively high concentration compared to that required in vertebrate preparations, but the potency of muscarinic drugs is lower in insects than vertebrates, and there are fewer binding sites for muscarinic ligands in insect nervous tissue compared to vertebrate (see Breer & Sattelle, 1987). Cholinergic agonists were also applied successfully at a concentration of 10^{-4} M in motoneurone D_f of the cockroach (David & Pitman, 1993a). The agonists were applied for 15 min and measurements taken after 1, 5, 10 and 15 min to allow a study of the time dependence of the response.

4.2.2.1. Carbachol

After pretreating the preparation with 10^{-6} M α-BTX for 1 h, 10^{-4} M CCh was applied to the cell (n=5), and the effect of the agonist is shown in Figure 4.3. Fifteen minutes' exposure to CCh resulted in a decrease in the amplitude of the sustained outward current in all preparations (Figure 4.3a) and the transient outward current evoked at -20 (n=2) and 0 mV (n=4). Carbachol induced an inward (n=4) or an outward (n=1) shift in the holding current.

The effect of CCh on the I/V relationship is shown in Figure 4.3b, while the CCh-induced current is shown in Figure 4.3c. The drug-induced current was obtained by subtracting the control currents from those produced in the presence of agonist. At potentials negative to -40 mV CCh evoked a small inward current in four cells out of five, which increased as the command potential became more negative from a minimum at -40 (n=4) or -60 mV (n=1). In the presence of CCh, this current component either increased to a maximum after five or ten minutes then decreased (n=3; Figure 4.3c), or decreased only (n=1). The maximum inward

Figure 4.3a. The effect of 15 min exposure to 10^{-4} M carbachol in the presence of 10^{-6} M α-BTX on the current evoked by stepping the membrane to -20 and 0 mV from a holding potential of -50 mV. Both the 'control' and 'carbachol' currents were recorded in the presence of α-BTX. Carbachol decreased the amplitude of the sustained outward current in all preparations and induced an inward shift in the holding current. Where a transient outward current was evoked (-20 mV, n=2; 0 mV, n=4), the amplitude was decreased.

Scale: vertical 50 nA
horizontal 100 ms

Figure 4.3b. The currents evoked in the motoneurone in (a) were measured after 50 ms and used to construct an I/V relationship of the neurone in the absence and presence (5, 15 min) of 10^{-4} M carbachol (in the presence of 10^{-6} M α-BTX).

Figure 4.3c. The carbachol-induced current, obtained by subtracting the 'control' currents from those obtained in the presence of agonist in (b). The drug induced an inward current at all potentials, small at potentials negative to approximately -40 mV, and increasing in size at more positive potentials.

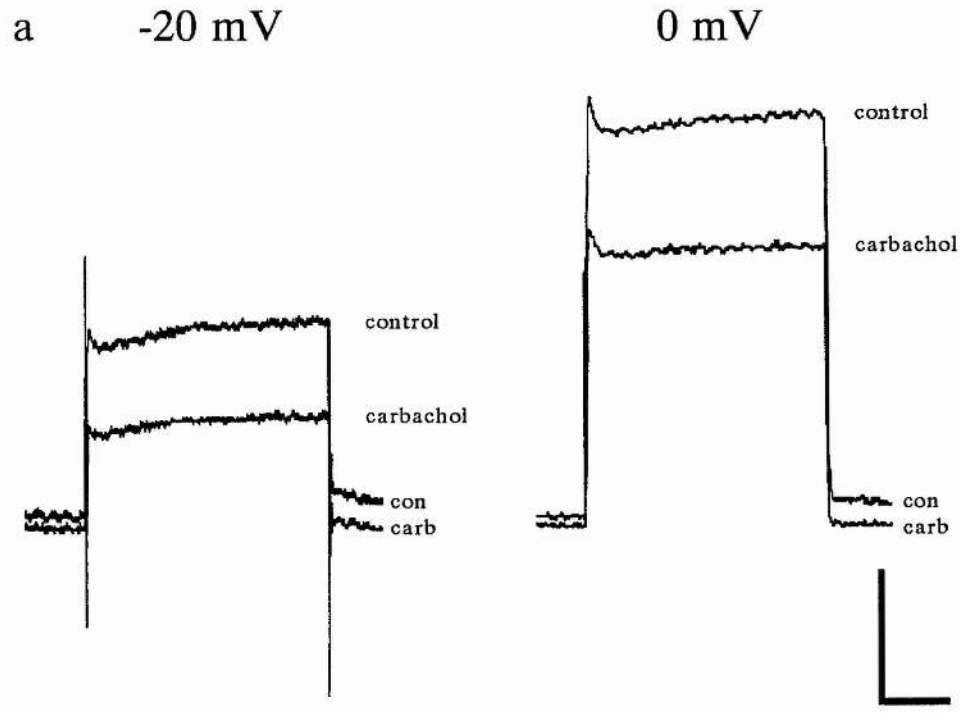

b

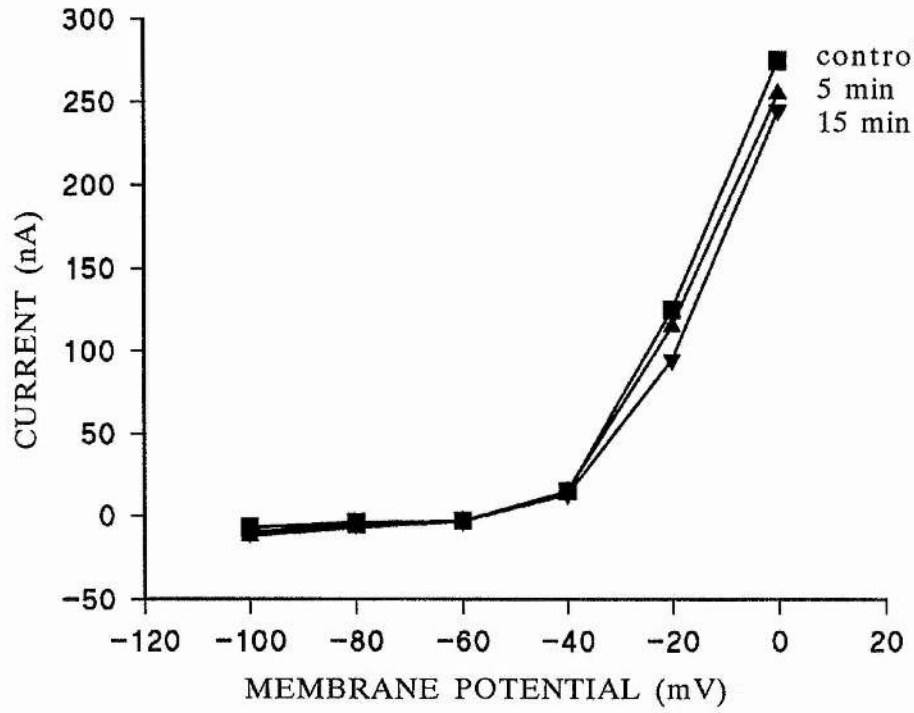
300
250
200
150
100
50
0
−50
CURRENT (nA)
control
5 min
15 min
−120
−100
−80
−60
−40
−20
0
20
MEMBRANE POTENTIAL (mV)

c

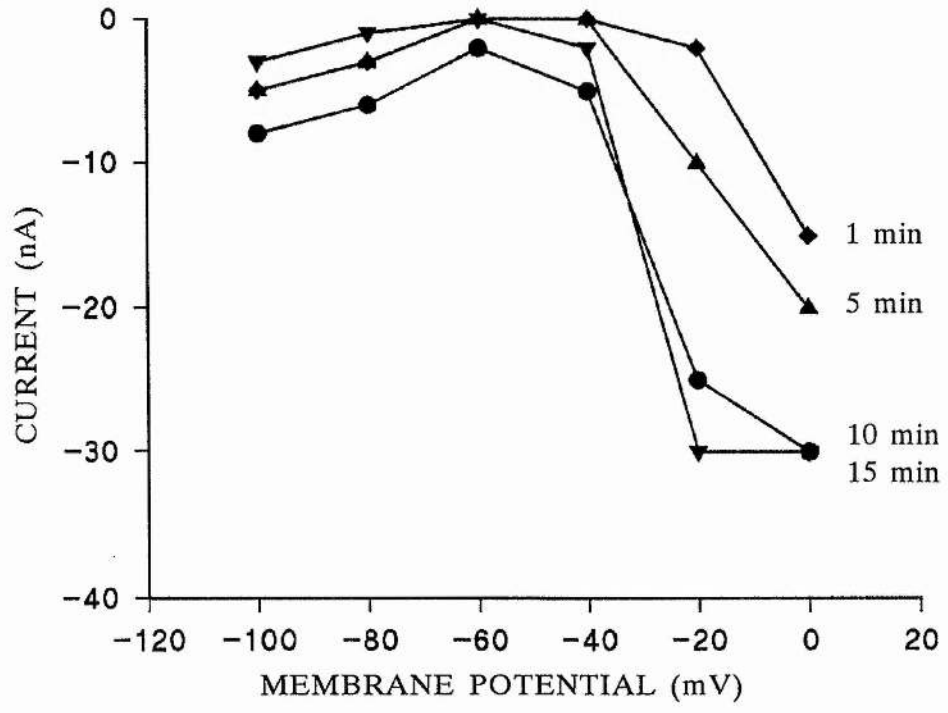
0
−10
−20
−30
−40
CURRENT (nA)
1 min
5 min
10 min
15 min
−120
−100
−80
−60
−40
−20
0
20
MEMBRANE POTENTIAL (mV)

current attained at -100 mV was 14·6 ± 3·2 nA (n=4). An outward increasing current, 10 nA after 15 min, was evoked in one cell. At potentials more positive than -40 mV, a larger inward current was evoked by CCh, increasing as the command potential became more positive. During exposure to agonist, the amplitude of this inward current component increased: after 15 min the amplitude was 65·0 ± 19·2 nA (n=5).

4.2.2.2. Muscarine

The effect of 10^{-4} M muscarine on the first basalar motoneurone was investigated (n=3) and typical results are shown in Figure 4.4. The sustained outward currents evoked in the motoneurone were reduced after 15 min exposure to agonist (Figure 4.4a; n=3), and there was an inward shift in the holding current.

The effect of muscarine on the I/V relationship of a neurone is shown in Figure 4.4b, and the muscarine-induced current in Figure 4.4c. The current evoked by muscarine is very similar to that produced by CCh in the presence of α-BTX (Figure 4.3). Muscarine had least effect at a command potential of -40 mV. At potentials negative to -40 mV an inward current was evoked by muscarine in two preparations, which increased as the command potential became more negative. During exposure to agonist, this inward current component increased to a maximum at 10 min and then decreased (n=1), or increased steadily over 15 min (n=1). In the third neurone, an inward current, which was relatively constant over 15 min, was evoked at -100 and -80 mV; at more positive potentials the current reversed, but became inwardly directed again at potentials positive to -20 mV. The maximum inward current evoked when the membrane was stepped to -100 mV was 21·7 ± 12·5 nA (n=3). At potentials more positive than -40 mV, muscarine initially evoked an outward current in two preparations, with an amplitude of 22·5 ± 1·8 nA (n=2) at 0 mV. This current component decreased and became inward after 5 min. In the third cell, in which the current reversed at -80 mV, the muscarine-induced current evoked at 0 mV was inward, and increased over time.

Figure 4.4a. The effect of 15 min exposure to 10^{-4} M muscarine on the current evoked by stepping the membrane from -50 mV to command potentials of -40, -20 and 0 mV. The drug decreased the amplitude of the sustained outward current and induced an inward shift in the holding current.

Scale: vertical 50 nA
horizontal 100 ms

Figure 4.4b. The currents evoked in the motoneurone in (a) were measured after 50 ms and used to construct an I/V relationship of the neurone in the absence and presence (5, 15 min) of 10^{-4} M muscarine.

Figure 4.4c. The muscarine-induced current obtained from the preparation in (b). An inward current was induced at potentials negative to approximately -40 mV. At potentials positive to -40 mV, an initial outward current was evoked, which decreased and became inward after 5 or 10 min.

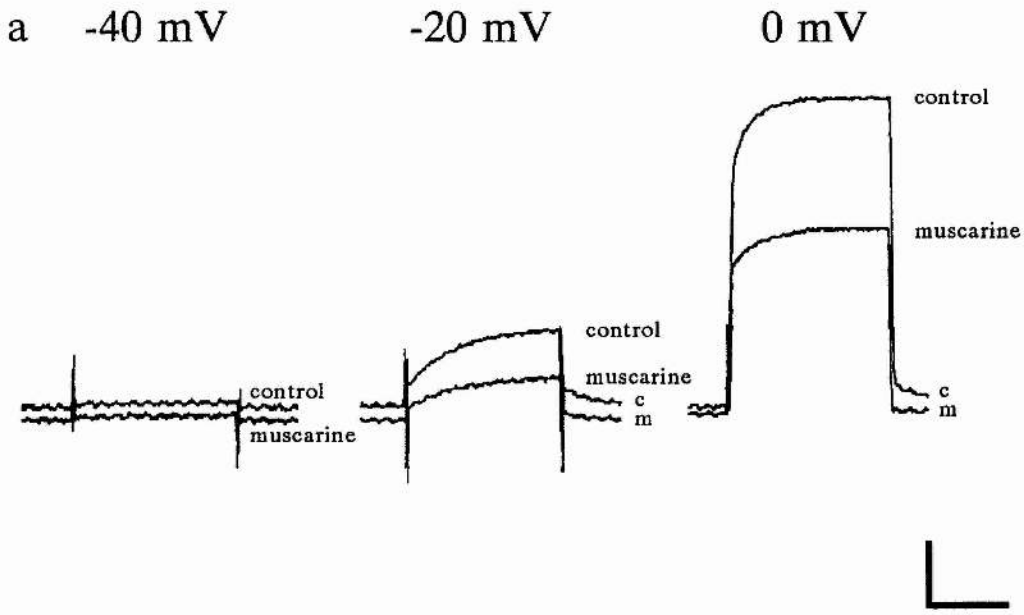

b

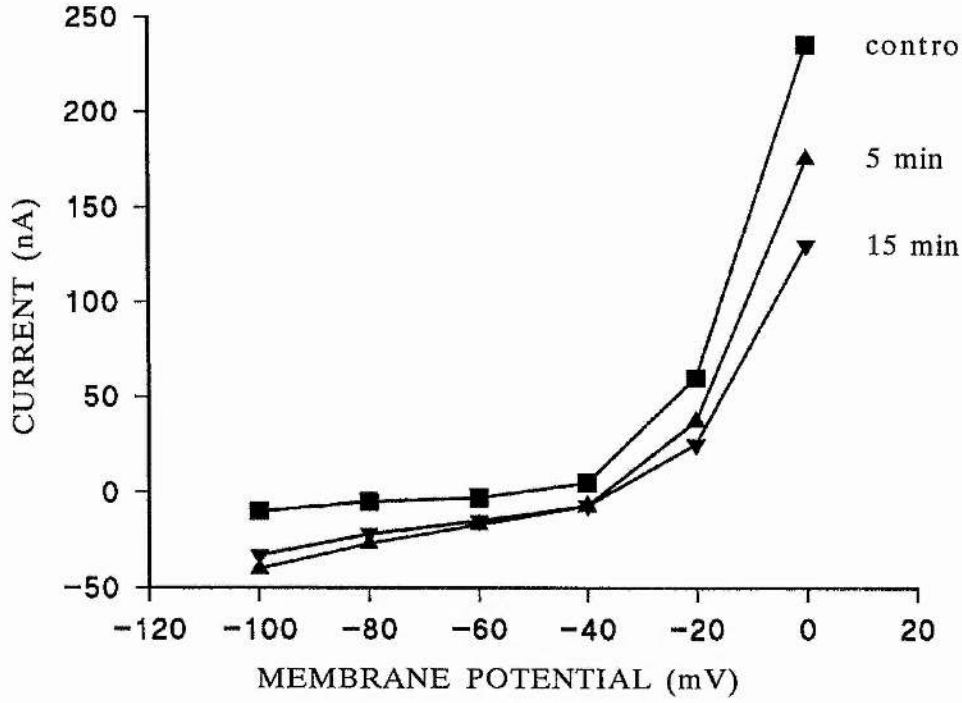
250
200
150
100
50
0
−50
CURRENT (nA)
−120
−100
−80
−60
−40
−20
0
20
MEMBRANE POTENTIAL (mV)
control
5 min
15 min

c

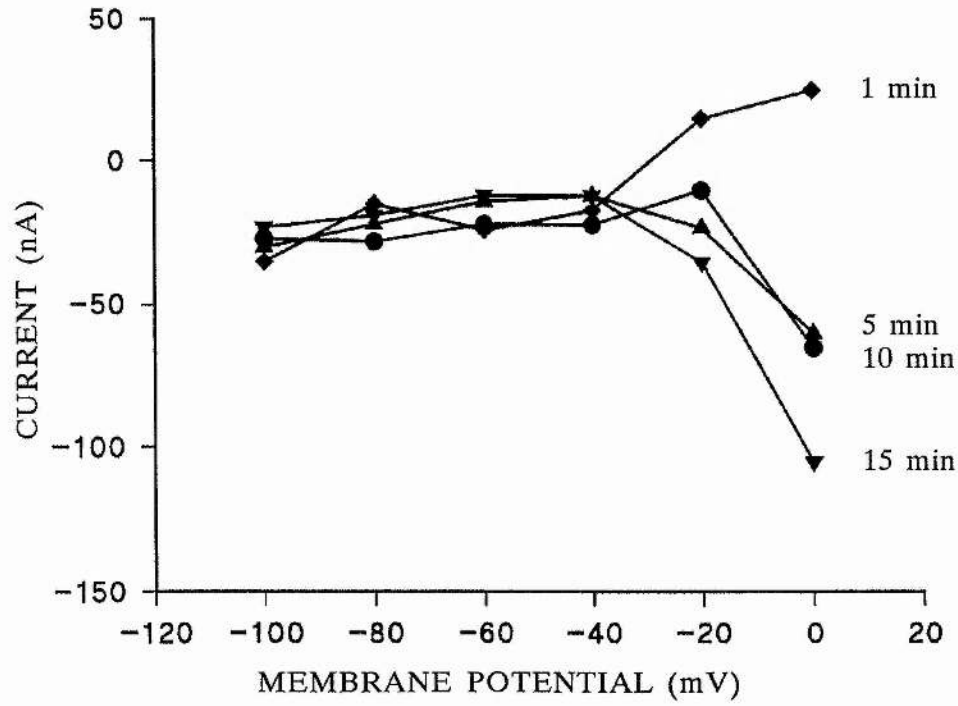
50
0
−50
−100
−150
CURRENT (nA)
−120
−100
−80
−60
−40
−20
0
20
MEMBRANE POTENTIAL (mV)
1 min
5 min
10 min
15 min

Both the outward and inward currents evoked positive to -40 mV increased as the command potential was made more positive. The maximum inward current reached at 0 mV after 15 min was 63·3 ± 9·6 nA (n=3).

4.2.2.3. McN-A-343

A typical response of a neurone to 10^{-4} M McN-A-343 is shown in Figure 4.5. McN-A-343 had a similar effect to CCh in the presence of α-BTX (n=3). After 15 min exposure to McN-A-343, the amplitude of both the sustained outward current (n=3) and the transient current evoked at 0 mV (n=1) was decreased. McN-A-343 induced an inward shift in the holding current.

The effect of McN-A-343 on the I/V relationship is shown in Figure 4.5b, while the McN-A-343-induced current is shown in Figure 4.5c. When the membrane potential was stepped to potentials negative to -40 mV, a small inward current was evoked, which increased as the command potential became more negative from a minimum at -40 mV. This current component increased during 15 min exposure to agonist (n=2) or increased to a maximum after 10 min and then decreased (n=1), as shown in Figure 4.5c. The maximum amplitude attained at -100 mV was 6·7 ± 2·2 nA (n=3). McN-A-343 also evoked an inward current at potentials positive to -40 mV, increasing as the command potential became more positive. With increasing time of exposure to McN-A-343, the amplitude of this current component increased. In one preparation, an outward current was initially evoked over this potential range, which decreased in size from 5 nA at a command potential of 0 mV and became inwardly directed after 5 min. The amplitude of the inward current at 0 mV was 58·3 ± 25·2 nA (n=3) after 15 min.

4.2.2.4. Nicotine

10^{-4} M nicotine was applied to the neurone after 1 h exposure to 10^{-6} M α-BTX (n=4). After 15 min, nicotine decreased the amplitude of the sustained outward current in all preparations (Figure 4.6a), and decreased the amplitude of

Figure 4.5a. The effect of 15 min exposure to 10^{-4} M McN-A-343 on the current evoked by stepping the membrane to -40, -20 and 0 mV from a holding potential of -50 mV. The drug decreased the amplitude of the sustained current and decreased the amplitude of the transient outward current evoked at 0 mV (n=1), and induced an inward shift in the holding current.

Scale: vertical 100 nA
horizontal 100 ms

Figure 4.5b. The currents evoked in the motoneurone measured 50 ms from the start on the command potential were used to construct an I/V relationship of the neurone in the absence and presence (5, 15 min) of 10^{-4} M McN-A-343 (different preparation to (a)).

Figure 4.5c. The McN-A-343-induced current obtained from the preparation in (b). The drug induced an inward current at potentials negative to -40 mV in all preparations (n=3). At more positive potentials, McN-A-343 evoked an inward current, which increased during exposure to drug; in this preparation, the inward current was preceded by an initial outward current.

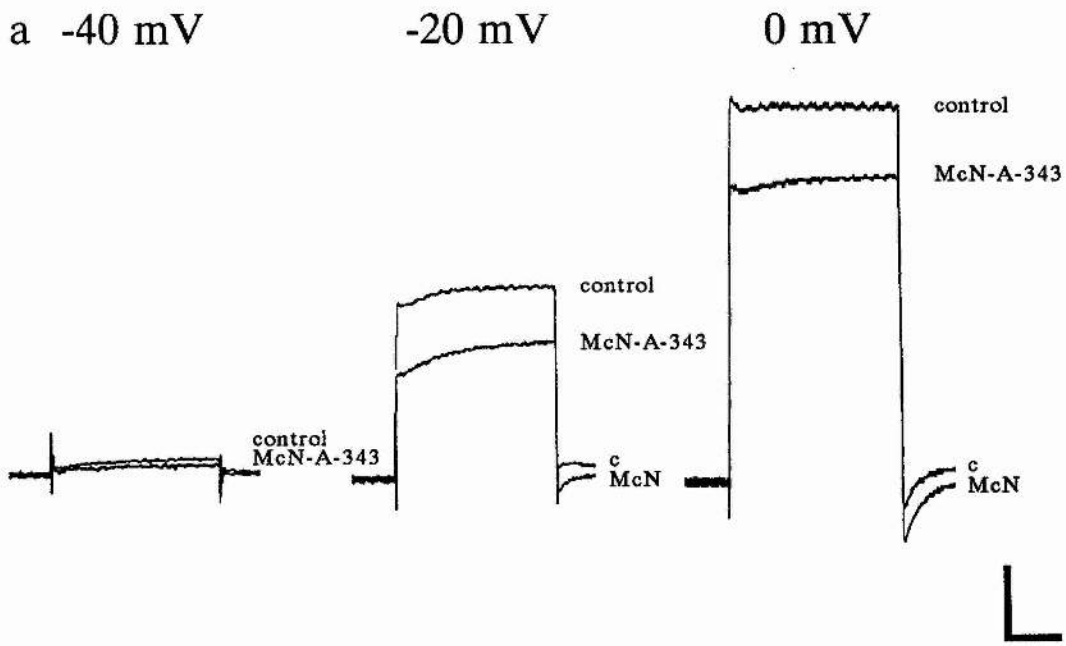

b

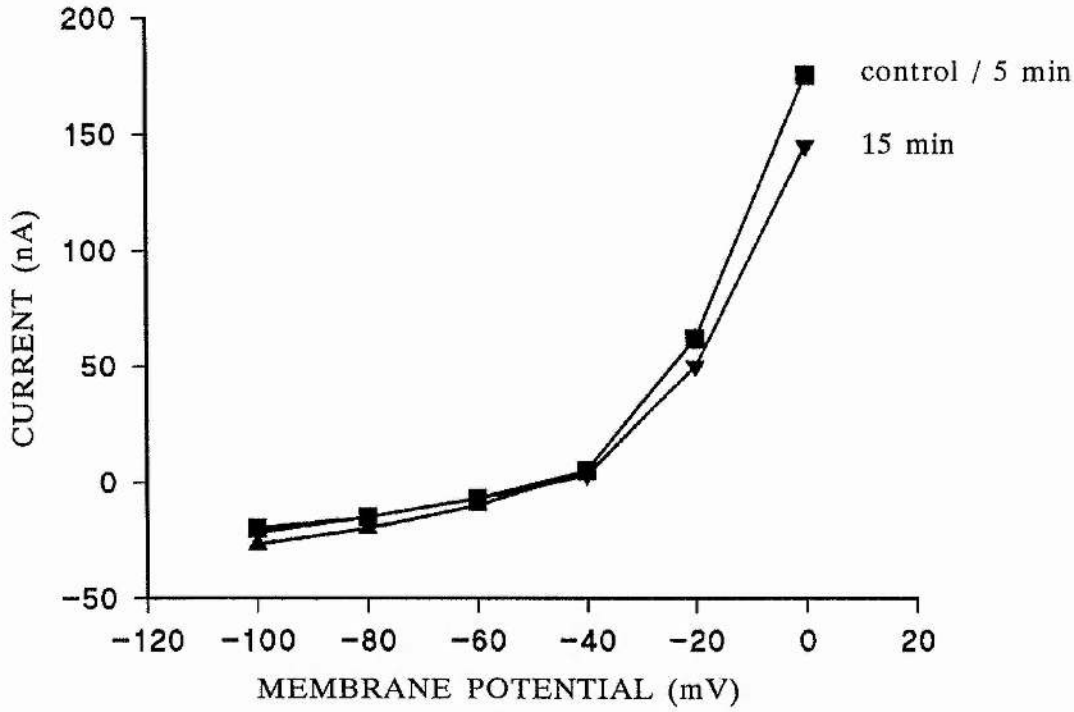
200
150
100
50
0
−50
CURRENT (nA)
−120
−100
−80
−60
−40
−20
0
20
MEMBRANE POTENTIAL (mV)
control / 5 min
15 min

c

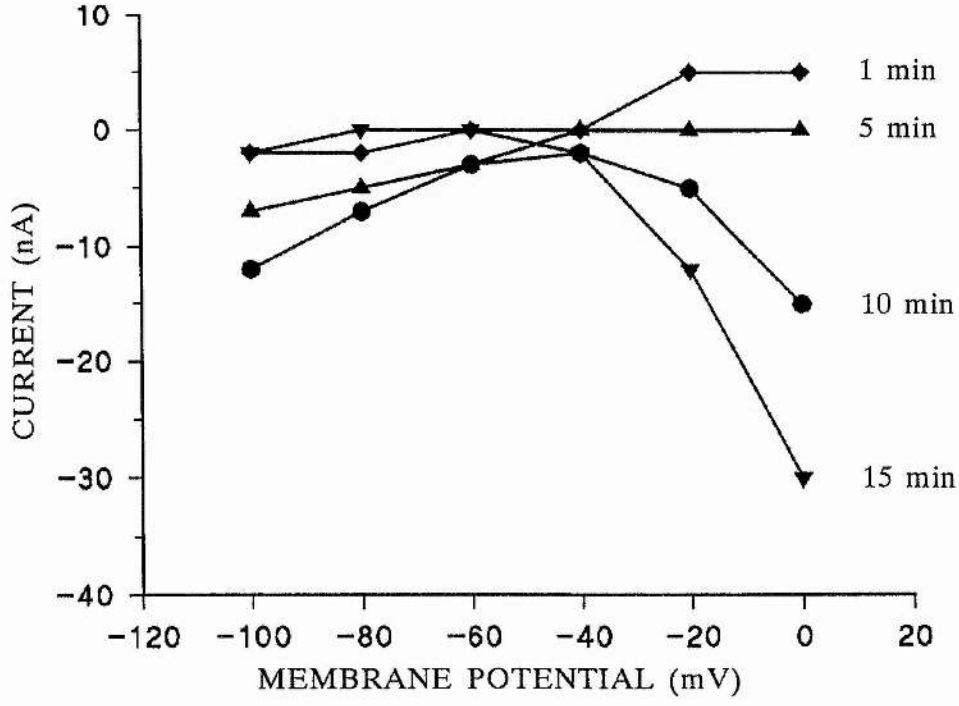
10
0
−10
−20
−30
−40
CURRENT (nA)
−120
−100
−80
−60
−40
−20
0
20
MEMBRANE POTENTIAL (mV)
1 min
5 min
10 min
15 min

Figure 4.6a. The effect of 15 min exposure to 10^{-4} M nicotine in the presence of 10^{-6} M α-BTX on the current evoked by stepping the membrane from -50 mV to command potentials of -20 and 0 mV. Nicotine decreased the amplitude of the sustained outward current in all preparations and induced an inward shift in the holding current. Where a transient outward current was evoked (0 mV, n=1), the amplitude was decreased.

Scale: vertical 100 nA
horizontal 100 ms

Figure 4.6b. The currents evoked in the motoneurone (different preparation to (a)) were measured after 50 ms and used to construct an I/V relationship of the neurone in the absence and presence (5, 15 min) of 10^{-4} M nicotine (in the presence of 10^{-6} M α-BTX).

Figure 4.6c. The nicotine-induced current obtained from the preparation in (b). An inward current was induced at potentials negative to approximately -40 mV. At potentials positive to -40 mV, an initial outward current was evoked in most preparations, which decreased and became inward after 5 or 10 min.

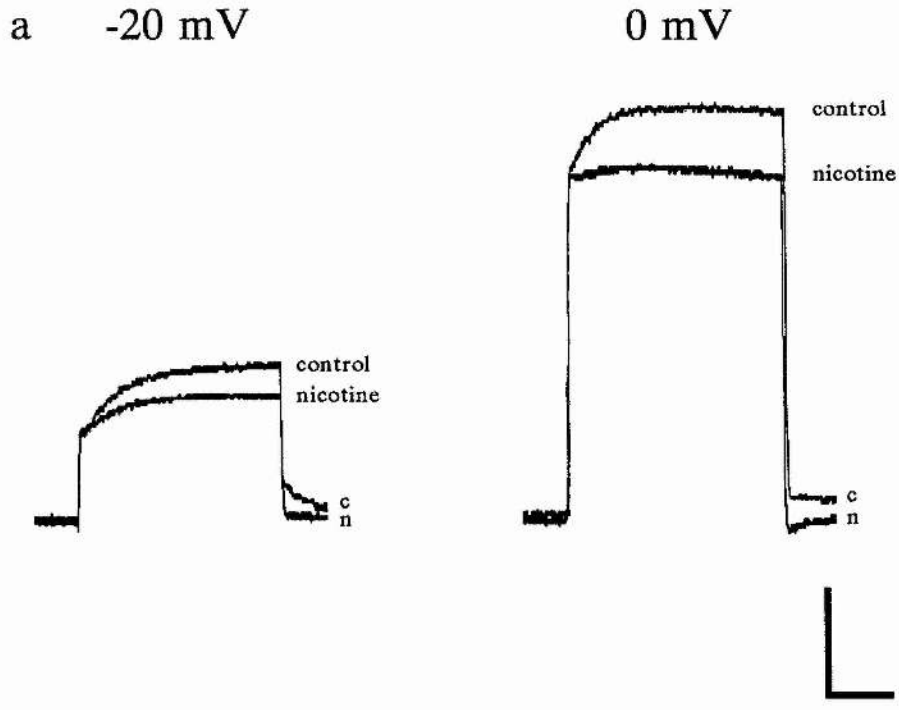

b

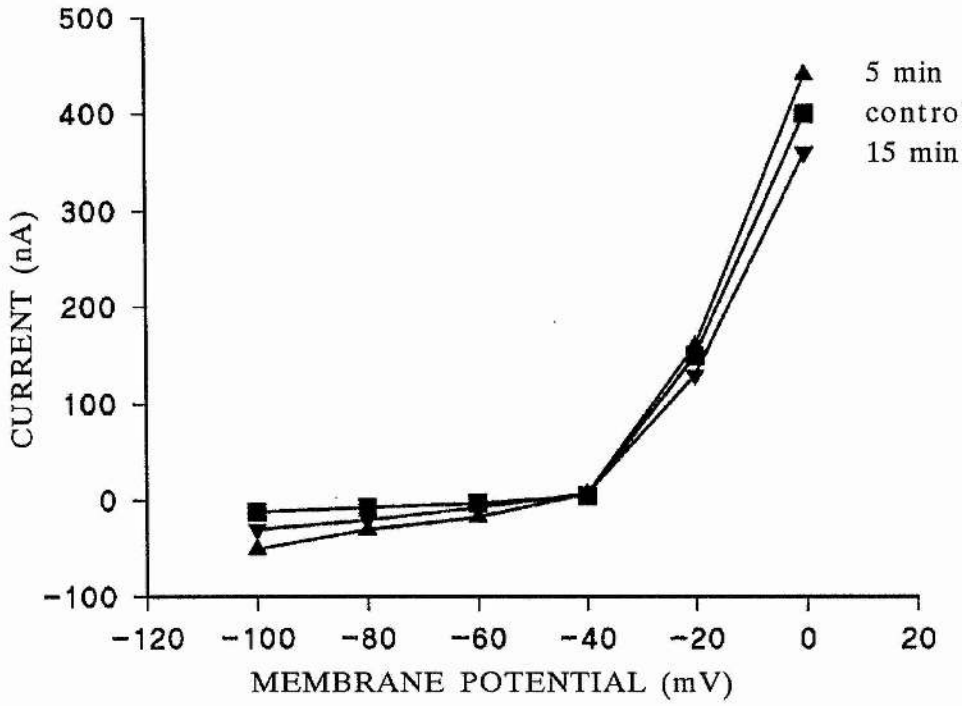
500
400
300
200
100
0
−100
CURRENT (nA)
−120
−100
−80
−60
−40
−20
0
20
MEMBRANE POTENTIAL (mV)
5 min
control
15 min

c

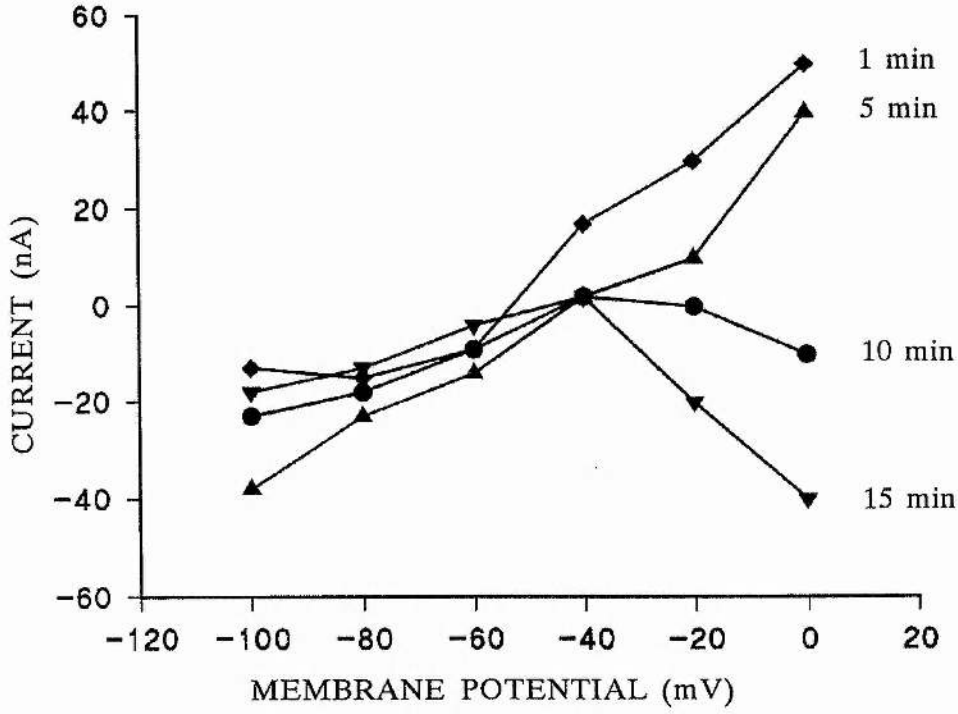
60
40
20
0
−20
−40
−60
CURRENT (nA)
−120
−100
−80
−60
−40
−20
0
20
MEMBRANE POTENTIAL (mV)
1 min
5 min
10 min
15 min

the outward transient currents evoked in one neurone at -20 and 0 mV. Exposure to agonist resulted in an inward shift in the holding current.

The effect of nicotine on the I/V relationship of a neurone can be found in Figure 4.6b, and the nicotine-induced current in Figure 4.6c. Nicotine had least effect at a command potential of -40 mV. An inward current was evoked at potentials negative to -40 mV, increasing as the command potential was made more negative. In the presence of nicotine, this current component increased to a maximum after 5 or 10 min, then decreased (n=3), and in the fourth it increased only (Figure 4.6c). The maximum amplitude attained at -100 mV was 26·0 ± 5·5 nA (n=4). At potentials positive to -40 mV, nicotine initially induced an outward current in three preparations, which increased as the command potential became more positive. At 0 mV the current reached 30·0 ± 9·4 nA (n=3) after 1 min, and subsequently decreased and became inwardly directed after 5 or 10 min. The fourth cell exhibited an inward current only, which increased over 15 min. The inward currents evoked at 0 mV reached a maximum of 62·5 ± 19·4 nA (n=4).

4.2.3. EFFECT OF SCOPOLAMINE ON THE RESPONSE TO McN-A-343 AND NICOTINE IN THE PRESENCE OF α-BTX

To further investigate the pharmacology of these α-BTX-resistant receptors, 10^{-7} M of the muscarinic antagonist (-)scopolamine hydrochloride was added to establish whether the responses to McN-A-343 and nicotine are blocked by this muscarinic antagonist. If this were the case, it implies that the agonists are binding to muscarinic receptors.

These experiments were carried out over a longer period of time than those described above. To limit the redistribution of ions the following changes were made to the command pulse protocol: 1. the membrane potential was jumped from -50 mV to 0 mV once every minute, instead of a range of potentials between -100 and 0 mV; 2. the pulse duration was reduced from 250-300 ms to 50 ms.

4.2.3.1. McN-A-343

Figure 4.7a shows the effect of 10^{-7} M scopolamine on the current induced by 10^{-4} M McN-A-343. The addition of McN-A-343 after 10 min exposure to scopolamine had no effect on the amplitude of the outward current.

After washing the preparation with fresh saline, 10^{-4} M McN-A-343 was reapplied (Figure 4.7b). This time there was a significant decrease in the current amplitude: over the period of application, the current decreased steadily: after 15 min the outward current was decreased by approximately 30 nA. After washing the preparation with fresh saline, the amplitude of the outward currents increased towards the control values.

4.2.3.2. Nicotine

To examine whether nicotine is operating on the same receptors as the muscarinic agonists, it was applied in the presence of 10^{-7} M scopolamine. The results of this experiment are illustrated in Figure 4.8. 10^{-4} M nicotine was applied 10 min after scopolamine and Figure 4.8a shows that it had no detectable effect over a period of 15 min. When 10^{-4} M nicotine was reapplied after washing the preparation with fresh saline, an inward current was evoked, as depicted in Figure 4.8b. There is a small degree of current run-down before addition of the drug, probably due to the fact that the cell has been voltage clamped for several hours, but there appears to be a decrease in the outward current on addition of nicotine, shown by the arrow. The outward current decreases continually in the presence of nicotine: after 15 min it has fallen by approximately 30 nA.

4.2.4. EFFECT OF McN-A-343 ON AN ISOLATED CELL BODY

To determine whether these 'mixed' receptors are located on the soma membrane of the motoneurone, the cell body was isolated from its axon by undercutting with a pair of fine scissors. The isolated cell body remained on the

Figure 4.7. The decrease in the outward current caused by 10^{-4} M McN-A-343 can be reversibly blocked by the muscarinic antagonist scopolamine (10^{-7} M). The cell was stepped from a holding potential of -50 mV to 0 mV (once every minute, pulse duration 50 ms).

Figure 4.7a. McN-A-343 was applied to the motoneurone 10 min after scopolamine, and had no effect on the amplitude of the outward current over the 15 min period of exposure to drug.

Figure 4.7b. After washing scopolamine from the preparation, McN-A-343 was reapplied, and caused a decrease in the amplitude of the outward current. The amplitude of the outward currents returns towards the control amplitude when McN-A-343 was removed from the preparation.

Scale: vertical 200 nA
horizontal 10 min

a

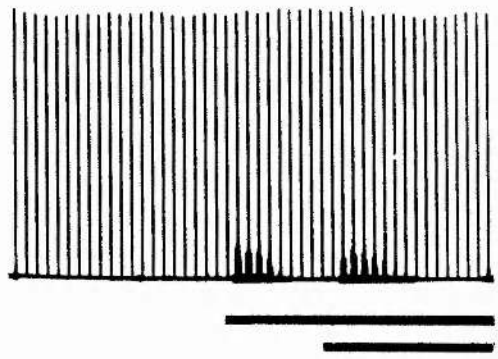

scopolamine
McN-A-343

b

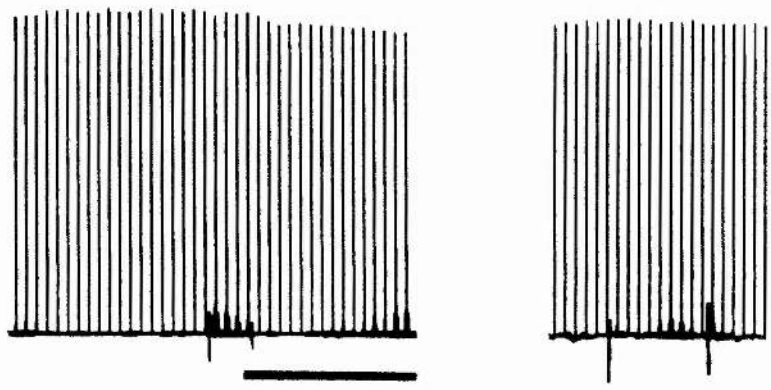

McN-A-343

wash

Figure 4.8. The effect of 10^{-7} M scopolamine on the suppression of the outward current caused by 10^{-4} M nicotine in the presence of 10^{-6} M α-BTX. The cell was stepped from a holding potential of -50 mV to 0 mV (once every minute, pulse duration 50 ms).

Figure 4.8a. After pretreating the preparation with scopolamine for 10 min, the addition of nicotine had no detectable effect over a period of 15 min.

Figure 4.8b. After washing scopolamine from the preparation, the addition of nicotine appears to have decreased the amplitude of the current evoked at 0 mV, as shown by the arrow.

Scale: vertical 100 nA
horizontal 10 min

a

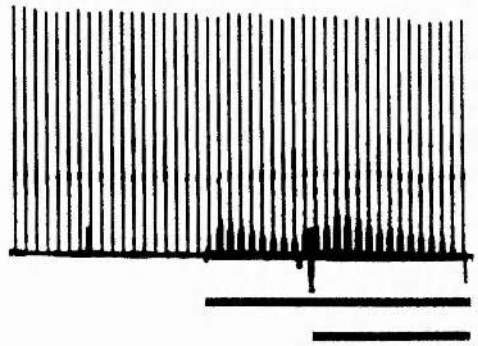

b

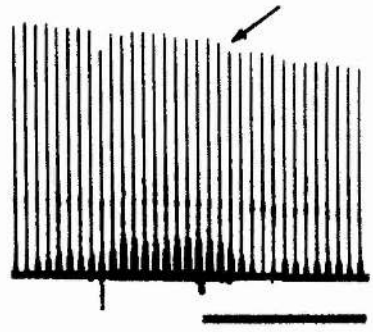

surface of the ganglion for the duration of the experiment. The protocol was similar to that used to examine the effects of the cholinergic agonists above, with two small changes: the pulse duration was decreased to 50 ms, and the holding potential was increased to -80 mV. An axotomised neurone will be less stable than an intact cell, and making these small changes in the protocol will minimise the probability that cell death will occur. At the more positive holding potential, the cell is slightly more depolarised than normal (mean -54 mV) and it is possible that a proportion of voltage-dependent ion channels are open; this was satisfactory in the previous experiments on an intact neurone, but in the present experiments could contribute to the instability of the neurone.

The effect of 15 min exposure to 10^{-4} M McN-A-343 on the outward currents evoked in the first basalar motoneurone (n=2) is displayed in Figure 4.9. The amplitude of the sustained outward current was reduced, and there was an inward shift in the holding current.

The I/V relationship in the presence of McN-A-343 is shown in Figure 4.9b, and the McN-A-343-induced current is shown in Figure 4.9c. The I/V relationship illustrates that the isolated cell body, like the intact cell, shows rectification positive to -40 mV. At potentials negative to -40 mV an inward current was produced, which increased from a minimum at -60 mV as the command potential became more negative. During 15 min exposure to agonist, this current component increased; the maximum amplitude reached at -100 mV was 5 or 20 nA. A larger inward current was evoked at potentials more positive than -40 mV. This current component increased as the command potential was made more positive. In the presence of McN-A-343 the amplitude of the current increased and reached an amplitude of 50 or 75 nA at 0 mV after 15 min. In the preparation shown here, a small (3 nA) outward current was evoked after 1 min at -40 and -30 mV, which was not observed in the other preparation. When the effect of McN-A-343 on an isolated cell body is compared with the McN-A-343-induced current in an intact preparation at a holding potential of -80 mV (Figure 5.6) there

Figure 4.9a. The effect of 15 min exposure to 10^{-4} M McN-A-343 on the current evoked in a functionally isolated cell body by stepping the membrane from a holding potential of -80 mV to command potentials of -20 and 0 mV. McN-A-343 decreased the amplitude of the sustained outward current, and induced an inward shift in the holding current in both preparations.

Scale: vertical 50 nA
horizontal 50 ms

Figure 4.9b. The currents evoked in the isolated cell body in (a) were measured after 50 ms and used to construct an I/V relationship of the neurone in the absence and presence (5, 15 min) of 10^{-4} M McN-A-343.

Figure 4.9c. The McN-A-343-induced current obtained from the preparation in (b). An inward current was evoked at potentials negative to -40 mV, which increased in amplitude over the 15 min period of exposure to agonist. A larger inward current was produced at more positive potentials.

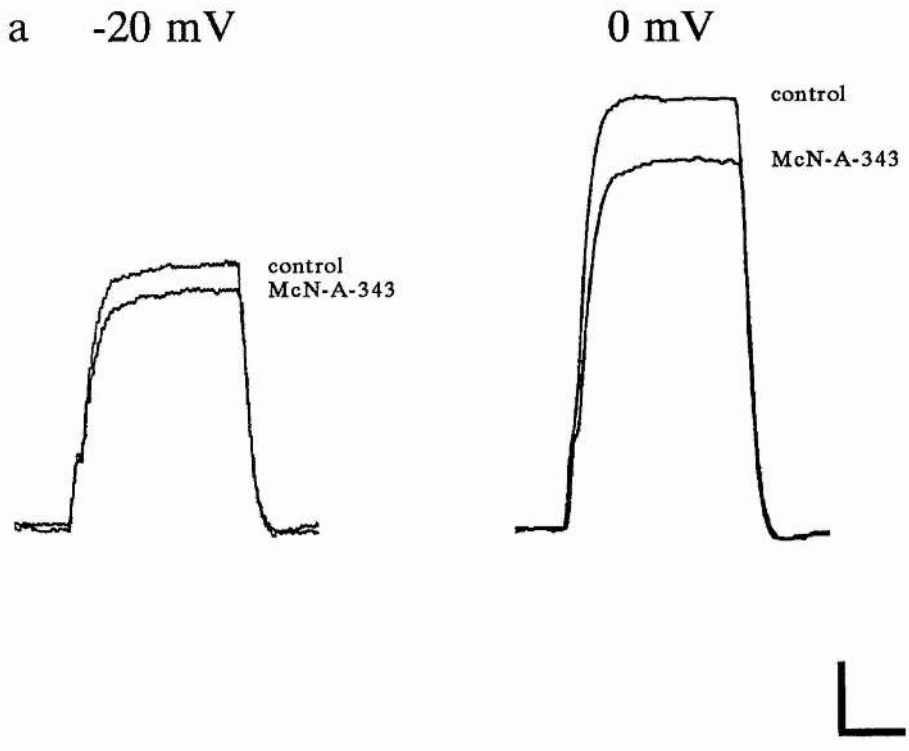

b

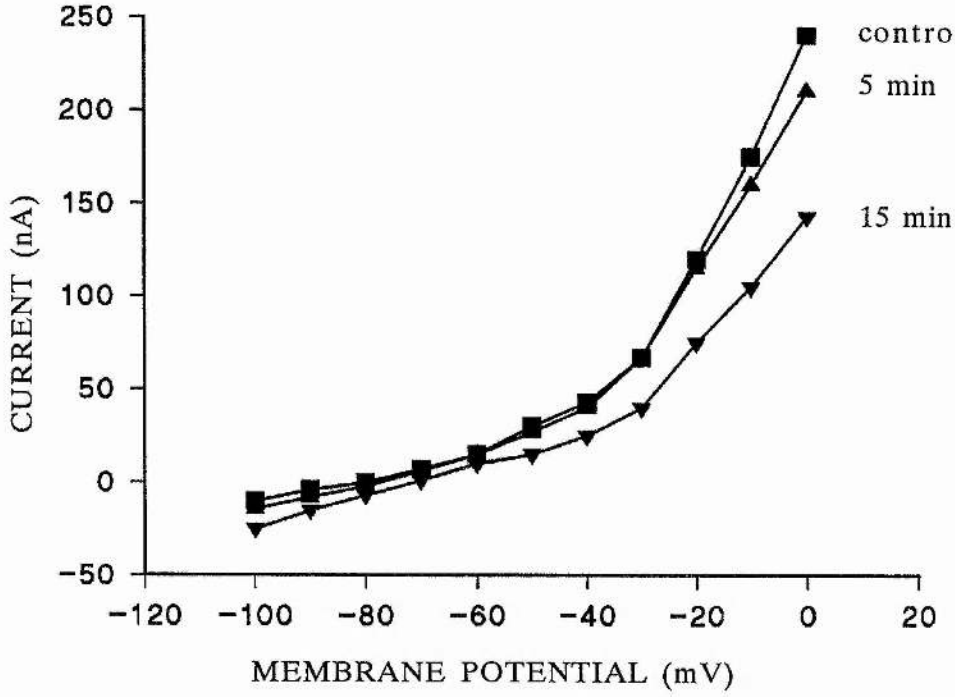
250
200
150
100
50
0
−50
CURRENT (nA)
−120
−100
−80
−60
−40
−20
0
20
MEMBRANE POTENTIAL (mV)
control
5 min
15 min

c

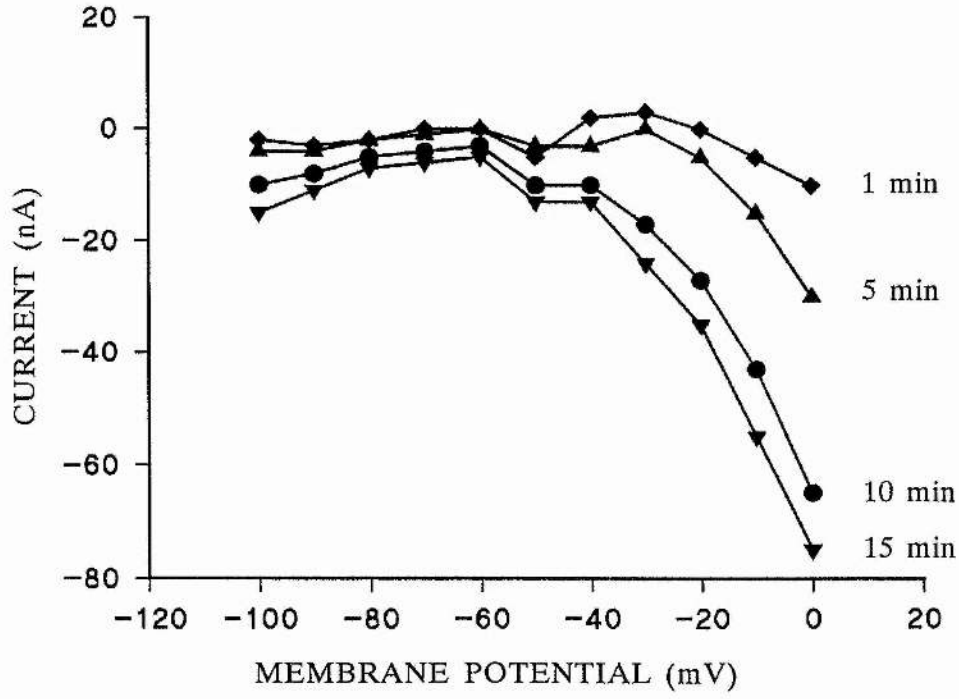
20
0
−20
−40
−60
−80
CURRENT (nA)
−120
−100
−80
−60
−40
−20
0
20
MEMBRANE POTENTIAL (mV)
1 min
5 min
10 min
15 min

is little difference, implying that these receptors must be located on the soma membrane.

4.3. DISCUSSION

The data presented here confirm that there is a population of α-bungarotoxin-resistant cholinergic receptors on the first basalar motoneurone of the locust, *Schistocerca gregaria*. They are activated by the cholinergic agonists carbachol, muscarine, McN-A-343 and nicotine, and thus appear to have a 'mixed' cholinergic pharmacology.

An inward current was evoked in the motoneurone when the membrane potential was stepped to potentials more negative than the holding potential. At command potentials more positive than the holding potential an outward current was evoked. In approximately 50 % of cells, the outward current consisted of a relaxation that gave way to a sustained outward current. The currents evoked in the remainder of cells exhibited an initial transient current preceding the sustained outward current. The transient component of the outward current was activated at potentials positive to -40 mV, and increased in amplitude as the command potential was moved further from the holding potential. The transient current recorded in motoneurone D_f of the cockroach (David & Pitman, in preparation) showed similar voltage dependency, and increased in amplitude with increasing command potential to a maximum at 20 mV before decreasing. A transient current, activated at command potentials more positive than -60 to -40 mV, was also recorded from the basalar/coxal depressor motoneurone of the cockroach by Nightingale & Pitman (1989). The amplitude of the transient could be increased by applying a hyperpolarising prepulse as negative as -140 mV, and also by increasing the command potential.

The cholinergic agonists applied to the motoneurone all decreased the amplitude of both the sustained current and the transient current. The sustained outward current of the first basalar motoneurone could be compared to the M-current: a non-inactivating, voltage-sensitive K^+ current that is inhibited by

muscarine (the M-current is also inhibited by substances such as bradykinin and LHRH: see Introduction, 1.3.1.5.). It was first described in bullfrog sympathetic neurones (Brown & Adams, 1980) and has since been identified in several vertebrate preparations including rat sympathetic neurones, hippocampal cells, human neocortical cells, spinal motoneurones, NG108-15 cells and toad smooth muscle (reviewed by Brown, 1988). The current is activated by stepping the membrane to command potentials more positive than the resting potential. In the presence of muscarinic agonists, the M-current is inhibited, leading to a decrease in the outward current. Thus the muscarinic agonist-sensitive current recorded from the first basalar motoneurone may be analogous to the M-current of vertebrate cells; if so, it would be the first invertebrate example. However, the kinetics of the M-current are slower than those of the muscarinic-agonist-sensitive current recorded from the first basalar motoneurone. Further analysis of the current, including the second messengers involved, is required to confirm whether it is comparable to the vertebrate M-current. Muscarinic agonists also decreased the transient outward current in cultured rat hippocampal neurones (Nakajima et al, 1986) and bullfrog sympathetic neurones (Kurenny et al, 1994). However, muscarinic agonists increased the amplitude of the transient in rat neostriatal neurones (Akins et al, 1990).

The currents evoked in the motoneurone were measured after 50 ms and the amplitudes used to construct an I/V relationship for the cell. The current evoked at potentials more negative than -40 mV was small, generally a few nA in amplitude. At potentials positive to -40 mV the I/V relationship shows strong rectification and a large outward current is evoked in the neurone.

The cholinergic agonists applied to the neurone all had a similar effect. At membrane potentials between -100 and 0 mV an inward current was evoked. A small current was induced negative to -40 mV, which increased at more positive potentials. The current was time dependent, and generally increased over 15 min

exposure to agonist; in some preparations at potentials negative to -40 mV, however, a maximum was reached after 5 or 10 min, after which the amplitude of the current began to decrease. This could suggest the involvement of a second messenger, and the decrease in current amplitude could be due to its sequestration, degradation or turnover. The greatest effect of the agonists was at potentials more positive than -40 mV, the region of the I/V relationship exhibiting strong outward rectification. In approximately 50 % of the preparations tested, the inward current at potentials positive to -40 mV was preceded by an outward current. This current decreased until after 5 or 10 min when it reversed and became inwardly directed. The dual effect of the agonists at potentials more positive than -40 mV suggests that McN-A-343 modulates two currents over this potential range: an outward current which is evoked within 1 min of receptor activation, and a more slowly-developing inward current. The ionic currents involved in the response to muscarinic agonists are investigated in the following chapter.

The results from the previous chapter showed that the α-BTX-resistant receptors on the first basalar motoneurone have a muscarinic pharmacology because the response to exogenous ACh could be reduced by muscarinic antagonists. The experiments presented here confirm this result because the muscarinic agonists muscarine and McN-A-343 decreased the amplitude of the outward current evoked in the neurone. In addition, the McN-A-343-induced current could be blocked by the muscarinic antagonist scopolamine, verifying that this agonist is acting on muscarinic receptors. It is assumed that muscarine and the non-selective cholinergic agonist carbachol are acting on the same receptors because of the similarity of the drug-induced currents. However, unlike the 'classical' muscarinic receptors described in vertebrate preparations, these receptors also respond to nicotine, and are therefore more correctly described as 'mixed' cholinergic receptors. This effect of nicotine could not be attributed to an

action on nicotinic receptors that remained unblocked by α-BTX, or to a non-specific action on non-cholinergic receptors because the response was blocked by scopolamine. Many of the examples of 'mixed' cholinergic receptors described so far are in invertebrate preparations, for example the cockroach motoneurone D_f (David & Pitman, 1993a), locust central neurones (Benson, 1992) and housefly heads (Aziz & Eldefrawi, 1973). Benson (1992) has described cholinergic receptors on isolated, unidentified neurones of *Locusta* which are activated by nicotine and can be blocked by the muscarinic antagonists HHSiD and 4-DAMP. However, the receptors are also blocked by α-BTX, so cannot be directly compared with the receptors on the first basalar motoneurone or the other examples described above. 'Mixed' cholinergic receptors have also been found in vertebrate preparations such as bovine chromaffin cells (Shirvan et al, 1991) and frog tadpole skin (Cox, 1993). It is quite possible that receptors in other preparations which have been assumed to be 'classical' muscarinic receptors also respond to nicotinic agonists, but the effect of these agents upon the receptors has never been studied.

In most of the experiments presented here, the currents evoked in the presence of the agonists did not return to control values after washing with fresh saline. The rate of saline flow during washing was relatively slow in these experiments; however, recovery could be demonstrated by increasing the flow rate, as in the experiments in which the effect of scopolamine on the currents evoked by McN-A-343 (Figure 4.7), and the input resistance and spike threshold were measured (Chapter 3). A long period of time was required for the currents to return to the control amplitude: measurements were taken after 1 h. This proves that the decrease in current amplitude caused by the drugs was not due to cell death. David & Pitman (1993a) showed recovery from agonist application in motoneurone D_f after the addition of cholinergic agonists at a concentration of 10^{-4} M, although it required over 40 min to return to control values. They

suggested that the long period required for recovery was indicative of the involvement of a second messenger. Applying the agonist for 15 min, as in the experiments presented here, may have caused near maximal stimulation of the enzyme synthesising the second messenger with the result that a very large amount of second messenger would be produced under these conditions. If the rate of synthesis is greater than the rate of breakdown, accumulation of the second messenger will occur. When the agonist is removed, the second messenger concentration would be far higher than normal physiological levels, and would take a relatively long time to return to the basal level. This may result in the effects of the agonist outlasting the period of drug application. Indeed, Felder et al (1989) found that the carbachol-stimulated increase in the levels of second messengers in A9 L cells was sustained for at least 15 min after removal of the agonist.

The 'mixed' cholinergic receptors described in this study appear to be present on the soma membrane of the first basalar motoneurone, since the McN-A-343-induced current recorded from an isolated cell body was similar to that evoked in an intact cell. There are no known examples of chemical synapses onto the cell bodies of insect neurones, but several studies have demonstrated that neurones respond to ionophoretically-applied neurotransmitters, which is persuasive evidence for the presence of receptors on the cell body of neurones (see Pitman, 1985 for review). In addition, experiments on somata freshly isolated from locust ganglia have demonstrated the presence of somatic receptors (there are no reports of similar experiments in other insect species). ACh receptors are present on the isolated cell bodies of *Locusta* (Benson, 1992) and *Schistocerca* (Usherwood et al, 1980; Suter & Usherwood, 1985). GABA receptors have been found on isolated somata of *Schistocerca* (Giles & Usherwood, 1985; Lees et al, 1987; Whitton et al, 1994) and *Locusta* (Lees et al, 1987). L-glutamate (Usherwood et al, 1980; Giles & Usherwood, 1985), octopamine (Usherwood et

al, 1980; Suter, 1986) and serotonin (Usherwood et al, 1980; Bermudez et al, 1992) receptors are also present on isolated somata of *Schistocerca*. The question arises from these data, what is the function, if any, of these extrasynaptic receptors? A possible explanation is that the receptors are newly-synthesised, and are transported in the cell membrane from the cell body to the synapses. They would therefore be unlikely to be functional, somatic receptors. However, the possibility also exists that somatic receptors could be available to respond to neuromodulatory compounds more widely released throughout the ganglion.

SUMMARY

When the membrane potential was stepped from a holding potential of -50 mV to more negative potentials, small, square, inward currents were produced. At potentials positive to -50 mV outward currents were evoked. The addition of agonist decreased the amplitude of the sustained outward current; if a transient outward current was recorded under control conditions it was decreased by the agonists.

The four cholinergic agonists applied to the first basalar motoneurone had similar effects on the amplitudes of the evoked currents and the responses showed a characteristic time dependency. At potentials negative to -40 mV an inward current was induced in fifteen out of sixteen preparations, and an outward current in one. The inward current increased during exposure to drug, and in about half the neurones, reached a maximum after 5 or 10 min before decreasing. The amplitude of this current was generally small, between 5 and 10 nA, but could sometimes be as large as 35 or 40 nA. When the membrane was stepped to more positive potentials a large inward current was evoked by each agonist, which increased in amplitude over the 15 min exposure to agonist. Seven of these cells exhibited an initial outward current at these potentials, which over the first few minutes of drug application, decreased and became inwardly directed. The inward

current was usually between 30 and 60 nA, although in four preparations it was as large as 100 nA.

The response to McN-A-343 can be blocked by the muscarinic antagonist scopolamine, implying that the drug-induced current is a result of the agonist binding to muscarinic receptors, rather than a non-specific effect. In addition, scopolamine blocks the nicotine-induced current, supporting the theory that the 'muscarinic' receptors of the motoneurone have a 'mixed' cholinergic pharmacology. These receptors are present on the soma membrane of the motoneurone.

These experiments demonstrate that muscarinic stimulation of the first basalar motoneurone results in the production of an inward current. This can be interpreted as either the activation of an inward current or the inhibition of an outward current. The fact that in some preparations an initial outward current is evoked suggests that two currents may be involved in the response of the motoneurone to muscarinic agonists. This is investigated in the following chapter.

CHAPTER 5

Ionic mechanism of α-BTX-resistant cholinergic receptor-mediated current, and the possible involvement of cAMP and Ca^{2+} in signal transduction

5.1. INTRODUCTION

Muscarinic cholinergic receptors are not directly coupled to ion channels, and therefore must bind to and activate G proteins to effect a change in membrane conductance (Hulme et al, 1990). In the majority of known examples, the activated G protein modulates the production of diffusible second messengers which in turn modulate membrane ion channels. However, muscarinic inhibition of a class of K^+ channel located in cardiac muscle is caused by the binding of an activated G protein directly to the channel and does not involve a diffusible second messenger (Sakmann et al, 1983; Noma, 1986).

Muscarinic receptors which activate second messenger pathways, generally produce either an increase in PI turnover or a decrease in adenylate cyclase activity (Nathanson, 1987; Hulme et al, 1990). This has been confirmed by expression studies in which reconstituted vertebrate muscarinic receptor subtypes couple preferentially to either stimulation of PIP_2 hydrolysis (m_1, m_3, m_5) or inhibition of adenylate cyclase activity (m_2, m_4) (Fukuda et al, 1988; Peralta et al, 1988; Pinkas-Kramarski et al, 1988; Liao et al, 1989). There have also been reports of muscarinic receptor-mediated increases in cAMP levels in rat olfactory bulb (Olianas & Onali, 1990), human neuroblastoma cell lines SK-N-SH (Baumgold & Fishman, 1988; Baumgold et al, 1992) and SH-SY5Y (Jansson et al, 1991) and canine iris smooth muscle (Tachado et al, 1994). This apparent adenylate cyclase stimulation, however, appears to be produced indirectly, since Jansson et al (1991) and Tachado et al (1994) have found that carbachol-stimulated cAMP accumulation could be reduced by the addition of protein kinase C inhibitors (Jansson et al, 1991) or intracellular injection of the Ca^{2+} chelator BAPTA (Jansson et al, 1991; Tachado et al, 1994); cAMP formation therefore appears to be secondary to PIP_2 hydrolysis. However, in SK-N-SH human neuroblastoma cell lines, where muscarinic receptors are coupled to PIP_2 hydrolysis, carbachol-stimulated cAMP accumulation appears to be independent

of both Ca^{2+} and protein kinase C, because neither intracellular BAPTA (Baumgold et al, 1992) nor activation of protein kinase C by phorbol esters (Baumgold & Fishman, 1988) affected cAMP formation. Further evidence for muscarinic receptor-mediated enhancement of adenylate cyclase activity occurring independently of PIP_2 hydrolysis comes from work on rat olfactory bulb, where cAMP accumulation is unaffected by either intracellular Ca^{2+} buffering or phorbol esters (Olianas & Onali, 1990).

In the insect CNS, there is evidence for muscarinic receptor mediated-modulation of either adenylate cyclase activity or PI turnover in different preparations. Muscarinic agonists decrease cAMP levels and increase PIP_2 hydrolysis in the supraoesophageal ganglia of locusts (Trimmer & Berridge, 1985; Qazi & Lunt, 1991) and whole nerve cords of *Manduca* (Qazi & Trimmer, 1993). PIP_2 hydrolysis is also enhanced by muscarinic agonists in whole nerve cords of the cockroach (David & Pitman, 1994) and mouse Y1 adrenal cells (Shapiro et al, 1989) and COS-7 cells (Blake et al, 1993) expressing cloned *Drosophila* muscarinic receptors. Experiments carried out on locust synaptosomes have shown that activation of the muscarinic receptors results in a decrease in cAMP accumulation (Knipper & Breer, 1988). The inward current evoked by muscarinic agonists in motoneurone D_f of the cockroach is mimicked by the addition of dibutyryl cAMP, a membrane-permeable analogue of cAMP, suggesting that the current may be mediated by an increase in adenylate cyclase activity (David & Pitman, 1991, 1993b).

Muscarinic receptor activation results in the modulation of membrane conductance; different ion channels may be affected in different types of neurone, including Ca^{2+} and K^+ channels. Muscarinic receptor activation enhances the Ca^{2+} current in the human neuroblastoma cell lines SH-SY5Y (Murphy et al, 1991) and N1E-115 (Mathes & Thompson, 1994) and guinea-pig ventricular myocytes (Gallo et al, 1993). Inhibition of a K^+ current may be an indirect effect due to a decrease in the Ca^{2+} current which causes a reduction of the Ca^{2+}-

dependent K^+ current (Brezina, 1988, David & Pitman, 1993b, 1995). Alternatively, the Ca^{2+}-dependent K^+ current can also be inhibited by muscarinic agonists directly, independent of an effect on intracellular free Ca^{2+} concentration, as described in rat hippocampal neurones (Knöpfel et al, 1990). Muscarinic receptors mediate suppression of the voltage-dependent M-current found in many vertebrate excitable cells including bullfrog sympathetic ganglion neurones, NG108-15 human neuroblastoma cell lines, rat sympathetic neurones, hippocampal cells, human neocortical cells, and toad smooth muscle (reviewed by Brown, 1988). Muscarinic agonists also decrease the K^+ conductance of cockroach giant interneurones (Le Corronc & Hue, 1993), lobster pyloric neurones (Nagy et al, 1985) and crayfish motoneurones (Cattaert et al, 1994).

The experiments described in Chapter 4 showed that activation of a population of α-BTX-insensitive cholinergic receptors on the first basalar motoneurone resulted in the production of an inward current, and in some neurones, an initial outward current. The experiments in this section were performed to establish whether cAMP may be involved in mediating the response to activation of the 'mixed' receptors, and if the apparent inward current evoked by muscarinic agonists is due to the production of an inward current or the inhibition of an outward current. In the latter context, the effects of the muscarinic agonist McN-A-343 on the Ca^{2+} and K^+ currents of the neurone were studied. The effect of receptor activation on the release of intracellular Ca^{2+} was also examined by loading the motoneurone with the Ca^{2+} chelator BAPTA. The holding potential was increased from -50 to -80 mV for the majority of the experiments, therefore a comparison of the currents evoked by stepping the membrane from both -50 and -80 mV was carried out, and the current evoked by McN-A-343 in a cell held at -80 mV was measured.

5.2. RESULTS

5.2.1. EFFECT OF INCREASING INTRACELLULAR cAMP

The concentration of intracellular cAMP can be increased by applying a membrane permeable analogue such as dibutyryl cAMP, or by adding theophylline, a phosphodiesterase inhibitor which prevents the breakdown of endogenous cAMP. Both methods were employed, and the drugs were applied for 15 min to compare the currents evoked under these conditions with those produced by the muscarinic agonists.

5.2.1.1. Dibutyryl cAMP

A typical response to externally applied dibutyryl cAMP (10^{-3} M; n=3) is shown in Figure 5.1. The holding potential was -50 mV. The amplitude of the sustained outward current decreased after 15 min (Figure 5.1a), and there was an inward shift in the holding current.

The effect of dibutyryl cAMP on the I/V relationship of the neurone is shown in Figure 5.1b, and the voltage-dependence of the dibutyryl cAMP-induced current in Figure 5.1c. At potentials negative to -40 mV an inward current was evoked, which, after 5 min exposure to drug, increased from a minimum at -40 (n=2; Figure 5.1.) or -60 mV (n=1) to a maximum at -100 mV. The current evoked after 1 min is essentially constant over this voltage range. In two preparations, this current component increased over 15 min, and in the third a maximum was reached at 10 min, after which it decreased. The maximum amplitude attained at -100 mV was 20·0 ± 4·7 nA (n=3). An inward current was also evoked at membrane potentials positive to -40 mV in all preparations, increasing as the command potential was stepped further from -50 mV. This current component increased during exposure to dibutyryl cAMP. After 15 min, the amplitude reached 85·3 ± 14·9 nA (n=3) at a command potential of 0 mV. In two neurones, including the example shown in Figure 5.1c, this current

Figure 5.1a. The effect of 15 min exposure to 10^{-3} M dibutyryl cAMP on the current evoked by stepping the membrane to -40, -20 and 0 mV from a holding potential of -50 mV. There was an inward shift in the holding current, and a decrease in the amplitude of the sustained outward current in all preparations.

Scale: vertical 20 nA (i)
50 nA (ii, iii)
horizontal 100 ms

Figure 5.1b. The currents evoked in the motoneurone in (a) were measured after 50 ms (arrow in (a)) and used to construct an I/V relationship of the neurone in the absence and presence (5, 15 min) of 10^{-3} M dibutyryl cAMP.

Figure 5.1c. The dibutyryl cAMP-induced current obtained from the preparation in (b). A relatively small, inward current was evoked at potentials negative to -40 mV. An inward current, which increased during exposure to dibutyryl cAMP, was induced positive to -40 mV. In this preparation, an outward current was evoked after 1 min exposure at potentials positive to -40 mV, which reversed and was inwardly directed after 5 min.

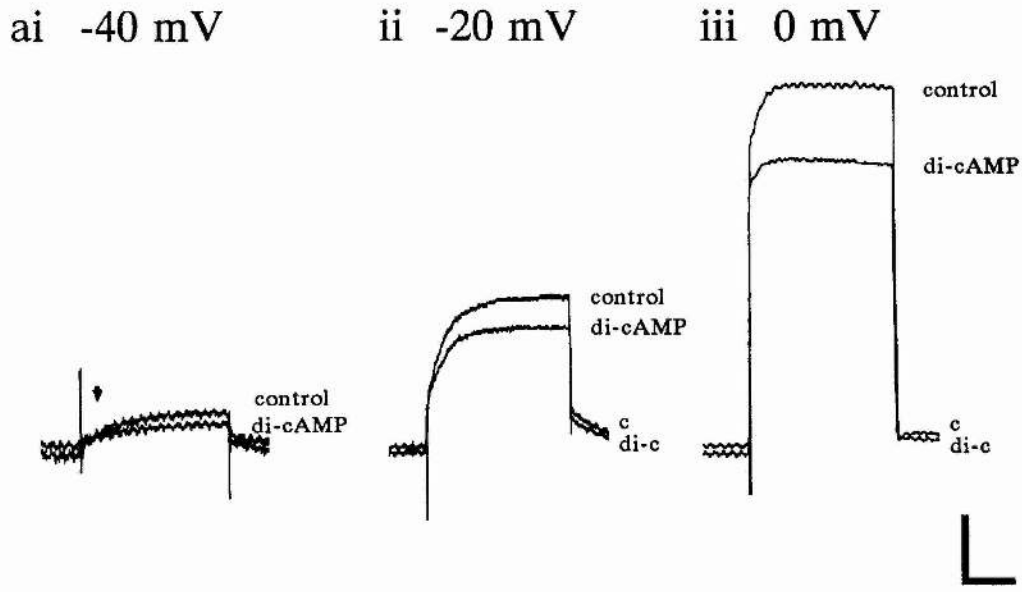

b

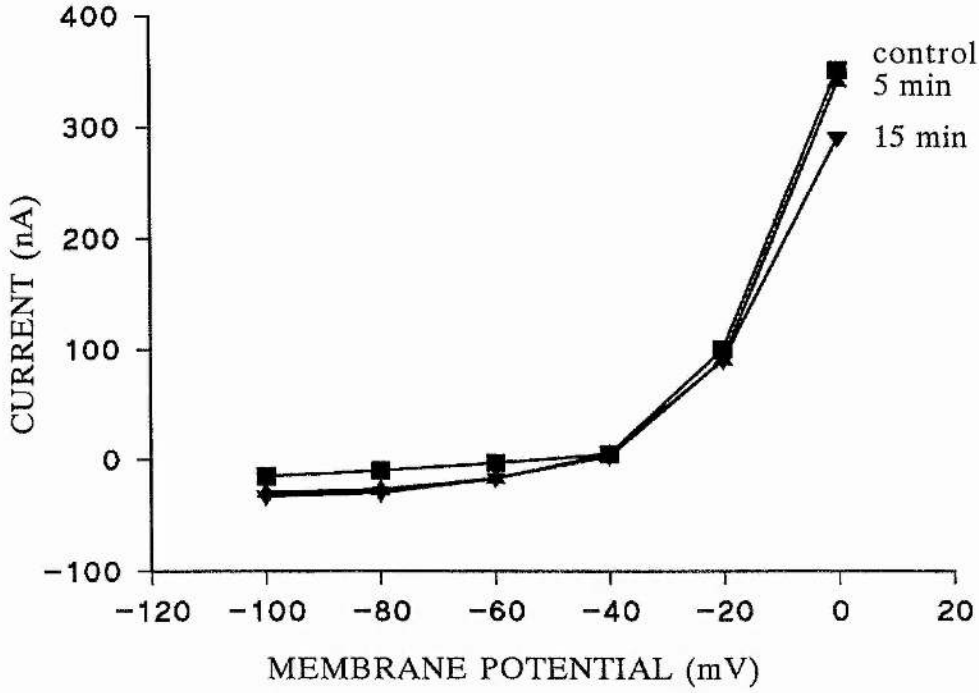
400
300
200
100
0
−100
CURRENT (nA)
−120
−100
−80
−60
−40
−20
0
20
MEMBRANE POTENTIAL (mV)
control
5 min
15 min

c

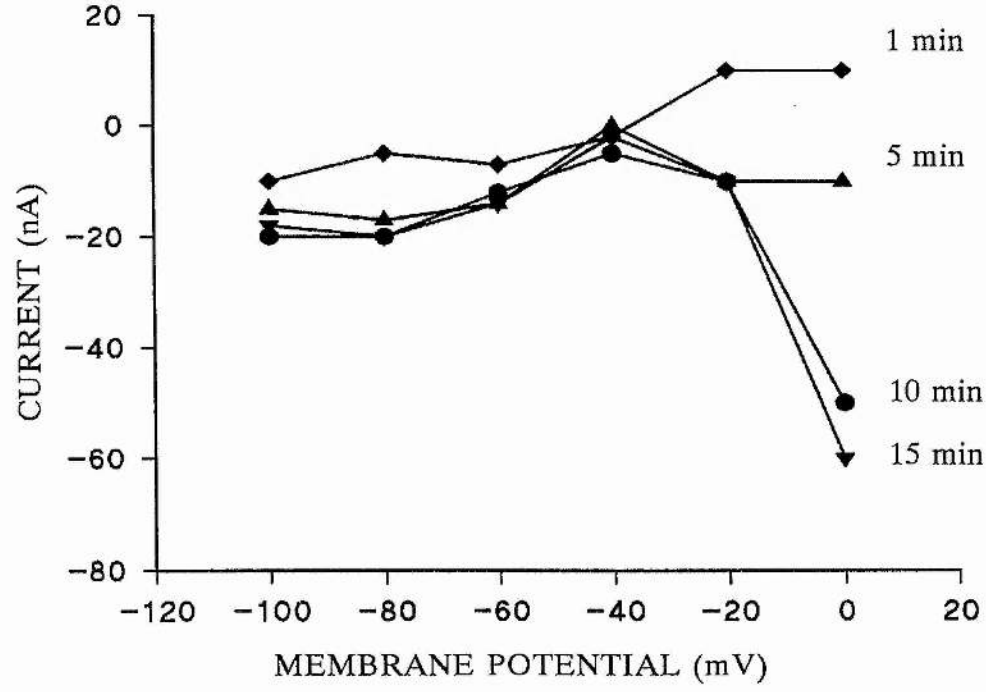
20
0
−20
−40
−60
−80
CURRENT (nA)
−120
−100
−80
−60
−40
−20
0
20
MEMBRANE POTENTIAL (mV)
1 min
5 min
10 min
15 min

component was preceded by an outward current, with an amplitude of 10 nA at 0 mV after 1 min; after 5 min this current had reversed and become inward.

5.2.1.2. Theophylline

The action of 10^{-4} M theophylline (n=4), which was similar to that of dibutyryl cAMP, is shown in Figure 5.2. As Figure 5.2a shows, the sustained outward current was reduced after 15 min exposure to theophylline. In preparations in which a transient current was evoked under control conditions (-40 mV, n=1; -20 mV, n=3; 0 mV, n=4), the addition of theophylline decreased the amplitude. Theophylline also induced a small inward shift in the holding current.

Figure 5.2b shows the effect of 10^{-4} M theophylline on the I/V relationship, and Figure 5.2c shows the theophylline-induced current. At all potentials between -100 and 0 mV an inward current was produced, with a minimum amplitude at -60 (n=1) or -40 mV (n=3) but increasing as the membrane was stepped further away from the holding potential. At potentials between -100 and -40 mV this current component generally increased during exposure to theophylline (in the preparation shown in Figure 5.2b & c, however, there was no current evoked at -100 or -60 mV); after 15 min the current evoked at -100 mV was 16·3 ± 3·7 nA (n=4). At command potentials more positive than -40 mV the inward current increased continually over the 15 min period of drug application. The amplitude of this current component when the membrane was stepped to 0 mV was 53·8 ± 13·6 nA (n=4). Unlike cAMP, theophylline did not evoke an initial outward current at potentials positive to the holding potential.

Figure 5.2a. The effect of 15 min exposure to 10^{-4} M theophylline on the current evoked by stepping the membrane from -50 mV to -20 and 0 mV. The amplitudes of both the sustained outward current and the transient current (-20 mV, n=3; 0 mV, n=4) were decreased in all preparations after 15 min exposure to theophylline. Theophylline evoked an inward shift in the holding current.

Scale: vertical 50 nA
horizontal 100 ms

Figure 5.2b. The currents evoked in the motoneurone were measured after 50 ms and used to construct an I/V relationship of the neurone in the absence and presence (5, 15 min) of 10^{-4} M theophylline (different preparation to (a)).

Figure 5.2c. The theophylline-induced current obtained from the preparation in (b). A relatively small, inward current was evoked at potentials negative to -40 mV. An inward current, which increased during exposure to theophylline, was induced positive to -40 mV.

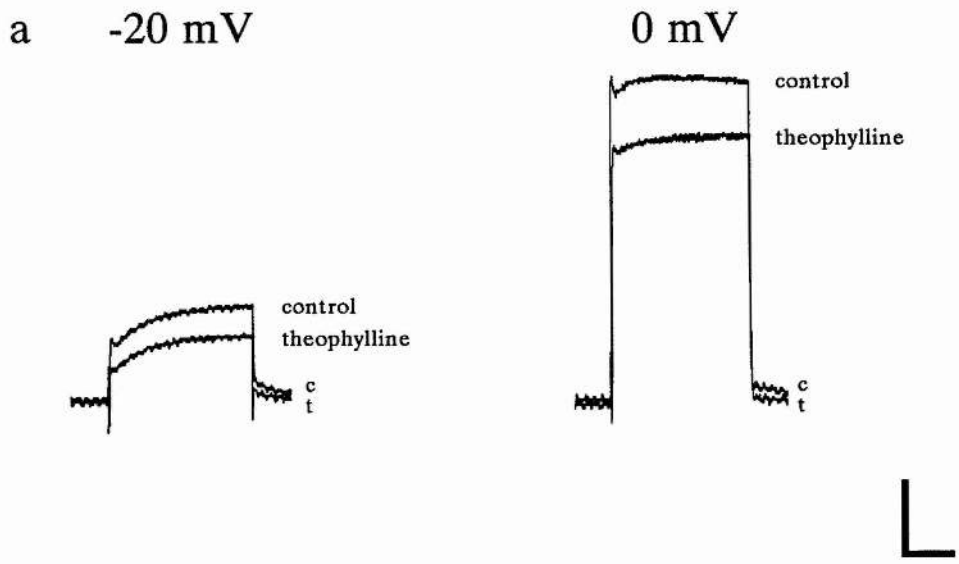

b

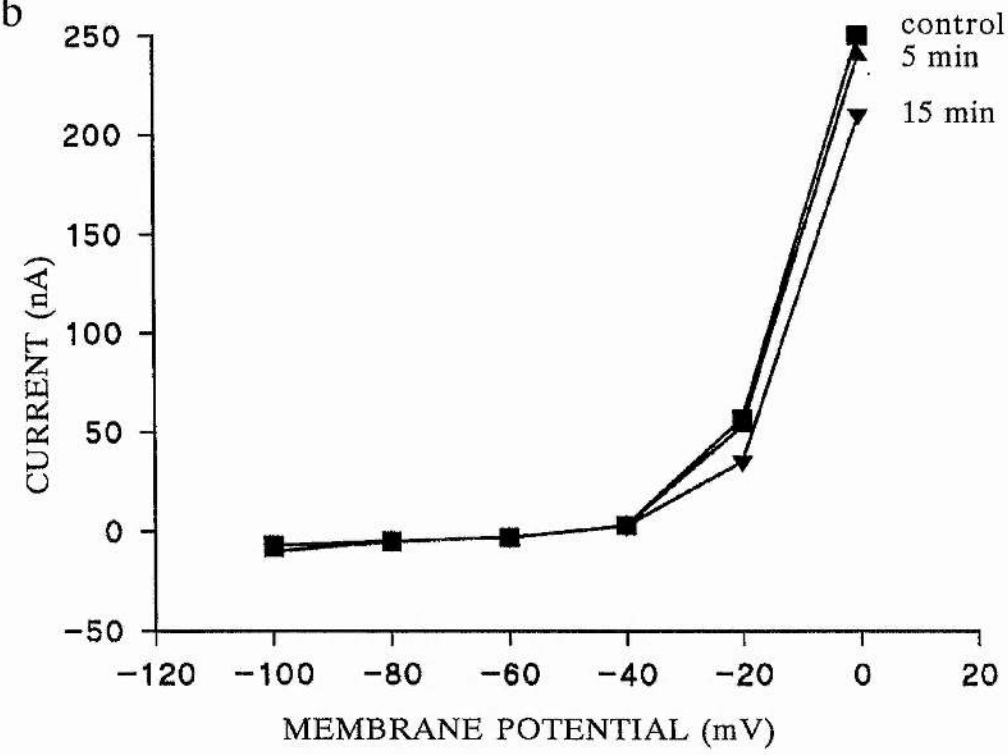
250
200
150
100
50
0
−50
CURRENT (nA)
−120
−100
−80
−60
−40
−20
0
20
MEMBRANE POTENTIAL (mV)
control
5 min
15 min

c

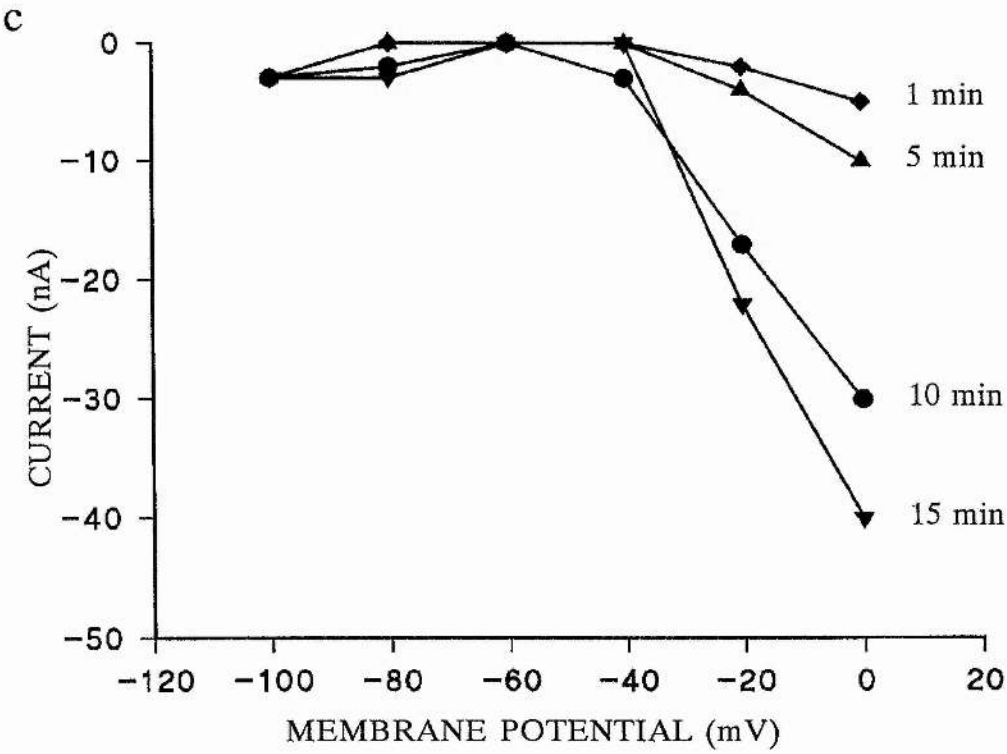
0
−10
−20
−30
−40
−50
CURRENT (nA)
−120
−100
−80
−60
−40
−20
0
20
MEMBRANE POTENTIAL (mV)
1 min
5 min
10 min
15 min

5.2.2. EFFECT OF THE HOLDING POTENTIAL ON THE CURRENTS EVOKED IN THE FIRST BASALAR MOTONEURONE

In the following experiments investigating the ionic mechanism of the response to muscarinic stimulation of the first basalar motoneurone, the holding potential was increased from -50 mV to -80 mV, and the pulse duration decreased from 250-300 ms to 50-100 ms. The mean membrane potential varied between approximately -45 and -60 mV, therefore a holding potential of -50 mV was selected. Although this is slightly more depolarised than the membrane potential in some neurones, it was satisfactory in the previous experiments investigating the response to cholinergic agonists in normal saline. However, the experiments described here investigated the properties of the cell after blocking Ca^{2+} or K^{+} channels. This procedure may perturb the ionic gradients across the cell membrane, and the impaled neurone will be more unstable and susceptible to death. It is possible that at a holding potential of -50 mV there are some voltage-dependent ion channels open, which would contribute to the instability of the cell. Increasing the holding potential to -80 mV will result in a greater proportion of these ion channels being closed. In addition, decreasing the pulse duration from 250-300 ms to 50-100 ms will reduce the ion flow across the membrane, therefore limiting the redistribution of ions.

The membrane was held at -80 mV and stepped to potentials between -100 and 0 mV. The evoked currents were measured after 50 ms to construct an I/V relationship for each neurone. In previous experiments, command potential increments were 20 mV as this was deemed sufficient to study the drug-induced currents in the motoneurone. However, initial experiments investigating the currents evoked in the neurone in the presence of Ba^{2+}, TEA^{+} and Cs^{+} ions (see Figure 5.7) revealed a current which was produced over a limited potential range; to allow a more comprehensive study of this current, the command potential increments were decreased to 10 mV.

To determine whether the increase in holding potential affects the currents evoked in the motoneurone, I/V relationships obtained from holding potentials of -50 and -80 mV were compared (n=4). The effect of increasing the holding potential on the currents evoked in two typical neurones is shown in Figure 5.3. When the holding potential was increased from -50 to -80 mV, there was an inward shift in the holding current, shown in Figure 5.3 by the dotted lines. At a holding potential of -50 mV three preparations exhibited no outward transient at command potentials positive to the holding potential (Figure 5.3ai); in the fourth, a transient was present at 0 mV (Figure 5.3bi). However, increasing the holding potential to -80 mV increased the amplitude of the net outward current and elicited a transient (Figure 5.3aii, 0 mV; Figure 5.3bii, -20 mV), or increased the amplitude of the transient (Figure 5.3bii, 0 mV), in all four cells.

Experiments were performed on a total of 26 neurones at a holding potential of -80 mV, and typical currents evoked under control conditions are shown in Figure 5.4. The currents were similar to those recorded at a holding potential of -50 mV (Figure 4.1): currents evoked between -100 and -60 mV were square-shaped (n=26), and were inwardly directed at command potentials negative to the holding potential and outwardly directed at more positive potentials. At potentials positive to -40 mV, the current evoked in several neurones consisted of an outward relaxation that gave way to a non-inactivating outward current. This was recorded at command potentials of -40 (n=22), -20 (n=19) and 0 mV (n=12), and a typical example is shown in Figure 5.4a. At 0 mV, the sustained outward current was reached within 20 ms. At -40 (n=12) and -20 mV (n=5) a steady-state was not reached. The outward currents in the remaining preparations consisted of an initial transient outward current preceding the sustained outward current, as shown in Figure 5.4b. A transient current was recorded at -40 (n=4), -20 (n=7) and 0 mV (n=14). The duration of the transient current evoked at 0 mV was between 10 and 20 ms with an amplitude of 15 to 25 nA.

Figure 5.3. The effect of the holding potential on currents evoked by stepping the membrane from -50 mV (Figures ai & ii) or -80 mV (Figures bi & ii) to -100, -40, -20 and 0 mV in two different neurones. Increasing the holding potential from -50 to -80 mV increased the amplitude of the outward currents evoked at -40, -20 and 0 mV but had no effect on the inward current evoked at -100 mV. There was an inward shift in the holding current when the holding potential was increased, as shown by the dotted lines. In cells in which no transient current was evoked when the cell was stepped from a holding potential of -50 mV, a transient current became apparent when the holding potential was increased to -80 mV (Figure a, 0 mV; b, -20 mV); when a transient current was present on jumping from -50 mV, it increased when the holding potential was made more negative (Figure b, 0 mV).

Scale: vertical 100 nA (a)
200 nA (b)
horizontal 25 ms

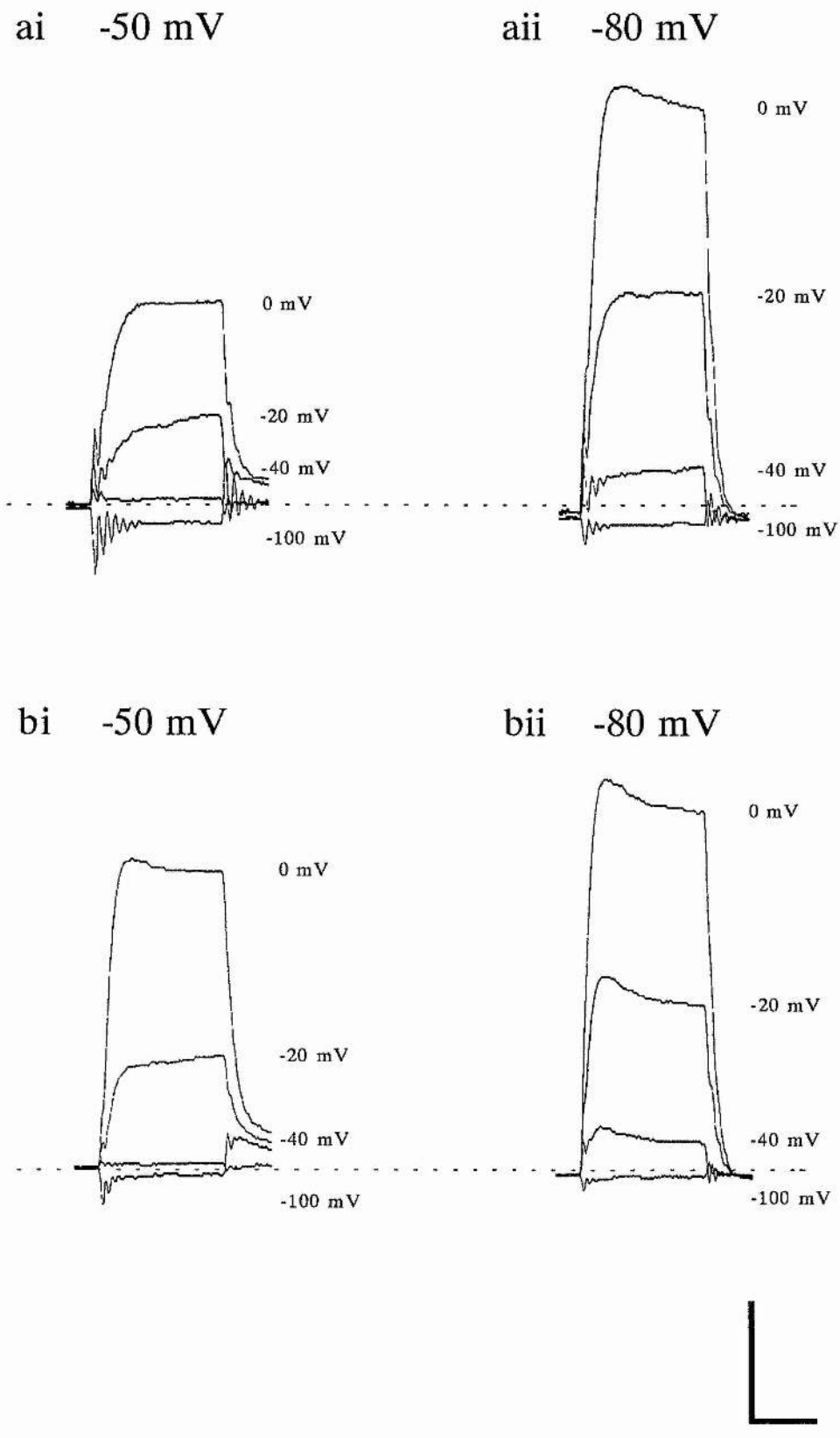
ai -50 mV
aii -80 mV
0 mV
-20 mV
-40 mV
-100 mV
0 mV
-20 mV
-40 mV
-100 mV
bi -50 mV
bii -80 mV
0 mV
-20 mV
-40 mV
-100 mV
0 mV
-20 mV
-40 mV
-100 mV

Figure 5.4. Currents evoked in the first basalar motoneurone by stepping the membrane from a holding potential of -80 mV to -100 mV, -40 mV, -20 mV and 0 mV. Inward currents evoked at -100 mV were small and appeared square-shaped; however, outward currents produced at potentials positive to the holding potential varied between preparations. The arrow in (a) shows the point at which current amplitude was measured to construct the I/V relationships of each neurone.

Figure 5.4a. The outward currents produced in this cell exhibited an outward relaxation into a non-inactivating outward current. This was recorded at -40 (n=22), -20 (n=20) and 0 mV (n=12). The steady state current was reached within 20 ms at 0 mV.

Figure 5.4b. The sustained outward current could be preceded by a transient outward current, with a duration at 0 mV of between 10 and 20 ms and amplitude of 15 to 25 nA. A transient current was recorded at -40 (n=4), -20 (n=6) and 0 mV (n=14).

Scale: vertical 100 nA
horizontal 25 ms

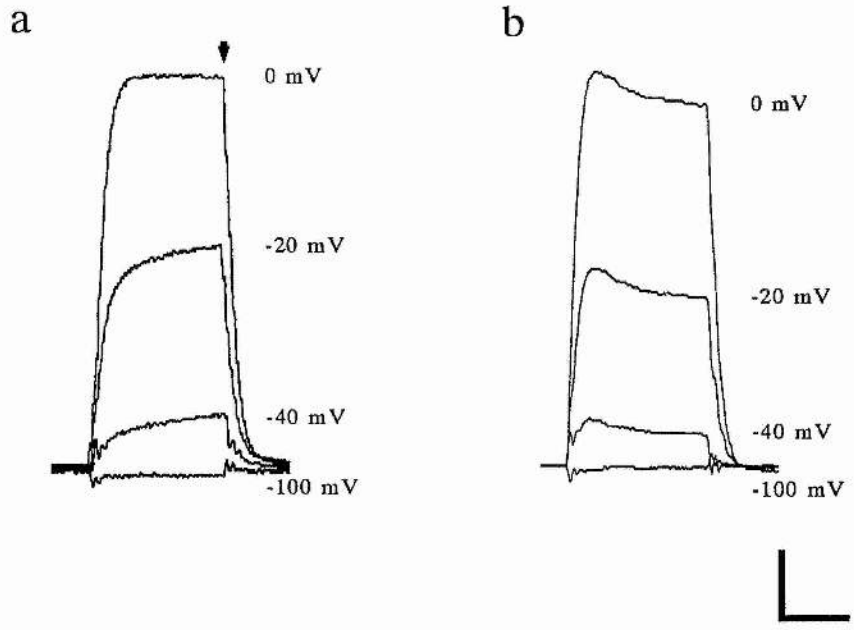

The effect of changing the holding potential on the I/V relationship is shown in Figure 5.5. There was no significant effect at potentials negative to -50 mV, but increasing the holding potential to -80 mV increased the amplitude of the currents evoked by stepping the membrane to potentials positive to -50 mV. Increasing the holding potential to -80 mV caused rectification to occur at a more negative potential (n=4): when the neurone was held at -50 mV rectification occurred at -40 mV, whereas when the holding potential was increased to -80 mV it occurred closer to -50 mV.

These data illustrate that increasing the holding potential from -50 to -80 mV increases the amplitude of the currents evoked at command potentials more positive than -40 mV. This is unlikely to affect the interpretation of the following experiments when they are compared with the results from the previous chapter.

5.2.3. CURRENTS EVOKED BY McN-A-343 IN A NEURONE AT A HOLDING POTENTIAL OF -80 mV

In these experiments the M_1 subtype-selective muscarinic agonist McN-A-343 (10^{-4} M) was employed rather than the non-selective cholinergic agonist carbachol: this avoided the requirement to block the nicotinic receptors by pretreatment with α-BTX. Typical results are shown in Figure 5.6. After 15 min exposure to 10^{-4} M McN-A-343, the amplitude of the sustained outward current decreased in all preparations (n=5); if a transient current was present prior to the addition of agonist, exposure to the drug decreased the amplitude at both -20 and 0 mV (n=2; Figure 5.6.a). A fifteen minute exposure to McN-A-343 induced an inward shift in the holding current.

The effect of 10^{-4} M McN-A-343 on the I/V relationship is shown in Figure 5.6b, and the McN-A-343-induced current is shown in Figure 5.6c. McN-A-343 evoked an inward current at all command potentials between -100 and 0 mV (n=5). At potentials negative to approximately -40 mV, the inward current

Figure 5.5. The currents evoked in the motoneurone were measured after 50 ms and used to construct an I/V relationship of the neurone at two different holding potentials, -50 mV and -80 mV. The holding potential had no effect on the I/V relationship at command potentials negative to -50 mV. Rectification occurred at a more negative potential when the cell was held at -80 mV.

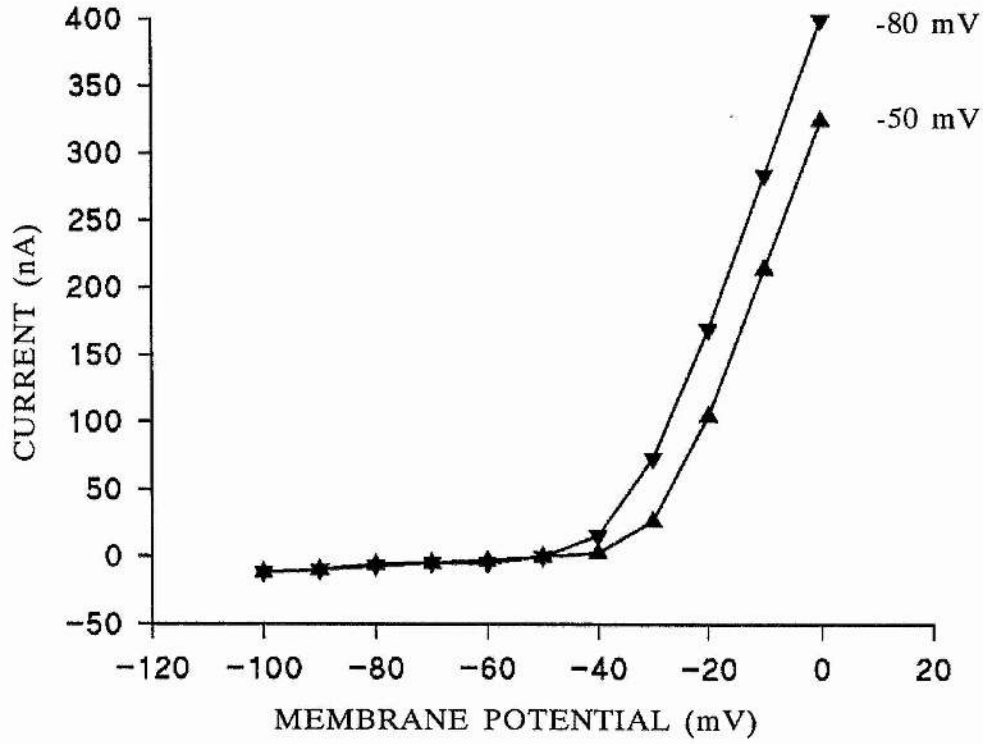

Figure 5.6a. The effect of 10^{-4} M McN-A-343 on the current evoked by stepping the membrane from a holding potential of -80 mV to -20 and 0 mV. After 15 min exposure to McN-A-343, the amplitude of the sustained current, and the transient outward current evoked at -20 mV and 0 mV (n=2) in two preparations, were decreased. The agonist also produced an inward shift in the holding current.

Scale: vertical 100 nA
horizontal 25 ms

Figure 5.6b. The currents evoked in the motoneurone were measured after 50 ms (arrow) and used to construct an I/V relationship of the first basalar motoneurone in the absence and presence (5 min, 15 min) of 10^{-4} M McN-A-343 (different preparation to (a)). Currents were measured after 50 ms.

Figure 5.6c. The McN-A-343-induced current in a cell at a holding potential of -80 mV, obtained from the preparation in (b). The agonist evoked an inward current at all potentials: small in amplitude at potentials negative to -40 mV in this example, and increasing in size at more positive potentials. The evoked current increased during the 15 min of exposure to agonist.

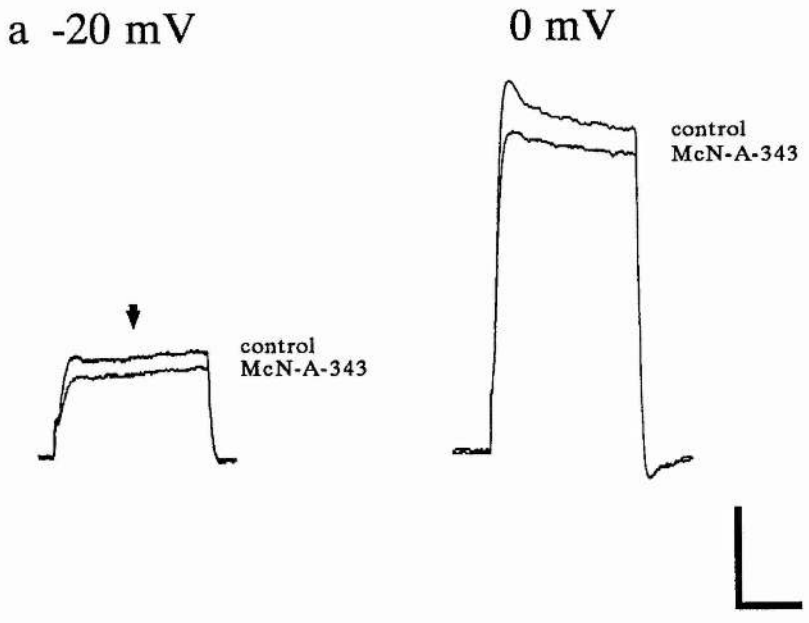

b

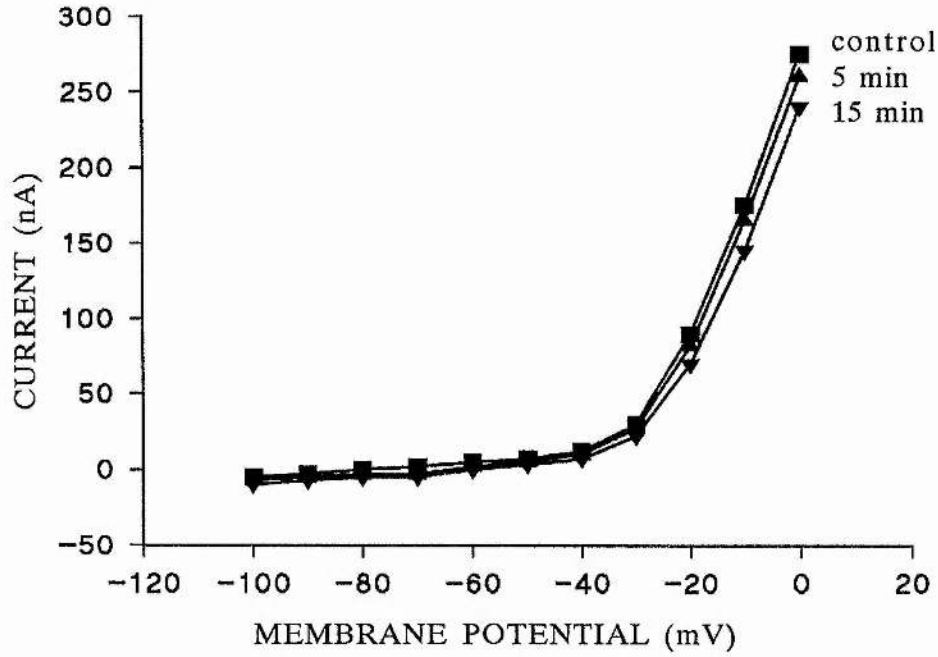
300
250
200
150
100
50
0
−50
CURRENT (nA)
control
5 min
15 min
−120
−100
−80
−60
−40
−20
0
20
MEMBRANE POTENTIAL (mV)

c

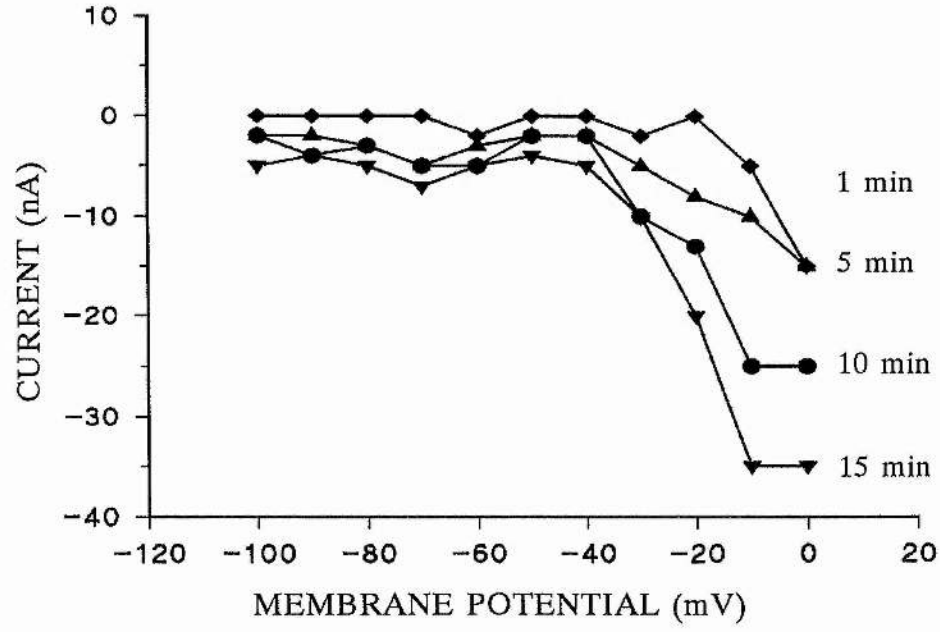
10
0
−10
−20
−30
−40
CURRENT (nA)
1 min
5 min
10 min
15 min
−120
−100
−80
−60
−40
−20
0
20
MEMBRANE POTENTIAL (mV)

was relatively voltage-independent. During exposure to agonist, this current component increased over 15 min. The maximum current amplitude reached at -100 mV after 15 min was 6·0 ± 1·6 nA (n=5). The inward current produced at potentials more positive than -40 mV was larger than that evoked at potentials negative to -40 mV, and increased as the command potential became less negative. This current component was also time-dependent and increased in amplitude over the 15 min period of exposure to agonist. After 15 min the magnitude of the current evoked at 0 mV was 48·0 ± 14·8 nA (n=5).

This experiment shows that the McN-A-343-induced current at a holding potential of -80 mV is similar to that produced in a cell held at -50 mV (Figure 4.5). However, whereas an initial outward current was produced at command potentials positive to -40 mV in approximately 50 % of the preparations held at -50 mV, it was not observed when the holding potential was increased to -80 mV. This implies that the holding potential has little effect on the current induced by McN-A-343.

5.2.4. IONIC BASIS OF THE INWARD CURRENT EVOKED BY McN-A-343

The inward current evoked by McN-A-343 may be due to the opening of channels which allow an inward flow of current such as Ca^{2+}, Na^{+} or H^{+}, or the closure of channels carrying an outward current (for example K^{+} or Cl^{-}). These two possibilities were examined by blocking K^{+} and Ca^{2+} channels respectively. The modulation of other ion currents by McN-A-343 was not examined because the results of the experiments described here suggested that K^{+} were the current carrying ions.

5.2.4.1. Modulation of a Ca^{2+} current

The Ca^{2+} currents of a cell can be observed under conditions in which K^{+} currents are blocked with extracellular Ba^{2+} (an equimolar replacement of Ca^{2+}

with Ba^{2+}) and TEA^+ (40 mM). K^+ current block can be further increased by injecting the cell with Cs^+ by filling the electrodes with 2 M CsCl.

The effect of blocking the K^+ channels of the neurone on the evoked currents is shown in Figure 5.7 (n=3). Using electrodes filled with 2 M KAc, the currents evoked at command potentials positive to the holding potential exhibited an outward relaxation into a non-inactivating outward current (Figure 5.7a). The electrodes were then replaced with two containing 2 M CsCl, and the normal bathing solution replaced by one containing 4 mM Ba^{2+} and 40 mM TEA^+. The outward currents were greatly reduced and a steady state was reached within ten minutes of changing the bathing medium. During this time, the membrane was stepped to 0 mV (50 ms; 1 Hz) to promote the entry of Cs^+ ions into the cell. The effect of Ba^{2+}, TEA^+ and Cs^+ on the evoked currents is shown in Figure 5.7b. There was no effect on the amplitude of the currents evoked at -100 mV, but the outward currents evoked at -40, -20 and 0 mV were greatly reduced and were inward at -20 (n=3). At -20 mV the inward current showed inactivation (n=3), which decreased as the command potential was moved away from -20 mV; at -40 and 0 mV the current appeared square.

The effect of Ba^{2+}, TEA^+ and Cs^+ on the I/V relationship of the motoneurone (n=3) is illustrated in Figure 5.7e. There is no effect on the currents evoked between -100 and -60 mV. At potentials more positive than -60 mV, the amplitude of the outward current is greatly reduced, and an inward current develops at potentials positive to -50 mV. The maximum amplitude of this inward current occurred at a command potential of -20 mV; at more positive potentials the current decreased in size. In one preparation the current remained inwardly directed at all potentials, but in the other two preparations the current became outward at either -10 (n=1) or 0 mV (n=1; Figure 5.7). The I/V relationship in the presence of Ba^{2+}, TEA^+ and Cs^+ can be seen more clearly in Figure 5.7f.

To examine whether this inward current was caused by Ba^{2+} entry through Ca^{2+} channels, the Ca^{2+} channel blocker verapamil (100 μM) was applied to the

Figure 5.7. The effect of blocking K^+ channels with 4 mM Ba^{2+}, 40 mM TEA^+ and 2 M Cs^+ on the currents evoked in the motoneurone at a holding potential of -80 mV.

Figure 5.7a. Control currents recorded with 2 M KAc-containing electrodes prior to the addition of 4 mM Ba^{2+} and 40 mM TEA^+. The currents were obtained by stepping the membrane from the holding potential of -80 mV to -100, -40, -20 and 0 mV. Outward currents exhibited an outward relaxation into a non-inactivating current.

Figure 5.7b. Currents evoked in the same cell after replacing the electrodes with two containing 2 M CsCl, and changing the saline to that containing 4 mM Ba^{2+} (Ca^{2+}-free saline) and 40 mM TEA^+, the outward currents were greatly reduced at -40, -20 and 0 mV, and were inwardly directed -20 (n=3) and 0 mV (n=1). In one preparation, the current remained inward, but in the remaining two, the current reversed at either -10 (n=1) or 0 mV (n=1). The inward current evoked at -20 mV showed inactivation, which decreased as the command potential was moved further from -20 mV. The current evoked at a command potential of -40 mV has been omitted from the figure for clarity due to a high level of oscillation which masked the other currents. There was no effect on the currents evoked at -100 mV.

Figure 5.7c. The inward current is a Ba^{2+} current because it can be reduced by the addition of 100 μM verapamil. As well as a decrease in the amplitude of the inward current, the current inactivation observed at -20 mV decreased.

Figure 5.7d. The effect of verapamil was reversible when the cell was washed with Ba^{2+}/ TEA^+ saline.

Scale: vertical 100 nA (a)
10 nA (b-d)
horizontal 25 ms

a control

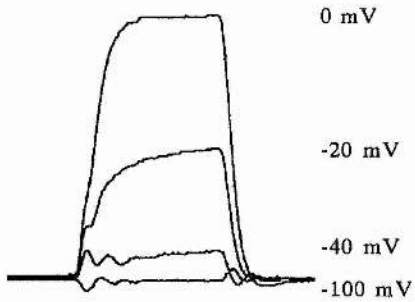

b Ba/TEA/CsCl

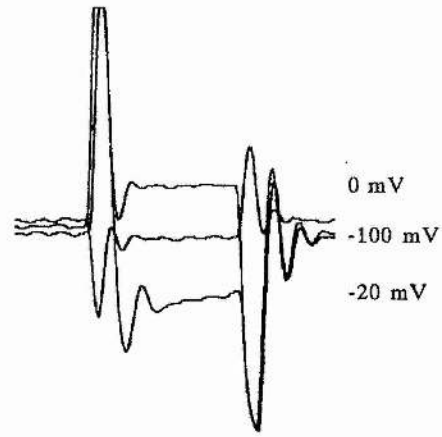

c Ba/TEA/CsCl/verap

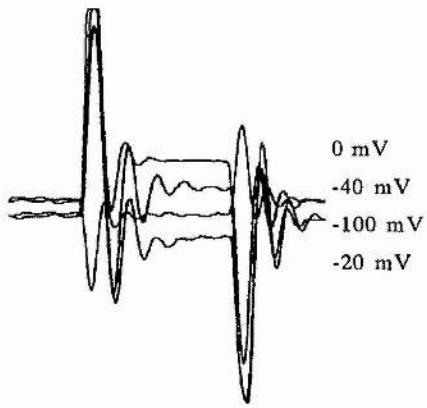

d wash

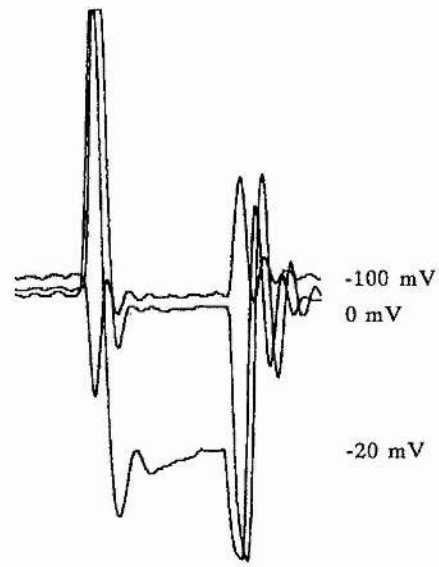

Figure 5.7e. The effect of blocking K^+ channels on the I/V relationship of the first basalar motoneurone. The currents evoked in the neurone in (a) to (d) were measured after 50 ms. There is no effect on the region negative to -60 mV, but at more positive potentials the current becomes inward, reaching a peak at -20 mV. The current reversed at 0 mV in this example.

Figure 5.7f. The effect of 100 μM verapamil in the presence of Ba^{2+}, TEA^+ and Cs^+ on the I/V relationship of the neurone in (a) to (d). The graph was constructed from the amplitude of the currents evoked in the neurone after 50 ms. There is an outward shift in the I/V curve, which is greatest in the 'U' shaped region of the relationship.

The effect of verapamil is reversible: when the preparation is washed with saline containing Ba^{2+} and TEA^+ the current evoked at potentials between -100 mV and -60 mV returns to the control values, and the inward current produced at more positive potentials increases in size.

Note the different current scales in (e) and (f).

e

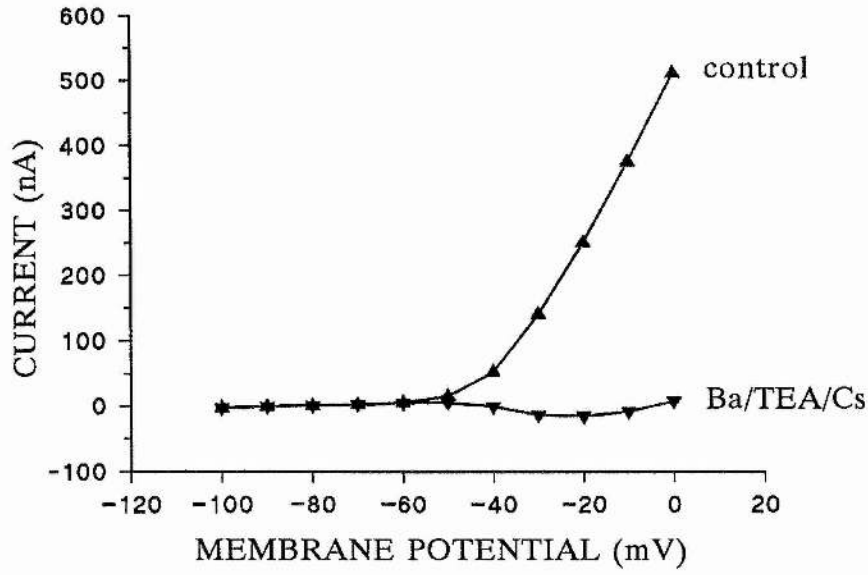
600
500
400
300
200
100
0
-100
CURRENT (nA)
control
Ba/TEA/Cs
-120
-100
-80
-60
-40
-20
0
20
MEMBRANE POTENTIAL (mV)

f

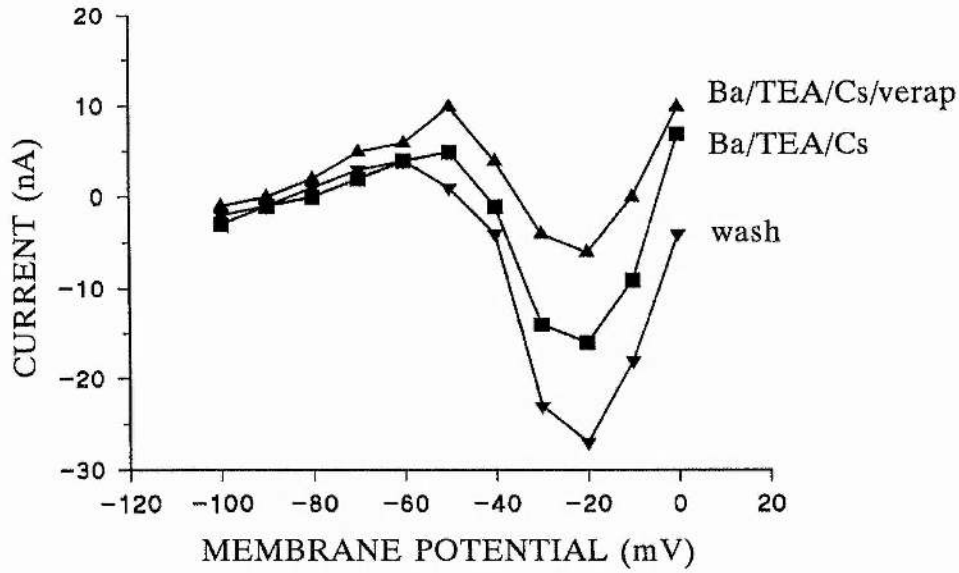
20
10
0
-10
-20
-30
CURRENT (nA)
Ba/TEA/Cs/verap
Ba/TEA/Cs
wash
-120
-100
-80
-60
-40
-20
0
20
MEMBRANE POTENTIAL (mV)

neurone (n=3). Figure 5.7c shows the effect of 100μM verapamil on the currents evoked in the motoneurone. A steady state was reached within 10 min of verapamil application. The amplitude of the inward currents was decreased, and that of the outward currents was increased. In addition, the inactivation of the inward current at -20 mV was blocked. After washing the preparation with Ba^{2+}/TEA^{+} saline the amplitudes of the inward currents evoked at -20 and 0 mV were greater than those obtained prior to the addition of verapamil (Figure 5.7d).

The effect of verapamil on the I/V relationship obtained in the presence of Ba^{2+}, TEA^{+} and Cs^{+} is illustrated in Figure 5.7f. The whole I/V curve was shifted in an outward direction. This effect was most marked, however, in the 'U' shaped region of the relationship, which appears, therefore, to correspond to an inward Ba^{2+} current through Ca^{2+} channels. Upon washing with Ba^{2+}/TEA^{+} saline, the amplitude of the inward current evoked positive to -50 mV increased to exceed that of the control currents (Figure 5.7f). The current evoked at potentials more negative than -50 mV returned towards the control value.

10^{-4} M McN-A-343 was added in the presence of Ba^{2+}, TEA^{+} and Cs^{+} to investigate the effect of activation of the 'mixed' cholinergic receptors on the Ca^{2+} channels of the neurone (n=4). In these experiments, the concentration of CsCl in the microelectrode was 1 M. Figure 5.8a shows the effect of McN-A-343 on the I/V relationship, while Figure 5.8b shows the McN-A-343-induced current obtained by subtraction of the traces in Figure 5.8a. In all four preparations, McN-A-343 evoked only very small currents, less than 5 nA in amplitude and which were variable in direction. The larger current evoked by McN-A-343 in normal saline (Figure 5.6, different preparation), which showed time- and voltage-dependency, was not observed in the presence of Ba^{2+}, TEA^{+} and Cs^{+}. Thus it appears that the small changes in current amplitude were unrelated to the presence of agonist, and that McN-A-343 does not modulate the Ca^{2+} current of the motoneurone.

Figure 5.8a. The currents evoked in the motoneurone were measured after 50 ms and used to construct an I/V relationship of the first basalar motoneurone in the presence of extracellular Ba^{2+} (4 mM; Ca^{2+} free saline), TEA^{+} (40 mM) and intracellular Cs^{+}, before and after (5 min, 15 min) the addition of 10^{-4} M McN-A-343. The current evoked by McN-A-343 was very small, varied in direction and showed no time- or voltage-dependence as recorded from neurones in normal saline.

Figure 5.8b. The McN-A-343-induced current after blocking K^{+} channels with Ba^{2+}, TEA^{+} and CsCl, obtained from the preparation in (a).

The holding potential was -80 mV.

a

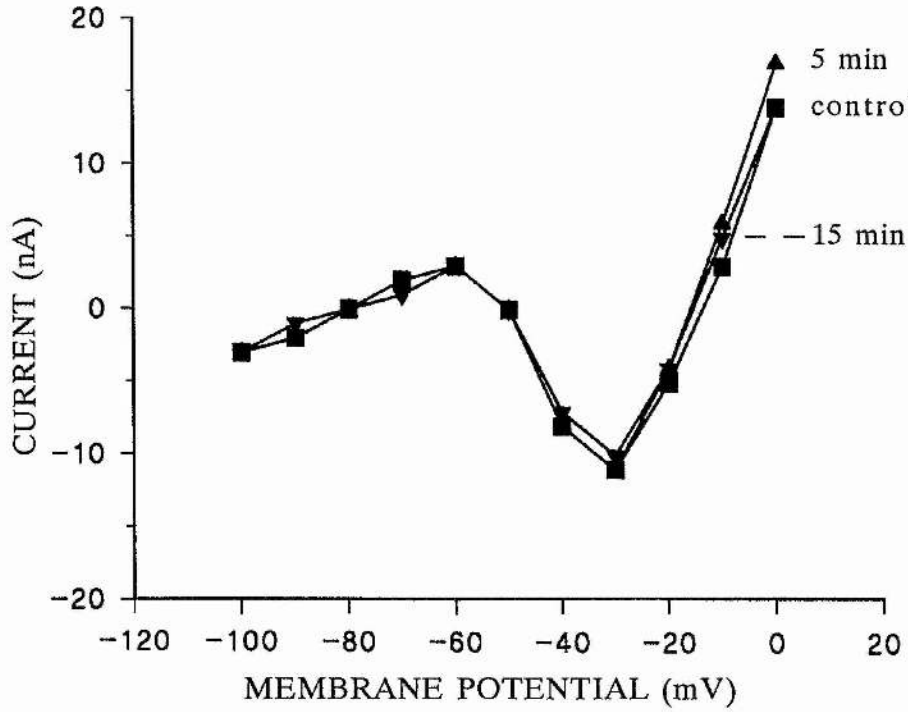
20
10
0
−10
−20
CURRENT (nA)
−120
−100
−80
−60
−40
−20
0
20
MEMBRANE POTENTIAL (mV)
5 min
control
15 min

b

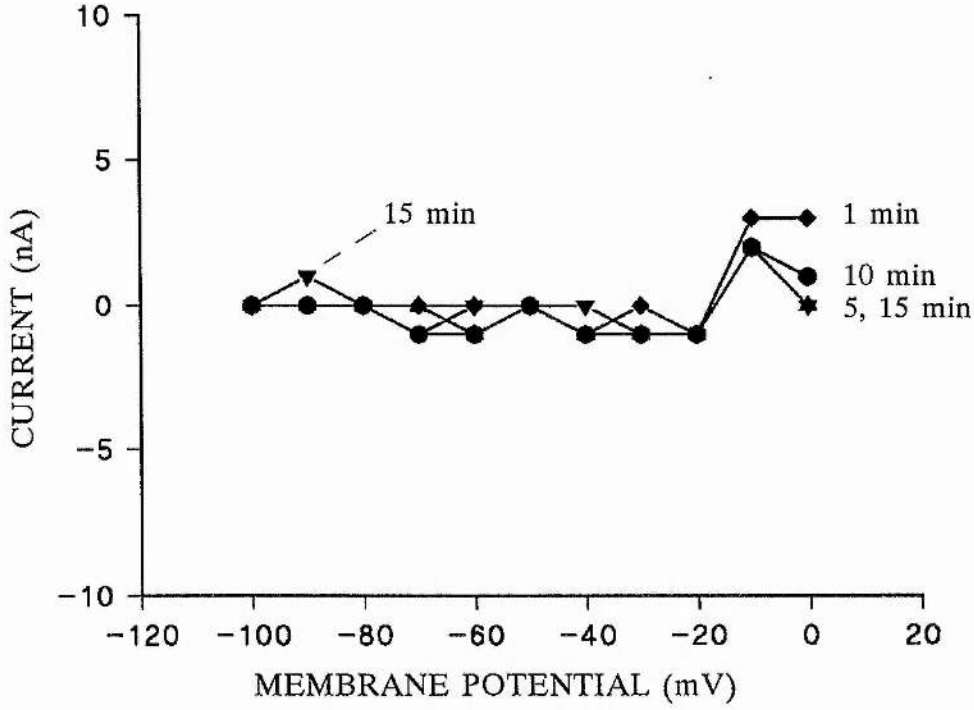
10
5
0
−5
−10
CURRENT (nA)
−120
−100
−80
−60
−40
−20
0
20
MEMBRANE POTENTIAL (mV)
15 min
1 min
10 min
5, 15 min

5.2.4.2. Modulation of a K^+ current

The previous experiment demonstrated that the apparent inward current evoked by McN-A-343 is not due to modulation of the influx of Ca^{2+} through the surface membrane channels. The experiments described here were carried out to confirm these observations by blocking the Ca^{2+} channels using either Cd^{2+} ions or verapamil.

5.2.4.2.1. Cd^{2+} ions

To examine the effect of Cd^+ ions on the currents evoked in the motoneurone, a concentration of 200 (n=2) or 500 μM (n=2) was used. The time course of the effect of Cd^{2+} was followed by measuring the amplitude of the current produced by jumping the membrane potential from -80 mV to 0 mV at a frequency of 1 Hz. Cd^{2+} affected the currents evoked in the motoneurone within 1 min of application, and a steady state was reached after 15 to 20 min. The effect of Cd^{2+} on the currents evoked in the motoneurone was investigated by stepping the membrane from -80 mV to command potentials between -100 and 0 mV. Figure 5.9 shows the effect of Cd^{2+} (200 or 500 μM) on the currents evoked in the neurone. At a concentration of either 200 or 500 μM, Cd^+ ions decreased the amplitude of both the sustained outward current (Figure 5.9a & b) and the transient current evoked at -20 (n=1) and 0 mV (n=2) in the control (Figure 5.9a), and induced an inward shift in the holding current. The extent to which the outward current was decreased was not concentration-dependent at the two concentrations tested: in Figure 5.9a, 200 μM Cd^{2+} has had a larger effect on the amplitude of the outward current than 500 μM Cd^{2+} (Figure 5.9b). However, in the other two preparations, 500 μM Cd^{2+} decreased the outward current by a greater amount than 200 μM Cd^{2+}.

The effect of Cd^+ on the I/V relationship is displayed in Figure 5.9c. In this example 500 μM Cd^+ was added, but the lower concentration of Cd^+ had a similar effect. The outward current was reduced at all potentials (n=4). At

Figure 5.9a, b. The effect of 200 (a) or 500 μM (b) Cd^{2+} on the outward current evoked by stepping the membrane from a holding potential of -80 mV to 0 mV in two different preparations. Both concentrations of Cd^{2+} decreased the amplitude of the sustained outward current and induced an inward shift in the holding current. In preparations in which a transient current was evoked at -20 (n=1) and 0 mV (n=2) in normal saline, it was blocked after exposure to Cd^{2+} (Figure 5.9a). The transient current was blocked by both 200 and 500 μM (b) Cd^{2+}.

Scale: vertical 100 nA
horizontal 25 ms

Figure 5.9c. The currents evoked in the motoneurone were measured after 50 ms and used to construct an I/V relationship of the first basalar motoneurone in the absence and presence of 500 mM Cd^{2+}. A relatively small inward current was evoked at potentials more negative than -40 mV; at potentials positive to -40 mV this current increased in amplitude.

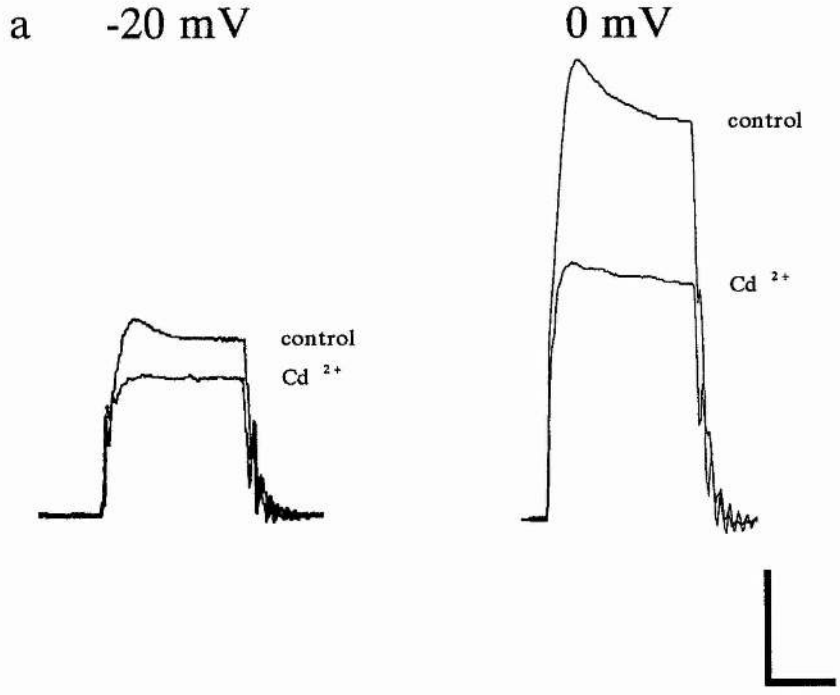

b

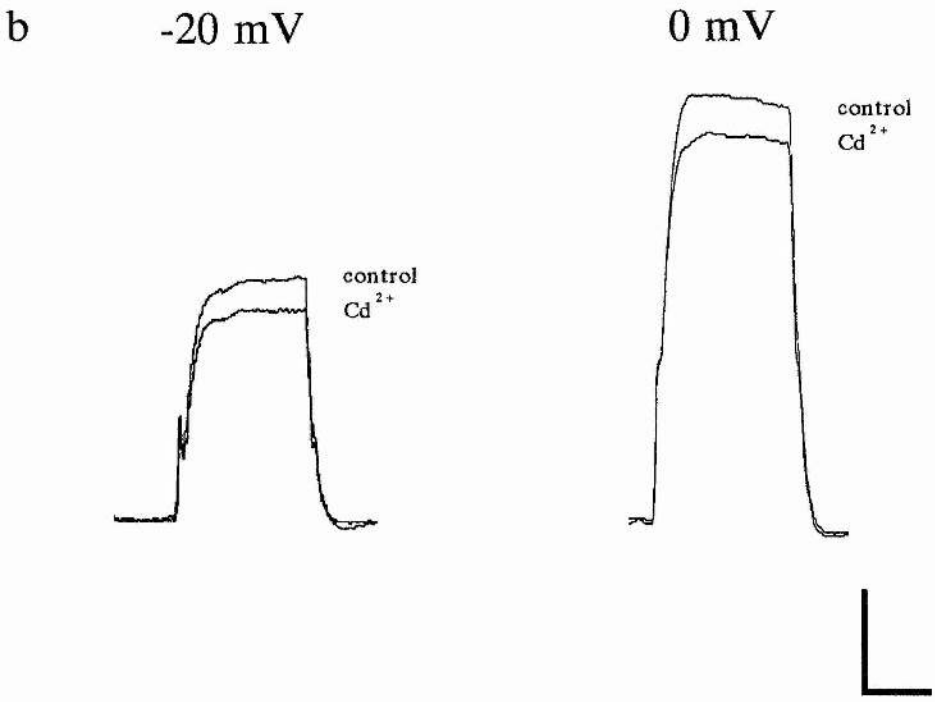
-20 mV
0 mV
control
Cd 2+
control
Cd 2+

c

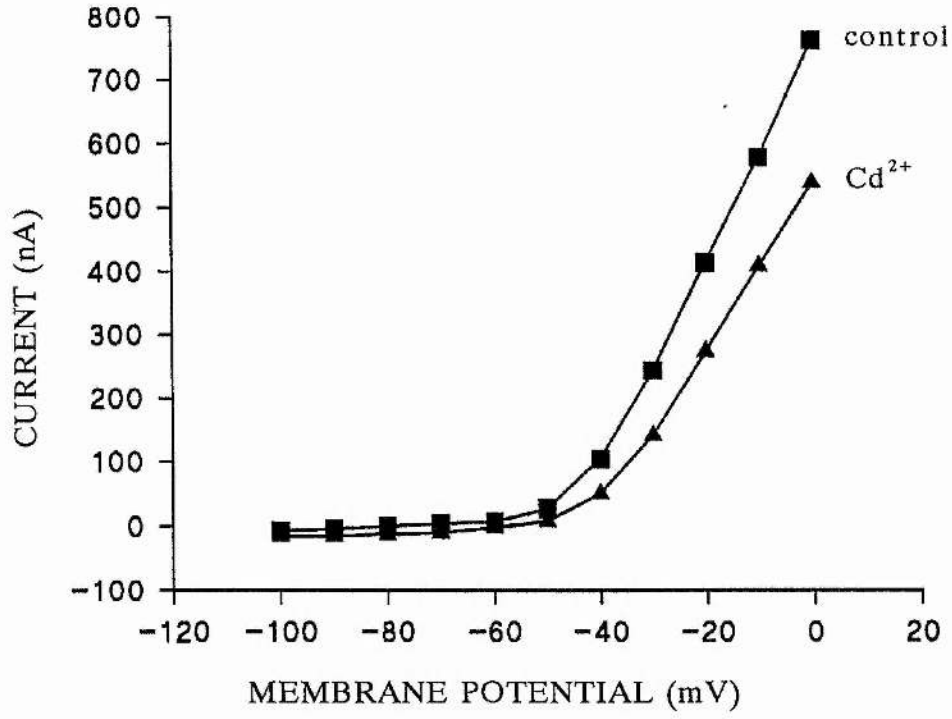
800
700
600
500
400
300
200
100
0
-100
CURRENT (nA)
-120
-100
-80
-60
-40
-20
0
20
MEMBRANE POTENTIAL (mV)
control
Cd2+

potentials negative to -40 mV, the current was decreased by less than 10 nA at a command potential of -100 mV. Cd^{2+} had a greater effect on the outward current at potentials more positive than -40 mV; over this potential range the effect of Cd^{2+} was voltage dependent and increased as the command potential became more positive. The proportion of Cd^{2+}-sensitive current was variable, and ranged between 6 and 42 % of the total outward current, which represents a decrease in the current measured at 0 mV of 40 nA (200 μM, n=1; 500 μM, n=1), 150 nA (200 μM, n=1) or 230 nA (500 μM, n=1; Figure 5.9c).

From the experiment in which McN-A-343 was applied to a motoneurone in the presence of the K^+ channel blockers Ba^{2+}, TEA^+ and Cs^+ (Section 5.2.4.1.), it would appear that the agonist does not act directly on the Ca^{2+} current of the cell. To confirm this, the effect of McN-A-343 in the presence of Cd^{2+} was investigated (n=4). Preliminary data showed that the effect of McN-A-343 in the presence of 500 μM Cd^{2+} was variable (n=2), which probably reflected sub-maximal block of Ca^{2+} channels. For this reason the concentration was increased to 1 mM; this concentration was found to block cockroach neuronal Ca^{2+} channels (Nightingale & Pitman, 1989). The results of this experiment are displayed in Figure 5.10. The effect of 15 min exposure to McN-A-343 on the outward currents evoked at -40, -20 and 0 mV is shown in Figure 5.10a. McN-A-343 induced an outward (n=2; Figure 5.10ai) or an inward (n=2; Figure 5.10aii) shift in the holding current. In all preparations, the outward current evoked at -20 and 0 mV became inactivating. The amplitude of the outward currents evoked at -40 and -20 mV, measured at the end of the current pulse, increased after drug treatment (n=4); at 0 mV the outward currents either decreased (n=2; Figure 5.10ai) or increased (n=2; Figure 5.10aii). The amplitude of the tail currents evoked at the end of the command pulse were increased in the presence of McN-A-343. The amplitude was dependent on the size of the outward current, and increased as the command potential was made less negative.

Figure 5.10a. The effect of 10^{-4} M McN-A-343 in the presence of 1 mM Cd^{2+} on the current evoked by stepping the membrane from a holding potential of -80 mV to-40, -20 and 0 mV.

Figure 5.10ai. In two preparations, 15 min exposure to McN-A-343 increased the amplitude of the sustained outward current evoked at -40 and -20 mV and decreased it at 0 mV; the outward current at -20 and 0 mV also became inactivating. In the presence of McN-A-343 a tail current was produced which increased as the command potential became more positive. In this preparation there was an outward shift in the holding current.

Figure 5.10aii. In the remaining two preparations, McN-A-343 increased the amplitude of the sustained outward current at all potentials, and the outward current evoked at -20 and 0 mV became inactivating. In the presence of McN-A-343 a tail current was produced which increased as the command potential became more positive. In this preparation there was an inward shift in the holding current.

Scale: vertical 50 nA
horizontal 25 ms (ai)
50 ms (aii)

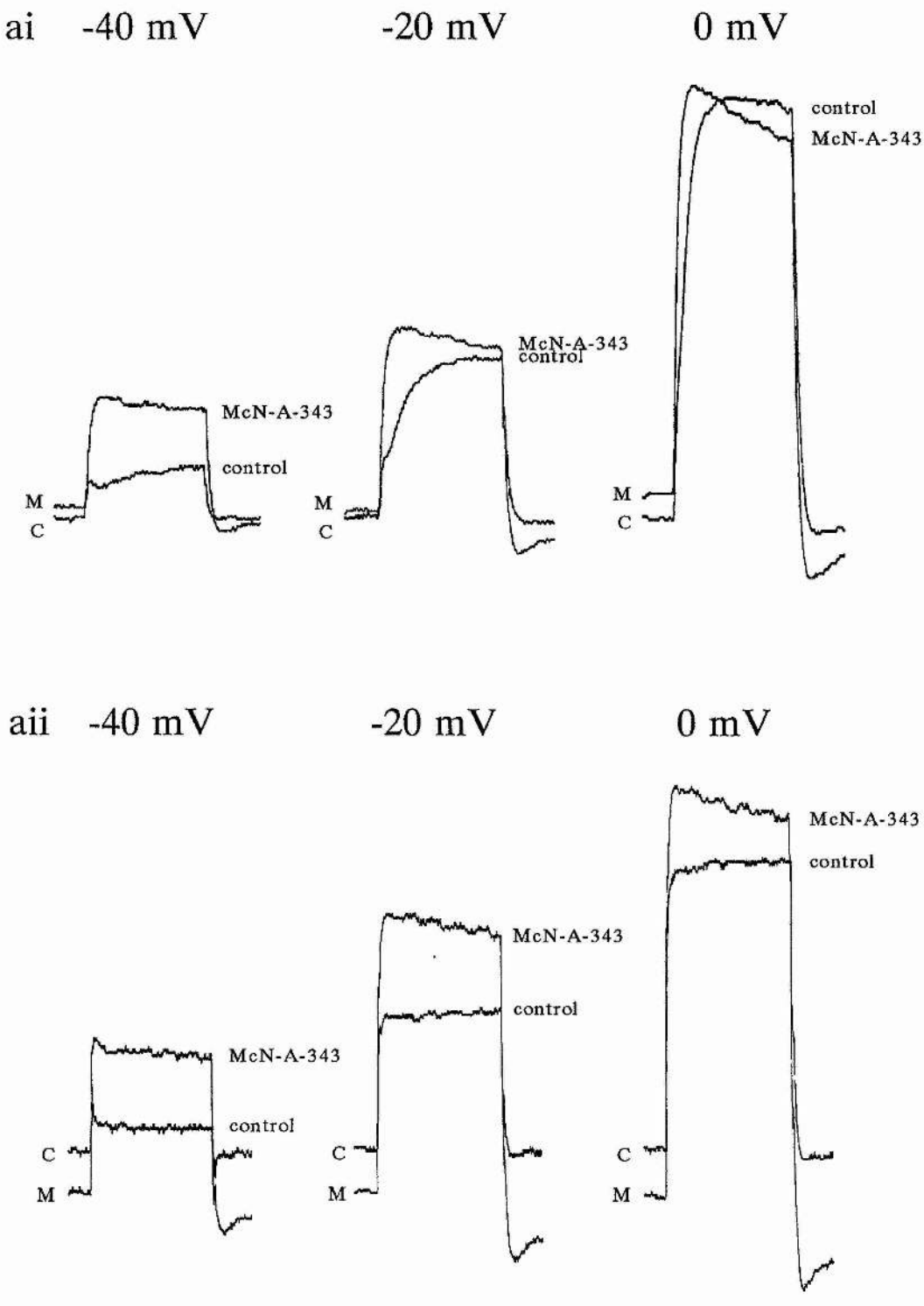
ai
-40 mV
-20 mV
0 mV
McN-A-343
control
M
C
McN-A-343
control
M
C
control
McN-A-343
M
C
aii
-40 mV
-20 mV
0 mV
McN-A-343
control
C
M
McN-A-343
control
C
M
McN-A-343
control
C
M

Figure 5.10bi. The currents evoked in the motoneurone were measured after 50 ms and used to construct an I/V relationship of the first basalar motoneurone in the presence of 1 mM Cd^{2+} before and after (5, 15 min) the addition of 10^{-4} M McN-A-343. The addition of the agonist greatly reduced the rectification and the relationship became almost linear.

Figure 5.10ci. The McN-A-343-induced current in the presence of 1 mM Cd^{2+}, obtained from the preparation in (bi). In this neurone, the amplitude of the current increased from -100 mV to a maximum at -30 mV, then decreased. There was little change in the amplitude of the current evoked at command potentials between -100 and -30 mV during exposure to McN-A-343. At potentials more positive than -30 mV, the current decreased and reversed at 0 mV. Over this potential range, the current decreased with continued exposure to agonist.

bi

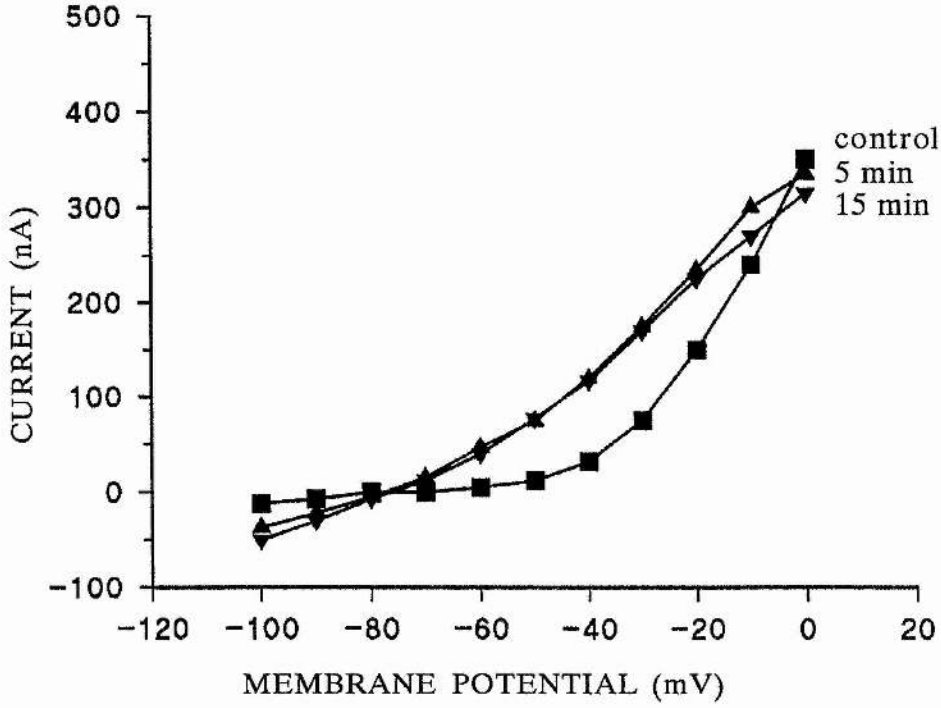
500
400
300
200
100
0
-100
CURRENT (nA)
control
5 min
15 min
-120
-100
-80
-60
-40
-20
0
20
MEMBRANE POTENTIAL (mV)

ci

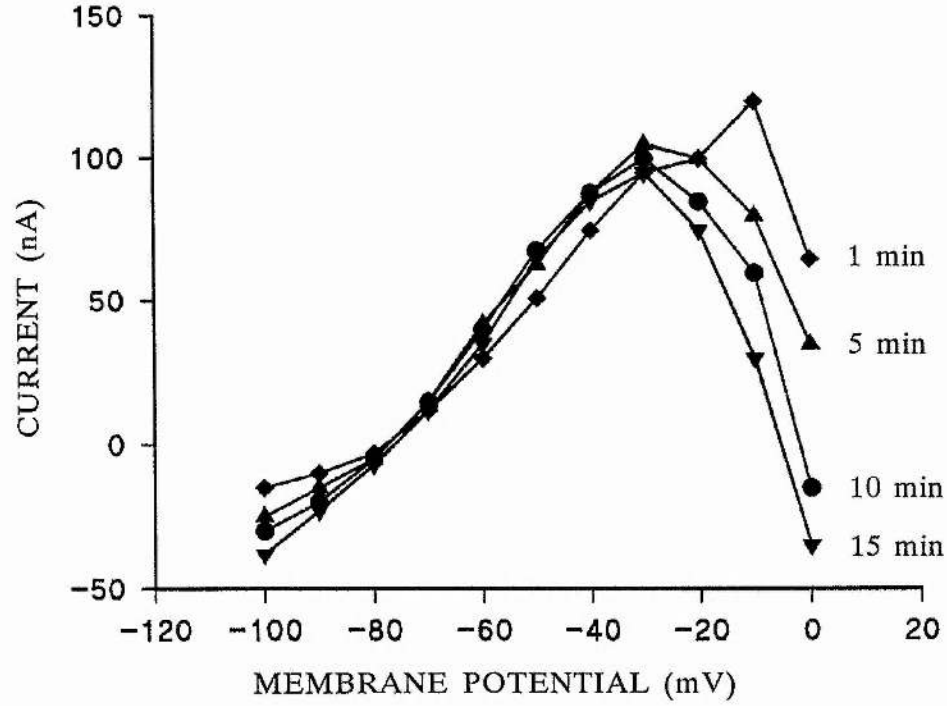
150
100
50
0
-50
CURRENT (nA)
1 min
5 min
10 min
15 min
-120
-100
-80
-60
-40
-20
0
20
MEMBRANE POTENTIAL (mV)

Figure 5.10bii. The currents evoked in the motoneurone were measured after 50 ms and used to construct an I/V relationship of the first basalar motoneurone in the presence of 1 mM Cd^{2+} before and after (5, 15 min) the addition of 10^{-4} M McN-A-343. The addition of the agonist greatly reduced the rectification and the relationship became almost linear.

Figure 5.10cii. The McN-A-343-induced current in the presence of 1 mM Cd^{2+}, obtained from the preparation in (bii). In this preparation, the amplitude of the current increased from -100 mV to a maximum at -20 mV, then decreased. The agonist had a smaller effect after 1 min than the example shown in Figure 5.10bi & ci. After 5 min, there was little change in the amplitude of the current evoked at command potentials between -100 and -20 mV. At potentials more positive than -20 mV, the current decreased but did not become inward. Over this potential range, the current decreased with continued exposure to agonist.

bii

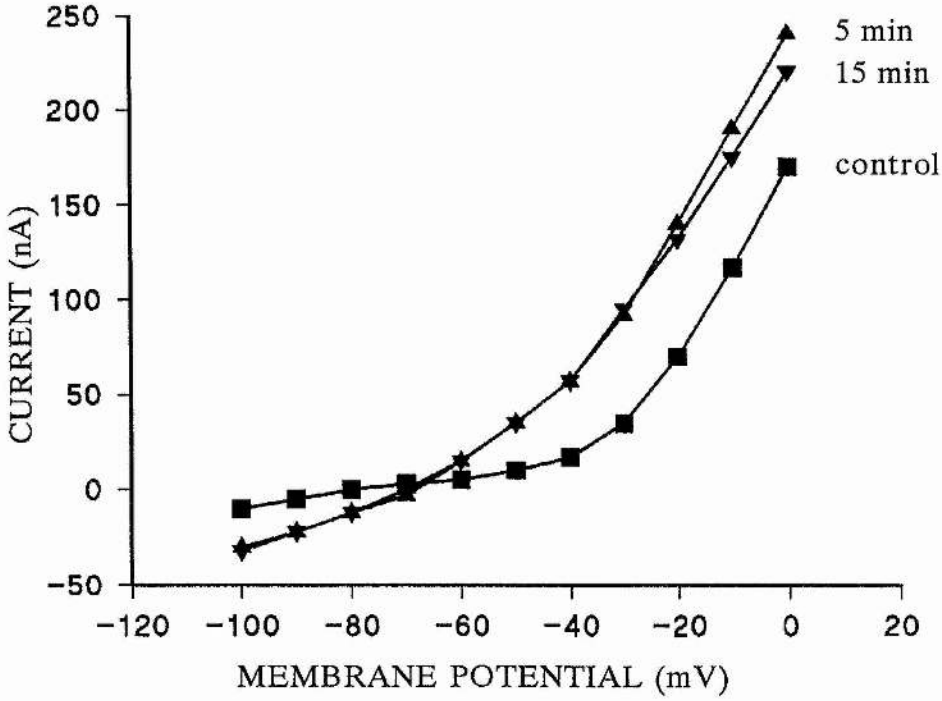
250
200
150
100
50
0
−50
CURRENT (nA)
−120
−100
−80
−60
−40
−20
0
20
MEMBRANE POTENTIAL (mV)
5 min
15 min
control

cii

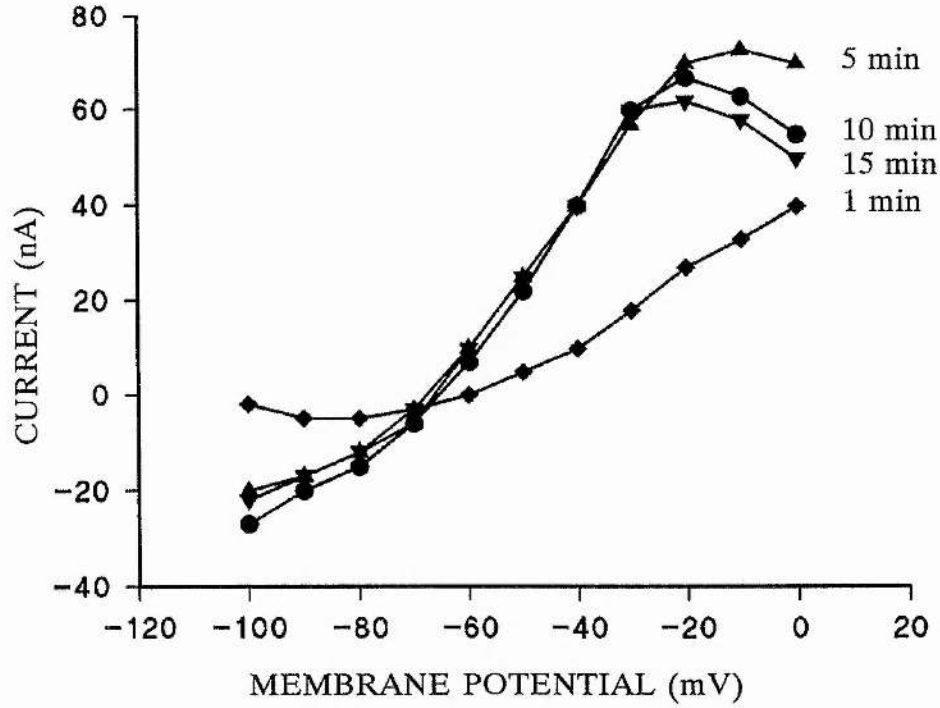
80
60
40
20
0
−20
−40
CURRENT (nA)
−120
−100
−80
−60
−40
−20
0
20
MEMBRANE POTENTIAL (mV)
5 min
10 min
15 min
1 min

Figure 5.10bi shows the effect of McN-A-343 in the presence of 1 mM Cd^{2+} ions on the I/V relationship of a neurone in which the outward current evoked at 0 mV decreased and reversed after 15 min exposure to McN-A-343 (n=2). The effect of McN-A-343 on the I/V relationship of a neurone in which the current did not reverse is shown in Figure 5.10bii (n=2). Prior to the addition of McN-A-343, the I/V relationship was similar to that produced in the presence of 500 μM Cd^{+} ions (n=4; Figure 5.8c, different preparation). When 10^{-4} M McN-A-343 was applied to the motoneurone, however, rectification was greatly reduced and the relationship became almost linear. The minimum current was evoked between -70 and -80 mV. Over the potential range -100 to -40 mV, the conductance of the membrane is greater than that in the control, as shown by the increase in the gradient of the graph. At potentials more positive than -40 mV, however, the membrane conductance is less than the control. The voltage-dependence of the current evoked by McN-A-343 can be seen more clearly in Figures 5.10ci & ii. The current produced by McN-A-343 in the example shown in Figure 5.10cii is similar to that evoked in the example in Figure 5.10ci, except that the maximum current was evoked at -20 mV rather than -30 mV. The current component produced at potentials between -100 and -20 or -30 mV was inwardly directed at potentials negative to between -70 and -80 mV, and outward at more positive potentials. There was little change in the amplitude of this current over 15 min exposure to agonist. The maximum inward current attained at -100 mV was 33·8 ± 2·7 nA (n=4); the peak outward current at -20 or -30 mV was 84·0 ± 6·5 nA (n=4). At potentials more positive than -20 or -30 mV the outward current decreased. The current component evoked over this potential range in the presence of Cd^{+} showed a time-dependency similar to that observed in normal saline, decreasing in amplitude during exposure to McN-A-343. The effect of McN-A-343 in the presence of Cd^{+} was irreversible one hour after washing the preparation: the input resistance was very low and the neurone was no longer viable.

Although the McN-A-343-induced current differs in some respects from that evoked in normal saline (Figure 5.6, different preparation), it is not abolished by blocking Ca^{2+} channels with Cd^{2+}, therefore it is unlikely that McN-A-343 acts on Ca^{2+} channels.

5.2.4.2.2. Verapamil

Verapamil was applied to the motoneurone at a concentration of 50 μM and the development of its effect was followed by monitoring the amplitude of the current evoked by stepping the membrane from the holding potential to 0 mV at a frequency of 1 Hz. The currents reached a steady state after 10 to 15 min, after which no further change in current amplitude was observed.

Once the membrane currents had stabilised, the effect of verapamil on the currents evoked in the motoneurone was investigated by stepping the membrane from -80 mV to command potentials between -100 and 0 mV. Figure 5.11a & b shows the outward currents evoked in two neurones before and after the addition of 50 μM verapamil (n=5). In all preparations, verapamil reduced the amplitude of the outward current, and caused the sustained current to become inactivating. Figure 5.11b shows that verapamil has much less effect on the transient outward current evoked at -20 (n=1) and 0 mV (n=2) than Cd^{2+} (Figure 5.9a).

The effect of 50 μM verapamil on the I/V relationship is illustrated in Figure 5.11c. In all preparations (n=5) the net outward current was reduced over the range of potentials tested. The current evoked at potentials negative to -40 mV was decreased by only 1 or 2 nA. At potentials more positive than -40 mV the effect on the outward current was greater, and increased as the command potential was made more positive. The verapamil-sensitive current varied between preparations: the net outward current, measured at 0 mV, was decreased by between 65 and 170 nA, which can be represented by a reduction of the outward current of between 15 and 25 %.

Figure 5.11a, b. The effect of 50 μM verapamil on the outward currents evoked by stepping the membrane from a holding potential of -80 mV to -40 (in (b) only), -20 and 0 mV in two different preparations. In the presence of verapamil the amplitude of the outward current decreased and the sustained outward current became inactivating. Verapamil does not have the same effect on the transient outward current as Cd^{2+} ((b)).

Scale: vertical 100 nA
horizontal 25 ms

Figure 5.11c. The currents evoked in the motoneurone were measured after 50 ms and used to construct an I/V relationship of the first basalar motoneurone in the absence and presence of 50 μM verapamil. At potentials negative to -40 mV a small inward current of only 1 or 2 nA was induced; this current increased in magnitude at potentials more positive than -40 mV.

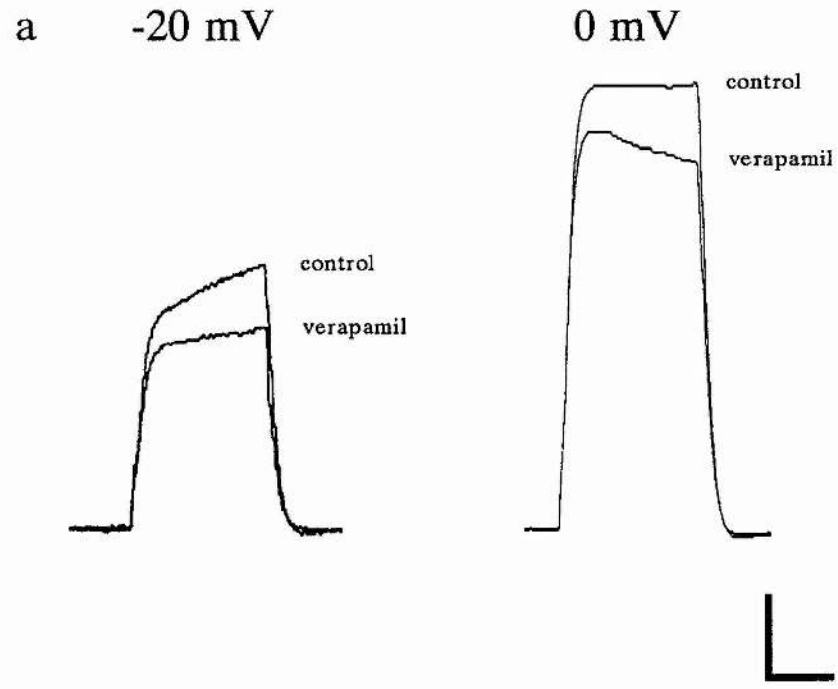

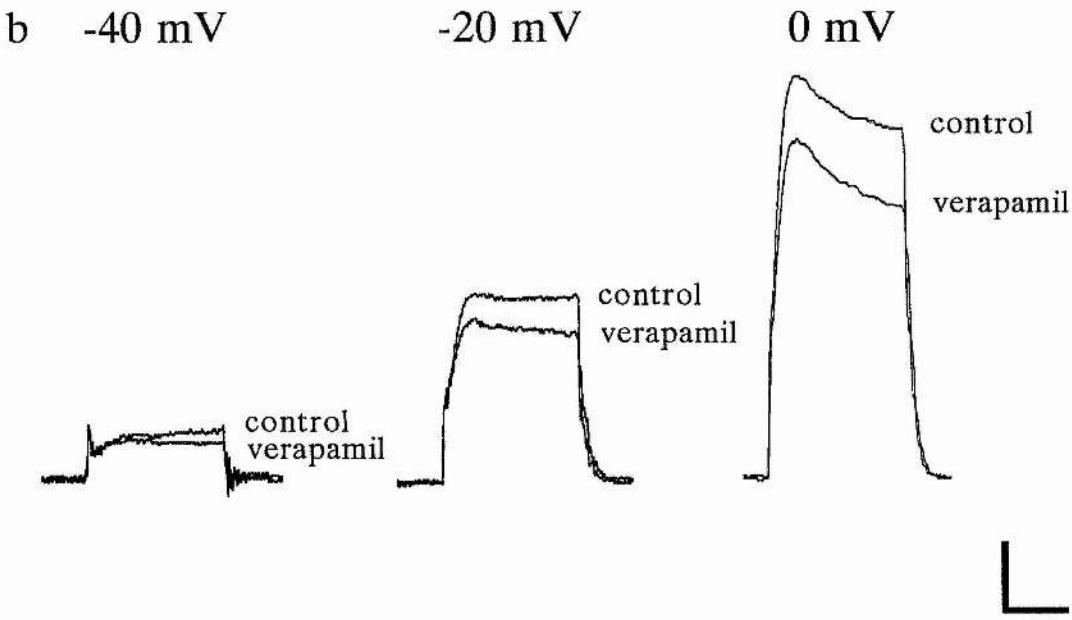
b
-40 mV
-20 mV
0 mV
control
verapamil
control
verapamil
control
verapamil

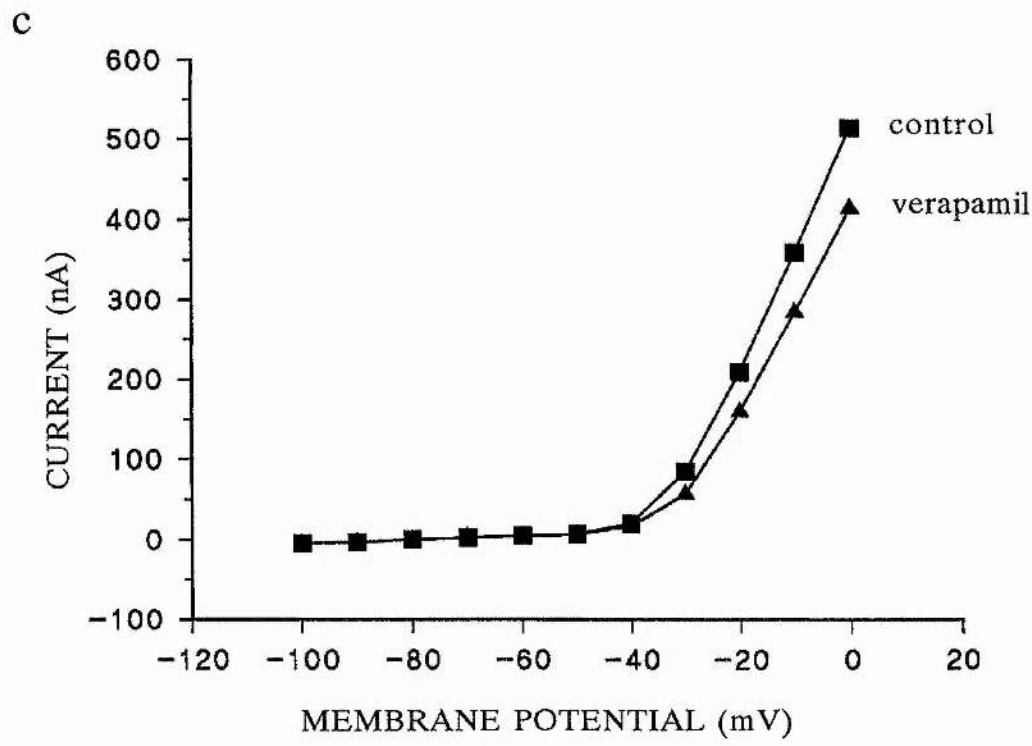
c
600
500
400
300
200
100
0
−100
CURRENT (nA)
−120
−100
−80
−60
−40
−20
0
20
MEMBRANE POTENTIAL (mV)
control
verapamil

After treating the neurone with 50 μM verapamil, 10^{-4} M McN-A-343 was applied (n=4) and the results are displayed in Figure 5.12. In the presence of verapamil, McN-A-343 decreased the amplitude of the outward current and induced an inward shift in the holding current, as shown in Figure 5.12a.

The effect of McN-A-343 on the I/V relationship of the neurone in the presence of verapamil is shown in Figure 5.12b, and the McN-A-343-induced current is shown in Figure 5.12c. An inward current was evoked at all potentials, which increased during 15 min exposure to McN-A-343. The minimum current was evoked at -60 (n=1) or -70 mV (n=3). The current component at potentials negative to -40 mV was relatively small, reaching a maximum of $4{\cdot}7 \pm 0{\cdot}3$ nA (n=4) after 15 min. At more positive potentials the current component was larger, and after 15 min was $30{\cdot}0 \pm 4{\cdot}1$ nA (n=4) at 0 mV.

The production of a current by McN-A-343 after block of Ca^{2+} channels with either Cd^{2+} or verapamil implies that the agonist does not act upon Ca^{2+} channels. When this is combined with the observation that McN-A-343 has no effect on the currents evoked in the motoneurone in the presence of the K^+ channel blockers Ba^{2+}, TEA^+ and Cs^+, it can be concluded that the apparent inward current evoked by activation of the 'mixed' receptors is due to the closure of K^+ channels.

5.2.5. EFFECT OF McN-A-343 ON INTRACELLULAR Ca^{2+} RELEASE

The experiments described above in Section 5.2.4. excluded the modulation by McN-A-343 of a Ca^{2+} influx through the surface membrane, but there remains the possibility that McN-A-343 stimulates the release of Ca^{2+} from intracellular stores. To investigate whether McN-A-343 may cause the release of Ca^{2+} from the intracellular stores of the first basalar motoneurone, cytosolic Ca^{2+} was chelated with BAPTA, which should buffer any change in intracellular Ca^{2+} concentration caused by release of Ca^{2+} from intracellular stores. Ca^{2+} is an intracellular messenger associated with several neurotransmitter receptors.

Figure 5.12a. In the presence of 50 μM verapamil, 15 min exposure to 10^{-4} M McN-A-343 decreased the outward currents evoked by stepping the membrane from a holding potential of -80 mV to -40, -20 and 0 mV and induced an inward shift in the holding current.

Scale: vertical 100 nA
horizontal 25 ms

Figure 5.12b. The currents evoked in the motoneurone in (a) were measured after 50 ms and used to construct an I/V relationship of the first basalar motoneurone in the presence of 50 μM verapamil before and after (5, 15 min) the addition of 10^{-4} M McN-A-343.

Figure 5.12c. The McN-A-343-induced current in the presence of 50 μM verapamil, obtained from the preparation in (b). An inward current was evoked over the potential range -100 mV to 0 mV. It was relatively small at potentials negative to -50 mV, and increased in size at more positive potentials.

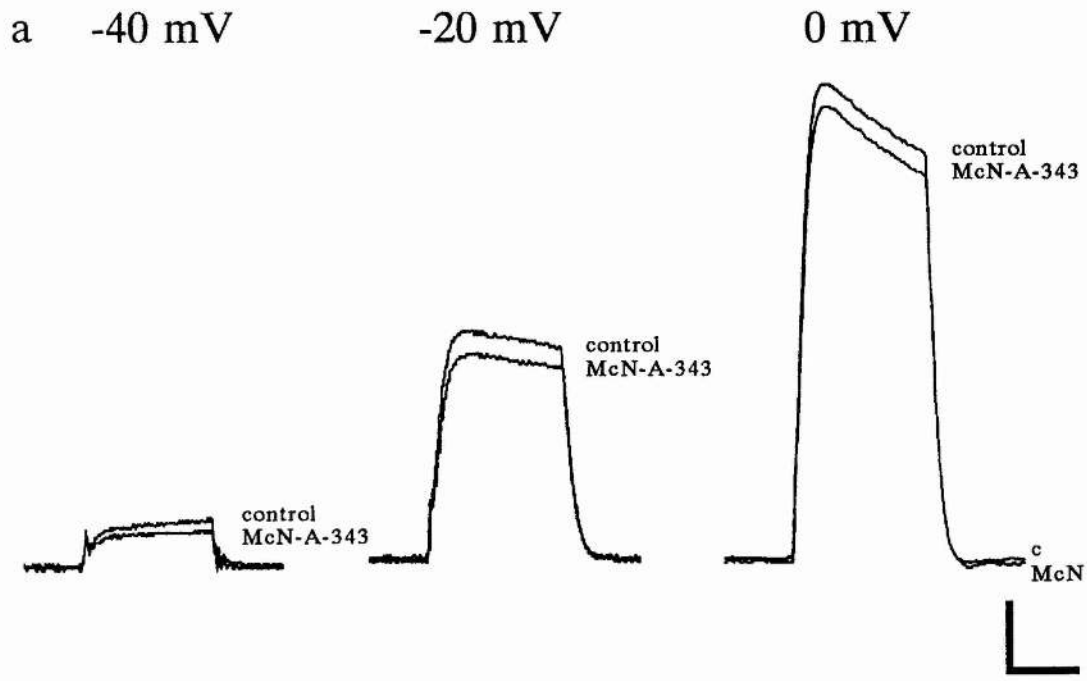

b

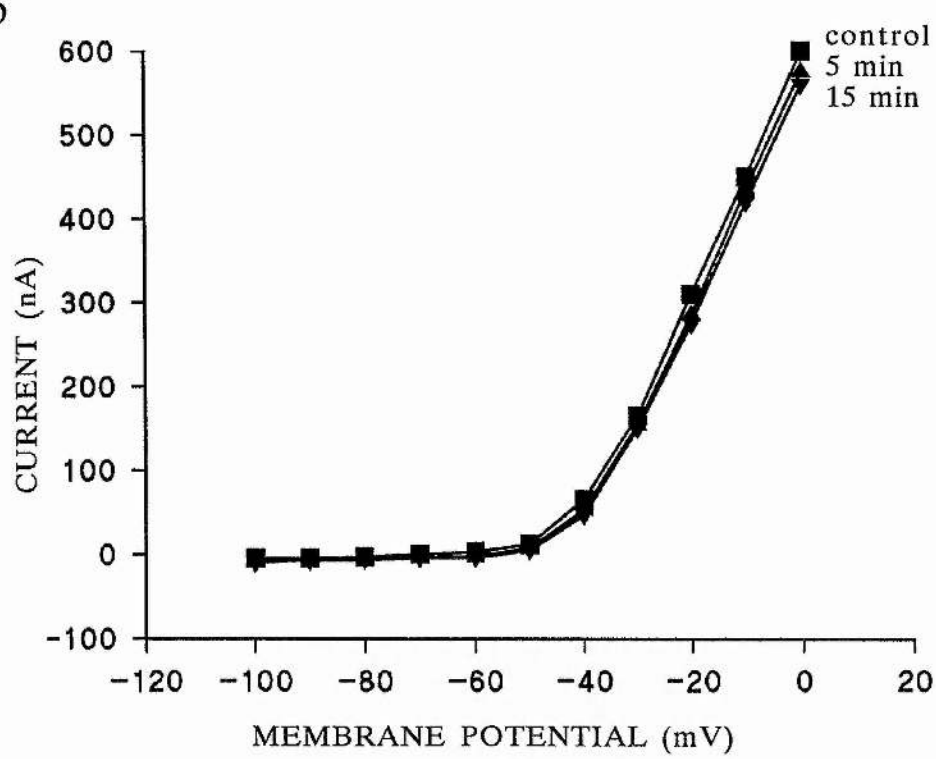
control
5 min
15 min
600
500
400
300
200
100
0
-100
CURRENT (nA)
-120
-100
-80
-60
-40
-20
0
20
MEMBRANE POTENTIAL (mV)

c

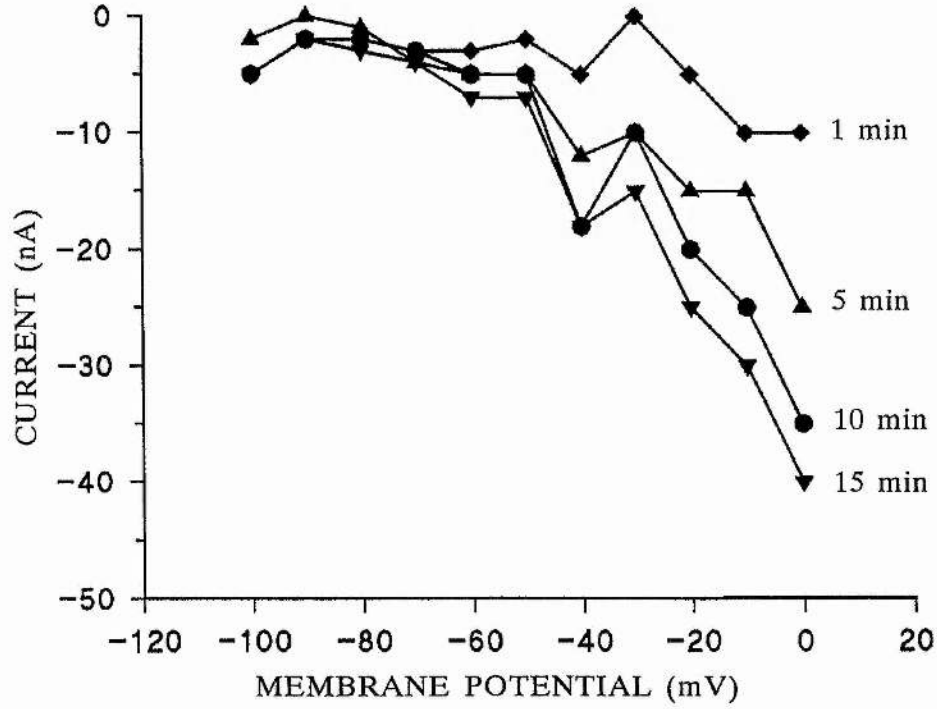
0
-10
-20
-30
-40
-50
CURRENT (nA)
1 min
5 min
10 min
15 min
-120
-100
-80
-60
-40
-20
0
20
MEMBRANE POTENTIAL (mV)

Therefore it is possible that the agonist-evoked reduction of the outward current at potentials more positive than -40 mV may be caused by the release of Ca^{2+} from intracellular stores, leading to the activation of calmodulin and the subsequent modulation of protein kinases (see Section 1.2.4.). Additionally, the outward current evoked by McN-A-343 in the presence of 1 mM Cd^{2+} may be a Ca^{2+}-dependent K^+ current, stimulated by an increase in intracellular Ca^{2+} (see Section 1.3.1.4.). The voltage-dependence of the McN-A-343-induced current would be due to the voltage-dependence of the Ca^{2+}-dependent K^+ current. The experiments were carried out both in the absence and presence of 1 mM Cd^{2+}: in the absence, to determine whether the reduction of the outward K^+ current evoked at potentials positive to -40 mV in normal saline may be mediated by Ca^{2+}, and in the presence, to investigate whether the outward current evoked by McN-A-343 at potentials negative to approximately -30 mV in the presence of Cd^{2+} may be a Ca^{2+}-dependent K^+ current.

The effect of injecting the cell with BAPTA is shown in Figure 5.13. The control was obtained with electrodes containing 2 M KAc, after which the current electrode was replaced with one in which the tip was filled with 100 mM BAPTA. The shaft of the electrode was filled with 2 M KAc. Hyperpolarising pulses were applied in current clamp mode (typically 5 to 8 nA to hyperpolarise the cell membrane by 30 mV; 500 ms, 1 Hz) to inject BAPTA anions (n=10). To determine whether BAPTA had been injected into the cell, the effect of the chelator on the action potentials evoked in the neurone was studied: decreasing the concentration of intracellular free Ca^{2+} by injecting a Ca^{2+} chelator results in the production of action potentials in insect neurones (Pitman, 1979), due to the increased driving force on Ca^{2+} across the membrane and the suppression of $I_{K(Ca)}$. Injecting BAPTA into the cell increased the amplitude of the action potential and evoked an after-hyperpolarisation after 10 min (n=10; Figure 5.13a).

Figure 5.13a. The effect of intracellular injection of BAPTA on the action potential (ai) evoked in the first basalar motoneurone by current injection (aii). Ten minutes after commencing the injection, the amplitude of the action potential was increased and an afterhyperpolarisation was produced.

Scale: vertical 20 mV
40 nA
horizontal 10 ms

Figure 5.13b. The effect of intracellular injection of BAPTA on the currents evoked by stepping the membrane from a holding potential of -80 mV to -40, -20 and 0 mV (different preparation to (a)). BAPTA decreased the amplitude of the outward current evoked at -40 (n=3), -20 (n=3) and 0 mV (n=6). In this example BAPTA induced an inward shift in the holding current.

Figure 5.13c. The effect of intracellular injection of BAPTA on the currents evoked by stepping the membrane from a holding potential of -80 mV to -20 and 0 mV (different preparation to (a) & (b)). BAPTA increased the amplitude of the outward current evoked at -20 (n=7) and 0 mV (n=4). In this example BAPTA induced an inward shift in the holding current.

Scale: vertical 100 nA
horizontal 25 ms

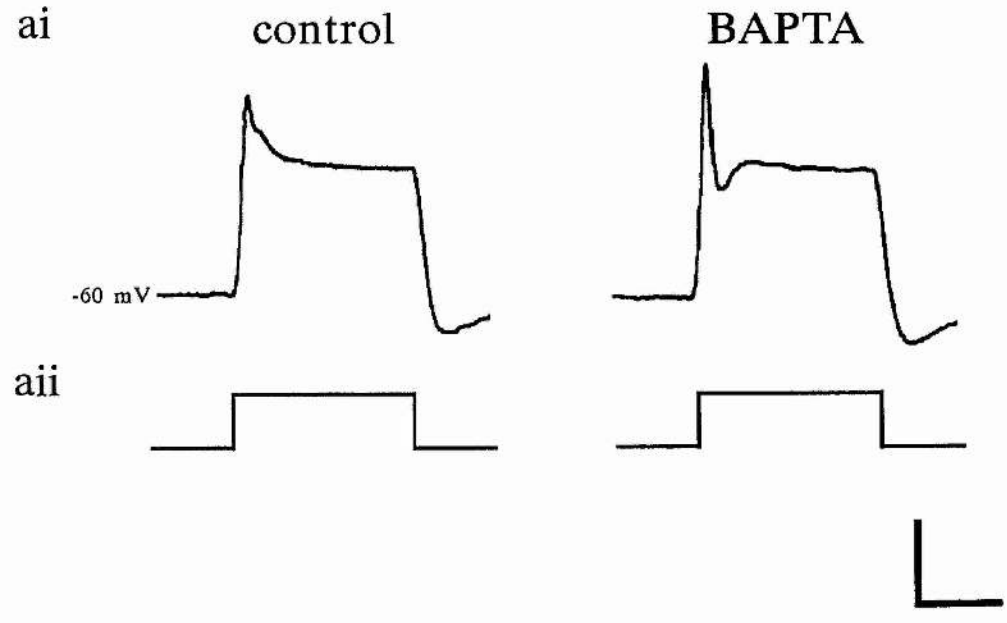

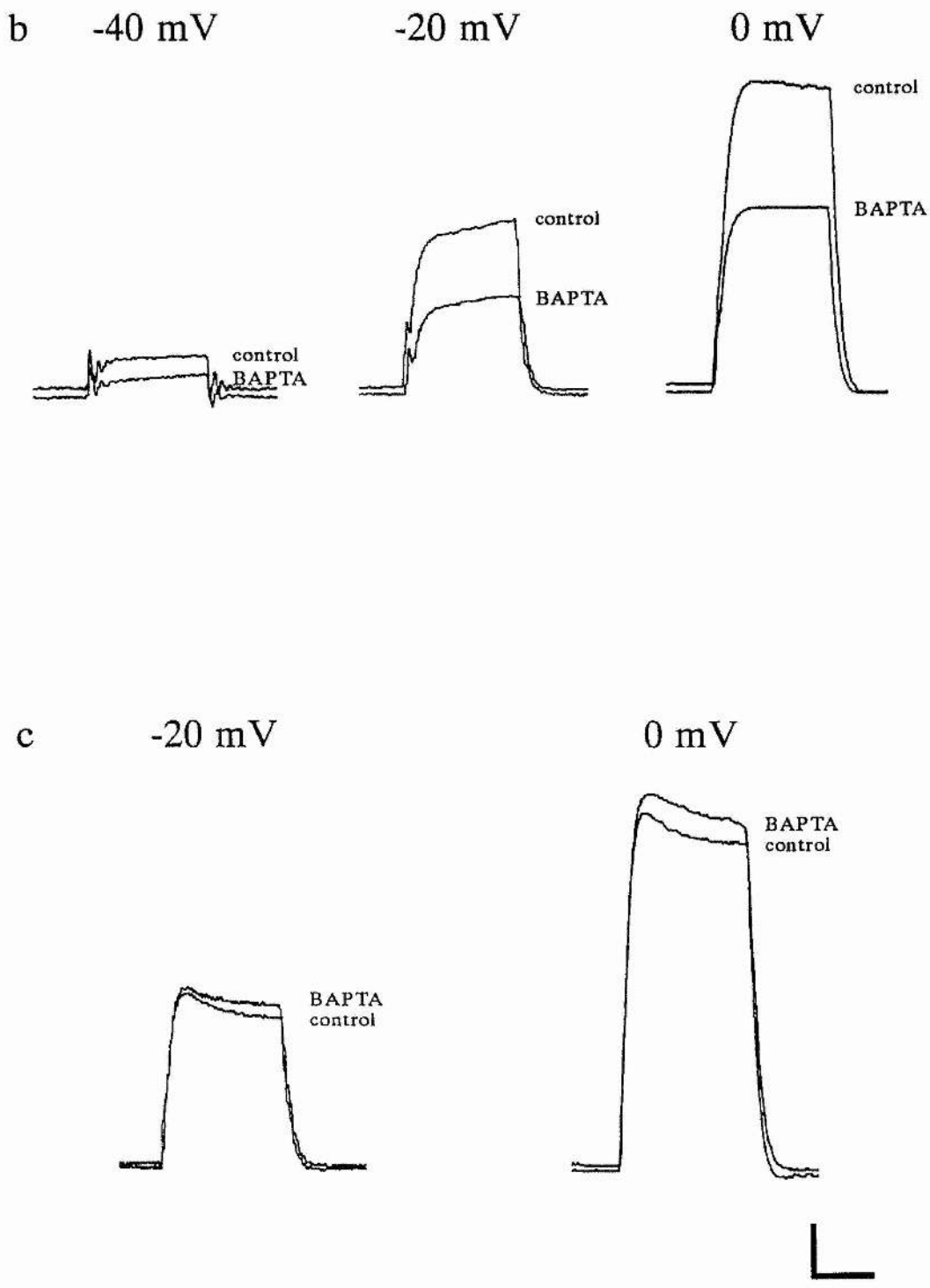
b
-40 mV
-20 mV
0 mV
control
BAPTA
control
BAPTA
control
BAPTA
c
-20 mV
0 mV
BAPTA
control
BAPTA
control

Figure 5.13d & e. The currents evoked in the motoneurone were measured after 50 ms and used to construct an I/V relationship of the first basalar motoneurone before and after injection of BAPTA.

Figure 5.13d. In the majority of neurones (n=8) BAPTA evoked an outward current at potentials positive to approximately -50 mV, increasing to a maximum in this cell at -30 mV and reversing at potentials positive to -10 mV. A small current, measuring a few nA, was evoked at potentials more negative to approximately -50 mV, which could be either inward or outward. The inset shows the BAPTA-induced current.

Figure 5.13e. The I/V relationship of the motoneurone before and after injection of BAPTA in the remaining preparations (n=2). BAPTA induced an inward current at potentials between -100 and 0 mV. The current evoked at potentials negative to -50 mV was relatively small compared with the current produced at more positive potentials. The inset shows the BAPTA-induced current.

d

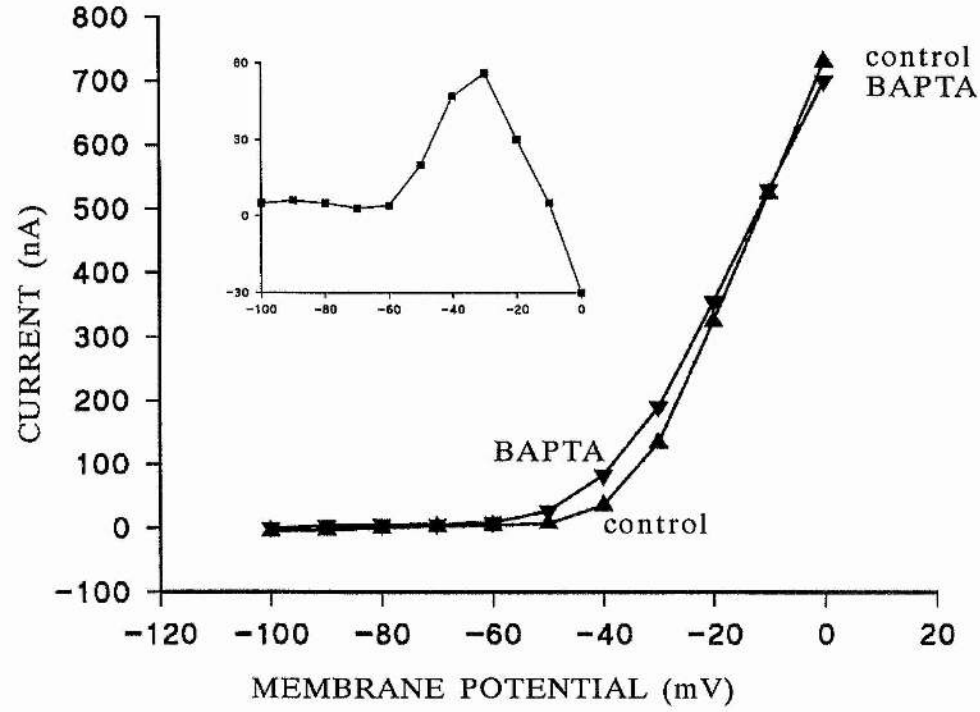
800
700
600
500
400
300
200
100
0
-100
CURRENT (nA)
-120
-100
-80
-60
-40
-20
0
20
MEMBRANE POTENTIAL (mV)
control
BAPTA
BAPTA
control

e

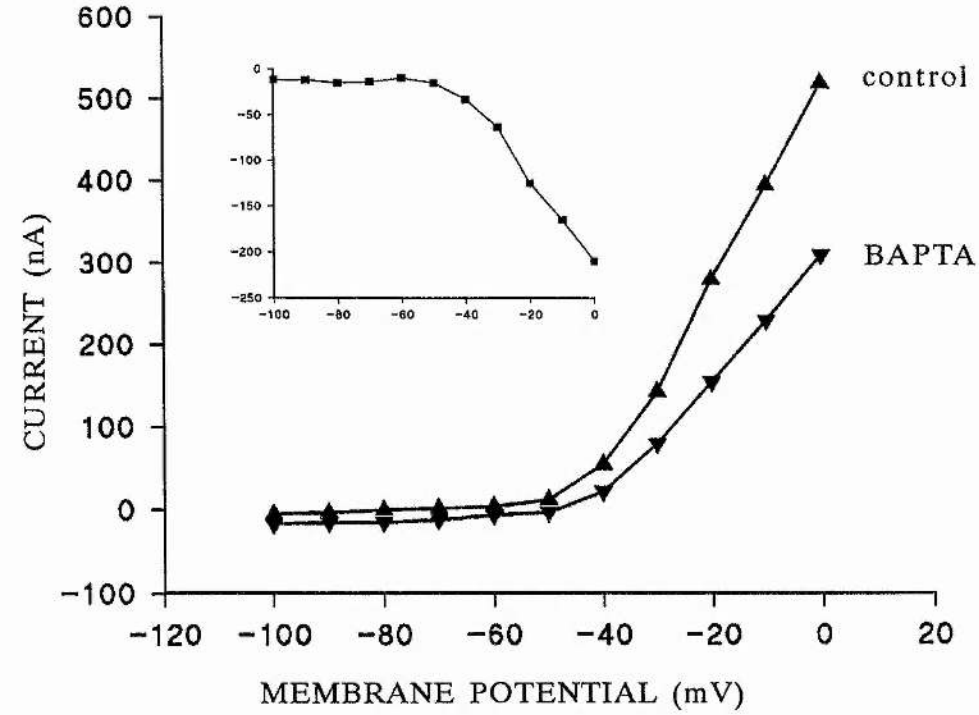
600
500
400
300
200
100
0
-100
CURRENT (nA)
-120
-100
-80
-60
-40
-20
0
20
MEMBRANE POTENTIAL (mV)
control
BAPTA

The effect of BAPTA injection (n=10) on the currents evoked in the motoneurone at potentials positive to -40 mV is displayed in Figure 5.13b & c. BAPTA decreased the outward currents evoked at -40 (n=3), -20 (n=3) and 0 mV (n=6), as shown in Figure 5.13b. In the remaining preparations, BAPTA increased the outward currents evoked at -40 (n=7), -20 (n=7) and 0 mV (n=4; Figure 5.13); BAPTA-induced action potentials were similar in these neurones and those in which the outward current was decreased. BAPTA induced an inward (n=5; Figure 5.13b & c) or an outward (n=5) shift in the holding current.

BAPTA was found to have one of two effects on the I/V relationship. In all cells (n=10) a small current, a few nA in amplitude, was evoked at potentials negative to approximately -50 mV. This current was inwardly directed in five preparations, and outward in the remaining five, and may be a result of re-impalement. At potentials positive to -50 mV, an outward current was produced in eight preparations (Figure 5.13d). The BAPTA-induced current is shown in the inset. The current increased to a maximum at potentials between -40 mV and -10 mV, before decreasing; in three preparations it reversed at -10 (n=1) or 0 mV (n=2). In the remaining two neurones, the current evoked by BAPTA was inwardly directed at potentials positive to -50 mV, as shown in Figure 5.13e. The inset shows the BAPTA-induced current. If the effect on the I/V relationships was an artefact caused by re-impaling the cells, there would probably be a change in the input resistance of the neurones, which, as Figures 5.13d & e show, is clearly not the case.

To examine whether the McN-A-343-induced current is mediated by the release of intracellular Ca^{2+}, the agonist was applied at a concentration of 10^{-4} M to three preparations which had been injected with BAPTA. The chelator had evoked an outwardly-directed current in two of these cells (similar to Figure 5.13d) and an inwardly-directed current in one (Figure 5.13e). After 15 min exposure to McN-A-343 the amplitudes of both the sustained current and transient current evoked at 0 mV (n=2) were reduced, as displayed in Figure 5.14a.

Figure 5.14a. The effect of 10^{-4} M McN-A-343 on the current evoked by stepping the membrane potential from a holding potential of -80 mV to -20 and 0 mV in a BAPTA-loaded cell. The amplitudes of both the sustained outward current and the transient current evoked at 0 mV (n=2) were reduced by McN-A-343.

Scale: vertical 100 nA
horizontal 25 ms

Figure 5.14b. The currents evoked in the motoneurone were measured after 50 ms and used to construct an I/V relationship of a BAPTA-loaded neurone in the absence and presence (5, 15 min) of 10^{-4} M McN-A-343 (different preparation to (a)).

Figure 5.14c. The McN-A-343-induced current in a neurone injected with BAPTA, obtained from the preparation in (b). An inward current was evoked at all potentials, small in amplitude negative to -50 mV, and larger at more positive potentials.

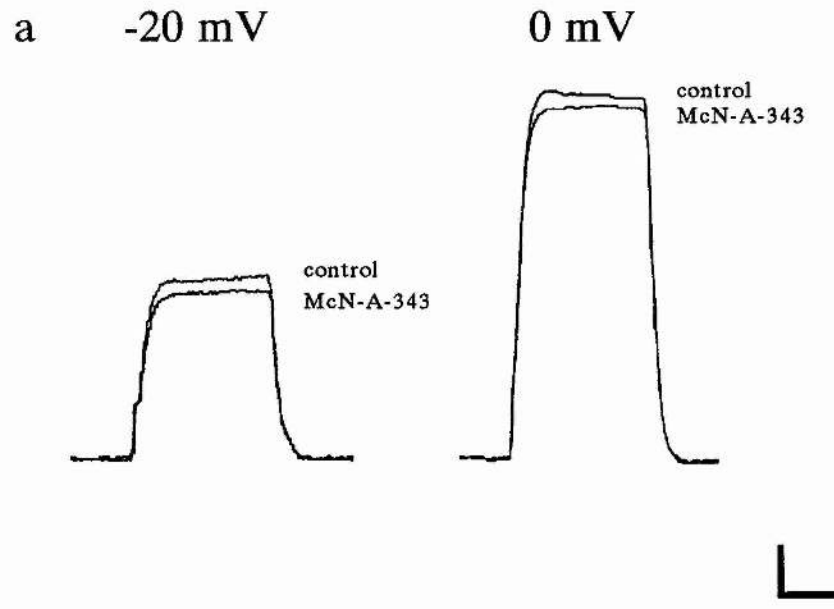

b

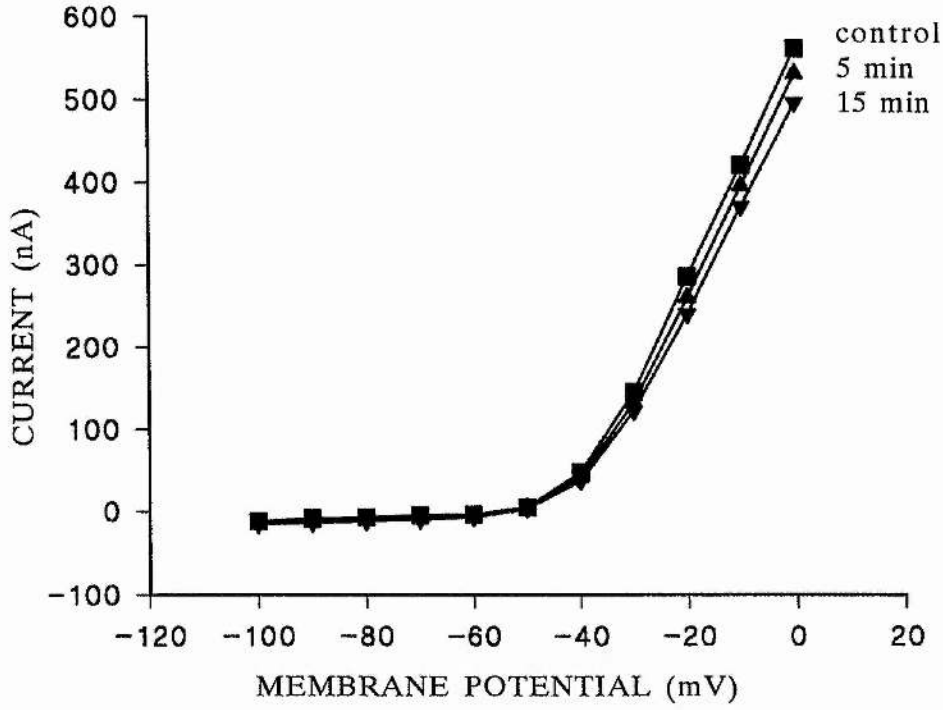
600
500
400
300
200
100
0
−100
CURRENT (nA)
control
5 min
15 min
−120
−100
−80
−60
−40
−20
0
20
MEMBRANE POTENTIAL (mV)

c

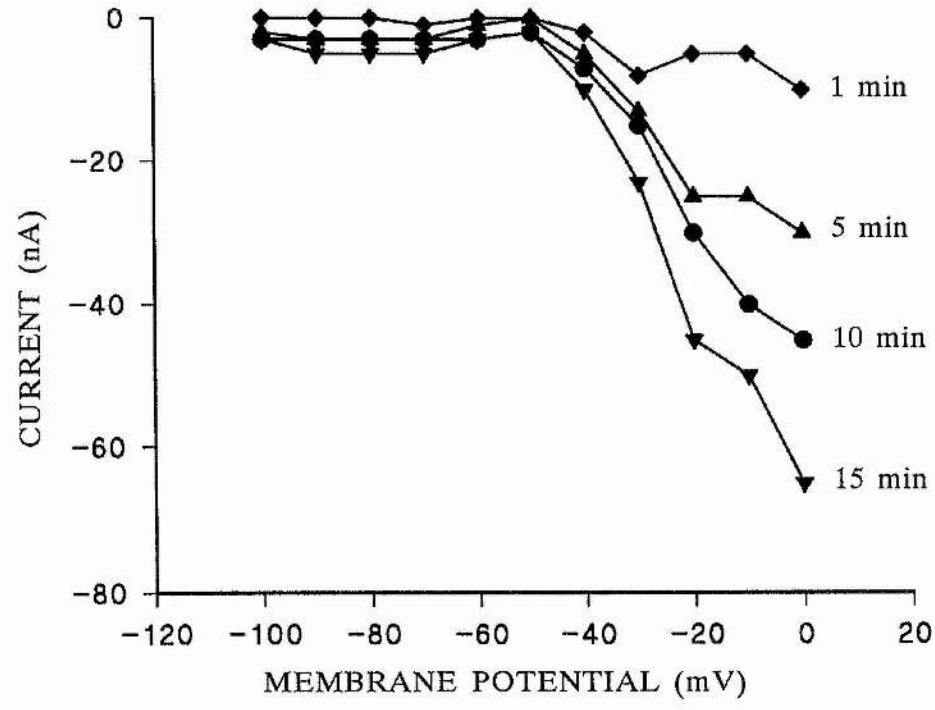
0
−20
−40
−60
−80
CURRENT (nA)
1 min
5 min
10 min
15 min
−120
−100
−80
−60
−40
−20
0
20
MEMBRANE POTENTIAL (mV)

The effect of McN-A-343 on the I/V relationship of a neurone injected with BAPTA is shown in Figure 5.14b, and the agonist-induced current is displayed in Figure 5.14c. Intracellular injection of BAPTA had little effect on the McN-A-343-induced current: an inward current was produced at all potentials, with a similar time- and voltage-dependency to the McN-A-343-induced current in an untreated neurone (Figure 5.6, different preparation). The current component evoked at potentials between -100 and -50 mV was voltage-independent. At more positive potentials the amplitude of the current increased as the command potential became more positive. The evoked current was time dependent and increased over the 15 min period of exposure to agonist. At potentials between -100 mV and -50 mV this current was only small, with an amplitude at -100 mV after 15 min of approximately 5 nA. At potentials more positive than -50 mV the magnitude of the current increased; after 15 min the outward current at 0 mV was 70 nA in two preparations, and 30 nA in the third.

These experiments suggest that the current induced by McN-A-343 at potentials positive to -40 mV is Ca^{2+} independent. The current evoked at more negative potentials in normal saline is too small to determine whether BAPTA has had an effect. There remains the possibility that the large, outward current induced by McN-A-343 in the presence of 1 mM Cd^{2+} ions (Figure 5.10) is mediated by a rise in free Ca^{2+}, which stimulates the production of a Ca^{2+}-dependent K^+ current. To test this hypothesis, McN-A-343 was applied to BAPTA-loaded neurones (n=3) in the presence of 1 mM Cd^{2+} ions (Figure 5.15). The agonist decreased the amplitude of the outward currents and induced an inward shift in the holding current, shown in Figure 5.15a.

The effect of McN-A-343 on the I/V relationship of a BAPTA-loaded neurone in the presence of 1 mM Cd^{2+} is displayed in Figure 5.15b, and the McN-A-343-induced current is shown in Figure 5.15c. Prior to the addition of Cd^{2+} and McN-A-343, the chelator had evoked an outwardly-directed current in all three preparations (similar to Figure 5.13d). The current produced by McN-A-343

Figure 5.15a. The effect of 10^{-4} M McN-A-343 on the current evoked by stepping the membrane potential from a holding potential of -80 mV to -20 and 0 mV in a BAPTA-loaded cell in the presence of 1 mM Cd^{2+}. The amplitudes of the outward currents were decreased and an inward shift in the holding current was produced.

Scale: vertical 100 nA
horizontal 25 ms

Figure 5.15b. The currents evoked in the motoneurone were measured after 50 ms and used to construct an I/V relationship of a BAPTA-loaded neurone in the presence of 1 mM Cd^{2+}, in the absence and presence (5 min, 15 min) of 10^{-4} M McN-A-343 (different preparation to (a)).

Figure 5.15c. The McN-A-343-induced current in a cell filled with BAPTA in the presence of Cd^{2+}, obtained from the preparation in (b). A small inward current was produced at potentials negative to -40 mV, increasing in amplitude during exposure to McN-A-343. At more positive potentials, a larger inward current was evoked, which also increased over the 15 min exposure period.

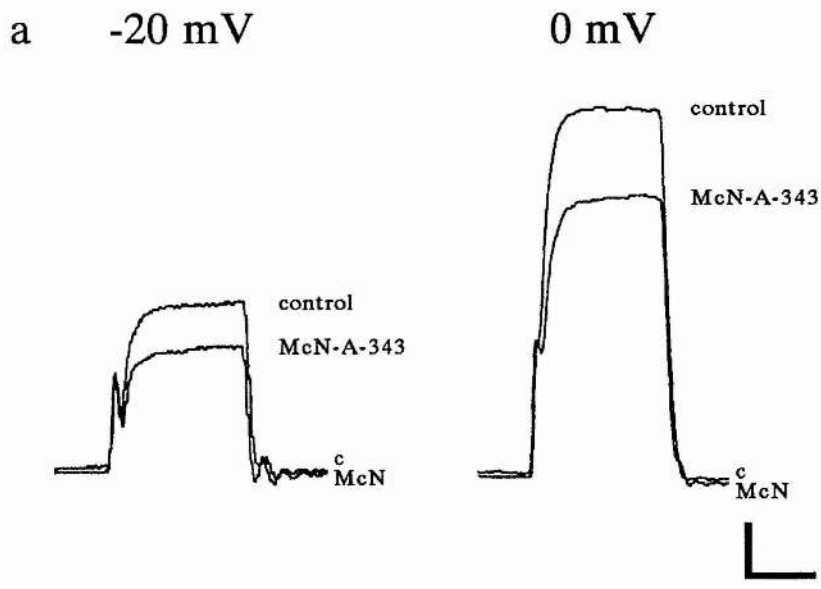

b

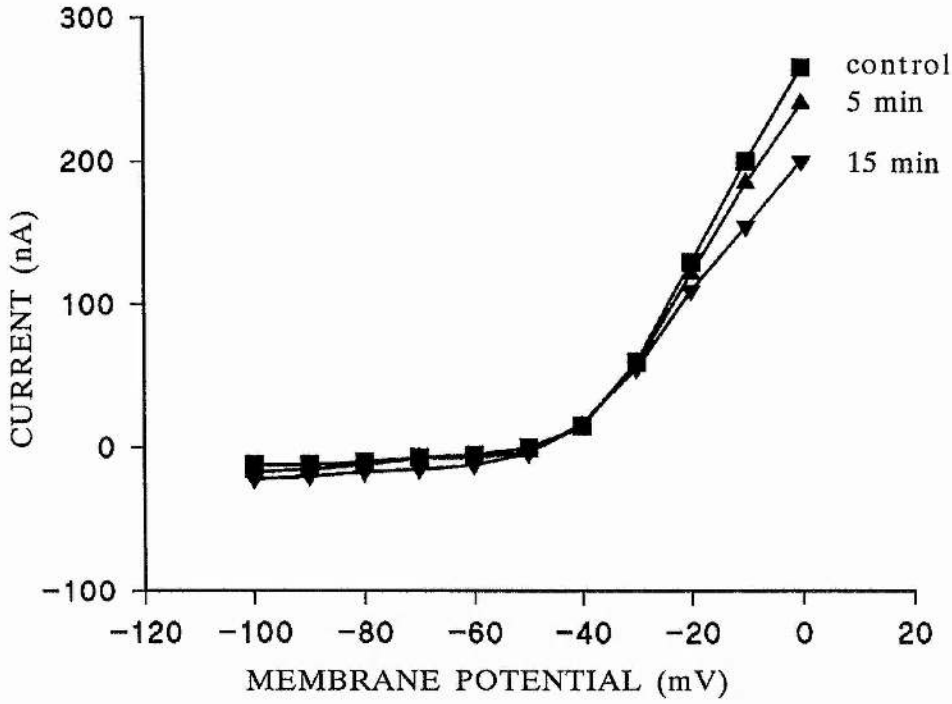
300
200
100
0
−100
CURRENT (nA)
−120
−100
−80
−60
−40
−20
0
20
MEMBRANE POTENTIAL (mV)
control
5 min
15 min

c

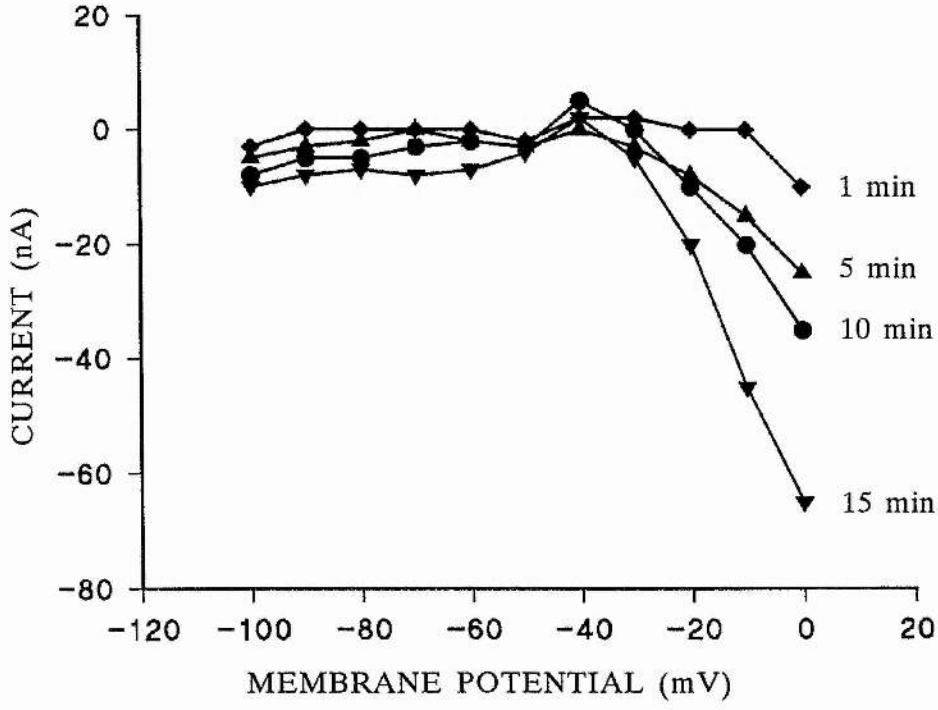
20
0
−20
−40
−60
−80
CURRENT (nA)
−120
−100
−80
−60
−40
−20
0
20
MEMBRANE POTENTIAL (mV)
1 min
5 min
10 min
15 min

(Figure 5.15c) was similar to that produced under normal conditions (in the absence of BAPTA and Cd^{2+}) (Figure 5.6, different preparation). A relatively small current was evoked at potentials more negative than -40 mV, with a minimum current evoked at -50 mV, and increased during exposure to agonist. This current component was relatively voltage-independent. After 15 min the current was approximately 10 nA at -100 mV. A small (less than 5 nA) outward current was evoked at -40 mV in two preparations, which reached a maximum after 10 min then decreased. This is shown in Figure 5.15c. At potentials more positive than -40 mV an inward current was produced, which increased in the presence of McN-A-343. At 0 mV the amplitude of the current was 78·3 ± 5·9 nA (n=3) after 15 min.

This experiment indicates that the McN-A-343-induced current at potentials positive to -40 mV is Ca^{2+} independent. However, it appears that McN-A-343 stimulates the release of Ca^{2+} from intracellular stores, resulting in the production of a large outward current in the presence of 1 mM Cd^{2+}. This current can be blocked by the Ca^{2+} chelator BAPTA.

5.3 DISCUSSION

5.3.1. MEMBRANE CURRENTS

The currents evoked in the motoneurone when the membrane was stepped from -80 mV to potentials between -100 and 0 mV were similar to those produced when the holding potential was -50 mV. Inward currents were produced at potentials negative to -80 mV and outward currents at more positive potentials. The currents evoked between -100 and -50 mV were square shaped. At potentials more positive than -50 mV, the currents either exhibited an outward relaxation into a non-inactivating outward current or a transient current preceding the sustained current.

Increasing the holding potential from -50 to -80 mV increased the amplitudes of both the sustained outward current and the transient outward current. This is probably due to a proportion of ion channels being inactivated at -50 mV, which is removed by increasing the holding potential to -80 mV. The inactivated channels are unable to conduct current, therefore a smaller current will be produced when the cell is jumped from -50 rather than -80 mV. The generation of a transient current does not appear to be due simply to the increase in the amplitude of the outward current. This is most clearly seen in Figure 5.3c & d, comparing the current evoked from a jump from -50 mV to 0 mV, and that produced by a step from -80 mV to -20 mV. The sustained current of the latter is smaller in amplitude, but the transient current is larger. This supports the theory that at the more positive holding potential there is a degree of channel inactivation which is removed by increasing the holding potential to -80 mV. The A-current, a transient outward K^+ current first described in molluscan neurones by Connor & Stevens in 1971 (Connor & Stevens, 1971b), is activated by depolarising steps from holding potentials negative to the normal resting potential; if the cell is held at a more positive holding potential, the current is inactivated. Increasing the amplitude of a hyperpolarising prepulse increases the amplitudes of the transient

currents recorded from the basalar/coxal depressor motoneurone of the cockroach (Nightingale & Pitman, 1989) and the marine ciliate *Euplotes vannus* (Krüppel et al, 1991). In the cockroach, increased activation was observed when hyperpolarising pre-pulses up to about -140 mV were applied; the same effect was recorded in *Euplotes* with hyperpolarising pulses up to -25 mV (more negative pulses were not applied because the activation threshold for this current is approximately -10 mV) (Krüppel et al, 1991). Similarly, the amplitude of the transient outward current evoked in bullfrog sympathetic neurones (MacDermott & Weight, 1982) was increased as the holding potential was increased to -100 mV.

The outward transient currents recorded from calf cardiac Purkinje fibres (Siegelbaum & Tsien, 1980), bullfrog sympathetic neurones (MacDermott & Weight, 1982), the marine ciliate *Euplotes* (Krüppel et al, 1991) and motoneurone D_f of the cockroach (David & Pitman, in preparation) appear to be mediated by an increase in intracellular Ca^{2+} because they can be reduced or blocked by intracellular injection of the Ca^{2+} chelators EGTA (Siegelbaum & Tsien, 1980; David & Pitman, in preparation) or BAPTA (Krüppel et al, 1991), the removal of Ca^{2+} from the extracellular solution (Siegelbaum & Tsien, 1980; MacDermott & Weight, 1982; David & Pitman, in preparation) or the addition of Ca^{2+} channel blockers such as D600 or Cd^{2+} ions (Siegelbaum & Tsien, 1980; MacDermott & Weight, 1982; Krüppel et al, 1991). Interestingly, EGTA had no effect on the transient current evoked in *Euplotes* (Krüppel et al, 1991). The transient outward current recorded from the first basalar motoneurone was blocked by external application of Cd^{2+} ions or intracellular injection of BAPTA, suggesting that it too is a Ca^{2+}-dependent K^+ current, which is activated by the influx of Ca^{2+} ions. In the presence of verapamil, the outward currents peak and then decline progressively during command pulses. However, this may not be a true transient current, but may represent a transformation in the properties of the sustained current caused by the application of verapamil. Although Cd^{2+} ions and verapamil

both decreased the amplitude of the sustained outward current, verapamil caused it to inactivate. Verapamil has been observed to increase the rate of inactivation of K^+ currents independently of an action on Ca^{2+} channels in human tracheal cells (Galietta et al, 1991), lung tumour cells (Pancrazio et al, 1991), kidney cells expressing heart K^+ channels (Rampe et al, 1993) and guinea-pig villus enterocytes (Tatsuta et al, 1994). It has been postulated that the inactivation of the outward current could be due to verapamil either blocking the open ion channel (Galietta et al, 1991; Pancrazio et al, 1991; Rampe et al, 1993), or affecting gating kinetics (Galietta et al, 1991; Tatsuta et al, 1994). To determine whether the inactivation of the outward current by verapamil observed in the first basalar motoneurone is a direct action on K^+ channels rather than by the drug's effect on Ca^{2+} channels, the preparation could be bathed in Ca^{2+}-free saline and the effect of verapamil on the K^+ current examined. The observation that verapamil decreases the amplitude of the Ba^{2+} current through Ca^{2+} channels without increasing the rate of inactivation of the Ba^{2+} current (Figure 5.7c) supports the theory that verapamil inactivates the K^+ current directly. Verapamil has, however, been found to increase the inactivation of Ca^{2+} channels in *Helix* neurones (Oyama et al, 1986).

The decrease in the amplitude of the sustained outward current by Cd^{2+} ions and verapamil implies that a proportion of this current is also Ca^{2+}-dependent. Ca^{2+}-dependent K^+ currents are a ubiquitous feature of cells (Rudy, 1988). The Ca^{2+}-dependent component of the outward current in the first basalar motoneurone appears to be voltage-dependent because Cd^{2+} and verapamil have the greatest effect on the I/V relationship of the cell at potentials positive to -40 mV. The extent to which the outward current was blocked varied between preparations, but was not a reflection of the concentration of Cd^+ ions applied (200 or 500 μM). This observation is probably due to a difference in either the density of Ca^{2+} channels, or the proportion of the outward current that is activated by Ca^{2+}.

Injecting a neurone with the Ca^{2+} chelator BAPTA decreases the outward current in some neurones, presumably because the Ca^{2+}-dependent K^+ current is suppressed (Connor, 1979; Lancaster & Nicoll, 1987). However, this was observed in only a minority of preparations in the experiments presented here. In the remainder, the amplitude of the outward current was increased, reaching a maximum at potentials between -40 and -10 mV before decreasing. The most likely explanation is that lowering the intracellular free Ca^{2+} concentration removes some of the Ca^{2+}-dependent Ca^{2+} channel inactivation (see Section 1.3.2.), resulting in an enhancement of the Ca^{2+} current, and therefore of the Ca^{2+}-dependent K^+ current. This hypothesis is supported by the observation that the voltage dependency of the outward current reflects that of the Ca^{2+} current (Figure 5.7e, f), which was maximal at -20 mV. However, BAPTA was present in the cell, because the shape of the action potential was affected and the McN-A-343-induced Ca^{2+}-dependent K^+ current in the presence of Cd^{2+} was blocked.

An inward Ca^{2+} current is revealed in the motoneurone when the outward K^+ currents are suppressed (Figure 5.7). This is achieved by the addition of 40 mM TEA^+ to saline containing 4 mM Ba^{2+} (Ca^{2+}-free saline), and using 2 M CsCl as an electrolyte. The current is confirmed as the entry of Ba^{2+} ions through Ca^{2+} channels because it can be reversibly reduced by verapamil. After washing verapamil from the preparation, the Ba^{2+} (or Ca^{2+}) current was increased in amplitude, which is probably due to an increase in the concentration of Ba^{2+} ions in the intercellular space surrounding the first basalar motoneurone, resulting in a greater driving force on the ions and therefore a larger current. The Ba^{2+} current was activated at potentials more positive than -50 mV, and increased in amplitude at increasingly positive command potentials, reaching a maximum at -20 mV. The reversal potential for Ca^{2+} is approximately + 50 mV (Hille, 1992), therefore it is unlikely that the decrease in the amplitude of the inward current at potentials positive to -20 mV is due to a decrease in the driving force on the Ba^{2+} ions;

rather, it is probably due to incomplete block of the voltage-dependent outward K^+ current, which is activated at potentials positive to -40 mV. At potentials between -40 and -20 mV, the Ba^{2+} current is larger than the K^+ current, and the net current will be inward. The K^+ current increases as the command potential becomes more positive than -40 mV, so that at -20 mV it is larger than the Ba^{2+} current. The net inward current will thus decrease in amplitude positive to -20 mV and eventually become outwardly directed. This theory is supported by the I/V relationship of the neurone shown in Figure 5.8, which was recorded from a different neurone using electrodes filled with 1 M CsCl. The outward current evoked at potentials more positive than -20 mV under these conditions was consistently larger than when 2 M CsCl was used. In addition, the peak inward current occurred at -30 rather than -20 mV in some preparations in which 1 M CsCl was used, which is consistent with the theory that there was less K^+ channel block in the presence of 1 M CsCl. It would be interesting to increase the K^+ channel block to attempt to characterise the Ca^{2+} current at potentials more positive than -20 mV.

5.3.2. MODULATION OF MEMBRANE CURRENTS BY McN-A-343

It was necessary to examine the effect of the increased holding potential on the McN-A-343-induced current in order to compare the results obtained here with those of the previous chapter. The holding potential appears to have little effect on the McN-A-343-induced current, although an initial outward current, evoked after 1 min exposure to agonist in approximately 50 % of preparations held at -50 mV, was not seen in the neurones held at -80 mV.

At potentials more positive than -40 mV, McN-A-343 induces a relatively large inward current which is time dependent and increases during exposure to the agonist. This current may be caused by the stimulation of an inward current such as Ca^{2+}, or the inhibition of an outward current such as K^+, which may or may not be Ca^{2+} dependent. Activation of muscarinic receptors leads to the production of a

Ca^{2+} current in SH-SY5Y human neuroblastoma cells (Murphy et al, 1991), guinea-pig ventricular myocytes (Gallo et al, 1993) and N1E-115 mouse neuroblastoma cells (Mathes & Thompson, 1994). The K^+ current may be reduced because of an inhibition of the Ca^{2+} current leading to the reduction of the Ca^{2+}-dependent K^+ current (Brezina, 1988, David & Pitman, 1993b, 1995), a direct action of muscarinic agonists on the Ca^{2+}-dependent K^+ current (Knöpfel et al, 1990) or the inhibition of a Ca^{2+}-independent K^+ current (Brown & Adams, 1980; Nagy et al, 1985; Brown & Higashida, 1988b; Le Corronc & Hue, 1993; ffrench-Mullen et al, 1994).

The effect of McN-A-343 on the Ca^{2+} current of the cell can be examined by applying the drug in the presence of the K^+ channel blockers Ba^{2+}, TEA^+ and Cs^+. No current was evoked, implying that the apparent inward current evoked by McN-A-343 in the first basalar motoneurone is not due to the stimulation of a Ca^{2+} current. However, in the presence of either Cd^{2+} ions or verapamil, McN-A-343 induces a current in the motoneurone. Although the current evoked in the presence of Cd^{2+} ions appears to be different to that produced either in normal saline or after the addition of verapamil, it is presumably mediated by K^+ ions because the Ca^{2+} current has been blocked. The McN-A-343-induced current in the presence of 1 mM Cd^{2+} ions consisted of a large outward current, reaching a maximum amplitude at -40 mV before decreasing. The current evoked at potentials more positive than -40 mV showed a similar time-dependency to that produced over this potential range in normal saline. The difference is that the current produced under normal conditions is an inward current, increasing in amplitude during exposure to agonist. The current evoked in the presence of Cd^{2+} is outwardly directed and decreases during exposure to agonist. It is proposed that these two currents are the same, but the one produced in the presence of Cd^{2+} is superimposed on an outward current. This suggests that McN-A-343 activates two currents: a current that is inward at potentials negative to between -70 and -80 mV and outward at more positive potentials, and an apparent inward current at

potentials more positive than -40 mV. These currents are presumably carried by K^+ ions rather than Ca^{2+} ions because the Ca^{2+} channels are blocked.

The Ca^{2+} dependency of these two currents was examined by loading the neurone with the Ca^{2+} chelator BAPTA. This had no apparent effect on the current evoked positive to -40 mV either in the absence or presence of Cd^{2+}. However, in the presence of Cd^{2+}, loading the cell with BAPTA blocked the outward current evoked negative to -40 mV and the McN-A-343-induced current resembled that evoked in normal saline. This implies that the outward current component is a Ca^{2+}-dependent K^+ current, which is activated by the release of Ca^{2+} from intracellular stores. The current evoked by McN-A-343 at potentials more positive than -40 mV is Ca^{2+}-insensitive. The voltage dependency of this current is similar to the outward current evoked in the neurone at command potentials positive to -40 mV and it suggests that McN-A-343 inhibits this voltage-dependent K^+ current.

There are two possible explanations as to why the McN-A-343-induced current in the presence of Cd^{2+} ions appears 'bell-shaped': one reason is that the effect on the voltage-dependent K^+ current evoked at potentials more positive than -40 mV is larger than the effect on the Ca^{2+}-dependent K^+ current, therefore as the voltage-dependent current is suppressed at potentials positive to -40 mV, the net current moves in an inward direction. A second, although less likely, explanation is that the Ca^{2+}-dependent K^+ current may be voltage-dependent and inactivate at approximately -40 mV, thus revealing the second current; this would represent a novel voltage- and Ca^{2+}-dependent K^+ current because the only such current reported to date (BK current; see Section 1.3.1.4.) is activated with depolarisation.

In two preparations out of four, the current evoked by McN-A-343 in the presence of Cd^{2+} reached a maximum at -30 mV before decreasing, and reversed direction at 0 mV (Figure 5.10ci). The currents evoked in the remaining neurones were largest at -20 mV and did not reverse (Figure 5.10cii). It is feasible that, because McN-A-343 modulates two currents, both the potential at which the peak

current is attained and the magnitude of the inward current are dependent upon the relative size of the agonist effects upon the two currents: if McN-A-343 evoked a relatively small Ca^{2+}-dependent K^+ current but a comparatively large decrease in the voltage-dependent K^+ current, the maximum current will be produced at a more negative potential. Conversely, if the Ca^{2+}-dependent K^+ current evoked by McN-A-343 is relatively large compared to the inhibition of the voltage-dependent K^+ current, the maximum amplitude of the current will not occur until a more positive potential.

The transient outward current evoked in the first basalar motoneurone upon depolarising pulses to potentials more positive than -40 mV is probably a Ca^{2+}-dependent K^+ current because it can be blocked by Cd^{2+} ions (Figure 5.9). In the presence of Cd^{2+}, McN-A-343 appears to stimulate the release of Ca^{2+} from intracellular stores, which may result in the activation of the transient Ca^{2+}-dependent outward current; under these conditions, the transient current may be enhanced sufficiently to dominate the outward current; therefore causing an apparent inactivation of the outward currents (Figure 5.10a).

Why the Ca^{2+}-dependent K^+ current was so large in the presence of Cd^{2+} ions is unclear. Cd^{2+} can be transported into cells (Toescu, 1991; Hinkle et al, 1992), and there is evidence that intracellular Cd^{2+} disturbs the Ca^{2+} homeostasis of the cell: it inhibits ATP-dependent Ca^{2+} uptake (Verbost et al, 1987; Shah & Pant, 1991) and Na^+/Ca^{2+} exchange (Smith et al, 1987) and also impairs the degradation of IP_3 (Storey et al, 1984). These effects will result in a prolongation of the effects of Ca^{2+}: in the absence of Cd^{2+}, the Ca^{2+} released by McN-A-343 would quickly be sequestered or expelled from the cell, resulting in a relatively brief Ca^{2+}-dependent K^+ current. However, in the presence of Cd^{2+} the increase in intracellular free Ca^{2+} concentration stimulated by McN-A-343 would be sustained, resulting in the continued production of a Ca^{2+}-dependent K^+ current. It also explains why there was no recovery after the addition of McN-A-343 in the presence of Cd^{2+}: there is evidence that prolonged exposure to a high

concentration of intracellular Ca^{2+} causes cell death (Schanne et al, 1979; Nicotera et al, 1986; Boobis et al, 1990).

The decrease in the outward current evoked by activation of the 'mixed' cholinergic receptors on the first basalar motoneurone was mimicked by application of the membrane permeable form, dibutyryl cAMP, or the phosphodiesterase inhibitor theophylline, both of which might be expected to increase intracellular cAMP. In addition, dibutyryl cAMP evoked an outward current during the first minute of exposure in some neurones. Theophylline did not evoke an outward current, which may be because it was too small to be resolved: further experiments must be performed to determine whether theophylline does evoke an initial outward current. The results presented here would therefore suggest that receptor activation leads to the production of cAMP, which modifies ion channels in the membrane, resulting in the currents observed. However, it is possible that cAMP is not directly involved in the production of the currents: increasing the concentration of cAMP may bring about currents similar to those evoked by activation of the 'mixed' receptors, but by a different mechanism. This theory is supported by the results obtained for motoneurone D_f of the cockroach: muscarinic agonists decrease the amplitude of the outward current in the neurone by suppressing the Ca^{2+} influx, thereby decreasing the Ca^{2+}-dependent K^+ current (David & Pitman, 1991, 1993b). Although the addition of dibutyryl cAMP to the neurone decreases the outward current in a similar manner to muscarinic agonists (David & Pitman, 1991, 1993b), it has no effect on the Ca^{2+} current (David & Pitman, personal communication). To determine whether muscarinic agonists stimulate the production of cAMP in the first basalar motoneurone, an adenylate cyclase inhibitor should be injected into the neurone prior to the addition of McN-A-343.

If both cAMP production and intracellular Ca^{2+} release are stimulated by activation of the 'mixed' cholinergic receptors, there remains the question of whether there is crosstalk between the two second messenger pathways. It seems unlikely that a rise in the concentration of intracellular free Ca^{2+} stimulates the production of cAMP, because in a BAPTA-loaded cell the McN-A-343-induced current is not suppressed. If it is assumed that cAMP does mediate the inhibition of the K^+ current, then this hypothesis could be investigated by the addition of cAMP to a neurone injected with BAPTA. However, from the results presented in this thesis, it is more likely that cAMP stimulates the release of Ca^{2+}, which has also been suggested for neurones of the mollusc *Euhadra* (Onozuka et al, 1988) and sarcoplasmic reticulum from both rabbit smooth muscle (Meissner, 1984) and guinea-pig cardiac muscle (Boller & Pott, 1989). An experiment which could be performed is the addition of cAMP to a neurone in the presence of 1 mM Cd^{2+} ions: under these conditions, if cAMP triggers Ca^{2+} release from intracellular stores, a Ca^{2+}-dependent K^+ current, similar to that evoked by McN-A-343 in the presence of Cd^{2+} ions, would be evoked.

SUMMARY

Increasing the holding potential of the motoneurone from -50 to -80 mV results in an increase in the amplitude of both the sustained outward current evoked at potentials positive to -40 mV, and the transient outward current, which implies that at a holding potential of -50 mV there is a degree of channel inactivation which is removed by increasing the holding potential to -80 mV.

The outward currents evoked in the neurone appear to be largely carried by K^+, since they can be greatly reduced by the K^+ channel blockers Ba^{2+}, TEA^+ and Cs^+. This treatment revealed the presence of an inward current, activated at potentials positive to -50 mV. It could be reversibly reduced by verapamil and was therefore concluded to be due to the entry of Ba^{2+} through Ca^{2+} channels. A maximum amplitude was reached at -20 mV; at more positive potentials the

current decreased. This was probably due to the development of a residual unblocked voltage-dependent K^+ current, since the reversal value is considerably more negative than the predicted Ca^{2+} equilibrium potential.

Both the sustained outward current and the transient outward current are Ca^{2+}-sensitive, because they were decreased in the presence of Cd^{2+} and verapamil. However, whereas Cd^{2+} simply decreased the amplitude of the sustained outward current, verapamil caused it to inactivate. This may be due to a direct effect on open K^+ channels rather than a secondary effect caused by the suppression of the Ca^{2+} current by verapamil.

Chelating intracellular Ca^{2+} with BAPTA in different preparations could increase or decrease the outward current. The increase in the outward current may be due to insufficient BAPTA present in the cell: when the steady-state concentration of free Ca^{2+} is decreased, a proportion of the Ca^{2+}-dependent Ca^{2+} channel inactivation may be removed (Eckert & Tillotson, 1981), resulting in an enhancement of the Ca^{2+} current, and therefore of the Ca^{2+}-dependent K^+ current. At higher concentrations of BAPTA, the transient increase in influx of Ca^{2+} ions may be buffered and enhancement of the Ca^{2+}-dependent K^+ current will not occur.

The apparent inward current evoked by McN-A-343 at potentials more positive than -40 mV is due to the reduction of an outward K^+ current rather than the activation of an inward Ca^{2+} current. This K^+ current is voltage-dependent because McN-A-343 has the largest effect at potentials positive to -40 mV, and Ca^{2+}-independent because it persists in a BAPTA-loaded cell. In the presence of Cd^{2+}, McN-A-343 evoked a large outward current which was shown to be a Ca^{2+}-dependent K^+ current, mediated by a rise in free Ca^{2+} due to release from intracellular stores. Therefore, two separate currents are differentially modulated by McN-A-343.

Increasing the intracellular concentration of cAMP by external application of dibutyryl cAMP or theophylline mimics the currents evoked by muscarinic

agonists, which suggests that activation of adenylate cyclase is involved in mediating the effects of receptor activation.

6. CONCLUSIONS & FUTURE WORK

This study has presented evidence for the existence of a population of α-BTX-resistant cholinergic receptors on the soma membrane of the first basalar motoneurone of the locust, *Schistocerca gregaria*. These receptors appear to have a predominantly muscarinic pharmacology, because the response to pressure-applied ACh in the presence of the toxin could be reversibly decreased by muscarinic antagonists. However, the receptors cannot strictly be classified as 'muscarinic' receptors due to the observation that under voltage clamp conditions, nicotine (in the presence of α-BTX) evokes a current similar to those produced by the muscarinic agonists muscarine and McN-A-343. This effect was not due to incomplete block of the nicotinic receptors or to a non-specific action on a non-cholinergic receptor because the nicotine-induced current could be blocked by the muscarinic antagonist scopolamine. Therefore the 'muscarinic' receptors are more accurately termed 'mixed' cholinergic receptors.

Whether these receptors are present on the synaptic membrane as well as the soma cannot be determined from the results obtained here. This could be examined by applying brief pulses of McN-A-343 in the neuropil of the ganglion in the region of the dendritic tree of the first basalar motoneurone, which would be expected to preferentially activate synaptically-located receptors rather than somatic receptors. Therefore, if the 'mixed' receptors are indeed present on the postsynaptic membrane, McN-A-343 would depolarise the neurone. Application of muscarinic agonists in this way depolarises cockroach giant interneurones (Le Corronc & Hue, 1993), motoneurone PPR of *Manduca* (Trimmer & Weeks, 1989) and the locust VPLI neurone (Baines & Bacon, 1994). However, injecting a muscarinic agonist into the neuropil may affect the first basalar motoneurone indirectly: the agonist may depolarise neurones other than the first basalar motoneurone, causing the release of ACh (or other neurotransmitters) which could in turn result in depolarisation of the first basalar motoneurone. In addition, if

there is a spontaneous release of ACh, the application of a muscarinic agonist could result in the hyperpolarisation of the first basalar motoneurone because of the decrease in neurotransmitter release caused by activation of the presynaptic muscarinic autoreceptors. This latter effect should be minimised by the use of the vertebrate M_1 subtype-selective agonist McN-A-343, because presynaptic muscarinic receptors in the insect CNS appear to have a pharmacology similar to vertebrate M_2 receptors (Knipper & Breer, 1988; Le Corronc et al, 1991).

Under voltage clamp, activation of the 'mixed' receptors results in the production of an apparent inward current over the potential range -100 to 0 mV; however, at potentials more positive than -40 mV, an initial outward current was evoked in approximately 50 % of neurones voltage clamped at -50 mV. This outward current was not recorded from neurones at a holding potential of -80 mV, and therefore warrants further investigation. The apparent inward current evoked at potentials positive to -40 mV is due to the inhibition of a voltage-dependent K^+ current rather than the production of a Ca^{2+} current, because it is suppressed in the presence of K^+ channel blockers but remains in the presence of Ca^{2+} channel blockers.

The initial outward current evoked in a proportion of neurones voltage clamped at -50 mV may be a Ca^{2+}-dependent K^+ current, but is unlikely to be the same current as recorded from neurones bathed in saline containing Cd^{2+} ions: the initial outward current is voltage-dependent and is activated only at potentials more positive to -40 mV, whereas the Ca^{2+}-dependent K^+ current evoked by McN-A-343 in the presence of Cd^{2+} is activated at potentials negative to -40 mV. Nevertheless, the Ca^{2+}-dependency of this current cannot be ruled out without further tests because a voltage-dependent, Ca^{2+}-dependent K^+ current does exist (see Section 1.3.1.4.). To investigate this, the effects of raising the concentration of intracellular free Ca^{2+} on the outward currents evoked in the motoneurone could be studied. One method to increase the concentration of intracellular free Ca^{2+} is to inject caged Ca^{2+} ions associated with Nitr-5 into the neurone, from

which they can be released by exposure to ultraviolet light. A second experiment is to examine the effects of the addition of charybdotoxin, a scorpion toxin which specifically blocks insect Ca^{2+}-dependent K^+ channels (J. Mills, personal communication).

Alternatively, since the initial outward current has the same voltage dependency as the K^+ current which is inhibited by McN-A-343, it is possible that it is the same current. This would imply that McN-A-343 has a dual effect on the voltage-dependent K^+ current, suppressing it in all neurones, but initially enhancing it in a proportion of neurones, which may involve two second messengers. There is evidence for dual modulation of ion channels by protein kinases A and C: protein kinase A activates K^+ channels in rat cortical collecting duct cells of the kidney (Wang & Giebisch, 1991) and Cl^- channels in human airway epithelial cells (Li et al, 1988), whereas these same channels are inhibited by protein kinase C (Wang & Giebisch, 1991; Li et al, 1989). A third possibility is that the outward current is produced by an action of McN-A-343 on an as yet unidentified current. From the work presented here, it is not possible to determine which of these two hypotheses is more likely.

Vertebrate muscarinic receptors are not integral receptor-ion channel complexes, and must therefore couple to a G protein to effect a change in membrane conductance. In the majority of known examples, activated G proteins subsequently modulate a second messenger cascade (see Section 1.2.). In the experiments presented here, the possible involvement of cAMP and Ca^{2+} were investigated. Both the inhibition of the voltage-dependent K^+ current and the initial outward current evoked at potentials positive to -40 mV were mimicked by the addition of dibutyryl cAMP, suggesting that the effects of muscarinic agonists on these currents may be mediated by cAMP; however, this is not conclusive proof because it is possible that increasing the concentration of cAMP may suppress the outward currents evoked in the motoneurone, producing similar effects to those resulting from activation of the 'mixed' receptors, but by a

different mechanism. A more conclusive result would be obtained by injecting an adenylate cyclase inhibitor into the neurone prior to the addition of McN-A-343: if cAMP synthesis mediates the suppression of the K^+ current by muscarinic agonists, then this procedure should block the effects of McN-A-343.

It would also be interesting to examine whether other second messenger pathways may be modulated by muscarinic agonists. In vertebrates, muscarinic receptor activation can result in the increased production of cyclic guanosine monophosphate (cGMP) (Kebabian et al, 1975; Wamsley et al, 1979; Castoldi et al, 1993; Sheng et al, 1993). Although there are no reports of muscarinic modulation of cGMP production in insects, cGMP is produced in response to eclosion hormone stimulation in moths (Truman et al, 1979; Morton & Truman, 1985). cGMP activates non-specific cation channels in silk moth olfactory neurones (Zufall & Hatt, 1991), inhibits K^+ channels in cultured olfactory neurones of *Manduca* (Zufall et al, 1991) and induces action potentials in sugar taste receptors of the fly, *Phormia regina* (Amakawa et al, 1990).

The results of the experiments performed in the presence of 1 mM Cd^{2+} ions provided evidence that McN-A-343 stimulates the release of Ca^{2+} from intracellular stores. An outward current was evoked, which was identified as a Ca^{2+}-dependent K^+ current because it could be blocked by intracellular injection of BAPTA. This current was apparent in the presence of Cd^{2+} because these ions upset the Ca^{2+} homeostasis of the cell (see Chapter 5). The subsequent effects of the increase in cytosolic Ca^{2+} concentration under normal conditions are unclear: Ca^{2+} ions do not appear to be involved in the inhibition of the voltage-dependent K^+ current because buffering cytosolic Ca^{2+} with BAPTA did not reduce the effect of McN-A-343. However, Ca^{2+} involvement in the suppression of the outward current cannot be ruled out without further tests, such as examining the effects of releasing caged Ca^{2+} as described above.

It is possible that the inward current at command potentials more negative than -40 mV may be a Ca^{2+}-dependent K^+ current. In a proportion of neurones,

this current increased to a maximum after 10 min before decreasing in the continued presence of agonist; this time dependency could be due to a net decrease in second messenger accumulation due to sequestration or metabolism of the second messenger. At first, it may seem unlikely that this current may be mediated by K^+ because the minimum current is evoked between -60 and -40 mV, which is more positive than the expected K^+ equilibrium potential. However, the reversal potential of the Ca^{2+}-dependent K^+ current of motoneurone D_f of the cockroach was calculated to be approximately -70 mV, although the reversal potential of tail currents evoked after depolarising pulses was more positive than this (Thomas, 1984). The discrepancy was postulated to be due to extracellular K^+ accumulation in the convolutions of the cell membrane. A similar explanation was put forward by Nightingale & Pitman (1989) for the lack of effect of extracellular K^+ concentration on the tail current reversal potential. Therefore, it is possible that the K^+ equilibrium potential of the first basalar motoneurone undergoes a positive shift as a consequence of the depolarising pulses applied to the neurone to construct an I/V curve, which could result in the accumulation of K^+ in the membrane infoldings. This would explain why the inward current evoked at potentials negative to -40 mV reached a minimum between -60 and -40 mV. The current does not actually reverse at these potentials, probably because the decrease in the amplitude of the outward current produced by inhibition of the voltage-dependent K^+ current is larger than the K^+ current activated by the rise in intracellular free Ca^{2+} concentration. The possible involvement of Ca^{2+} in mediating this current can be investigated with caged Ca^{2+} as described above. Additionally, the effects of charybdotoxin on this current can be examined.

In current clamp, bath application of McN-A-343 either increased or decreased the input resistance. Both observations can be explained by the inhibition of the voltage-dependent K^+ current. In neurones in which the input resistance increased, the membrane potential was unaffected: the increase in input

resistance is caused by the closure of K^+ channels, which has no effect on the membrane potential because the K^+ equilibrium potential is close to the resting membrane potential, therefore the driving force on the ions is low. The decrease in the input resistance, accompanied by a depolarisation of the membrane, may be a secondary effect of inhibition of the K^+ current: in some cases, the closure of K^+ channels may produce a small depolarisation, sufficient to reach the activation threshold of voltage-dependent Ca^{2+} and Na^+ channels. These channels would open, resulting in a decrease in input resistance and depolarisation of the membrane.

The inhibition of the voltage-dependent K^+ current by muscarinic agonists would therefore be expected to lead to an increase in the excitability of the motoneurone, a theory supported by the experiments investigating the effects of McN-A-343 on the spike threshold. However, the decrease in the spike threshold was small compared with the results obtained from the PPR motoneurone of *Manduca* (Trimmer & Weeks, 1993), cockroach giant interneurones (Le Corronc & Hue, 1993) and locust VPLI interneurones (Baines & Bacon, 1994). Clearly, more experiments must be performed to clarify this. If the 'mixed' receptors do modulate the excitability of the neurone, then muscarinic antagonists would be expected to increase the spike threshold. It is also important to examine whether the effects of nicotine are potentiated in the presence of muscarinic agonists, which was found to be the case in locust VPLI interneurones (Baines & Bacon, 1994). An alternative protocol is to examine the effects of McN-A-343 on the threshold for a synaptically evoked action potential (in the absence of α-BTX), a technique employed by Le Corronc & Hue (1991).

The muscarinic agonist-sensitive, voltage-dependent K^+ current thus appears to be analogous to the M-current, a muscarine-sensitive, voltage-dependent K^+ current present in many types of vertebrate excitable cells (reviewed by Brown, 1988; also see Section 1.3.1.5.). Muscarinic receptors mediate a slow epsp, caused by the inhibition of the M-current, which increases the excitability of

the cell. To date, there have been no reports of the M-current in invertebrate cells: although the muscarinic agonist-sensitive current in the first basalar motoneurone is similar, and probably performs the same function (modulation of the neurone's excitability), the kinetics of the M-current are slower.

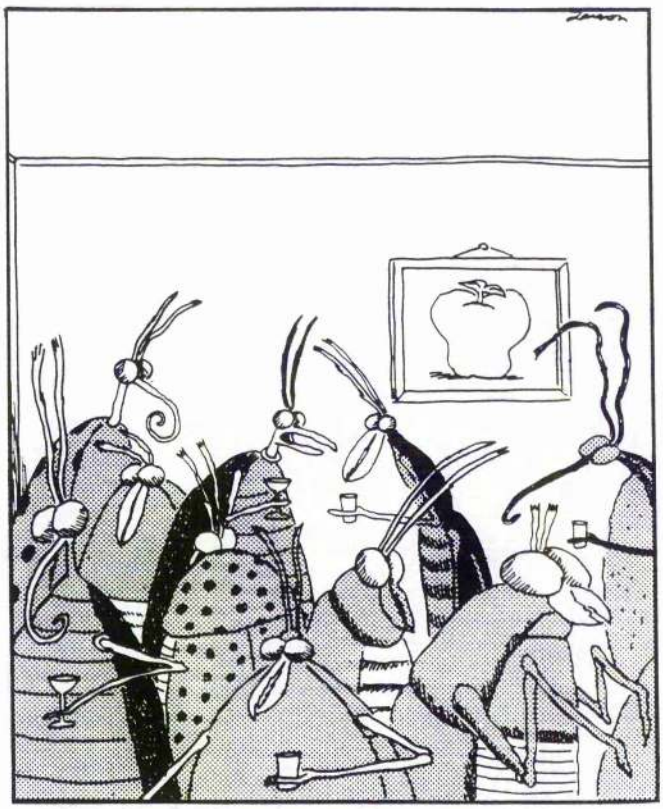

"Think about it, Ed.... the class Insecta contains 26 orders, almost 1,000 families, and over 750,000 described species — but I can't shake the feeling we're all just a bunch of bugs."

Cartoon by Gary Larson
From: The Prehistory of The Far Side: A 10th Anniversary Exhibit. Warner Books, London.

REFERENCES

Abdallah, E.A.M., Eldefrawi, M.E. & Eldefrawi, A.T. 1991. Pharmacologic characterization of muscarinic receptors of insect brains. *Arch. Insect. Biochem. Physiol.* **17**, 107-118.

Abrams, T.W., Karl, K.A. & Kandel, E.R. 1991. Biochemical studies of stimulus convergence during classical conditioning in *Aplysia*: dual regulation of adenylate cyclase by Ca^{2+}/calmodulin and transmitter. *J. Neurosci.* **11**(9), 2655-2665.

Adams, P.R. Constanti, A., Brown, D.A. & Clark, R.B. 1982a. Intracellular Ca^{2+} activates a fast voltage-sensitive K^+ current in vertebrate sympathetic neurones. *Nature (Lond.).* **296**, 746-749.

Adams, P.R., Brown, D.A. & Constanti, A. 1982b. Pharmacological inhibition of the M-current. *J. Physiol. (Lond.).* **332**, 223-262.

Adrian, R.H., Chandler, W.K. & Hodgkin, A.L. 1968. Voltage clamp experiments in striated muscle fibers. *J. Gen. Physiol.* **51**, 188S-192S.

Aguilar, J.S. & Lunt, L.G. 1984. Cholinergic binding sites with muscarinic properties on membranes from the supraoesophageal ganglion of the locust (*Schistocerca gregaria*). *Neurochem. Int.* **6**(4), 510-507.

Akil, M. & Fisher, S.K. 1989. Muscarinic receptor-stimulated phosphoinositide turnover in human SK-N-SH neuroblastoma cells: differential inhibition by agents that elevate cyclic AMP. *J. Neurochem.* **53**, 1479-1486.

Akins, P.T., Surmeier, D.J. & Kitai, S.T. 1990. Muscarinic modulation of a transient K^+ conductance in rat neostriatal neurons. *Nature (Lond.).* **344**, 240-242.

Alkondon, M. & Albequerque, E.X. 1994. Presence of α-bungarotoxin-sensitive nicotinic acetylcholine receptors in rat olfactory bulb neurons. *Neurosci. Lett.* **176**, 152-156.

Altman, J.S. 1980. Toluidine blue as a rapid stain for nerve cell bodies in insect ganglia. In: *Neuroanatomical Techniques: insect nervous system.* 21-24. Ed. Strausfeld, N.J. & Miller, T.A. Springer-Verlag.

Altman, J.S. & Tyrer, N.M. 1977. The locust wing hinge stretch receptors. I. Primary sensory neurones with enormous central arborizations. *J. Comp. Neurol.* **172**, 409-430.

Amakawa, T., Ozaki, M. & Kawata, K. 1990. Effects of cyclic GMP on the sugar taste receptor cell of the fly, *Phormia regina*. *J. Insect. Physiol.* **36**(4), 281-286.

Armstrong, C.M. & Binstock, L. 1965. Anomalous rectification in the squid giant axon injected with tetraethylammonium chloride. *J. Gen. Physiol.* **48**, 859-872.

Armstrong, C.M., Swenson, R.P. & Taylor, S.R. 1982. Block of squid axon K channels by internally and externally applied barium ions. *J. Gen. Physiol.* **80**, 663-682.

Ascher P., Large, W.A. & Rang, H.P. 1979. Studies on the mechanism of action of acetylcholine antagonists on rat parasympathetic ganglion cells. *J. Physiol. (Lond.).* **295**, 139-170.

Augustinsson, K.B. & Grahn, M. 1954. The occurrence of choline esters in the honey-bee. *Acta Physiol. Scand.* **32**, 174-190.

Aziz, S.A. & Eldefrawi, M.E. 1973. Cholinergic receptors of the central nervous system of insects. *Pest. Biochem. Physiol.* **3**, 168-174.

Bai, D., Erdbrugger, H., Breer, H., & Sattelle, D.B. 1992. Acetylcholine receptors of thoracic dorsal midline neurones in the cockroach, *Periplaneta americana*. *Arch. Insect. Biochem. Physiol.* **21**, 289-301.

Baines, R.A. & Bacon, J.P. 1994. Pharmacological analysis of the cholinergic input to the locust VPLI neuron from an extraocular photoreceptor system. *J. Neurophysiol.* **72**(6), 2864-2874.

Baker, P.F., Hodgkin, A.L. & Ridgway, E.B. 1971. Depolarisation and calcium entry in squid giant axons. *J. Physiol. (Lond.).* **218**, 709-755.

Baker, P.S., Gewecke, M. & Cooter, R.J. 1981. The natural flight of the migratory locust, *Locusta migratoria* L. III. Wing-beat frequency, flight speed and attitudes. *J. Comp. Physiol.* **141**, 233-237.

Barlow, R.B., Berry, K.J., Glenton, P.A.M., Nikolaou, N.M. & Soh, K.S. 1976. A comparison of affinity constants for muscarine-sensitive acetylcholine receptors in guinea-pig atrial pacemaker cells at 29° C and in ileum at 29° C and 37° C. *Br. J. Pharmacol.* **5**, 613-620.

Barnard, E.A., Wieckowski, J. & Chiu, T.H. 1971. Cholinergic receptor molecules and cholinesterase molecules at mouse skeletal muscle junctions. *Nature (Lond.).* **234**, 207-209.

Baumgold J. & Fishman, P.H. 1988. Muscarinic receptor-mediated increase in cAMP levels in SK-N-SH human neuroblastoma cells. *Biochem. Biophys. Res. Comm.* **154**(3), 1137-1143.

Baumgold, J., Paek, R. & Fiskum, G. 1992. Calcium independence of phosphoinositide hydrolysis-induced increase in cAMP accumulation in SK-N-SH human neuroblastoma cells. *J. Neurochem.* **58**, 1754-1759.

Ben-barak, J.B. & Dudai, Y. 1979. Cholinergic binding sites in rat hippocampal formation: properties and ontogenesis. *Brain Res.* **166**, 245-257.

Benishin, C.G., Sorensen, R.G., Brown, W.E., Krueger, B.K. & Blaustein, M.P. 1988. Four polypeptide components of green mamba venom selectively block certain potassium channels in rat brain synaptosomes. *Mol. Pharmacol.* **34**, 152-159.

Benson, J.A. 1989. M1-like muscarinic receptors mediate cholinergic activation of an inward current in isolated neuronal somata from locust thoracic ganglia. *Soc. Neurosci. Abstr.* **15**, 365.

Benson, J.A. 1992. Electrophysiological pharmacology of the nicotinic and muscarinic cholinergic responses of isolated neuronal somata from locust thoracic ganglia. *J. exp. Biol.* **170**, 203-233.

Benson, J.A. & Adams, W.B. 1987. The control of rhythmic neuronal firing. In: *Neuromodulation: the biochemical control of neuronal excitability*. 100-118. Ed. Kaczmarek L.K. & Levitan, B. *Oxford University Press*.

Benson, J.A. & Neumann, R. 1987. Nicotine and muscarine evoke different responses in isolated, neuronal somata from locust thoracic ganglia. *Soc. Neurosci. Abstr.* **13**, 938.

Bentley, D.R. 1970. A topological map of the locust flight system motor neurons. *J. Insect. Physiol.* **16**, 905-918.

Berg, D.K., Kelly, R.B., Sargent, P.B., Williamson, P. & Hall, Z.W. 1972. Binding of α-bungarotoxin to acetylcholine receptors in mammalian muscle. *Proc. Natl. Acad. Sci. U.S.A.* **69**, 147-151.

Bermudez, I. Beadle, D.J. & Benson, J.A. 1992. Multiple serotonin-activated currents in isolated, neuronal somata from locust thoracic ganglia. *J. exp. Biol.* **165**, 43-60.

Berridge, M.J. 1985. The molecular basis of communication within the cell. *Sci. Am.* **253**(4), 124-134.

Berridge, M.J. & Irvine, R.F. 1984. Inositol trisphosphate, a novel second messenger in cellular signal transduction. *Nature (Lond.)*. **312**, 315-321.

Bertrand, D., Ballivet, M., Gomez, M., Bertrand, S., Phannavong, B. & Gundelfinger, E.D. 1994. Physiological properties of neuronal nicotinic receptors reconstituted from the vertebrate β2 subunit and *Drosophila* α subunits. *Eur. J. Neurosci.* **6**(5), 869-875.

Bezanilla, F. & Armstrong, C.M. 1972. Negative conductance caused by entry of sodium and cesium into the potassium channels of squid giant axons. *J. Gen. Physiol.* **60**, 588-608.

Bezprozvanny, I., Watras, J. & Ehrlich, B.E. 1991. Bell-shaped calcium-response curves of Ins(1,4,5)P_3- and calcium-gated channels from endoplasmic reticulum of cerebellum. *Nature (Lond.).* **351**, 751-754.

Blake, A.D., Anthony, N.M., Chen, H.H., Harrison, J.B., Nathanson, N.M. & Sattelle, D.B. 1993. Drosophila nervous system muscarinic acetylcholine receptor: transient functional expression and localization by immunocytochemistry. *Mol. Pharmacol.* **44**, 716-724.

Blatz, A.L. & Magleby, K.L. 1986. Single apamin-blocked Ca-activated K^+ channels of small conductance in cultured rat skeletal muscle. *Nature (Lond.).* **323**, 718-720.

Blaustein, M.P. 1988. Calcium transport and buffering in neurons. *Trends Neurosci.* **11**(10), 438-443.

Boller, M. & Pott, L. 1989. β-Adrenergic modulation of transient inward current in guinea-pig cardiac myocytes. Evidence for regulation of Ca^{2+}-release from sarcoplasmic reticulum by a cAMP dependent mechanism. *Pflügers Arch.* **415**, 276-288.

Bonner, T.I. 1989. The molecular basis of muscarinic receptor diversity. *Trends Neurosci.* **12**(4), 148-151.

Bonner, T.I., Buckley, N.J., Young, A.C. & Brann, M.R. 1987. Identification of a family of muscarinic acetylcholine receptor genes. *Science (N.Y.).* **237**, 527-532.

Boobis, A.R., Seddon, C.E., Nasseri-Sina, P. & Davies, D.S. 1990. Evidence for a direct role of intracellular calcium in paracetamol toxicity. *Biochem. Pharmacol.* **39**(8), 1277-1281.

Bosmann, H.B. 1972. Acetylcholine receptor. I. Identification and biochemical characteristics of a cholinergic receptor of guinea pig cerebral cortex. *J. Biol. Chem.* **247**(1), 130-145.

Bossy, B., Ballivet, M. & Spierer, P. 1988. Conservation of neural nicotinic acetylcholine receptors from *Drosophila* to vertebrate central nervous system. *EMBO J.* 7(3), 611-618.

Bourque, C.W., Randle, J.C.R. & Renaud, L.P. 1985. Calcium-dependent potassium conductance in rat supraoptic nucleus neurosecretory cells. *J. Neurophysiol.* **54**(6), 1375-1382.

Bowman, W.C. & Rand, M.J. 1980. *Textbook of Pharmacology. Blackwell Scientific Publications.*

Boyett, M.R. 1981. Two transient outward currents in cardiac Purkinje fibers. *J. Physiol. (Lond.).* **320**, P32.

Brandt, D.R., Asano, T., Pederson, S.E. & Ross, E.M. 1983. Reconstitution of catecholamine-stimulated guanosine triphosphatase activity. *Biochem.* **22**, 4357-4362.

Brann, M.R., Buckley, N.J. & Bonner, T.I. 1988. The striatum and cerebral cortex express different muscarinic receptors mRNAs. *FEBS Lett.* **230**(1-2), 90-94.

Brann, M.R., Klimkowski, V.J. & Ellis, J. 1993a. Structure/function relationships of muscarinic acetylcholine receptors. *Life Sci.* **52**, 405-412.

Brann, M.R., Jorgensen, H., Burstein, E.S., Spalding T.A., Ellis, J., Jones., S.V.P. & Hill-Eubanks, D. 1993b. Studies of the pharmacology, localization, and structure of muscarinic acetylcholine receptors. *Ann. N.Y. Acad. Sci.* **707**, 225-236.

Bräu, M.E., Dreyer, F., Jonas, P., Repp, H. & Vogel, W. 1990. A K^+ channel in *Xenopus* nerve fibres selectively blocked by bee and snake toxins: binding and voltage-clamp experiments. *J. Physiol. (Lond.).* **420**, 365-385.

Breer, H. 1981a. Comparative studies on cholinergic activities in the central nervous system of *Locusta migratoria*. *J. Comp. Physiol.* **141**, 271-275.

Breer, H. 1981b. Properties of putative nicotinic and muscarinic cholinergic receptors in the central nervous system of *Locusta migratoria*. *Neurochem. Int.* **3**(1), 43-52.

Breer, H. 1982. Uptake of [N-Me-3H] choline by synaptosomes from the central nervous system of *Locusta migratoria*. *J. Neurobiol.* **13**(2), 107-117.

Breer, H. 1983. Choline transport by synaptosomal membrane vesicles isolated from insect nervous tissue. *FEBS Lett.* **153**(2), 345-348.

Breer, H. & Sattelle, D.B. 1987. Molecular properties and functions of insect acetylcholine receptors. *J. Insect. Physiol.* **33**(11), 771-790.

Breer, H. & Knipper, M. 1984. Characterization of acetylcholine release from insect synaptosomes. Insect *Biochem.* **14**(3), 337-344.

Breer, H., Kleene, R. & Hinz, G. 1985. Molecular forms and subunit structure of the acetylcholine receptor in the central nervous system of insects. *J. Neurosci.* **5**, 3386-3392.

Brehm, P. & Eckert, R. 1978. Calcium entry leads to inactivation of calcium channel in *Paramecium*. *Science (N.Y.).* **202**, 1203-1206.

Brezina, V. 1988. Acetylcholine suppresses calcium current in neurons of *Aplysia californica*. *Comp. Biochem. Physiol.* **91C**(1), 219-228.

Brisson, A. & Unwin, P.N.T. 1985. Quaternary structure of the acetylcholine receptor. *Nature (Lond.).* **315**, 474-477.

Brockes, J.P. & Hall, Z.W. 1975. Acetylcholine receptors in normal and denervated muscle. I. Purification and interaction with [^{125}I]-α-bungarotoxin. *Biochem.* **14**(10), 2092-2099.

Brostrom, C.O., Huang, Y.-C., Breckenridge, B.M. & Wolff, D.J. 1975. Identification of a calcium-binding protein as a calcium-dependent regulator of brain adenylate cyclase. *Proc. Natl. Acad. Sci. U.S.A.* **72**, 64-68.

Brown, A.M., Morimoto, K., Tsuda, Y. & Wilson, D.L. 1981. Calcium current-dependent and voltage-dependent inactivation of calcium channels in *Helix aspersa*. *J. Physiol. (Lond.).* **320**, 193-218.

Brown, D.A. 1988. M-currents: an update. *Trends Neurosci.* **11**(7), 294-299.

Brown, D.A. & Adams, P.R. 1980. Muscarinic suppression of a novel voltage-sensitive K^+ current in a vertebrate neurone. *Nature (Lond.).* **283**, 673-676.

Brown, D.A. & Adams, P.R. 1987. Effects of phorbol dibutyrate on M currents and M current inhibition in bullfrog sympathetic neurons. *Cell. Mol. Neurobiol.* 7(3), 255-269.

Brown, D.A. & Fumagalli, L. 1977. Dissociation of the α-bungarotoxin binding and receptor block in the rat superior cervical ganglion. *Brain Res.* **129**, 165-168.

Brown, D.A. & Higashida, H. 1988a. Voltage- and calcium-activated potassium currents in the mouse neuroblastoma x rat glioma hybrid cells. *J. Physiol. (Lond.).* **397**,149-165.

Brown, D.A. & Higashida, H. 1988b. Membrane current responses of NG108-15 mouse neuroblastoma x rat glioma hybrid cells to bradykinin. *J. Physiol. (Lond.).* **397**, 167-184.

Brown, D.A., Marrion, N.V. & Smart, T.G. 1989. On the transduction mechanism for muscarine-induced inhibition of M-current in cultured rat sympathetic neurones. *J. Physiol. (Lond.).* **413**, 469-488.

Buck, M.A. & Fraser, C.M. 1990. Muscarinic acetylcholine receptor subtypes which selectively couple to phospholipase C: pharmacological and biochemical properties. *Biochem. Biophys. Res. Comm.* **173**(2), 666-672.

Buckley, N.J., Bonner, T.I. & Brann, M.R. 1988. Localization of a family of muscarinic receptor mRNAs in rat brain. *J. Neurosci.* **8**(12), 4646-4652.

Burrows, M. 1975. Monosynaptic connexions between wing stretch receptors and flight motoneurones of the locust. *J. exp. Biol.* **62**, 189-219.

Bursztajn, S. & Gershon, M.D. 1977. Discrimination between nicotinic receptors in vertebrate ganglia and skeletal muscle by alpha-bungarotoxin and cobra venoms. *J. Physiol. (Lond.).* **269**, 17-31.

Burton, F.L. & Hutter, O.F. 1990. Sensitivity to flow of intrinsic gating in inwardly rectifying potassium channel from mammalian skeletal muscle. *J. Physiol. (Lond.)*. **424**, 253-261.

Callec, J.-J. & Boistel, J. 1967. Les effets de l'acétylcholine aux niveaux synaptique et somatique dans le cas du dernier ganglion abdominal de la blatte *Periplaneta americana*. *C. r. Séanc. Soc. Biol.* **161**, 442-446.

Carbone, E. & Lux, H.D. 1988. ω-Conotoxin blockade distinguishes Ca from Na permeable states in neuronal calcium channels. *Pflügers Arch.* **413**, 14-22.

Carbone, E., Prestipino, G., Spadavecchia, L., Franciolini, F. & Possani, L.D. 1987. Blocking of the squid axon K^+ channel by noxiustoxin: a toxin from the venom of the scorpion *Centruroides noxius*. *Pflugers Arch.* **408**, 423-431.

Carbone, E. & Swandulla, D. 1989. Neuronal calcium channels: kinetics, blockade and modulation. *Prog. Biophys. Mol. Biol.* **54**, 31-58.

Carr, C.E. & Fourtner, C.R. 1980. Pharmacological analysis of a monosynaptic reflex in the cockroach, *Periplaneta americana*. *J. exp. Biol.* **86**, 259-273.

Cassel, D. & Pfeuffer, T. 1978. Mechanism of cholera toxin action: covalent modification of the guanyl nucleotide-binding protein of the adenylate cyclase system. *Proc. Natl. Acad. Sci. U.S.A.* **75**, 2669-2673.

Castoldi, A.F., Manzo, L. & Costa, L.G. 1993. Cyclic GMP formation induced by muscarinic receptors is mediated by nitric oxide synthesis in rat cortical primary cultures. *Brain Res.* **610**, 57-61.

Cattaert, D., Araque, A., Buno, W. & Clarac, F. 1994. Nicotinic and muscarinic activation of motoneurons in the crayfish locomotor network. *J. Neurophysiol.*. **72**(4), 1622-1633.

Chandler, W.K. & Meves, H. 1965. Voltage clamp experiments on internally perfused giant axons. *J. Physiol. (Lond.)*. **180**, 788-820.

Chang, C.C. & Lee, C.Y. 1963. Isolation of neurotoxins from the venom of *Bungarus multicinctus* and their modes of neuromuscular blocking action. *Arch. Int. Pharmacodyn.* **144**, 241-257.

Changeux, J.P., Kasai, M. & Lee, C-Y. 1970. Use of a snake venom toxin to characterize the cholinergic receptor protein. *Proc. Natl. Acad. Sci. USA*. **67**, 1241-1247.

Chen, I. & Yates, R.D. 1981. Alpha-bungarotoxin binding sites in the rat carotid body. *Anat. Rec.* **199**(3), 49A.

Cheung, W.Y., Bradham, L.S., Lynch, T.J., Lin, Y.M. & Tallant, E.A. 1975. Protein activator of cyclic 3':5'-nucleotide phosphodiesterase of bovine or rat brain also activates its adenylate cyclase. *Biochem. Biophys. Res. Comm.* **66**(3), 1055-1062.

Chiappinelli, V.A. & Zigmond, R.E. 1978. α-bungarotoxin blocks nicotinic transmission in the aviary ciliary ganglion. *Proc. Natl. Acad. Sci. U.S.A.* **75**, 2999-3003.

Claudio, T., Ballivet, M., Patrick, J. & Heinemann, S. 1983. Nucleotide and deduced amino acid sequences of *Torpedo californica* acetylcholine receptor γ subunit. *Proc. Natl. Acad. Sci. U.S.A.* **80**, 1111-1115.

Cole, A.E. & Nicoll, R.A. 1984. Characterization of a slow cholinergic post-synaptic potential recorded in vitro from rat hippocampal pyramidal cells. *J. Physiol. (Lond.).* **352**, 173-188.

Cole, K.S. 1949. Dynamic electrical characteristics of the squid giant axon membrane. *Arch. Sci. Physiol.* **3**, 253-258.

Colhoun, E.H. 1958a. Acetylcholine in *Periplaneta americana* L. I. Acetylcholine levels in nervous tissue. *J. Insect. Physiol.*. **2**, 108-116.

Colhoun, E.H. 1958b. Distribution of choline acetylase in insect conductive tissue. *Nature (Lond.).* **182**, 1378.

Connor, J. 1979. Calcium current in molluscan neurones: measurement under similar conditions which maximise its visibility. *J. Physiol. (Lond.).* **286**, 41-60.

Connor, J.A. & Stevens, C.F. 1971a. Inward and delayed outward currents in isolated neural somata under voltage clamp. *J. Physiol. (Lond.).* **213**, 1-19.

Connor, J.A. & Stevens, C.F. 1971b. Voltage clamp studies of a transient outward membrane current in gastropod neural somata. *J. Physiol. (Lond.).* **213**, 21-30.

Constanti, A., Adams, P.R. & Brown, D.A. 1981. Why do barium ions imitate acetylcholine? *Brain Res.* **206**, 244-250.

Constanti, A. & Galvan, M. 1983. Fast inward-rectifying current accounts for anomalous rectification in olfactory cortex neurones. *J. Physiol. (Lond.).* **335**, 153-178.

Conti-Tronconi, S.M., McLane, K.E., Raftery, M.A., Grando, S.A. & Protti, M.P. 1994. The nicotinic acetylcholine receptor - structure and autoimmune pathology. *Crit. Rev. Biochem. Mol. Biol.* **29**(2), 69-123.

Cox, T. 1993. Low-affinity mixed acetylcholine-responsive receptors at the apical membrane of frog tadpole skin. *Am. J. Physiol.* **264**(Cell Physiol. 33), C552-C558.

Crest, M., Jaquet, G., Gola, M., Zerrouk, H., Benslimane, A., Rochat, H., Mansuelle, P. & Martin-Eauclaire, M.-F. 1992. Kaliotoxin, a novel peptidyl inhibitor of neuronal BK-type Ca^{2+}-activated K^+ channels characterized from *Androctonus mauretanicus mauretanicus* venom. *J. Biol. Chem.* **267**(3), 1640-1647.

Curró Dossi, R., Paré, D. & Steriade, M. 1991. Short-lasting nicotinic and long-lasting muscarinic depolarizing responses of thalamocortical neurons to stimulation of mesopontine cholinergic nuclei. *J. Neurophysiol.*. **65**(3), 393-406.

Curtis, C.A.M., Wheatley, M., Bansal, S., Birdsall, N.J.M., Eveleigh P., Pedder, E.K., Poyner, D. & Hulme, E.C. 1989. Propylbenzilylcholine mustard labels an acidic residue in transmembrane helix 3 of the muscarinic receptor. *J. Biol. Chem.* **264**(1), 489-495.

Dale, H.H. 1914. The action of certain esters and esters of choline, and their relation to muscarine. *J. Pharmacol. Exp. Ther.* **6**, 147-190.

David, J.A. & Pitman, R.M. 1990. Functional muscarinic receptors on an identified neurone in the isolated metathoracic ganglion of the cockroach *Periplaneta americana*. *J. Physiol. (Lond.)*. **429**, 66P.

David, J.A. & Pitman, R.M. 1991. Modulation of a calcium current by muscarinic receptors in an insect motoneurone. *Soc. Neurosci. Abstr.* **17**, 276.

David, J.A. & Pitman, R.M 1993a. The pharmacology of α-bungarotoxin-resistant acetylcholine receptors on an identified cockroach motorneurone. *J. Comp. Physiol. A*. **172**, 359-368.

David, J.A. & Pitman, R.M. 1993b. Activation of receptors with mixed muscarinic/nicotinic pharmacology modulates a calcium current in an insect motoneurone. *J. Physiol. (Lond.)*. **459**, 98P.

David, J.A. & Pitman, R.M. 1994. Inositol 1,4,5-trisphosphate production is linked to muscarinic acetylcholine receptors in the CNS of the cockroach, *Periplaneta americana*. *J. Physiol. (Lond.)*. **480**, 97P.

David, J.A. & Pitman, R.M. 1995. Muscarinic agonists modulate calcium-dependent outward currents in an identified insect motoneurone. *Brain Res.* **669**, 153-156.

Deitmer, J.W. & Eckert, R. 1985. Two Components of Ca-dependent potassium current in identified neurones of *Aplysia californica*. *Pflügers Arch.* **403**, 353-359.

Dolly, J.O. & Barnard, E.A. 1975. Complete purification of the acetylcholine receptor protein from mammalian muscle. *FEBS Lett.* **57**(3), 267-271.

Dörje, F., Levey, A.I. & Brann, M.R. 1991. Immunological detection of muscarinic receptor subtype proteins (m1-m5) in rabbit peripheral tissues. *Mol. Pharmacol.* **40**, 459-462.

Dudai, Y. 1977. Demonstration of an α-bungarotoxin-binding nicotinic receptor in flies. *FEBS Lett.* **76**(2), 211-213.

Dudai, Y. &.Amsterdam, A. 1977. Nicotinic receptors in the brain of *Drosophila melanogaster* demonstrated by autoradiography with [^{125}I]α-bungarotoxin. *Brain Res.* **130**, 551-555.

Dudai, Y. & Ben-Barak, J. 1977. Muscarinic receptor in *Drosophila melanogaster* demonstrated by binding of [^{3}H] quinuclidinyl benzilate. *FEBS Lett.* **81**(1), 134-136.

Dutar, P. & Nicoll, R.A. 1988a. Classification of muscarinic responses in hippocampus in terms of receptor subtypes and second messenger systems: electrophysiological studies in vitro. *J. Neurosci.* **8**(11), 4214-4224.

Dutar, P. & Nicoll, R.A. 1988b. Stimulation of phosphatidylinositol (PI) turnover may mediate the muscarinic suppression of the M-current in hippocampal pyramidal cells. *Neurosci. Lett.* **85**, 89-94.

Dwyer, B.P. 1991. Topological dispositions of Lysine α380 and Lysine α486 in the acetylcholine receptor from *Torpedo californica. Biochem.* **30**, 4105-4112.

Eaton, D.C. & Brodwick, M.S. 1980. Effects of barium on the potassium conductance of squid axon. *J. Gen. Physiol.*. **75**, 727-750.

Eckert, R. & Tillotson, D.L. 1981. Calcium-mediated inactivation of the calcium conductance in caesium-loaded giant neurones of *Aplysia californica. J. Physiol. (Lond.).* **314**, 265-280.

Ehrenstein, G. & Gilbert, D.L. 1966. Slow changes in potassium permeability in the squid giant axon. *Biophys. J.* **6**, 553-566.

Ehrlich, B.E., Kaftan, E. Bezprozvannaya, S. & Bezprozvanny, I. 1994. The pharmacology of intracellular Ca^{2+}-release channels. *Trends Pharmacol. Sci.* **15**, 145-149.

Eldefrawi, M.E., Eldefrawi, A.T. & O'Brien, R.D. 1971. Binding sites for cholinergic ligands in a particulate fraction of *Electrophorus* electroplax. *Proc. Natl. Acad. Sci. U.S.A.* **68**, 1047-1050.

Emson, P.C., Burrows, M. & Fonnum, F. 1974. Levels of glutamate decarboxylase, choline acetyltransferase and acetylcholinesterase in identified motorneurons of the locust. *J. Neurobiol.* **5**(1), 33-42.

Fasolato, C., Innocenti, B. & Pozzam, T. 1994. Receptor-activated Ca^{2+} influx: how many mechanisms for how many channels? *Trends Pharmacol. Sci.* **15**, 77-83.

Fatt, P. & Katz, B. 1953. The electrical properties of crustacean muscle fibres. *J. Physiol. (Lond.).* **120**, 171-204.

Felder, C.C., Kanterman, R.Y., Ma, A.L. & Axelrod, J. 1989. A transfected m1 muscarinic acetylcholine receptor stimulates adenylate cyclase via phosphatidylinositol hydrolysis. *J. Biol. Chem.* **34**, 20356-20362.

ffrench-Mullen, J.M.H., Plata-Salamán, C.R., Buckley, N.J., & Danks P. 1994. Muscarinic modulation by a G-protein α-subunit of delayed rectifier K^+ current in rat ventromedial hypothalamic neurones. *J. Physiol. (Lond.).* **474**, 21-26.

Fisher, S.K., McEwen, E.L., Lovell, S.C. & Landon, R.E. 1992. Cyclic-AMP potentiates receptor-stimulated phosphoinositide hydrolysis in human neuroepithelioma cells. *Mol. Pharmacol.* **42**,(2), 340-346.

Fox, A.P., Nowycky, M.C. & Tsien, R.W. 1987. Kinetic and pharmacological properties distinguishing three types of calcium currents in chick sensory neurones. *J. Physiol. (Lond.).* **394**, 149-172.

Fraser, C.M., Chung, F.-Z., Wang, C.-D. & Venter, J.C. 1988. Site-directed mutagenesis of human β-adrenergic receptors: substitution of aspartic acid-130 by asparagine produces a receptor with high-affinity agonist binding that is uncoupled from adenylate cyclase. *Proc. Natl. Acad. Sci. U.S.A.* **85**, 5478-5482.

Fraser, C.M., Wang, C.-D., Robinson, D.A., Gocayne, J.D. & Venter, J.C. 1989. Site-directed mutagenesis of m1 muscarinic acetylcholine receptors: conserved aspartic acids play important roles in receptor function. *Mol. Pharmacol.* **36**, 840-847.

Fukuda, K., Higashida, H., Kubo, T., Maeda, A., Akiba, I., Bujo, H., Mishina, M. & Numa, S. 1988. Selective coupling with K^+ currents of muscarinic acetylcholine receptor subtypes in NG108-15 cells. *Nature (Lond.).* **335**, 355-358.

Fumagalli, L., De Renzis, G. & Miani, N. 1976. Acetylcholine receptors: number and distribution in intact and deafferented superior cervical ganglion of the rat. *J. Neurochem.* **27**, 47-52.

Furukawa, K., Abe, Y., Sorimachi, M. & Akaike, N. 1994. Nicotinic and muscarinic acetylcholine responses in the embryo chick ciliary ganglion cells. *Brain Res.* **657**, (1-2), 185-190.

Galietta, L.J.V., Rasola, A., Barone, V., Gruenert, D.C. & Romeo, G. 1991. A forskolin and verapamil sensitive K^+ current in human tracheal cells. *Biochem. Biophys. Res. Comm.* **179**(3), 1155-1160.

Gallo, M.P., Alloatti, G., Eva, C., Oberto, A. & Levi, R.C. 1993. M1 muscarinic receptors increase calcium current and phosphoinositide turnover in guinea-pig ventricular myocytes. *J. Physiol. (Lond.).* **471**, 41-60.

Galvez, A., Gimenez-Gallego, G., Rueben, J.P., Roy-Contancin, L., Feigenbaum, P. Kaczorowski, G.J. & Garcia, M.L. 1990. Purification and characterization of a unique, potent, peptidyl probe for the high conductance calcium-activated potassium channel from the venom of the scorpion *Buthus tamulus*. *J. Biol. Chem.* **265**(19), 11083-11090.

Gay, L.A. & Stanfield, P.R. 1977. Cs^+ causes a voltage-dependent block of inward K currents in resting skeletal muscle fibres. *Nature (Lond.).* **267**, 169-170.

Gettrup, E. 1962. Thoracic proprioceptors in the flight system of locusts. *Nature (Lond.).* **193**, 498-499.

Giachetti, A., Micheletti, R. & Monagna, E. 1986. Cardioselective profile of AF-DX 116, a muscarinic M2 receptor antagonist. *Life Sci.* **38**, 1663-1672.

Giangiacomo, K.M., Garcia, M.L. & McManus, O.B. 1992. Mechanism of iberiotoxin block of the large-conductance calcium-activated potassium channel from bovine aortic smooth muscle. *Biochem.* **31**, 6719-6727.

Giles, D. & Usherwood, P.N.R. 1985. The effects of putative amino acid neurotransmitters on somata isolated from neurons of the locust central nervous system. *Comp. Biochem. Physiol.* **80C**, 231-236.

Giles, W.R. & van Ginneken, A.C.G. 1985. A transient outward current in isolated cells from the crista terminalis of rabbit heart. *J. Physiol. (Lond.).* **368**, 243-264.

Goh, J.W., Kelly, M.E.M., Pennefather, P.S., Chicchi, G.G., Cascieri, M.A., Garcia, M.L. & Kaczorowski, G.J. 1992. Effect of charybdotoxin and leiurotoxin I on potassium currents in bullfrog sympathetic ganglion and hippocampal neurones. *Brain Res.* **591**, 165-170.

Goodman, C.S. & Spitzer, N.C. 1980. Embryonic development of neurotransmitter receptors in grasshoppers. In: *Receptors for Neurotransmitters, Hormones and Pheromones in Insects.* 195-207. Ed. Sattelle, D.B., Hall, L.M. & Hildebrand, JG. *Elsevier/North Holland, Amsterdam.*

Greene, L.A., Sytkowski, A.J., Vogel, Z. & Nirenberg, M.W. 1973. α-bungarotoxin used as a probe for acetylcholine receptors of cultured neurones. *Nature (Lond.).* **243**, 163-166.

Gutnick, M.J., Lux, H.D., Swandulla, D. & Zucker, H. 1989. Voltage-dependent and calcium-dependent inactivation of calcium channel current in identified snail neurones. *J. Physiol. (Lond.).* **412**, 197-220.

Haga, K. & Haga, T. 1983. Affinity chromatography of the muscarinic acetylcholine receptor. *J. Biol. Chem.* **258**(2), 13575-13579.

Hagiwara, S. & Byerly, L. 1981. Calcium channel. *Ann. Rev. Neurosci.* **4**, 69-125.

Hagiwara, S. & Jaffe, L.A. 1979. Electrical properties of egg cell membranes. *Ann. Rev. Biophys. Bioeng.* **8**, 385-416.

Hagiwara, N., Irisawa, H. & Kameyama, M. 1988. Contribution of two types of calcium currents to the pacemaker potentials of rabbit sino-atrial node cells. *J. Physiol. (Lond.).* **395**, 233-253.

Hagiwara, S., Kusano, K. & Saito, N. 1961. Membrane changes of *Onchidium* nerve cell in potassium-rich media. *J. Physiol. (Lond.).* **155**, 470-489.

Hagiwara, S. Miyazaki, S., Moody, W. & Patlak, J. 1978. Blocking effects of barium and hydrogen ions on the potassium current during anomalous rectification in the starfish egg. *J. Physiol. (Lond.).* **279**, 167-185.

Hagiwara, S., Miyazaki, S. & Rosenthal, N.P. 1976. Potassium current and the effect of cesium on this current during anomalous rectification of the egg cell membrane of a starfish. *J. Gen. Physiol.*. **67**, 621-638.

Hagiwara, S. & Yoshii, M. 1979. Effects of internal potassium and sodium on the anomalous rectification of the starfish egg as examined by internal perfusion. *J. Physiol. (Lond.).* **292**, 251-265.

Halliwell, J.V., Othman, I.B., Pelchen-Matthews, A. & Dolly, J.O. 1986. Central action of dendrotoxin: selective reduction of a transient K conductance in hippocampus and binding to localized receptors. *Proc. Natl. Acad. Sci. U.S.A.* **83**, 493-497.

Hamilton, S.L., Pratt, D.R. & Eaton, D.C. 1985. Arrangement of the subunits of the nicotinic acetylcholine receptor of *Torpedo californica* as determined by α-neurotoxin cross-linking. *Biochem.* **24**, 2210-2219.

Hammer, R. Berrie, C.P., Birdsall, N.M.J., Burgen, A.S.V. & Hulme, E.C. 1980. Pirenzepine distinguishes between different subclasses of muscarinic receptor. *Nature (Lond.).* **283**, 90-92.

Hancox, J.C. 1991. Non-linear membrane properties of insect motoneurones. PhD Thesis, University of St. Andrews.

Hanke, W. & Breer, H. 1986. Channel properties of an insect neuronal acetylcholine receptor protein reconstituted in planar lipid bilayers. *Nature (Lond.).* **321**, 171-174.

Harris, R., Cattell, K.J. & Donnellan, J.F. 1981. The purification and molecular characterisation of a putative nicotinic-muscarinic acetylcholine receptor from housefly heads. *Insect. Biochem.* **11**(4), 371-385.

Harrow, I.D. & Sattelle, D.B. 1983. Acetylcholine receptors on the cell body membrane of giant interneurone 2 in the cockroach, *Periplaneta americana*. *J. exp. Biol.* **105**, 339-350.

Hepler, J.R. & Gilman, A.G. 1992. G proteins. *Trends. Biochem. Sci.* **17**, 383-387.

Hermann, A. & Erxleben, C. 1987. Charybdotoxin selectively blocks small Ca-activated K channels in *Aplysia* neurons. *J. Gen. Physiol.*. **90**, 27-47.

Hermans-Borgmeyer, I., Zopf, D., Ryseck, R.-P., Hovemann, B., Betz, H. & Gundelfinger, E.D. 1986. Primary structure of a developmentally regulated nicotinic acetylcholine receptor protein from *Drosophila*. *EMBO J.* **5**(7), 1503-1598.

Higashida, H. & Brown, D.A. 1986. Two polyphosphatidylinositide metabolites control two K^+ currents in a neuronal cell. *Nature (Lond.)*. **323**, 333-335.

Hille, B. 1967. The selective inhibition of delayed potassium currents in nerve by tetraethylammonium ion. *J. Gen. Physiol.*. **50**, 1287-1302.

Hille, B. 1992. *Ionic channels of excitable membranes. Sinauer Associates Inc. Mass.*

Hinkle, P.M., Shanshala, E.D. & Nelson, E.J. 1992. Measurement of intracellular cadmium ions with fluorescent dyes. Further evidence for the role of calcium channels in cadmium uptake. *J. Biol. Chem.* **267**(35), 25553-25559.

Hirning, L.D., Fox, A.P., McCleskey, E.W., Olivera, B.M., Thayer, S.A., Miller, R.J. & Tsien, R.W. 1988. Dominant role of N-type Ca^{2+} channels in evoked release of norepinephrine from sympathetic neurons. *Science (N.Y.)*. **239**, 57-61.

Hodgkin, A.L. & Huxley, A.F. 1952a. Currents carried by sodium and potassium ions through the membrane of the giant axon of *Loligo*. *J. Physiol. (Lond.)*. **116**, 449-472.

Hodgkin, A.L. & Huxley, A.F. 1952b. The components of membrane conductance in the giant axon of *Loligo*. *J. Physiol. (Lond.)*. **116**, 473-496.

Hodgkin, A.L. & Huxley, A.F. 1952c. A quantitative description of membrane current and its application to conduction and excitation. *J. Physiol. (Lond.)*. **116**, 500-544.

Hofmann, F., Biel, M. & Flockerzi, V. 1994. Molecular basis for Ca^{2+} channel diversity. *Ann. Rev. Neurosci.* **17**, 399-418.

Hösli, L., Hösli, E., Winter, T. & Stauffer, S. 1994. Coexistence of cholinergic and somatostatin receptors on astrocytes of rat CNS. *Neuroreport*. **5**, 1469-1472.

Huang, Z.-Y. & Knowles, C.O. 1990. Nicotinic and muscarinic cholinergic receptors in honey bee (*Apis mellifera*) brain. *Comp. Biochem. Physiol.* **97C**(2), 275-281.

Hue, B., Lapied, B. & Malecot, C.O. 1989. Do presynaptic muscarinic receptors regulate acetylcholine release in the central nervous system of the cockroach *Periplaneta americana*? *J. exp. Biol.* **142**, 447-451.

Huguenard, J.R. & Prince, D.A. 1992. A novel T-type current underlies prolonged Ca^{2+}-dependent burst firing in GABAergic neurons of rat thalamic reticular nucleus. *J. Neurosci.* **12**(10), 3804-3817.

Hulme, E.C., Birdsall, N.M.J. & Buckley, N.J. 1990. Muscarinic receptor subtypes. *Ann. Rev. Pharmacol. Toxicol.* **30**, 633-673.

Imoto, K., Konno, T., Nakai, J., Wang, F., Mishina, M. & Numa, S. 1991. A ring of uncharged polar amino acids as a component of channel constriction in the nicotinic acetylcholine receptor. *FEBS Lett.* **289**(2), 193-200.

Inoue, R., Kitamura, K. & Kuriyama, H. 1985. Two Ca-dependent K-channels classified by the application of tetraethylammonium distribute to smooth muscle membranes of the rabbit portal vein. *Pflügers Arch.* **405**, 173-179.

Irvine, R.F. 1990. 'Quantal' Ca^{2+} release and the control of Ca^{2+} entry by inositol phosphates - a possible mechanism. *FEBS Lett.* **263**(1), 5-9.

Jackel, C., Krenz, W.-D. & Nagy, F. 1994. Bicuculline/baclofen-insensitive GABA response in crustacean neurones in culture. *J. exp. Biol.* **191**, 167-193.

Jan, Y.N., Jan, L.Y. & Dennis, M.J. 1977. Two mutations of synaptic transmission in *Drosophila*. *Proc. R. Soc. Lond. B.* **198**, 87-108.

Jan, Y.N., Jan, L.Y. & Kuffler, S.W. 1979. A peptide as a possible transmitter in sympathetic ganglia of the frog. *Proc. Natl. Acad. Sci. U.S.A.* **76**, 1501-1505.

Jansson, C.C., Kukkonen, J. & Åkerman, K.E.O. 1991. Muscarinic receptor-linked elevation of cAMP in SH-SY5Y neuroblastoma cells is mediated by Ca^{2+} and protein kinase C. *Biochim. Biophys. Acta.* **1095**, 255-260.

Johns, A., Lategan, T.W., Lodge, N.J., van Breemen, C. & Adams, D.J. 1987. Calcium entry through receptor-operated channels in bovine pulmonary artery endothelial cells. *Tissue & Cell.* **19**(6), 733-745.

Jonas, P., Baumann, A., Merz, B. & Gundelfinger, E.D. 1990. Structure and developmental expression of the Dα2 gene encoding a novel nicotinic acetylcholine receptor protein of *Drosophila melanogaster*. *FEBS Lett.* **269**(1), 264-268.

Jones, S.W. 1987. A muscarine-resistant M-current in C cells of bullfrog sympathetic ganglia. *Neurosci. Lett.* **74**, 309-314.

Karlin, A. 1993. Structure of nicotinic acetylcholine receptors. *Curr. Op. Neurobiol.* **3**, 299-309.

Karlin, A. & Cowburn, D. 1973. The affinity-labelling of partially purified acetylcholine receptor from electric tissue of *Electrophorus*. *Proc. Natl. Acad. Sci. U.S.A.* **70**, 3636-3640.

Karlin, A., Holtzmann, E., Yodh, N., Lobel, P., Wall, J. & Hainfield, J. 1983. The arrangement of the subunits of the acetylcholine receptor of *Torpedo californica*. *J. Biol. Chem.* **258**(11), 6678-6681.

Katada, T. & Ui, M. 1982. ADP ribosylation of the specific membrane protein of C6 cells by islet-activating protein associated with modification of adenylate cyclase activity. *J. Biol. Chem.* **257**(12), 7210-7216.

Katz, B. 1949. Les constantes électriques de la membrane du muscle. *Arch. Sci. Physiol.* **2**, 285-299.

Kebabian, J.W., Steiner, A.L. & Greengard, P. 1975. Muscarinic cholinergic regulation of cyclic guanosine 3',5'-monophosphate in autonomic ganglia: possible role in synaptic transmission. *J. Pharmacol. Exp. Ther.* **193**(2), 474-488.

Kerkut, G.A., Newton, L.C., Pitman, R.M., Walker, R.J. & Woodruff, G.N. 1970. Acetylcholine receptors of invertebrate neurones. *Br. J. Pharmacol.* **40**(3), 586P.

Kerkut, G.A., Pitman, R.M. & Walker, R.J. 1969. Iontophoretic application of acetylcholine and GABA onto insect central neurones. *Comp. Biochem. Physiol.* **31**, 611-633.

Kishimoto, A., Takai, Y., Mori, T., Kikkawa, U. & Nishizuka, Y. 1980. Activation of calcium and phospholipid-dependent protein kinase by diacylglycerol, its possible relation to phosphatidylinositol turnover. *J. Biol. Chem.* **255**(6), 2273-2276.

Knipper, M. & Breer, H. 1988. Subtypes of muscarinic receptors in insect nervous system. *Comp. Biochem. Physiol.* **90C**(1), 275-280.

Knipper, M. & Breer, H. 1989. Muscarinic receptors modulating acetylcholine release from insect synaptosomes. *Comp. Biochem. Physiol.* **93C**(2), 287-292.

Knöpfel, T., Vranesic, I., Gahwiler, B.H. & Brown, D.A. 1990. Muscarinic and β-adrenergic depression of the slow Ca^{2+}-activated potassium conductance in hippocampal CA3 pyramidal cells is not mediated by a reduction of depolarization-induced cytosolic Ca^{2+} transients. *Proc. Natl. Acad. Sci. U.S.A.* **87**, 4083-4087.

Krüppel, T., Westermann, R. & Lueken, W. 1991. Calcium-dependent transient potassium outward current in the marine ciliate *Euplotes vannus*. *Biochim. Biophys. Acta*. **1062**, 193-198.

Kuba, K. & Kuketsu, K. 1986. Analysis of the slow excitatory post-synaptic potential in bullfrog sympathetic ganglion cells. *Jap. J. Physiol.* **26**, 651-669.

Kubo, T., Bujo, H., Akiba, I., Nakai, J., Mishina, M. & Numa, S. 1988. Location of a region of the muscarinic acetylcholine receptor involved in selective effector coupling. *FEBS Lett.* **241**(1-2), 119-125.

Kubo, T., Fukuda, K., Mikami, A., Maeda, A., Takahashi, H., Mishina, M., Haga, T., Haga, K., Ichiyama, A., Kangawa K., Kojima, M., Matsuo, H., Hirose, T. & Numa, S. 1986a. Cloning, sequencing and expression of complementary DNA encoding the muscarinic acetylcholine receptor. *Nature (Lond.)*. **323**, 411-416.

Kubo, T., Maeda, A., Sugimoto, K., Akiba, I., Mikami, A., Takahashi, H., Haga, T., Haga, K., Ichiyama, A., Kangawa K., Matsuo, H., Hirose, T. & Numa, S. 1986b. Primary structure of porcine cardiac muscarinic acetylcholine receptor deduced from the cDNA sequence. *FEBS Lett.* **209**(2), 367-372.

Kubo, T., Noda, M., Takai, T., Tanabe, T., Kayano, T., Shimizu, S., Tanaka, K., Takahashi, H., Hirose, T., Inayama, S., Kikuno, R., Miyata, T. & Numa, S. 1985. Primary structure of δ subunit precursor of calf muscle acetylcholine receptor deduced from cDNA sequence. *Eur. J. Biochem.* **149**, 5-13.

Kurenny, D.E., Chen, H. & Smith, P.A. 1994. Effects of muscarine on K^+-channel currents in the C-cells of bullfrog sympathetic ganglion. *Brain Res.* **658**, 239-251.

Kurtenbach, E., Curtis, C.A.M., Pedder, E.K., Aitken, A., Harris, A.C.M. & Hulme, E.C. 1990. Muscarinic acetylcholine receptors. Peptide sequencing identifies residues involved in antagonist binding and disulphide bond formation. *J. Biol. Chem.* **265**(23), 13702-13708.

Lambrecht, G., Feifel, R., Moser, U., Wagner-Roder, M., Choo, L.K., Camus, J., Tastenoy, M., Waelbroeck, M., Strohmann, C., Tacke, R., Rodrigues de Miranda, J.F., Christophe, J. & Mutschler, E. 1989. Pharmacology of hexahydro-difenidol, hexahydro-sila-difenidol and related selective muscarinic antagonists. *Trends Pharmacol. Sci.* **10**(Supplement - Subtypes of muscarinic receptors IV), 60-64.

Lancaster, B. & Nicoll, R.A. 1987. Properties of two calcium-activated hyperpolarizations in rat hippocampal neurones. *J. Physiol. (Lond.)*. **389**, 187-203.

Lapied, B. & Hue, B. 1991. Sensitive nicotinic, mixed and muscarinic receptors in isolated identified adult insect neurones. *Pestic. Sci.* **32**, 377-279.

Latorre, R., Oberhauser, A., Labarca, P. & Alvarez, O. 1989. Varieties of calcium-activated potassium channels. *Ann. Rev. Physiol.* **51**, 385-399.

Lechleiter, J., Hellmiss, R., Duerson, K., Ennulat, D., David, N., Clapham, D. & Peralta, E. 1990. Distinct sequence elements control the specificity of G protein activation by muscarinic receptor subtypes. *EMBO J.* **9**(13), 4381-4390.

Le Corronc, H. & Hue, B. 1993. Pharmacological and electrophysiological characterization of a postsynaptic muscarinic receptor in the central nervous system of the cockroach. *J. exp. Biol.* **181**, 257-278

Le Corronc, H., Lapied, B. & Hue, B. 1991. M2-like presynaptic receptors modulate acetylcholine release in the cockroach (*Periplaneta americana*) central nervous system. *J. Insect. Physiol.*. **37**(9), 647-652.

Lee, C.Y., Tseng, L.F & Chiu, T.H. 1967. Influence of denervation on localization of neurotoxins from elapid venoms in rat diaphragms. *Nature (Lond.)*. **215**, 1177-1178.

Leech, C.A. & Stanfield, P.R. 1981. Inward rectification in frog skeletal muscle fibres and its dependence on membrane potential and external potassium. *J. Physiol. (Lond.)*. **319**, 295-309.

Lees, G., Beadle, D. & Botham, R.P. 1983. Cholinergic receptors on cultured neurones from the central nervous system of embryonic cockroaches. *Brain Res.* **288**, 49-59.

Lees, G., Beadle, D.J., Neumann, R. & Benson, J.A. 1987. Responses to GABA by isolated insect neuronal somata: pharmacology and modulation by a benzodiazepine and a barbiturate. *Brain Res.* **401**, 267-278.

Leitch, B., Pitman, R.M. & Crockford, K.J. 1993. Muscarinic receptors at the synapse between locust wing hinge stretch receptors and an identified motoneurone. *Brain Research Assoc Abstr.* **10**, 31.

Levitan, I.B. 1988. Modulation of ion channels in neurons and other cells. *Ann. Rev. Neurosci.* **11**, 119-136.

Lewis, S.E. 1953. Acetylcholine in blowflies. *Nature (Lond.)*. **172**, 1004-1005.

Li, M., McCann, J.D., Liedtke, C.M., Nairn, A.C., Greengard, P. & Welsh, M.J. 1988. Cyclic AMP-dependent protein kinase opens chloride channels in normal but not cystic fibrosis airway epithelium. *Nature (Lond.)*. **331**, 358-360.

Li, M., McCann, J.D., Anderson, M.P., Clancy, J.P., Liedtke, C.M., Nairn, A.C., Greengard, P. & Welsh, M.J. 1989. Regulation of chloride channels by protein kinase C in normal and cystic fibrosis airway epithelia. *Science (N.Y.)*. **244**, 1352-1356.

Liao, C.-F., Themmen, A.P.N., Joho, R., Barberis, C., Birnbaumer, M. & Birnbaumer, L. 1989. Molecular cloning and expression of a fifth muscarinic acetylcholine receptor. *J. Biol. Chem.* **264**(12), 7328-7337.

Lindstrom, J., Criado, M., Hochschwender, S., Fox, J.L. & Sarin, V. 1984. Immunochemical tests of acetylcholine receptor subunit models. *Nature (Lond.).* **311**, 573-575.

Lindstrom, J., Merlie, J. & Yogeeswaran, G. 1979. Biochemical properties of acetylcholine receptor subunits from *Torpedo californica. Biochem.* **18**(21), 4465-4470.

Llinás, R., Sugimori, M., Hillman, D.E. & Cherksey, B. 1992. Distribution and functional significance of the P-type, voltage-dependent Ca^{2+} channels in the mammalian central nervous system. *Trends Neurosci.* **15**(9), 351-355.

Llinás, R., Sugimori, M., Lin, J.-W. & Cherksey, B. 1989. Blocking and isolation of a calcium channel from neurons in mammals and cephalopods utilizing a toxin fraction (FTX) from funnel web spider poison. *Proc. Natl. Acad. Sci. U.S.A.* **86**, 1689-1693.

Loewi, O. 1921. Über humorale Übertragbarkeit der Herznervenwirkung. *Pflügers. Arch. Gesamte Physiol.* **189**, 239-242.

Loirand, G., Mirroneau, C., Mirroneau, J. & Pacard, P. 1989. Two types of calcium currents in smooth muscle cells from rat portal vein. *J. Physiol. (Lond.).* **412**, 333-349.

Lummis, S.C.R. & Sattelle, D.B. 1985. Binding of N-[propionyl-^{3}H]propionylated α-bungarotoxin and L-[benzilic-4-4'-^{3}H] quinuclidinyl benzilate to CNS extracts of the cockroach *Periplaneta americana. Comp. Biochem. Physiol.* **80C**(1), 75-83.

Lux, H.D., Neher, E. & Marty, A. 1981. Single channel activity associated with the calcium dependent outward current in *Helix pomatia. Pflügers Arch.* **389**, 293-295.

MacDermott, A.B. & Weight, F.F. 1982. Action potential repolarization may involve a transient, Ca^{2+}-sensitive outward current in a vertebrate neurone. *Nature (Lond.).* **300**, 185-188.

Madison, D.V. & Nicoll, R.A. 1984. Control of the repetitive discharge of rat CA1 pyramidal neurones in vitro. *J. Physiol. (Lond.).* **354**, 319-331.

Mansour, N.A., Eldefrawi, M.E. & Eldefrawi, A.T. 1977. Isolation of putative acetylcholine receptor proteins from housefly brain. *Biochem.* **16**(18), 4126-4132.

Marder, E. & Paupardin-Tritsch, D. 1978. The pharmacological properties of some crustacean neuronal acetylcholine, γ-aminobutyric acid, and L-glutamate responses. *J. Physiol. (Lond.).* **280**, 213-236.

Marmot, G. 1949. Studies on the axon membrane. I. A new method. J. *Cell. Comp. Physiol.* **34**, 351-382.

Marrion, N.V. 1987. Probable role of a GTP-binding protein in mediating M-current inhibition by muscarine in rat sympathetic neurones. *J. Physiol. (Lond.).* **396**, 87P.

Marrion, N.V. 1994. M-current suppression by agonist and phorbol ester in bullfrog sympathetic neurons. *Pflügers Arch.* **426**, 296-303.

Marrion, N.V., Zucker, R.S., Marsh, S.J. & Adams, P.R. 1991. Modulation of M-current by intracellular Ca^{2+}. *Neuron.* **6**, 533-545.

Marshall, L.M. 1981. Synaptic localization of α-bungarotoxin binding which blocks nicotinic transmission at frog sympathetic neurons. *Proc. Natl. Acad. Sci. U.S.A.* **78**, 1948-1952.

Marshall, J., Buckingham, S.D., Shingai, R., Lunt, G.G., Goosey, M.W., Darlison, M.G., Sattelle, D.B. & Barnard, E.A. 1990. Sequence and functional expression of a single α subunit of an insect nicotinic acetylcholine receptor. *EMBO J.* **9**(13), 4391-4398.

Marty, A. 1981. Ca-dependent K channels with large unitary conductance in chromaffin cell membranes. *Nature (Lond.).* **291**, 497-500.

Mathes, C. & Thompson, S.H. 1994. Calcium current activated by muscarinic receptors and thapsigargin in neuronal cells. *J. Gen. Physiol.*. **104**, 107-121.

Matsuda, H., Saigusa, A. & Irisawa, H. 1987. Ohmic conductance through the inwardly rectifying K channel and blocking by internal Mg^{2+}. *Nature (Lond.).* **325**, 156-159.

McCrea, P.D., Popot, J.-L. & Engelman, D.M. 1987. Transmembrane topography of the nicotinic acetylcholine receptor δ subunit. *EMBO J.* **6**(12), 3619-3626.

Meech, RW. 1972. Intracellular calcium injection causes increased potassium conductance in Aplysia nerve cells. *Comp. Biochem. Physiol.* **42A**, 493-499.

Meech, RW. 1979. Membrane potential oscillations in molluscan 'burster' neurones. *J. exp. Biol.* **81**, 93-112.

Meissner, G. 1984. Adenine nucleotide stimulation of Ca^{2+}-induced Ca^{2+} release in sarcoplasmic reticulum. *J. Biol. Chem.* **259**(4), 2365-2374.

Melchiorre, C., Angeli, P., Lambrecht, G., Mutschler, E., Picchio, M.T. & Wess, J. 1987. Antimuscarinic action of methoctramine, a new cardioselective M-2 muscarinic receptor antagonist, alone and in combination with atropine and gallamine. *Eur. J. Pharmacol.* **144**, 117-124.

Meves, H. & Pichon, Y. 1977. The effect of internal and external 4-aminopyridine on the potassium currents in intracellularly perfused squid giant axons. *J. Physiol. (Lond.).* **268**, 511-532.

Meyer, M.R. & Edwards, J.S. 1980. Muscarinic cholinergic binding sites in an Orthopteran central nervous system. *J. Neurobiol.* **11**, 215-219.

Meyer, M.R. & Reddy, G.R. 1985. Muscarinic and nicotinic cholinergic binding sites in the terminal abdominal ganglion of the cricket, *Acheta domesticus*. *J. Neurochem.* **45**(4), 1101-1112.

Miledi, R., Molinoff, P. & Potter, L.T. 1971. Isolation of the cholinergic receptor protein of Torpedo electric tissue. *Nature (Lond.).* **229**, 554-557.

Miledi, R. & Potter, L.T. 1971. Acetylcholine receptors in muscle fibers. *Nature (Lond.).* **233**, 599-603.

Miller, C., Moczydlowski, E., Latorre, R. & Philips, M. 1985. Charybdotoxin, a protein inhibitor of single Ca^{2+}-activated K^+ channels from mammalian skeletal muscle. *Nature (Lond.).* **313**, 316-318.

Mishina, M., Takai, T., Imoto, K., Noda, M., Takahashi, T. & Numa, S. 1986. Molecular distinction between fetal and adult forms of muscle acetylcholine receptor. *Nature (Lond.).* **321**, 406-411.

Morton, D.B. & Truman, J.W. 1985. Steroid regulation of the peptide-mediated increase in cyclic GMP in the nervous system of the hawkmoth, *Manduca sexta*. *J. Comp. Physiol. A.* **157** (4), 423-432.

Murphy, N.P., Vaughan, P.F.T., Ball, S.G. & McCormack, J.G. 1991. The cholinergic regulation of intracellular calcium in the human neuroblastoma, SH-SY5Y. *J. Neurochem.* **57**, 2116-2123.

Nagy, F., Benson, J.A. & Moulins, M. 1985. Cholinergic inputs reduce a steady outward K^+ current allowing the activation of a Ca^{2+} conductance which underlies the burst-generating oscillations in lobster pyloric neurons. *Soc. Neurosci. Abstr.* **11**, 1022.

Nahorski, SR. 1988. Inositol polyphosphates and neuronal calcium homeostasis. *Trends Neurosci.* **11**(10), 444-448.

Nakajima, Y., Nakajima, S., Leonard, R.J. & Yamaguchi, K. 1986. Acetylcholine raises excitability by inhibiting the fast transient potassium current in cultured hippocampal neurons. *Proc. Natl. Acad. Sci. U.S.A.* **83**, 3022-3026.

Nakamura, T. & Gold, G.H. 1987. A cyclic-nucleotide-gated conductance in olfactory cilia. *Nature (Lond.).* **325**, 442-444.

Nathanson N.M. 1987. Molecular properties of the muscarinic acetylcholine receptor. *Ann. Rev. Neurosci.* **10**, 195-236.

Neher, E. 1971. Two fast transient current components during voltage clamp on snail neurons. *J. Gen. Physiol.* **58**, 36-53.

Neher, E. & Lux, H.D. 1972. Differential action of TEA^+ on two K^+ current components of a molluscan neurone. *Pflügers Arch.* **336**, 87-100.

Nicotera, P., Hartzell, P., Baldi, C., Svensson, S., Bellomo, G. & Orrenius, S. 1986. Cystamine induces toxicity in hepatocytes through the elevation of cytosolic Ca^{2+} and the stimulation of a nonlysosomal proteolytic system. *J. Biol. Chem.* **261**(31), 14628-14635.

Nightingale, W.D. & Pitman, R.M. 1989. Ionic currents in the soma of an identified cockroach motoneurone recorded under voltage clamp. *Comp. Biochem. Physiol.* **93A**(1), 85-93.

Nightingale, W.D. Electrical characteristics of an identified insect motoneurone cell body: a current- and voltage-clamp study. PhD Thesis, University of St. Andrews.

Nilius, B., Hess, P., Lansman, J.B. & Tsien, R.W. 1985. A novel type of cardiac calcium channel in ventricular cells. *Nature (Lond.).* **316**, 443-446.

Noda, M., Furutani, Y., Takahashi, H., Toyosato, M., Tanabe, T., Shimizu, S., Kikyotani, S., Kayano, T., Hirose, T., Inayama, S. & Numa, S. 1983b. Cloning and sequence analysis of calf cDNA and human genomic DNA encoding α-subunit precursor of muscle acetylcholine receptor. *Nature (Lond.).* **305**, 818-823.

Noda, M., Takahashi, H., Tanabe, T., Toyosata, M., Furutani, Y., Hirose, T., Asai, M., Inayama, S., Miyata, T. & Numa, S. 1982. Primary structure of α-subunit precursor of *Torpedo californica* acetylcholine receptor deduced from cDNA sequence. *Nature (Lond.).* **299**, 793-797.

Noda, M., Takahashi, H., Tanabe, T., Toyosata, M., Kikyotani, S., Hirose, T., Asai, M., Takashima, H., Inayama, S., Miyata, T. & Numa, S. 1983a. Primary structures of β- and δ-subunit precursors of *Torpedo californica* acetylcholine receptor deduced from cDNA sequences. *Nature (Lond.).* **301**, 251-255.

Noma, A. 1986. GTP-binding proteins couple cardiac muscarinic receptors to potassium channels. *Trends Neurosci.* **9**, 142-143.

Nowycky, M.C., Fox, A.P. & Tsien, R.W. 1985. Three types of neuronal calcium channel with different calcium agonist sensitivity. *Nature (Lond.).* **316**, 440-443.

Olianas, M.C. & Onali, P. 1990. Ca^{2+}-independent stimulation of adenylate cyclase activity by muscarinic receptors in rat olfactory bulb. *J. Neurochem.* **55**, 1083-1086.

Olsen, R.W., Meunier, J.-C. & Changeux, J.-P. 1972. Progress in the purification of the cholinergic receptor protein from *Electrophorus electricus* by affinity chromatography. *FEBS Lett.* **28**(1), 96-100.

Onai, T., FitzGerald, M.G., Arakawa, S., Gocayne, J.D., Urquhart, D.A., Hall, L.M., Fraser, C.M., McCrombie, W.R. & Venter, J.C. 1989. Cloning, sequence analysis and chromosome localization of a *Drosophila* muscarinic acetylcholine receptor. *FEBS Lett.* **255**(2), 219-225.

Onozuka, M., Imai, S., Kubo, K., Deura, S., Nishiyama, K. & Ozono, S. 1988. Cyclic AMP-dependent protein phosphorylation is involved in activation of the potassium current associated with endogenous cellular calcium in *Euhadra* neurons. *Brain Res.* **473**, 401-405.

Oyama, Y., Akaike, N., Kuraoka, S. & Nishi, K. 1986. Differences in the action of organic and inorganic Ca^{2+}-antagonists on the inactivation of the Ca^{2+} channel in a molluscan neurone. *Comp. Biochem. Physiol.* **83C**(2), 353-357.

Pancrazio, J.J., Viglione, M.P., Kleiman, R.G. & Kim, Y.I. 1991. Verapamil-induced blockade of voltage-activated K^+ current in small-cell lung cancer lines. *J. Pharmacol. Exp. Ther.* **257**(1), 184-189.

Pearson, K.G., Reye, D.N., Robertson, R.M. 1983. Phase-dependent influences of wing stretch receptors on flight rhythm in the locust. *J. Neurophysiol.*. **49**(5), 1168-1181.

Pennefather, P., Lancaster, B., Adams, P.R. & Nicoll, R.A. 1985. Two distinct Ca-dependent K currents in bullfrog sympathetic ganglion cells. *Proc. Natl. Acad. Sci. U.S.A.* **82**, 3040-3044.

Peralta, E.G., Ashkenazi, A., Winslow, J.W., Smith, D.H., Ramachandran, J. & Capon, D.J. 1987b. Distinct primary structures, ligand-binding properties and tissue-specific expression of four human muscarinic acetylcholine receptors. *EMBO J.* **6**(13), 3923-3929.

Peralta, E.G., Ashkenazi, A., Winslow, J.W., Ramachandran, J. & Capon, D.J. 1988. Differential regulation of PI hydrolysis and adenylyl cyclase by muscarinic receptor subtypes. *Nature (Lond.).* **334**, 434-437.

Peralta, E.G., Winslow, J.W., Peterson, G.L., Smith, D.H., Ashkenazi, A., Ramachandran, J., Schimerlik, M.I. & Capon, D.J. 1987a. Primary structure and Biochemical properties of an M2 muscarinic receptor. *Science (N.Y.).* **236**, 600-605.

Perrins, R. & Roberts, A. 1994. Nicotinic and muscarinic ACh receptors in rhythmically active spinal neurones in the *Xenopus laevis* embryo. *J. Physiol. (Lond.).* **478**, 221-228.

Peterson, G.L., Herron, G.S., Yamaki, M., Fullerton, D.S. & Schimerlik, M.I. 1984. Purification of the muscarinic acetylcholine receptor from porcine atria. *Proc. Natl. Acad. Sci. U.S.A.* **81**, 4993-4997.

Pfaffinger, P.J., Leibowitz, M.D., Subers, E.M., Nathanson, N.J., Almers, W. & Hille, B. 1988. Agonists that suppress M-current elicit phosphoinositide turnover and Ca^{2+} transients, but these events do not explain M-current suppression. *Neuron.* **1**, 477-484.

Pinkas-Kramarski, R., Stein, R., Zimmer, Y. & Sokolovsky, M. 1988. Cloned rat M3 muscarinic receptors mediate phosphoinositide hydrolysis but not adenylate cyclase inhibition. *FEBS Lett.* **239**(2), 174-178.

Pitman, R.M. 1979. Intracellular citrate or externally applied tetraethylammonium ions produce calcium-dependent action potentials in an insect motoneurone cell body. *J. Physiol. (Lond.).* **291**, 327-337.

Pitman, R.M. 1985. Nervous system. In: *Comprehensive Insect Physiology, Biochemistry and pharmacology.* 5-54. Eds. Kerkut, G.A. & Gilbert, L.I. *Pergamon Press, Oxford.*

Pitman, R.M. & Kerkut, G.A. 1970. Comparison of the actions of iontophoretically applied acetylcholine and gamma aminobutyric acid with the EPSP and IPSP in cockroach central neurons. *Comp. Gen. Pharmacol.* **1**(2), 221-230.

Qazi, S. & Lunt, G.G. 1991. Muscarinic receptors in locust ganglia are coupled to phosphatidyl inositol turnover and to adenylate cyclase. *Soc. Neurosci. Abstr.* **17**, 584.

Qazi, S. & Trimmer, B.A. 1993. Muscarinic modulation of second messengers in an insect CNS. *Soc. Neurosci. Abstr.* **19**, 743.

Raftery, M.A. 1973. Isolation of acetylcholine receptor-α-bungarotoxin complexes from *Torpedo californica* electroplax. *Arch. Biochem. Biophys.* **154**, 270-276.

Raftery, M.A., Vandlen, R.L., Reed, K.L. & Lee, T. 1975. Characterization of *Torpedo californica* acetylcholine receptor: its subunit composition and ligand-binding properties. *Symp. Quant. Biol.* **40**, 193-292.

Rall, T.W., Sutherland, E.W. & Berthet, J. 1957. The relationship of epinephrine and glucagon to liver phosphorylase. IV. Effect of epinephrine and glucagon on the reactivation of phosphorylase in liver homogenates. *J. Biol. Chem.* **224**, 463-475.

Ramirez, J.M. & Pearson, K.G. 1991a. Octopaminergic modulation of interneurones in the flight system of the locust. *J. Neurophysiol.* **66**(5), 1522-1537.

Ramirez, J.M. & Pearson, K.G. 1991b. Octopamine induces bursting and plateau potentials in insect neurons. *Brain Res.* **549**, 332-337.

Rampe, D., Wible, B., Fedida, D., Dage, R.C. & Brown, A.M. 1993. Verapamil blocks a rapidly activating delayed rectifier K^+ channel cloned from human heart. *Mol. Pharmacol.* **44**, 642-648.

Rang, H.P. & Dale, M.M. 1987. *Pharmacology. Churchill Livingstone, U.K.*

Reiter. M.J., Cowburn, D.A., Prives, J.M. & Karlin, A. 1972. Affinity labelling of the acetylcholine receptor in the electroplax: electrophoretic separation in sodium dodecyl sulfate. *Proc. Natl. Acad. Sci. U.S.A.* **69**, 1168-1172.

Reuter, H. 1984. Ionic channels in cardiac cell membranes. *Ann. Rev. Physiol.* **46**, 473-484.

Reye, D.N. & Pearson, K.G. 1987. Projections of the wing stretch receptors to central flight neurones in the locust. *J. Neurosci.* **7**(8), 2476-2487.

Reynolds, J.A. & Karlin, A. 1978. Molecular weight in detergent solution of acetylcholine receptor from *Torpedo californica*. *Biochem.* **17**(11), 2035-2038.

Robbins, J., Marsh, S.J. & Brown, D.A. 1993. On the mechanism of M-current inhibition by muscarinic m1 receptors in DNA-transfected rodent neuroblastoma x glioma cells. *J. Physiol. (Lond.).* **469**, 153-178.

Robertson, R.M. 1986. Neuronal circuits controlling flight in the locust: central generation of the rhythm. *Trends Neurosci.* **9**(6), 278-280.

Robertson, P.L., Bruno, G.R. & Datta, S.C. 1990. Glutamate-stimulated, guanine nucleotide-mediated phosphoinositide turnover in astrocytes is inhibited by cyclic AMP. *J. Neurochem.* **55**(5), 1727-1733.

Robertson, R.M. & Pearson, K.G. 1983. Interneurons in the flight system of the locust: distribution, connections and resetting properties. *J. Comp. Neurol.* **215**, 33-50.

Robertson, R.M. & Pearson, K.G. 1985. Neural circuits in the flight system of the locust. *J. Neurophysiol.*. **53**(1), 110-128.

Rodbell, M., Birnbaumer, L., Pohl, S.L. & Krans, M.J. 1971. The glucagon-sensitive adenyl cyclase system in plasma membranes of rat liver. V. An obligatory role of guanyl nucleotides in glucagon action. *J. Biol. Chem.* **246**(6), 1877-1882.

Rogawski, M.A. 1985. The A-current: how ubiquitous a feature of excitable cells is it? *Trends Neurosci.* **8**(5), 214-219.

Rudy, B. 1988. Diversity and ubiquity of K channels. *Neurosci.* **25**(3), 729-749.

Sakmann, B., Noma, A. & Trautwein, W. 1983. Acetylcholine activation of single muscarinic K^+ channels in isolated pacemaker cells of the mammalian heart. *Nature (Lond.).* **303**, 250-253.

Salkoff, L. 1983. *Drosophila* mutants reveal two components of fast outward current. *Nature (Lond.).* **302**, 249-251.

Salkoff, L.B. & Wyman, R.J. 1981a. Outward currents in developing *Drosophila* flight muscle. *Science (N.Y.).* **212**, 461-463.

Salkoff, L.B. & Wyman, R.J. 1981b. Genetic modification of potassium channels in *Drosophila* Shaker mutants. *Nature (Lond.).* **293**, 228-230.

Salkoff, L.B. & Wyman, R.J. 1983. Ion currents in *Drosophila* flight muscles. *J. Physiol. (Lond.).* **337**, 687-709.

Salvaterra, P.M. & Foders, R.M. 1979. [^{125}I]α-bungarotoxin and [^{3}H]quinuclidinyl benzilate binding in central nervous system of different species. *J. Neurochem.* **32**, 1509-1517.

Sanes, J.R. & Hildebrand, J.G. 1976. Acetylcholine and its metabolic enzymes in developing antennae of the moth, *Manduca sexta. Dev. Biol.* **52**, 105-120.

Sanes, J.R., Prescott, D.J. & Hildebrand, J.G. 1977. Cholinergic neurochemical development of normal and deafferented antennal lobes during metamorphosis of the moth, *Manduca sexta. Brain Res.* **119**, 389-402.

Sattelle, D.B. 1985. Acetylcholine receptors. In: *Comprehensive Insect Physiology, Biochemistry and pharmacology.* 395-434. Eds. Kerkut, G.A. & Gilbert, L.I. *Pergamon Press, Oxford.*

Sattelle, D.B., David, J.A., Harrow, I.D. & Hue, B. 1980. Actions of α-bungarotoxin on identified insect central neurones. In: *Receptors for neurotransmitters, hormones and pheromones.* 125-139. Eds. Sattelle, D.B., Hall, L.M. & Hildebrand, J.G. *Elsevier, Amsterdam.*

Sattelle, D.B., Harrow, I.D., Hue, B., Pelhate, M., Gepner, J.I. & Hall, L.M. 1983. α-Bungarotoxin blocks excitatory synaptic transmission between cercal sensory neurones and giant interneurone 2 of the cockroach, *Periplaneta americana. J. exp. Biol.* **107**, 473-489.

Sattelle, D.B., McClay, A.S., Dowson, R.J. & Callec, J.J. 1976. The pharmacology of an insect ganglion: actions of carbamylcholine and acetylcholine. *J. exp. Biol.* **64**, 13-23.

Sattelle, D.B., Pinnock, R.D., Wafford, K.A. & David, J.A. 1988. GABA receptors on the cell-body membrane of an identified insect motor neuron. *Proc. R. Soc. Lond. B.* **232**, 443-456.

Sawruk, E., Udri, C., Betz, H. & Schmitt, B. 1990. SBD, a novel structural subunit of the *Drosophila* nicotinic acetylcholine receptor, shares its genomic localization with two α-subunits. *FEBS Lett.* **273**(1-2), 177-181.

Schafer R. 1973. Acetylcholine: fast axoplasmic transport in insect chemoreceptor fibers. *Science (N.Y.).* **180**, 315-317.

Schäfer S., Béhé, P. & Meves, H. 1991. Inhibition of the M current in NG 108-15 neuroblastoma x glioma hybrid cells. *Pflügers Arch.* **418**, 581-591.

Schanne, F.A.X., Kane, A.B., Young, E.E. & Farber, J.L. 1979. Calcium dependence of toxic cell death: a final common pathway. *Science (N.Y.)*. **206**, 700-702.

Schloss, P., Betz, H., Schroeder, C. & Gundelfinger, E.D. 1991. Neuronal nicotinic acetylcholine receptors in *Drosophila*- antibodies raised against an α-like and a non-α-subunit recognise the same high affinity α-bungarotoxin binding complex. *J. Neurochem.* **57**(5), 1556-1562.

Schmidt, J. & Raftery, M.A. 1972. Use of affinity chromatography for acetylcholine receptor purification. *Biochem. Biophys. Res. Comm.* **49**(2), 572-578.

Schneider, M.J., Rogowski, R.S., Krueger, B.K. & Blaustein, M.P. 1989. Charybdotoxin blocks both Ca-activated K channels and Ca-independent voltage gated K channels in rat brain synaptosomes. *FEBS Lett.* **250**(2), 433-436.

Schramm, M. & Rodbell, M. 1975. A persistent active state of the adenylate cyclase system produced by the combined actions of isoproterenol and guanylyl imidodiphosphate in frog erythrocyte membranes. *J. Biol. Chem.* **250**(6), 2232-2237.

Schramm, M & Selinger, Z. 1984. Message transmission: receptor controlled adenylate cyclase system. *Science (N.Y.)*. **225**, 1350-1356.

Schweitz, H., Stansfield, C.E., Bidard, J.-N., Fagni, L., Maes, P. & Lazdunski, M. 1989. Charybdotoxin blocks dendrotoxin-sensitive voltage-activated K^+ channels. *FEBS Lett.* **250**(2), 519-522.

Schwindt, P.C., Spain, W.J., Foehring, R.C., Chubb, M.C. & Crill, W.E. 1988. Slow conductances in neurons from cat sensorimotor cortex in vitro and their role in slow excitability changes. *J. Neurophysiol.*. **59**(2), 450-467.

Selyanko, A.A., Stansfeld, C.E. & Brown, D.A. 1992. Closure of potassium M-channels by muscarinic acetylcholine-receptor stimulants requires a diffusible messenger. *Proc. R. Soc. Lond. B.* **250**, 119-125.

Shah, J. & Pant, H.C. 1991. Effect of cadmium on Ca^{2+} transport in brain microsomes. *Brain Res.* **566**, 127-130.

Shankland, D.L., Rose, J.A. & Donniger, C. 1971. The cholinergic nature of the cercal nerve-giant fiber synapse in the sixth abdominal ganglion of the American cockroach, *Periplaneta americana* (L.). *J. Neurobiol.* **2**(3), 247-262.

Shapiro, R.A., Wakimoto, B.T., Subers, E.M. & Nathanson, N.M. 1989. Characterization and functional expression in mammalian cells of genomic

and cDNA clones encoding a *Drosophila* muscarinic acetylcholine receptor. *Proc. Natl. Acad. Sci. U.S.A.* **86**, 9039-9043.

Sheng, H., Gagne, G.D., Matsumoto, T., Miller, M.F., Förstermann, U. & Murad, F. 1993. Nitric oxide synthase in bovine superior cervical ganglion. *J. Neurochem.* **61**, 1120-1126.

Shirvan, M.H., Pollard, H.B. & Heldman, E. 1991. Mixed nicotinic and muscarinic features of cholinergic receptor coupled to secretion in bovine chromaffin cells. *Proc. Natl. Acad. Sci. U.S.A.* **88**, 4860-4864.

Siegelbaum, S.A. & Tsien, R.W. 1980. Calcium-activated transient outward current in calf cardiac Purkinje fibres. *J. Physiol. (Lond.).* **299**, 485-506.

Silver, M.R. & DeCoursey, T.E. 1990. Intrinsic gating of inward rectifier in bovine pulmonary artery endothelial cells in the presence or absence of internal Mg^{2+}. *J. Gen. Physiol.*. **96**, 109-133.

Sims, S.M., Walsh, J.V. & Singer, J.J. 1986. Substance P and acetylcholine both suppress the same K^+ current in dissociated smooth muscle cells. *Am. J. Physiol.* **251**(Cell. Physiol. 20), C580-C587.

Smart, T.G. 1987. Single calcium-activated potassium channels recorded from cultured rat sympathetic neurones. *J. Physiol. (Lond.).* **389**, 337-360.

Smith, J.B., Cragoe, E.J. Jr. & Smith, L. 1987. Na^+/Ca^{2+} antiport in cultured arterial smooth muscle cells. Inhibition by magnesium and other divalent cations. *J. Biol. Chem.* **262**(25), 11988-11994.

Spedding, M. & Paoletti, R. 1992. Classification of calcium channels and the sites of action of drugs modifying channel function. *Pharmacol. Rev.* **44**(3), 363-376.

Standen, N.B. & Stanfield, P.R. 1978. A potential- and time-dependent blockade of inward rectification in frog skeletal muscle fibres by barium and strontium ions. *J. Physiol. (Lond.).* **280**, 169-191.

Standen, N.B. & Stanfield, P.R. 1980. Rubidium block and rubidium permeability of the inward rectifier of frog skeletal muscle fibres. *J. Physiol. (Lond.).* **304**, 415-435.

Stanfield, P.R. 1970a. The effect of the tetraethylammonium ion on the delayed currents of frog skeletal muscle. *J. Physiol. (Lond.).* **209**, 209-229.

Stanfield, P.R. 1970b. The differential effects of tetraethylammonium and zinc ions on the resting conductance of frog skeletal muscle. *J. Physiol. (Lond.).* **209**, 231-256.

Storey, D.J., Shears, S.B., Kirk, C.J. & Michell, R.H. 1984. Stepwise enzymatic dephosphorylation of inositol 1,4,5-trisphoshate to inositol in liver. *Nature (Lond.).* **312**, 374-376.

Streb, H., Irvine, R.F., Berridge, M.J. & Schulz, I. 1983. Release of Ca^{2+} from a nonmitochondrial intracellular store in pancreatic acinar cells by inositol-1,4,5-trisphosphate. *Nature (Lond.).* **306**, 67-69.

Stryer, L. 1988. *Biochemistry. W.H. Freeman & Co. New York.*

Sugden, D., Vanecek, J., Klein, D.C., Thomas, T.P. & Anderson, W.B. 1985. Activation of protein kinase C potentiates isoprenaline-induced cyclic AMP accumulation in rat pinealocytes. *Nature (Lond.).* **314**, 359-361.

Supattapone, S., Worley, P.F., Baraban, J.M. & Snyder, S.H. 1988. Solubilization, purification, and characterization of an inositol trisphosphate receptor. *J. Biol. Chem.* **263**(3), 1530-1534.

Suter, C. 1986. The actions of octopamine and other biogenic amines on locust central neurons. *Comp. Biochem. Physiol.* **84C**(1), 181-187.

Suter, C. & Usherwood, P.N.R. 1985. Action of acetylcholine and antagonists on somata isolated from locust central neurons. *Comp. Biochem. Physiol.* **80C**(2), 221-229.

Sutherland, E.W. & Rall, T.W. 1958. Fractionation and characterization of a cyclic adenine ribonucleotide formed by tissue particles. *J. Biol. Chem.* **232**, 1077-1091.

Tachado, S.D., Virdee, K., Akhtar, R.A. & Abdel-Latif, A.A. 1994. M3 muscarinic receptors mediate an increase in both inositol trisphosphate production and cyclic AMP formation in dog iris sphincter smooth muscle. *J. Ocular. Pharmacol.* **10**(1), 137-147.

Tachibana, M. 1983. Ionic currents of solitary horizontal cells isolated from goldfish retina. *J. Physiol. (Lond.).* **345**, 329-351.

Takahashi, K. & Akaike, N. 1991. Calcium antagonist effects on low-threshold (T-type) calcium current in rat isolated hippocampal CA1 pyramidal neurons. *J. Pharmacol. Exp. Ther.* **256**(1), 169-175.

Takai, Y., Iwasa, Y., Kawahara, Y., Mori, T. & Nishizuka, Y. 1979. Calcium-dependent activation of a multifunctional protein kinase by membrane phospholipids. *J. Biol. Chem.* **254**(10), 3692-3695.

Takai, T., Noda, M., Furutani, Y., Takahashi, H., Notake, M., Shimizu, S., Kayano, T., Tanabe, T., Tanaka, K., Hirose, T., Inayama, S. & Numa, S. 1984. Primary structure of γ subunit precursor of calf-muscle acetylcholine receptor deduced from the cDNA sequence. *Eur. J. Biochem.* **143**, 109-115.

Takai, T., Noda, M., Mishina, M., Shimizu, S., Furutani, Y., Kayano, T., Ikeda, T., Kubo, T., Takahashi, H., Takahashi, T., Kuno, M. & Numa, S. 1985. Cloning, sequencing and expression of cDNA for a novel subunit of acetylcholine receptor from calf muscle. *Nature (Lond.).* **315**, 761-764.

Tanabe, T., Noda, M., Furutani, Y., Takai, T., Takahashi, H., Tanaka, K., Hirose, T., Inayama, S. & Numa, S. 1984. Primary structure of β subunit precursor of calf muscle acetylcholine receptor deduced from cDNA sequence. *Eur. J. Biochem.* **144**, 11-17.

Tasaki, I. & Hagiwara, S. 1957. Demonstration of two stable potential states in the squid giant axon under tetraethylammonium chloride. *J. Gen. Physiol.*. **40**, 859-872.

Tatsuta, H., Ueda, S., Morishima, S. & Okada, Y. 1994. Voltage- and time-dependent K^+ channel currents in the basolateral membrane of villus enterocytes isolated from guinea-pig small intestine. *J. Gen. Physiol.*. **103**, 429-446.

Taylor, C.W. & Marshall, I.C.B. 1992. Calcium and inositol 1,4,5-trisphosphate receptors: a complex relationship. *Trends. Biochem. Sci.* **17**, 403-407.

Thomas, M.V. 1984. Voltage-clamp analysis of a calcium-mediated potassium conductance in cockroach (*Periplaneta americana*) central neurones. *J. Physiol. (Lond.).* **350**, 159-178.

Thomas, M.V. & Gorman, A.L.F. 1977. Internal calcium changes in a bursting pacemaker neuron measured with Arsenazo III. *Science (N.Y.).* **196**, 531-533.

Thompson, S.H. 1977. Three pharmacologically distinct potassium channels in molluscan neurones. *J. Physiol. (Lond.).* **265**, 465-488.

Tillotson, D. 1979. Inactivation of Ca conductance dependent on entry of Ca ions in molluscan neurones. *Proc. Natl. Acad. Sci. U.S.A.* **76**, 1497-1500.

Tobias, J.M., Kollross, J.J. & Savit, J. 1946. Acetylcholine and related substances in the cockroach, fly and crayfish, and the effect of DDT. *J. Cell. Comp. Physiol.* **28**, 159-182.

Toescu, E.C. 1991. Regulation of $^{109}Cd^{2+}$ uptake into isolated neurohypophysial peptidergic nerve terminals. *J. Neurochem.* **57**, 1827-1831.

Trimmer, B.A. 1995. Current excitement from insect muscarinic receptors. *Trends Neurosci.* **18**, 104-111.

Trimmer, B.A. & Berridge, M.J. 1985. Inositol phosphates in the insect nervous system. *Insect Biochem.* **15**(6), 811-815.

Trimmer, B.A. & Weeks, J.C. 1989. Effects of nicotinic and muscarinic agents on an identified motorneurone and its direct afferent inputs in larval *Manduca sexta*. *J. exp. Biol.* **144**, 303-337.

Trimmer, B.A., & Weeks, J. 1993. Muscarinic acetylcholine receptors modulate the excitability of an identified insect motoneuron. *J. Neurophysiol.*. **69**(6), 1821-1836.

Trube, G., Sakmann, B. & Trautwein, W. 1981. Inward rectifying potassium currents recorded from isolated heart cells by the patch clamp method. *Pflügers Arch.* **391**, R7.

Truman, J.W., Mumby, S.M. & Welch, S.K. 1979. Involvement of cyclic GMP in the release of stereotyped behaviour patterns in moths by a peptide hormone. *J. exp. Biol.* **84**, 201-212.

Tsien, R.W., Lipscombe, D., Madison, D.V., Bley, K.R. & Fox, A.P. 1988. Multiple types of neuronal calcium channels and their selective modulation. *Trends Neurosci.* **11**, 431-438.

Tsien, R.W., Lipscombe, D., Madison, D., Bley, K. & Fox, A. 1995. Reflections on Ca^{2+}-channel diversity, 1988-1994. *Trends Neurosci.* **18**(2), 52-54.

Tsien, R.W. & Tsien, R.Y. 1990. Calcium channels, stores and oscillations. *Ann. Rev. Cell Biol.* **6**, 715-760.

Tytgat, J., Vereecke, J. & Carmeliet, E. 1990. Mechanism of cardiac T-type Ca channel blockade by amiloride. *J. Pharmacol. Exp. Ther.* **254**(2), 546-551.

Uchitel, O.D. & Protti, D.A. 1994. P-type calcium channels and transmitter release from nerve terminals. *News Physiol. Sci.* **9**, 101-105.

Usherwood, P.N.R., Giles, D. & Suter, C. 1980. Studies of the pharmacology of insect neurons *in vitro*. In: *Insect Neurobiology and Pesticide Action (Neurotox 79)*, 115-128. *Soc. Chem. Ind., London.*

Vandenberg, C.A. 1987. Inward rectification of a potassium channel in cardiac ventricular cells depends on internal magnesium ions. *Proc. Natl. Acad. Sci. U.S.A.* **84**, 2560-2564.

Vanner, S., Evans, R.J., Matsumoto, S.G. & Surprenant, A. 1993. Potassium currents and their modulation by muscarine and substance P in neuronal cultures from adult guinea pig celiac ganglia. *J. Neurophysiol.*. **69**(5), 1632-1644.

Verbost, P.M., Senden, M.H.M.N. & van Os, C.H. 1987. Nanomolar concentrations of Cd^{2+} inhibit Ca^{2+} transport systems in plasma membranes and intracellular Ca^{2+} stores in intestinal epithelium. *Biochim. Biophys. Acta.* **902**, 247-252.

Vergara, C. & Latorre, R. 1983. Kinetics of Ca^{2+}-activated K^+ channels from rabbit muscle incorporated into planar bilayers. Evidence for a Ca^{2+} and Ba^{2+} blockade. *J. Gen. Physiol.*. **82**, 543-568.

Villaroel, A., Marrion, N.V., Lopez, H. & Adams, P.R. 1989. Bradykinin inhibits a potassium M-like current in rat pheochromocytoma PC12 cells. *FEBS Lett.* **255**, 42-46.

Waelbroeck, M., Tastenoy, M., Camus, J. & Christophe, J. 1991. Binding kinetics of quinuclidinyl benzilate and methyl-quinuclidinyl benzilate enantiomers at neuronal (M1), cardiac (M2), and pancreatic (M3) muscarinic receptors. *Mol. Pharmacol.* **40**, 413-420.

Walsh, D.A., Perkins, J.P. & Krebs, E.G. 1968. Adenosine 3',5'-monophosphate-dependent protein kinase from rabbit skeletal muscle. *J. Biol. Chem.* **243**(13), 3763-3765.

Wamsley, J.K., West, J.R., Black, A.C. Jr. & Williams, T.H. 1979. Muscarinic cholinergic and preganglionic physiological stimulation increase cyclic GMP levels in guinea-pig superior cervical ganglia. *J. Neurochem.* **32**, 1033-1035.

Wang, W. & Giebisch, G. 1991. Dual modulation of renal ATP-sensitive K^+ channel by protein kinases A and C. *Proc. Natl. Acad. Sci. U.S.A.* **88**, 9722-9725.

Washburn, M.S. & Moises, H.C. 1992. Muscarinic responses of rat basolateral amygdaloid neurons recorded *in vitro*. *J. Physiol. (Lond.).* **449**, 121-154.

Weight, ,F.F. & Votava, J. 1970. Slow synaptic excitation in sympathetic ganglion cells: evidence for synaptic inactivation of potassium conductance. *Science (N.Y.).* **170**, 755-758.

Weill, C.L., McNamee, M.G. & Karlin, A. 1974. Affinity-labeling of purified acetylcholine receptor from *Torpedo californica*. *Biochem. Biophys. Res. Comm.* **61**(3), 997-1003.

Weiner, D.M. & Brann, M.R. 1989. Distribution of m1-m5 muscarinic receptor mRNAs in rat brain. *Trends Pharmacol. Sci.* **10**(Supplement - Subtypes of muscarinic receptors IV), 115.

Wendler, G. 1974. The influence of proprioceptive feedback on locust flight co-ordination. *J. Comp. Physiol.*. **88**, 173-200.

Werman, R. 1966. A review- Criteria for identification of a central nervous system transmitter. *Comp. Biochem. Physiol.* **18**, 745-766.

Wess, J. 1993. Molecular basis of muscarinic acetylcholine receptor function. *Trends Pharmacol. Sci.* **14**, 308-313.

Wess, J., Brann, M.R. & Bonner, T.I. 1989. Identification of a small intracellular region of the muscarinic m3 receptor as a determinant of selective coupling to PI turnover. *FEBS Lett.* **258**(1), 133-136.

Wess, J., Gdula, D. & Brann, M.R. 1991. Site-directed mutagenesis of the m3 muscarinic receptor: identification of a series of threonine and tyrosine residues involved in agonist but not antagonist binding. *EMBO J.* **10**(12), 3729-3734.

Whitton, P.S., Nicholson, R.A. & Strang, R.H.C. 1994. Electrophysiological responses of isolated locust (*Schistocerca gregaria*) somata to taurine and GABA application. *J. Insect. Physiol.*. **40**(3), 195-199.

Wilson, D.M. 1961. The central nervous control of flight in a locust. *J. exp. Biol.* **38**, 471-490.

Wilson, D.M. & Gettrup, E. 1963. A stretch reflex controlling wingbeat frequency in grasshoppers. *J. exp. Biol.* **40**, 171-185.

Wilson, D.M. & Weis-Fogh, T. 1962. Patterned activity of co-ordinated motor units, studied in flying locusts. *J. exp. Biol.* **39**, 643-667.

Xu, X. & Lee, K.S. 1994. A selective blocker for rested T-type Ca^{++} channels in guinea pig atrial cells. *J. Pharmacol. Exp. Ther.* **268**(3), 1135-1142.

Yamamura, H.I., Kuhar, M.J., Greenberg, D. & Snyder, S.H. 1974. Muscarinic cholinergic receptor binding: regional distribution in monkey brain. *Brain Res.* **66**, 541-546.

Yamamura, H.I. & Snyder, S.H. 1974a. Muscarinic cholinergic binding in rat brain. *Proc. Natl. Acad. Sci. U.S.A.* **71**, 1725-1729.

Yamamura, H.I. & Snyder, S.H. 1974b. Muscarinic cholinergic receptor binding in the longitudinal muscle of the guinea-pig ileum with [^{3H}]quinuclidinyl benzilate. *Mol. Pharmacol.* **10**, 861-867.

Yarosh, C.A., Acosta, C. & Ashe, J.H. 1988. Modification of nicotinic ganglionic transmission by muscarinic slow postsynaptic potentials in the in vitro rabbit superior cervical ganglion. *Synapse*. **2**, 174-182.

Yeh, J.Z., Oxford, G.S., Wu, C.H. & Narahashi, T. 1976. Dynamics of aminopyridine block of potassium channels in squid axon membranes. *J. Gen. Physiol.*. **68**, 519-535.

Yellen, G. 1984. Ionic permeation and blockade in Ca^{2+}-activated K^+ channels of bovine chromaffin cells. *J. Gen. Physiol.*. **84**, 157-186.

Yoshimasa, T., Sibley, D.R., Bouvier, M., Lefkowitz, R.J. & Caron, M.G. 1987. Cross-talk between cellular signalling pathways suggested by phorbol-ester-induced adenylate cyclase phosphorylation. *Nature (Lond.)*. **327**, 67-70.

Young, E.F., Ralston, E., Blake, J., Ramachandran, J., Hall, Z.W. & Stroud, R.M. 1985. Topological mapping of acetylcholine receptor: evidence for a model with five transmembrane segments and a cytoplasmic COOH-terminal peptide. *Proc. Natl. Acad. Sci. U.S.A.* **82**, 626-630.

Yovell, Y., Kandel, E.R., Dudai, Y. & Abrams, T.W. 1992. A quantitative study of the Ca^{2+}/calmodulin sensitivity of adenylyl cyclase in *Aplysia*, *Drosophila*, and rat. *J. Neurochem.* **59**, 1736-1744.

Zhang, J.-F., Randall, A.D., Ellinor, P.T., Horne, W.A., Sather, W.A., Tanabe, T., Schwarz, T.L. & Tsien, R.W. 1993. Distinctive pharmacology and kinetics of cloned neuronal Ca^{2+} channels and their possible counterparts in mammalian CNS neurons. *Neuropharmacol.* **32**(11), 1075-1088.

Zbicz, K.L. & Weight, F.F. 1985. Transient voltage and calcium-dependent outward currents in hippocampal CA3 pyramidal neurons. *J. Neurophysiol.*. **53**(4), 1038-1058.

Zufall, F. & Hatt, H. 1991. Dual activation of a sex pheromone-dependent ion channel from insect olfactory dendrites by protein kinase-C activators and cyclic GMP. *Proc. Natl. Acad. Sci. U.S.A.* **88**, 8520-8524.

Zufall, F., Stengl, M., Franke, C., Hildebrand, J.G. & Hatt, H. 1991. Ionic currents of cultured olfactory neurons from antennae of male *Manduca sexta*. *J. Neurosci.* **11**(4), 956-965.

APPENDIX I
COMPOSITION OF LOCUST SALINE

SALINE	4 M NaCl (ml)	1 M KCl (ml)	1 M $CaCl_2$ (ml)	1 M $BaCl_2$ (ml)
normal	37.5	5	4	-
Ba^{2+} saline	37.5	5	-	4

Stock solutions were made up to approximately 950 ml with deionised, double distilled water (Milli Q) before the pH buffer, TES (N-tris[Hydroxymethyl]methyl-2-aminoethanesulfonic acid) was added ($2{\cdot}292\ g\ l^{-1}$; 10 mM). The pH was corrected to pH 7.4 with sodium hydroxide using a Kent EIL 3055 pH meter. The final volume was made up to 1000 ml.

(From Hancox, 1991)

APPENDIX II
SOURCES OF DRUGS AND CHEMICALS

Drugs:

acetylcholine chloride	Sigma
atropine sulphate	Sigma
BAPTA	Sigma
α-bungarotoxin	Sigma
carbamylcholine chloride	Sigma
4-DAMP methiodide	RBI
S(+)-dexetimide hydrochloride	RBI
dibutyryl cAMP	Sigma
McN-A-343	RBI
methoctramine 4HCl hydrate	RBI
L-(+)-muscarine	RBI
(-)-nicotine	Sigma
p-F-HHSiD	RBI
pirenzepine dihydrochloride	Sigma
theophylline	Sigma
(-)scopolamine hydrochloride	Sigma
(±)-verapamil hydrochloride	Sigma

Other chemicals:

barium chloride	AnalaR
borax	Sigma
boric acid	Griffin and Tatlock Ltd
caesium chloride	Fisons
cadmium chloride	BDH
calcium chloride	BDH
ethanol	BDH
fast green FCF	Gurr
formaldehyde	BDH
glacial acetic acid	BDH
lithium acetate	Sigma
lithium chloride	Sigma
Lucifer Yellow CH	Sigma
methyl benzoate	BDH
methyl salicylate	BDH
potassium acetate	BDH
potassium chloride	BDH
sodium chloride	BDH
tetraethylammonium chloride	Sigma
Toluidine Blue	Gurr

APPENDIX III

BLOCK DIAGRAM REPRESENTING SINGLE-ELECTRODE CURRENT CLAMP PRESSURE APPLICATION OF ACh

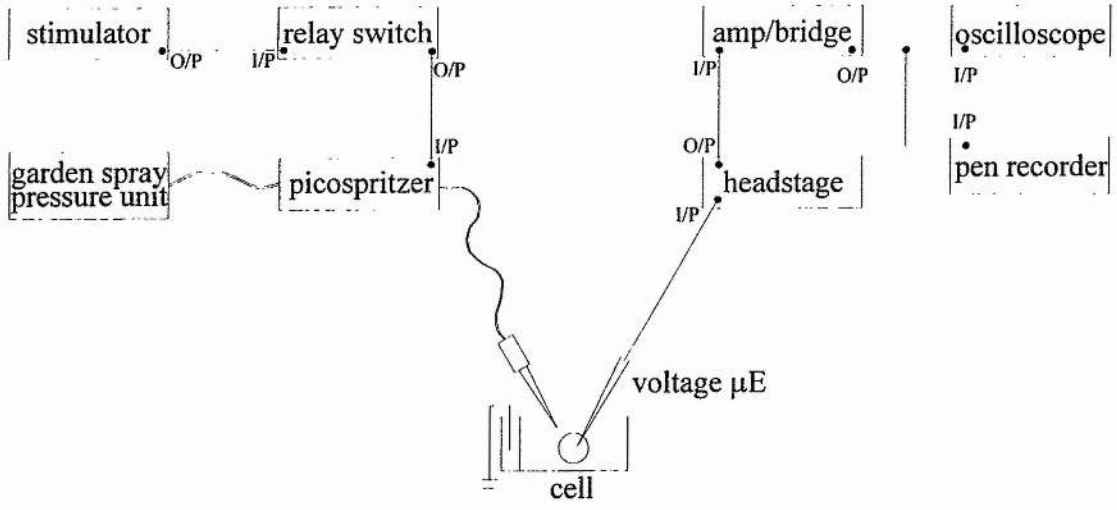

APPENDIX IV
BLOCK DIAGRAM REPRESENTING TWO-ELECTRODE CURRENT CLAMP INPUT RESISTANCE MEASUREMENTS

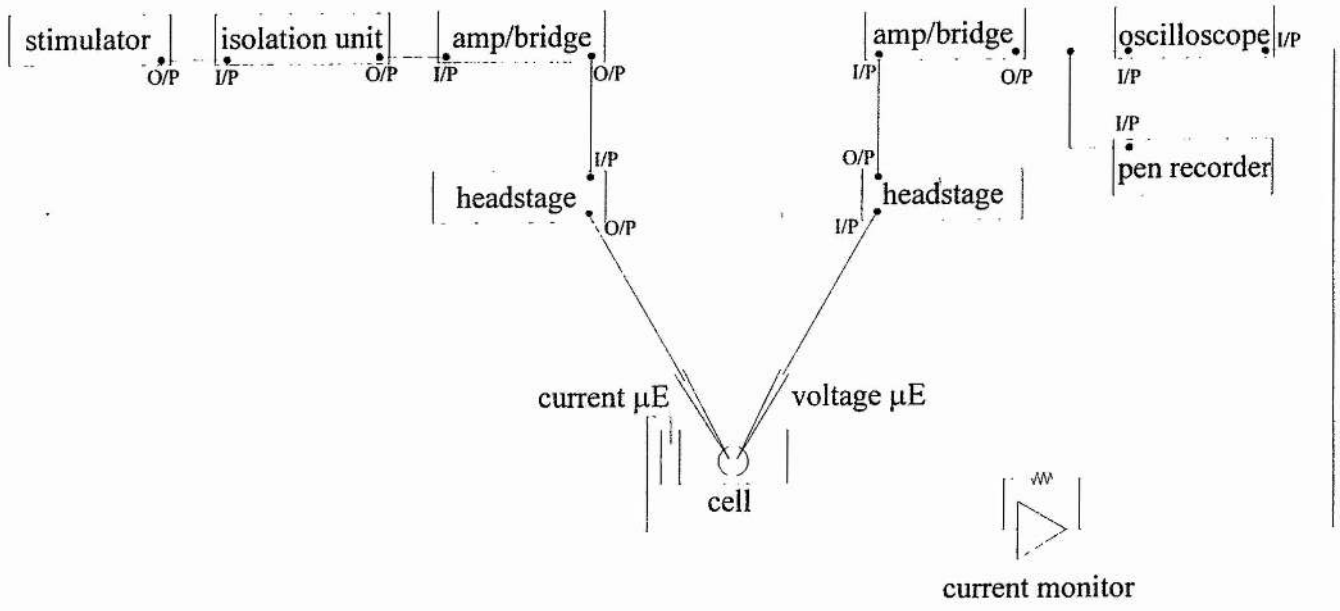

APPENDIX V
BLOCK DIAGRAM REPRESENTING TWO-ELECTRODE CURRENT CLAMP SPIKE THRESHOLD MEASUREMENTS

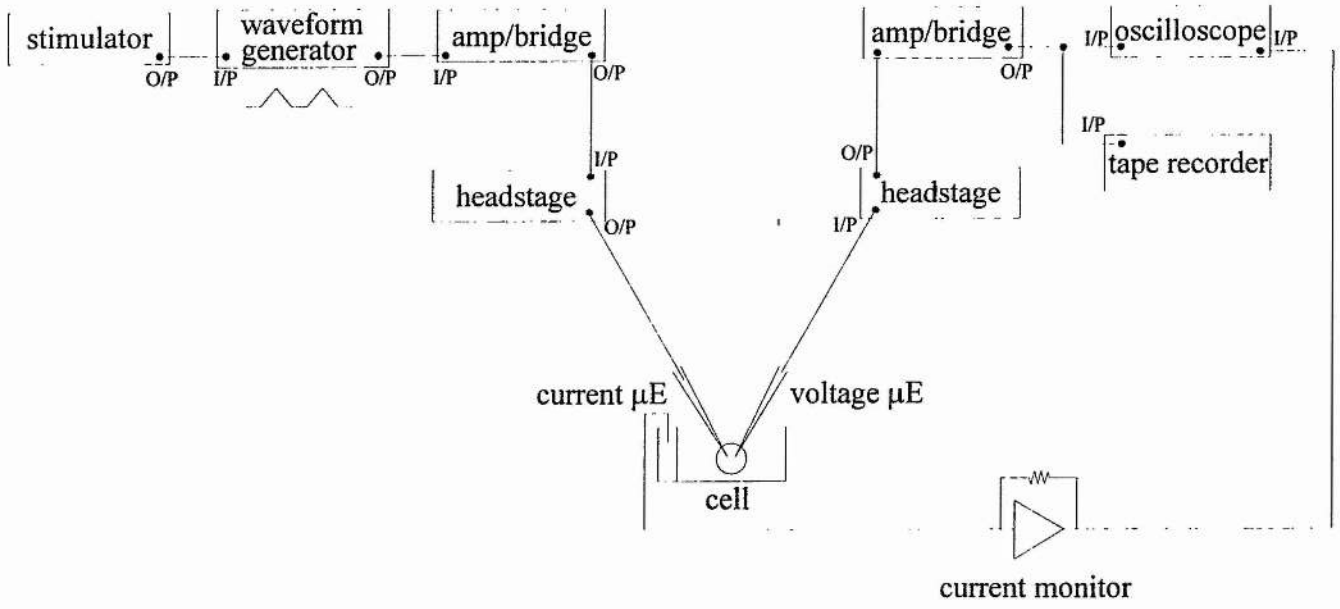

APPENDIX VI
BLOCK DIAGRAM REPRESENTING TWO-ELECTRODE VOLTAGECLAMP

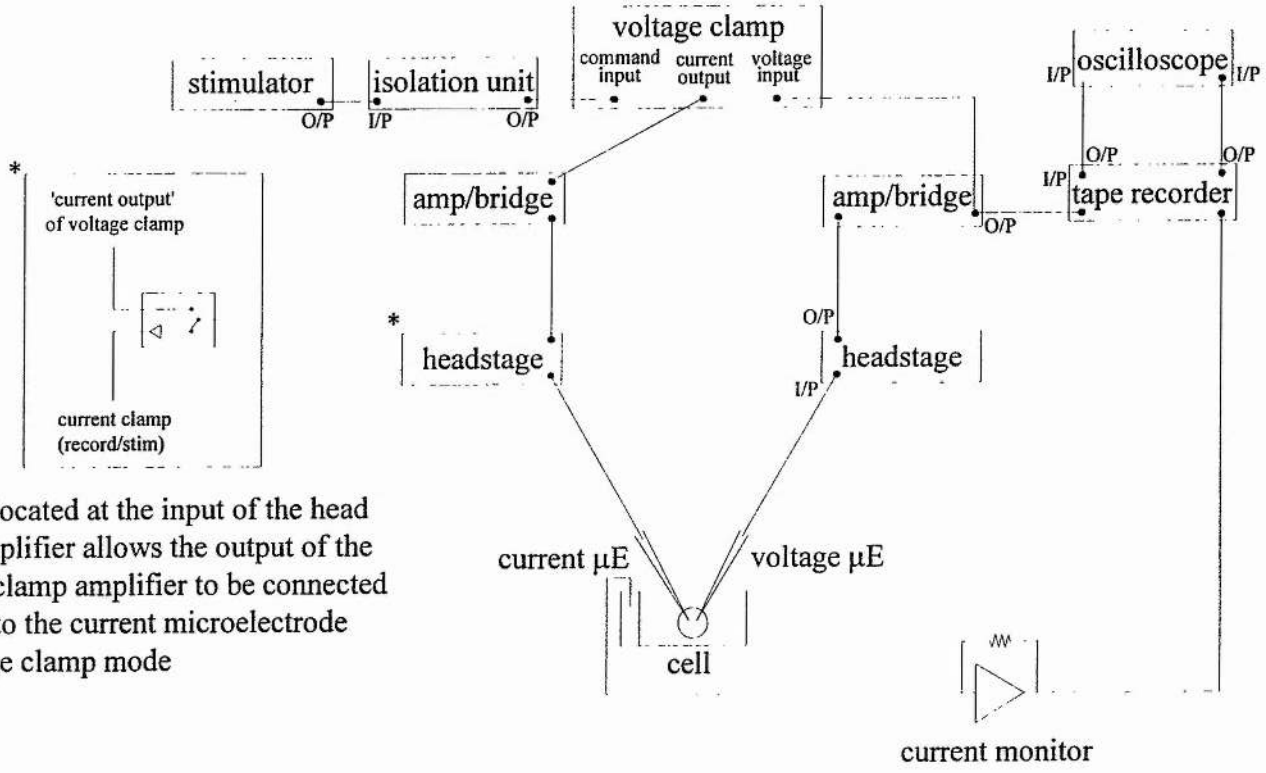

A relay located at the input of the head stage amplifier allows the output of the voltage-clamp amplifier to be connected directly to the current microelectrode in voltage clamp mode

APPENDIX VII
COMPOSITION OF TOLUIDINE BLUE STAIN AND BODIAN'S FIXATIVE

Toluidine Blue

1 g Toluidine Blue

6 g borax

1 g boric acid

100 ml distilled water

pH 7.6-9.0

Bodian's Fixative

5 ml formalin

5 ml glacial acetic acid

90 ml 80% ethanol

(From Altman, 1980)

LIST OF ABBREVIATIONS

ACh	acetylcholine
ADP	adenosine diphosphate
AHP	afterhyperpolarisation
4-AP	4-aminopyridine
ATP	adenosine triphosphate
BAPTA	*bis*-(o-aminophenoxy)-ethane-N,N,N,N'-tetraacetic acid
α-BTX	α-bungarotoxin
cAMP	cyclic adenosine monophosphate
cGMP	cyclic guanosine monophosphate
CCh	carbachol
ChAT	choline acetyltransferase
CNS	central nervous system
DAG	diacylglycerol
4-DAMP	4-diphenylacetoxy-N-methylpiperidine
DHP	dihydropyridine
DNA	deoxyribonucleic acid
DUM	dorsal unpaired midline
EGTA	ethyleneglycol-*bis*-(β-aminoethyl)-N,N,N,N'-tetraacetic acid
GABA	γ-aminobutyric acid
GDP	guanosine diphosphate
GTP	guanosine triphosphate
HVA	high voltage activated
IP_3	inositol trisphosphate
I/V	current/voltage
LHRH	luteinising hormone releasing hormone
LVA	low voltage activated
McN-A-343	(4-hydroxy-2-butynyl)-1-trimethylammonium-*m*-chlorocarbanilate chloride
p-F-HHSiD	p-Fluoro-hexahydrosiladifenidol
PI	phosphoinositide
PIP_2	phosphatidyl inositol 4,5-bisphosphate
PKA	protein kinase A
PKC	protein kinase C
PPR	principle planta retractor
QNB	quinuclidinyl benzilate
RNA	ribonucleic acid
SER	smooth endoplasmic reticulum
SIU	stimulus isolation unit
SR	sarcoplasmic reticulum
TEA^+	tetraethylammonium ions
VPLI	vasopressin-like immunoreactive